AD NUMBER
AD384581
CLASSIFICATION CHANGES
TO: **unclassified**
FROM: **confidential**
LIMITATION CHANGES
TO: **Approved for public release, distribution unlimited**
FROM: **Distribution authorized to U.S. Gov't. agencies and their contractors; Administrative/Operational Use; OCT 1967. Other requests shall be referred to U.S. Air Force Rocket Propulsion Laboratory, Attn: RPPR/STINFO, Edwards AFB, CA 93523.**
AUTHORITY
31 Oct 1979, per document marking, DoDD 5200.10; AFRPL ltr, 5 Feb 1982

19

AFRPL-TR-67-175

THRUST CHAMBER MATERIALS AND DESIGN CONCEPTS EVALUATION (U)

E. G. PARKS Jr.
et. al
TRW Inc.
23555 Euclid Avenue, Cleveland, Ohio

FINAL REPORT AFRPL-67-175

Project Number 3058—Program Structure No. 750G

OCTOBER 1967

AIR FORCE ROCKET PROPULSION LABORATORY
AIR FORCE SYSTEMS COMMAND
EDWARDS, CALIFORNIA

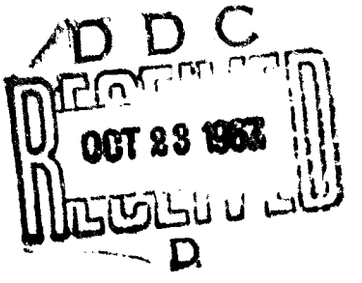

CONFIDENTIAL

AFRPL-TR-67-175

Copy [redacted] of 225 copies

Containing 248 pages.

THRUST CHAMBER MATERIALS AND DESIGN CONCEPTS EVALUATION (U)

E. G. PARKS Jr.
et. al

TRW Inc.
23555 Euclid Avenue, Cleveland, Ohio

FINAL REPORT AFRPL-67-175

Project Number 3058—Program Structure No. 750G

OCTOBER 1967

"THIS MATERIAL CONTAINS INFORMATION AFFECTING THE NATIONAL DEFENSE OF THE UNITED STATES WITHIN THE MEANING OF THE EPIONAGE LAWS. TITLE 18 U.S.C., SECTIONS 793 AND 794. THE TRANSMISSION OR REVELATION OF WHICH IN ANY MANNER TO AN UNAUTHORIZED PERSON IS PROHIBITED BY LAW."

"FOREIGN NATIONAL EMPLOYEES OF THE CONTRACTOR OR SUBCONTRACTOR(S), INCLUDING THOSE POSSESSING CANADIAN OR UNITED KINGDOM RECIPROCAL CLEARANCE, ARE NOT AUTHORIZED ACCESS TO CLASSIFIED INFORMATION RESULTING FROM OR USED IN THE PERFORMANCE OF, THIS CONTRACT UNLESS AUTHORIZED IN WRITING BY THE PROCURING CONTRACTING ACTIVITY."

"IN ADDITION TO SECURITY REQUIREMENTS WHICH MUST BE MET, THIS DOCUMENT IS SUBJECT TO SPECIAL EXPORT CONTROLS AND EACH TRANSMITTAL TO FOREIGN GOVERNMENTS OR FOREIGN NATIONALS MAY BE MADE ONLY WITH PRIOR APPROVAL OF AFRPL (RPPR/STINFO), EDWARDS, CALIFORNIA 93523."

AIR FORCE ROCKET PROPULSION LABORATORY

AIR FORCE SYSTEMS COMMAND

EDWARDS, CALIFORNIA

CLASSIFICATION: Confidential
REVIEWED BY: E. G. Parks Jr.
DATE: [illegible]
PROGRAM: [illegible]

DOWNGRADED AT 3 YEAR INTERVALS
DECLASSIFIED AFTER 12 YEARS
DOD DIR 5200.10

CONFIDENTIAL

TP-15250

34

FOREWARD

(U) This Final Report covers the work performed by TRW Equipment Laboratories (formerly TRW Structures Division), 23555 Euclid Avenue, Cleveland, Ohio, under USAF Contract No. AF 04(611)-10807. TRW Program Manager and Project Engineer were K. J. Smith and E. G. Parks Jr., respectively.

(U) This project was initiated under USAF Program Structure No. 750G, Project No. 3058, "Materials Investigation and Design Concepts for Non-Regenerative Thrust Chambers with Improved Capabilities." This program was accomplished under the technical direction of Captain R. W. Ogershok, RPRRE, Air Force Rocket Propulsion Laboratory, Edwards Air Force Base, California.

(U) In addition to those named on the cover, other authors of this report are D. N. Crump, E. N. Poulos, J. B. Pearson, and K. J. Smith. The technical assistance received from these individuals and Messrs. P. J. Cavano, W. E. Winters, J. R. Bohn, and G. S. Bell during this program is gratefully acknowledged. The latter two individuals are with TRW Systems Group, Redondo Beach, California.

(U) Test conditions and configuration designs for test articles provided in this report are UNCLASSIFIED. However, when performance results are associated with the test conditions and/or design configurations, this information will be classified CONFIDENTIAL.

(U) Classified information has been extracted from (asterisked) documents listed under References.

(U) This report has been given TRW internal Report No. ER 6383-19.

(U) The technical report has been reviewed and approved.

James A. Hintz, 1/Lt, USAF
AFRPL Project Engineer

ABSTRACT

(U) A program was conducted to investigate and evaluate new and unique designs of non-regenerative combustion chambers and nozzles using new materials or new techniques for applying the best materials. The technical effort on this program was divided into two phases. This is the final report on the program.

(U) The technical activity was pursued in three areas--literature survey, laboratory materials investigation, and design concept evaluation in rocket motor tests. The limitation that such parameters as chamber pressure, chemical reaction, firing duration, multiple starts, thermal shock, and structural requirements impose are evaluated in several design concepts. Scaling relations, effect of flow parameter changes on design requirements, and relative ratings on ease of fabrication and reliability of advanced thrust chamber design concepts are evaluated.

(U) Analysis of information obtained through literature search, contact with material suppliers, and laboratory testing indicates that materials which will have the best performance, i.e. lowest reactivity with high temperature fluorniated propellant combuation products, are essentially carbon base materials--graphites, carbides, pyrolyzed composites. Rocket motor tests were conducted using LF_2/ hydrazine blend propellant composition which is equivalent to a theoretical combustion temperature of over 7000°F to evaluate candidate materials and to demonstrate design concepts and scaling relations. Eight 100 pound and three 3750 pound thrust chambers were tested at chamber pressures of 150 and 200 psia. Material and design concepts included prestressed tantalum carbide, arc cast hypereutectic hafnium carbide, pyrolyzed compoistes of Carb-I-Tex 700 and PTB, heat sink design of pyrolytic graphite, tungsten, high-density graphite, hot-bonded Grafoil, and Thompsine Tape.

(U) The experimental findings were supplemented with technical and analytical support in an effort to establish the limitations that the propellant environment imposes on the selected materials and design concepts. The erosion or chemical reaction of liner materials appear to be diffusion controlled in most instances and a method for prediction of erosion based upon surface temperature and chamber pressure is reported. Conclusions and recommendations for further work are offered.

TABLE OF CONTENTS

LIST OF FIGURES

LIST OF TABLES

SECTION I

INTRODUCTION

(U) Rocket propulsion needed for space craft, ballistic missiles, and air-launched missiles of the future using advanced propellants requires non-regenerative thrust chambers with improved capabilities with high energy propellants in at least one of the following areas: higher chamber pressure; longer firing durations; and multiple restarts. Thus, the development of non-regenerative thrust chamber concepts which will advance the state-of-the-art in high energy upper-stage and attitude control systems, and show possible secondary applications to booster engines and air-launch propulsion systems are of interest. Concurrently, low cost, low weight, reliability, reproducibility, and decreased development time are factors which must be emphasized in considering future applications of new thrust chamber concepts.

(U) Research in the area of high temperature, non-corrosive, and thermal shock resistance has resulted in several promising materials which may enable thrust chambers to fulfill the aforementioned characteristics. It has been recognized from past experience, however, that analysis alone cannot resolve all the problems that occur in rocket chamber applications. Thus, it is relevant to investigate and evaluate materials which offer the greatest potential for uncooled thrust chambers by experimental means as well.

(U) This program was conducted to investigate and evaluate materials and design concepts for non-regenerative thrust chambers with improved capabilities for use with liquid fluorine oxidizer and hydrazine blend propellant systems for the Air Force Rocket Propulsion Laboratory, Edwards, California. This program was a 23 months effort completed in May 1967.

(U) The technical program was divided into two phases. Phase I was devoted to material evaluation and screening through design analysis, laboratory bench tests, and subscale rocket motor tests. The limitations that such parameters as chamber pressure, chemical reaction, firing duration, pulsing, and thermal shock impose on the thrust chamber material integrity and design concept were sought in this phase. During Phase II, the findings of Phase I supplemented by technical analysis were incorporated into the design, fabrication, and test evaluation of two full scale thrust chambers. A third full scale thrust chamber was designed to evaluate a new engineering material.

(U) This report is the final report and presents the results of the program activities. The results of the total program are presented and discussed in terms of actual and predicted performance. Relative ratings on ease of fabrication and reliability of advanced design concepts are presented and discussed. Recommendation for further investigation are offered.

(U) Appended to this report is the Material and Process, Research and Development Report. This report describes the details of the literature survey, laboratory investigation, and the application of a unique ablative composite material.

SECTION II

SUMMARY

(U) A program has been conducted to investigate and evaluate new and uniuqe designs of non-regenerative combustion chambers and nozzles using new materials or new techniques for applying the best materials. The technical effort on this program is divided into two phases. This report presents the results of the technical activities.

(U) The Phase I activities were designed to provide a systematic plan to accomplish the aforementioned objective. Specifically, the development of candidate materials and design concepts leading toward improved performance capabilities, the definition of operational limitations, the evaluation of thrust chambers and design concepts in a liquid fluorine/hydrazine blend propellant exhaust environment, and the analytical correlation of material performance and predicted behavior with test data are goals.

(U) During Phase I, technical activity was pursued in three areas--literature survey, laboratory materials investigation, and design concept evaluation. The literature survey provided the basis for subsequent investigations. Screening and evaluation of several advanced materials was accomplished both in laboratory bench tests and in subscale thrust chamber tests. The experimental findings were supplemented with technical and analytical support in an effort to establish the limitations that the propellant environment imposes on selected materials and passively cooled thrust chamber concepts.

(U) A comprehensive performance history was conducted. Approximately 90 reports and articles were reviewed in search for applicable data. The results of the survey implied several conclusions:

A. Analysis of the information indicates fairly conclusively that the materials which will have the best performance, i.e., lowest reactivity with the high temperature combustion products of fluorine propellants, are the essentially carbon base materials--the graphites, carbides, and pyrolyzed composites. This is true when the contents of the combustion gases are low in oxidizing species.

B. There is some theoretical information, and some meager test data, indicating that certain carbides--specifically TaC--may have superior resistance to HF reaction at very high temperatures, above 2500°K (5840°F) wall temperature.

C. The oxides do not appear promising because of reaction with HF to form either gaseous or liquid metal fluorides.

D. The refractory metals do not appear to offer any advantage over graphites in an environment dominated by fluorine reactions. However, where oxidizing species exist, or predominate, tungsten (as do the oxides) shows an improved performance capability.

(U) A laboratory materials screening program was designed to evaluate candidate materials with reference to their ability to resist attack by environments of hydrogen fluoride, the predominant specie in the combustion gases of the propellants under consideration. Two separate studies were conducted to determine the relative reactivity of various materials under consideration.

(U) A series of laboratory bench torch tests involving hydrogen-fluoride mixtures were performed on materials of interest for the prestressed nozzle

design. This design concept required critical components of materials other than that of a throat insert (such as a prestressing ring) which might be subjected to exhaust gases.

(U) A more extensive laboratory materials screening program was also conducted to evaluate candidate throat and chamber liner materials with reference to their ability to resist attack by hydrogen fluroide environments. Three different test conditions were examined in this series of tests--reaction of specimens with hydrogen fluoride in a static environment, reaction of specimens with hydrogen fluoride in a dynamic environment, and reaction of specimens with hydrogen fluoride plus a 0.1% volume of air to simulate the relative percentage of oxygen in the propellant exhaust specie. All tests were conducted with heated specimens.

(U) The results of the laboratory investigation indicated the graphite base materials had the lowest reaction rate. Carb-I-Tex 700, a prepyrolyzed graphite composite produced by Basic Carbon Corporation, showed no material loss at about 4400°F in hydrogen fluoride. Tantalum carbide ranked somewhat lower, as expected, since specimen temperatures were below 5500°F. Tungsten demonstrated favorable performance in the laboratory investigation, and, as a result, was selected for subscale thrust chamber evaluation.

(U) The subscale thrust chamber evaluation program was planned to systematically test several throat insert materials. A total of eight units were designed, fabricated, and tested for an accumulated duration in excess of 1100 seconds on all units. Throat materials tested included:

A. Tantalum Carbide

B. Hypereutectic Hafnium Carbide

C. Carb-I-Tex 700

D. Pyrolytic Graphite

E. Tungsten with 2% thoria

F. PTB (prepyrolyzed graphite composite, National Carbon Corporation)

G. Hot-Bond Grafoil (anisotropic graphite, High Temperature Materials Incorporated)

H. High Density CGW Graphite (National Carbon Corporation)

Chamber liner materials included carbon cloth phenolic, CGW graphite, Carb-I-Tex 700, pyrolytic graphite, and PTB.

(U) Thrust chambers were designed employing simple heat barrier or heat sink concepts. The pyrolytic graphite throat insert employed conically oriented "a-b" planes and was designed to take advantage of the inherent high conductivity of the material. A heat sink was provided in the chamber region. A prestressed throat insert design concept was utilized for the tantalum carbide throat insert to circumvent the thermal shock characteristics of the material.

(U) Test results revealed that the graphite base and carbide material demonstrated the lowest total erosion. An analytical correlation of test data eliminating the variability of the test conditions was used to rank the materials. This ranking was comparable to that determined in the laboratory except that tungsten also demonstrated low reactivity potential with HF due to the low laboratory test temperatures. In the subscale tests, tungsten reacted readily with the propellant environment.

(U) As a result of the Phase I technical activity and the state-of-the-art for design and fabrication of the several material and design concepts examined, Carb-I-Tex 700 was selected as a throat insert material based upon its good performance and design simplicity. A heat sink design concept employing pyrolytic graphite was utilized for the second full scale thrust design.

(U) In keeping with the major objective of material and design performance, the third full scale unit was constructed using Thompsine Tape,[1] a TRW developed material, in a portion of the chamber and in the throat region. Thompsine Tape is a unique ablative material which provides better end-product performance in ablative structures. The uniqueness of this material lies primarily in the elimination of the need for interface bond lines between the exposed material (gas side) and the insulative material (shell side). This is done by mechanically weaving the two materials together prior to resin impregnation and cure. The two sections are thus an integral part upon curing giving a much stronger interlaminar integrity. Secondary advantages, which are built into the tape weave, permit attainability of high diametral wrap ratios. Although an ablative Thompsine Tape structure is not recommended as a candidate throat material in a high pressure fluorine environment, tests on this unit were designed to provide the necessary date to evaluate the unique characteristics of this material.

(U) Full scale unit S/N 1 contained a Carb-I-Tex 700 throat insert with conventional carbon cloth-phenolic chamber and exit cone liner. Total test time on unit S/N 1 was 373 seconds and was comprised of four pulses--11, 61, 100, and 201 seconds, respectively. The chamber liner, which was 0.625 inches thick, was almost completely consumed and indications of separation and loss of the liner at the liner-insulator interface were evident at a few locations. Inspection between pulses indicated normal erosion with no chunking or spalling evident. Diametral erosion of the Carb-I-Tex 700 throat insert amounted to 0.686 inches over the total time. During the 11, 61, and 100 second pulses, only .009 inches of accumulated erosion was measured, with the remaining 0.677 inches occurring during the 201 second pulse (probably after 100 seconds of elapsed time).

(U) Full scale unit S/N 2 contained an oriented plane pyrolytic graphite throat insert in a design concept intended to "heat sink" the throat. The throat insert support and aft half of the chamber were CGW graphite. Total test time on unit S/N 2 was approximately 358 seconds and was comprised of 6 pulses--9, 39, 60, 72, 150, and 28 seconds respectively. Total throat erosion during the last three pulses was approximately 0.050 inches. .Again, the majority of the erosion occurred during the longer pulse durations. .The chamber section (CGW graphite) remained intact and eroded a minor amount.

---

[1] TRW has applied for a patent on this material.

(U) Full scale unit S/N 3, which was the all ablative chamber containing Thompsine Tape, was tested for a total duration of 206 seconds. Test run durations consisted of several pulses up to 20 seconds in length and one 55 second test. Erosion of the ablative throat was comparable to that of other ablative concepts. For test pulses up to 20 seconds in duration, throat area change was less than 3%. For the 55 second pulse, throat area change was approximately 20%. The Thompsine Tape was constructed with graphite and quartz for gas side and insulative materials respectively. The advantages of Thompsine Tape as an engineering material were demonstrated. It was shown that Thompsine Tape can be fabricated in thicknesses and at diameters not possible with conventional bias tape construction and that complete dissimilar interface integrity can be maintained in the charred condition.

(U) As a result of this program, pyrolytic graphite and Carb-I-Tex 700 have demonstrated satisfactory performance as throat insert materials in a rocket motor operating environment of a LF_2/N_2H_4 blend propellant system with a chamber pressure of 100 to 200 psia. The advantages of Thompsine Tape as an engineering material have been demonstrated. Future work is recommended to extend the state-of-the-art of the several material and design concepts examined including pyrolyzed Thompsine Tape and composite reinforced carbide structures.

SECTION III

TECHNICAL APPROACH

(U) The program encompasses a material and design concept investigation for non-regenerative thrust chambers with improved capabilities for operation in liquid fluorine oxidizer and hydrazine blend fuel propellant systems. The technical program was divided into two phases. Phase I was devoted to material evaluation and screening through laboratory bench tests and subscale rocket motor tests. During Phase II, the findings of Phase I supplemented by technical analysis were incorporated into the design, fabrication, and post firing evaluation of three full scale thrust chambers.

(U) In this section, objectives of the total program are presented. The plan to accomplish these objectives is presented and discussed.

1. OBJECTIVE

(U) The major objective of the program was to investigate and evaluate new and unique designs of uncooled combustion chambers and nozzles using new materials or new techniques for applying the best materials. Design concepts were limited to those materials or composites which involve passive responsiveness such as heat barrier, radiation, heat sink, or ablative techniques. Specific objectives were to:

A. Develop candidate materials and design concepts aimed toward improved performance capabilities.

B. Define operational limitations in terms of size, weight, chamber pressure, firing duration, restart capabilities, surface temperature, vacuum and near vacuum conditions, compatibility of materials with specified propellant combination, and structural requirements.

C. Evaluation of thrust chambers in the exhaust environments of the liquid rocket propellant LF_2/N_2H_4 blend.

D. Obtain scaling relations and effect of flow parameter changes on design requirements.

E. Obtain test data for concept evaluation and analytical correlation of materials performance and predicted behavior.

F. Obtain relative ratings on ease of fabrication and reliability of advanced nozzle design concepts.

2. PHASE I PLAN

(U) The Phase I activities were designed to provide a systematic plan to accomplish the aforementioned objectives. Specifically the development of candidate materials and design concepts leading toward improved performance capabilities, the definition of operational limitations, the evaluation of thrust chambers and design concepts in the required exhaust environment, and the analytical correlation of material performance and predicted behavior with test data were goals.

(U) During Phase I, technical activity was pursued in three areas--literature survey, laboratory materials investigation, and design concept evaluation. The following presents the approach used in each of these areas.

a. Literature Survey

(U) A comprehensive literature survey was conducted early in the program to serve as a basis for all subsequent work. The objective of this survey was to review and evaluate available information and to select promising materials that apply to passively cooled combustion chamber and nozzle components. Information was screened relative to use with LF_2/N_2H_4 blend propellants; however, consideration was given to potential use of Compound A oxidizer and LH_2 fuel. The survey considered the following factors: material performance in the specified propellant environments, thrust level, chamber pressure range, mixture ratio, structural size and weight, specific impulse, firing duration, performance degradation with time, vacuum operation, and cooling concept employed.

b. Material Investigation

(U) A laboratory materials screening program was conducted to evaluate candidate materials which suggested a high probability of being successfully applied to advanced design concepts. Since hydrogen fluoride is the predominate reactive specie in the specified propellant combustion gases, laboratory bench tests were designed to provide a low cost material screening under carefully controlled conditions. Materials were ranked according to resistance to hydrogen fluoride attack at elevated material temperatures. Thermal shock resistance was also examined and some strength data obtained.

c. Design Concept Evaluation

(U) The subscale thrust chamber evaluation program was planned to provide a systematic approach to the acquisition of useful design information. The results of the performance history survey were utilized in planning the details of the technical effort. Although the laboratory materials investigation and the design concept evaluation were initiated concurrently, they were planned such that the results of the laboratory investigation could be integrated into the subscale thrust chamber design evaluation.

(U) Seven tests were initially planned in the subscale test program to be conducted in three series. These tests were primarily intended to investigate throat insert materials. The first test series (three subscale thrust chambers) was designed to determine erosion as a function of temperature and maximum material operating temperature of the throat insert materials. Long on-time duty cycles were planned for this series of tests. The second test series (two subscale thrust chambers) were to employ a pulsing duty cycle to determine the effect on material performance and to evaluate and design configurations. Materials for the second series of tests were to be selected following evaluation of the first test series and the laboratory analysis. The last two subscale thrust chambers (third series) were to be designed to incorporate the best materials based upon results of the previous testing. The first six thrust chamber tests were to be conducted at a chamber pressure of 150 psia, while the last would be conducted at 200 psia chamber pressure. Nominal thrust level for all tests was 100 pounds.

(U) During the execution of the laboratory materials investigation task, several "hard" materials tested were deemed adequate for thrust chamber evaluation due both to their relatively low reactivity with hydrogen fluoride and their ability to be easily formed. As a result, the design concept evaluation approach

was altered to consider both the throat insert and the effect which different thrust chamber liner materials might have on total performance. In order to accommodate more materials, the number of thrust chambers tested was increased to eight. Thus, the subscale thrust chamber design evaluation program considered six units designed for 150 psia chamber pressure and two units designed for 200 psia chamber pressure. Eight different throst insert materials were evaluated and five different chamber materials.

3. PHASE II PLAN

(U) In terms of the original program, the Phase II plan was to incorporate the results of the Phase I investigations in design, fabrication, and post firing evaluation of three full size (3750 pound thrust) chambers. The first two units were to utilize the best materials and design concepts from Phase I. The third full size unit was to incorporate the best material and design concept from the previous two full size units with design improvements dictated by test evaluation.

(U) In keeping with the major objective of material and design performance evaluation, TRW recommended that the third full scale be constructed from a TRW developed material called Thompsine Tape. The objective of this unit was to provide information relative to the performance of a non-conventional weave pattern, to demonstrate improved dissimilar material interface integirty between exposed (gas side) and insulative ablative materials, and to provide additional information on the performance of ablative materials in the propellant environment. As a result the first two full scale units utilized the best materials and design concepts from Phase I, and the third full scale unit incorporated Thompsine Tape.

SECTION IV

MATERIALS SURVEY

(U) Early in the program an extensive materials survey was conducted to evaluate the characteristics of promising materials for application to thrust chamber design in a fluorinated propellant system. Three primary areas of concern for thrust chamber liner and throat materials exposed to the extreme environment of the LF_2/N_2H_4 blend propellant system are (a) melting or softening due to exposure to the extremely high temperatures of the propellant gases, (b) corrosion or erosion losses due to chemical reaction or mechanical impingement by the combustion products, and (c) cracking due to thermally induced stresses during firing.

(U) Chemical reaction problems complement those associated with surface softening due to the exponential increase in reactivity rates with increasing temperatures and pressures. As a result, severe degradation in nozzle performance can occur as a result of chemical reaction of the throat liner material with the propellant combustion products. The reactions become more critical as the component temperatures and system gas pressures are increased. This factor of high temperature chemical reactivity undoubtedly poses the major problem in selecting a suitable nozzle throat liner design capable of satisfactory performance for the specified firing times and pressures.

(U) The results of the literature materials survey and laboratory materials screening program are presented in this section. Details are included in the a appendix of this report.

1. PERFORMANCE HISTORY

(U) A comprehensive review of materials was made relative to the combination of high combustion gas temperature and chemical reactivity potential which exists in a luquid fluorine/hydrazine blend propellant system. The following is a summarization of information obtained from various reports of the work performed with materials exposed to the influence of high temperature, reactive rocket engine gases containing fluorine. The information was selected to closely apply to the conditions which would exist with hardware produced in support of this program. The results also incorporate applicable information obtained through contacts with materials suppliers.

a. Carbides

(U) Carbides appear to have a high resistance to high temperature fluorine environments. There is some information, however, that graphite materials have a superior reaction resistant for wall temperatures below 5840°F. This information is based on the reaction potential with HF, the predominant specie in the combustion gases of LF_2/N_2H_4 blend propellants.

(U) Test results of the carbides of tantalum, titanium, silicon, zirconium, hafnium and columbium were reported. Of these data, tantalum carbide appeared to perform the best. The major limitation in the application of carbide materials is the inherent brittleness and sensitivity to thermal shock cracking.

b. Graphites

(U) Graphite appears to give good performance in fluorine atmospheres. Test results of several graphites indicated edge-oriented pyrolytic graphite yields superior performance in short duration tests. These test suggested that

erosion is directly proportional to the pressure at the throat and that chemical corrosion is the major mechanism for removing material from the throat surface.

(U) Test results of alloys made from pyrolytic graphite and several carbides were not successful because of the low melting temperatures of the carbide-graphite composites tested.

c. Oxides

(U) Oxides are generally resistant to propellant environments containing oxidizing and fluorine specie for short test times. However, at higher temperatures, the oxides react with HF to form either gaseous or liquid metal fluorides. Two major disadvantages are their extreme thermal shock sensitivity and their relatively low melting points (below 6000°F). Based on either maximum useful temperature or chemical reactivity with fluorine compounds, there appears to be no advantage for at least some of the oxides over either graphite or carbides.

d. Pyrolyzed and Ablative Composites

(U) Little information was available in the industry on the performance of pyrolyzed and ablative materials in the corrosive environment of fluorine/hydrazine exhaust. There was some experimental data which demonstrated the stability of both carbon and graphite materials, and the instability of high silica materials. Improved performance was reported for ablative structures of carbon phenolic materials which were pyrolyzed prior to propellant testing.

e. Refractory Metals

(U) From the standpoint of thermal shock resistance and fabricability, the refractory metals are very acceptable as rocket nozzle materials. However, the high flame temperatures encountered with fluorine base propellants would limit the use to only short duration firings becuase of the relative low melting temperature of the refractory metals. Tungsten appears to be the most promising refractory material for this environment. According to thermodynamic calculations, the reaction resistance of tungsten to HF approaches that of graphite at temperatures very near the melting point of tungsten (6170°F).

2. MATERIALS INVESTIGATION

(U) A laboratory materials screening program was designed to evaluated candidate materials with reference to their ability to resist attach by environments of hydrogen fluoride. Two separate studies were conducted to determine the relative reactivity of the materials under consideration. A series of laboratory torch tests involving hydrogen fluoride mixtures were performed on materials of interest. Following this, a more intensive laboratory reactivity screening program was also conducted to evaluate selected throat and chamber liner materials.

(U) In the first set of tests, a hydrogen fluoride torch was used which produced an adiabatic flame temperature of 8512°F. The samples were tested after preheating so that thermal shock would not destroy the specimen. The criteria used for determining the resistance to the environment was the per cent weight loss. By using the theoretical density, the loss in volume could be determined. Table I presents the results of these tests in order of decreasing resistance to the environment. The test data substantiate the findings of the literature survey and demonstrate the superior behavior of graphite materials.

Table I (U) Propellant Exhaust Environment Test

Material	Density* gm/cm^3	Weight Before gm	Weight Loss gm	%Weight Loss	Volume Loss cm^3
ATJ	1.80	2.6461	nil	0	0
CFZ	1.90	2.9180	0.004	0.01	0.0021
PG	2.2	3.3650	0.019	0.56	0.0086
W	19.3	25.9003	0.190	0.73	0.0098
TaC	14.37	21.2939	0.160	0.75	0.0111
TZM	10.15	12.9617	0.114	0.88	0.0112
Z_rC	6.78	9.9777	0.111	1.11	0.0163
Ta (carburized)	16.6	23.6965	0.277	1.20	0.0166
HfC + C (arc cast)	10.0	21.5643	0.307	1.42	0.0307
Ta - 10 W (carburized)	16.6	22.2652	0.552	2.48	0.0328
FS 85	10.8	14.4328	0.372	2.58	0.0344
Ta	16.6	22.0227	0.742	3.37	0.0446
Ta - 10 W	16.8	23.3236	0.798	3.40	0.0475

Unclassified

* Densities are published values.

(U) In the second set of tests, the specimens were heated to a high temperature (approximately 4500°F) in a stagnant atmosphere of hydrogen fluoride and were held at these temperatures for varying periods of time. The degree of reactivity was determined by measuring the diameter change of the specimens with pin-tip mocrometers. The materials selected for these tests are presented in Table II and the results of these tests are recorded in Table III.

(U) The results of the second series of reactivity tests indicate that the graphite base Carb-I-Tex 700 material exhibited the greatest resistance to attack by HF at temperatures up to 4200°F. Wrought tungsten also showed moderately good resistance to attach at temperatures as high as 4500°F. Tantalum carbide ranked somewhat lower, as expected, since specimen temperatures were below 5500°F. Additions of 0.1% air, volume of air to simulate the relative percentage of oxygen in the propellant exhaust specie, and the use of an impinging gas stream did not significantly alter the results obtained with the static HF environment.

Table II (U) Materials for Evaluation in Fluorine Environments

Material	Type	Form	Vendor
Graphite	CGW	Blocks	Union Carbide
Graphite	Pyrolytic	1/4" dia. X 2" rods	Super Temp
Tungsten	Unalloyed	1/4" dia. X 2" rods	General Electric
Carbide	TaC (Hot pressed)	3/4" dia. X 2" rods	Carborundum
Carbide	HfC (Hot pressed)	3/4" dia. X 2" rods	Carborundum
Oxide	ZrO_2	0.010 plasma coating on 1/4"dia. X 2" W rods	TRW
Pyrolysed Plastic	Carb-I-Tex 700	1/4" dia. X 2" rods	Carborundum (Graphite Specialties)
Pyrolysed Plastic	Carb-I-Tex 100	1/4" dia. X 2" rods	Carborundum (Graphite Specialties)
Pyrolysed Plastic	Union Carbide PTB (PT-0145)	1/4" dia. X 2" rods	Union Carbide
Carbon Cloth Phenolic	MX-4926	Blocks	TRW

Table III (U) Summary of Reactivity Test Results with HF

Material	Test Temperature, °F	Test Time, Min.	Dia. Change 10^{-3} inches
Carb-I-Tex 700	4240	3	0
Carb-I-Tex 700	4200	3	0
W	4000	3	-2.1
W	4520	3	-2.2
W	4420	3	-2.3
W	4520	3	-2.5
PG	4000	3	-2.8
W	4500	6	-3.2
TaC	4480	3	-4.2
ZrO_2	4500	3	-5.0
CGW	4200	3	-5.5
HfC	4500	3	-5.5
Carb-I-Tex 100	3400	3	-6.0*
Carbon Cloth Phenolic	4000	3	+1.8 to 5.0

* Loss occurred only in one direction, normal to the plies, producing an elliptical cross-section.

Unclassified

SECTION V

SUBSCALE THRUST CHAMBER CONCEPT EVALUATION

(U) The subscale thrust chamber evaluation program was planned to permit a logical persuance of specific design information. Eight thrust chambers were designed, fabricated, and tested. The details of the thrust chamber concept evaluation are discussed in this section.

1. DESIGN

(U) The design requirements for subscale thrust chambers were specified to be compatible with the full scale design requirements of this program except for size and duration. Materials were selected based upon the results of the performance history survey and the laboratory materials evaluation. Each thrust chamber was then designed to accommodate the requirements and material constraints. In most areas, simple shapes were employed to minimize cost of fabrication since primary effort was to evaluate liner materials. Insulation and steel shells were conservatively designed for potential reuse.

a. Requirements

(U) The design requirements for the subscale thrust chamber evaluation were specified by the Air Force Rocket Propulsion Laboratory. The propellant combination and operating goals were as follows:

A. Propellants	LF_2/N_2H_4 blend (Weight percent: 66.7 N_2H_4, 24.0 MMH, 9.3 H_2O)
B. Thrust	100 pounds
C. Chamber Pressure	200 psia (exhaust to 14.7 psia)
D. Mixture Ratio	1.8 (design for 2.0)
E. Performance	96% theoretical specific impulse (min.)
F. Duration	600 cumulative seconds at rated thrust with the option of up to 30 restarts at any time during the 600 second duration

(U) The duration specified above was a full scale requirement. The subscale tests were not designed for the total duration. However, the test sequence was planned to examine the stringent requirements of full scale testing which require sustained burns and a pulsing duty cycle.

(U) The performance properties were calculated at mixture ratios of 1.8 and 2.0 using a TRW computer program. Theoretical performance calculations for the stated propellant combination at a chamber pressure of 200 psia and O/F ratios of 1.8 and 2.0 were made and the results of analysis are presented in Tables IV through VII. Variations in characteristic velocity and combustion temperature as a function of mixture ratio and chamber pressure are presented in Figures 1 through 3. The theoretical specific impulse is presented in Figure 4.

(U) For a chamber pressure of 200 psia at a mixture ratio of 2.0 and this propellant system, a throat area of 0.393 square inches in a nozzle exhausting

TABLE IV (U) Combustion Characteristics

Mixture Ratio	1.8	2.0	Notes
Theoretical Flame Temperature	4130 ^{o}K	4229 ^{o}K	
Theoretical Specific Impulse	293 sec	295 sec	1
C^{*}	6966 ft/sec	6988 ft/sec	1
C_p (Calculated assuming shifting equilibrium flow)	0.154 Kcal/100 gms ^{o}K	0.173 Kcal/100 gms ^{o}K	2
C_p (Calculated assuming frozen equilibrium flow)	0.0458 Kcal/100 gms	0.0445 Kcal/100 gms	2
Gas Viscosity	7143 x 10^{-7} gm/cm-sec	7322 x 10^{-7} gm/cm-sec	2, 3
Gas Conductivity	2926 x 10^{-7} cal/cm-sec-^{o}K	2836 x 10^{-7} cal/cm-sec-^{o}K Unclassified	2, 4

Notes:

1. Calculated assuming shifting equilibrium flow.
2. Calculated at chamber conditions.
3. Calculated using empirical relation: $\mu = 8322 \times 10^{-10} (M.W.)_{AVG}^{1/2} T^{0.6}$ where $(M.W.)_{AVG}$ is the average molecular weight of the combustion products in the chamber, T is the temperature in degrees Rankine, and the viscosity is expressed in gm/cm-sec.
4. Calculated using empirical relation: $k = \frac{15}{4} \frac{R}{(M.W.)_{AVG}} \cdot \mu$ where R is the universal gas constant, and the conductivity is expressed in cal/gm-sec-^{o}K.
5. Chamber conditions: P_c = 200 psia, P_a = 13.2 psia where P_c is the chamber pressure and P_a is the atmospheric pressure.

TABLE V (U) Principle Constituents of Gases in Combustion Chamber

	T = 4130 °K M.R. = 1.8	T = 4229 °K M.R. = 2.0
Constituent	Mole Fraction	
C	1.81141×10^{-5}	2.50497×10^{-5}
CN	4.30634×10^{-4}	4.62020×10^{-4}
CO	3.32063×10^{-2}	3.16796×10^{-2}
F	3.96858×10^{-2}	6.53810×10^{-2}
FCN	1.29197×10^{-5}	1.64615×10^{-5}
H	1.25372×10^{-1}	1.17064×10^{-1}
H_2	5.48911×10^{-2}	3.48120×10^{-2}
HF	5.76808×10^{-1}	5.88610×10^{-1}
H_2O	2.91401×10^{-5}	1.90960×10^{-5}
HCN	2.01206×10^{-4}	1.45531×10^{-4}
N	3.09360×10^{-4}	4.21911×10^{-4}
NH	6.92976×10^{-5}	6.77099×10^{-5}
N_2	1.68822×10^{-1}	1.61115×10^{-1}
NO	1.40119×10^{-5}	1.79121×10^{-5}
O	5.41021×10^{-5}	7.95111×10^{-5}
CF		1.45838×10^{-5}
OH		4.33796×10^{-5}

Unclassified

TABLE VI (U) Principle Constituents of Gases in Throat

Constituent	T = 3870 °K M.R. = 1.8 Mole Fraction	T = 3985 °K M.R. = 2.0 Mole Fraction
C	1.04519×10^{-5}	1.58937×10^{-5}
CN	3.64750×10^{-4}	4.01847×10^{-4}
CO	3.38437×10^{-2}	3.23278×10^{-2}
F	2.60825×10^{-2}	4.81766×10^{-2}
FCN	1.03717×10^{-5}	1.38422×10^{-5}
H	1.08727×10^{-1}	1.02800×10^{-1}
H_2	5.80675×10^{-2}	3.44316×10^{-2}
HF	6.00647×10^{-1}	6.17233×10^{-1}
H_2O	1.72748×10^{-5}	1.08898×10^{-5}
HCN	2.12426×10^{-4}	1.45314×10^{-4}
N	1.602579×10^{-4}	2.41379×10^{-4}
NH	3.75975×10^{-5}	3.80904×10^{-5}
N_2	1.71755×10^{-1}	1.64077×10^{-1}
O	1.95714×10^{-5}	3.27867×10^{-5}
OH	1.88313×10^{-5}	1.99111×10^{-5}

Unclassified

TABLE VII (U) Principle Constituents of Gases in Exit Cone

Constituent	T = 2913 °K M.R. = 1.8 Mole Fraction	T = 3070 °K M.R. = 2.0 Mole Fraction
CN	1.46110×10^{-4}	2.39104×10^{-4}
CO	3.56627×10^{-2}	3.41972×10^{-2}
F	1.67643×10^{-3}	5.25541×10^{-3}
H	3.70666×10^{-2}	4.37823×10^{-2}
H_2	8.67724×10^{-2}	4.58523×10^{-2}
HF	6.57475×10^{-1}	6.97018×10^{-1}
HCN	4.24016×10^{-4}	3.01421×10^{-4}
N_2	1.80761×10^{-1}	1.73328×10^{-1}

Unclassified

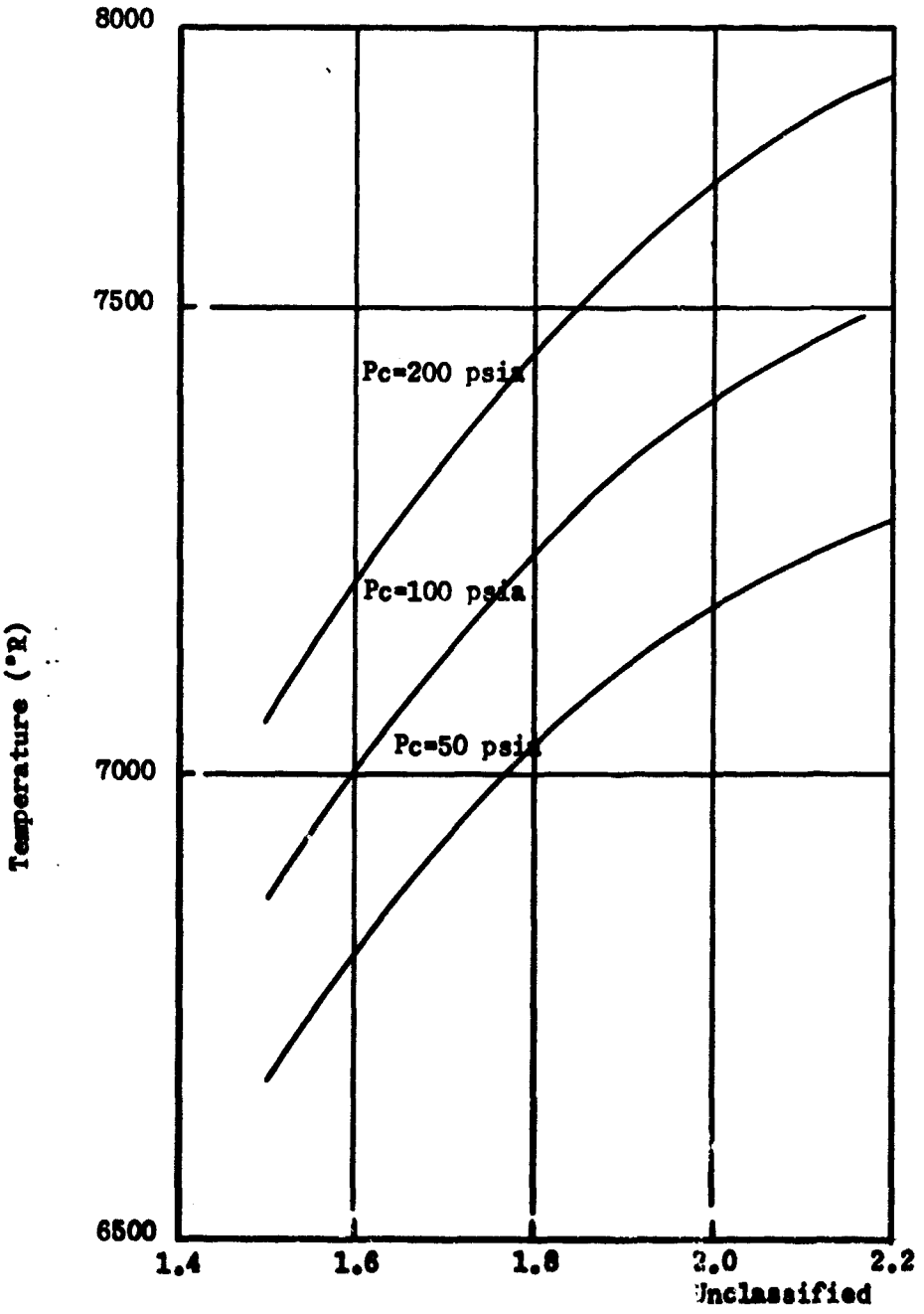

LF$_2$/N$_2$H$_4$ Blend Propellants

FIGURE 1 (U) Theoretical Combustion Temperature

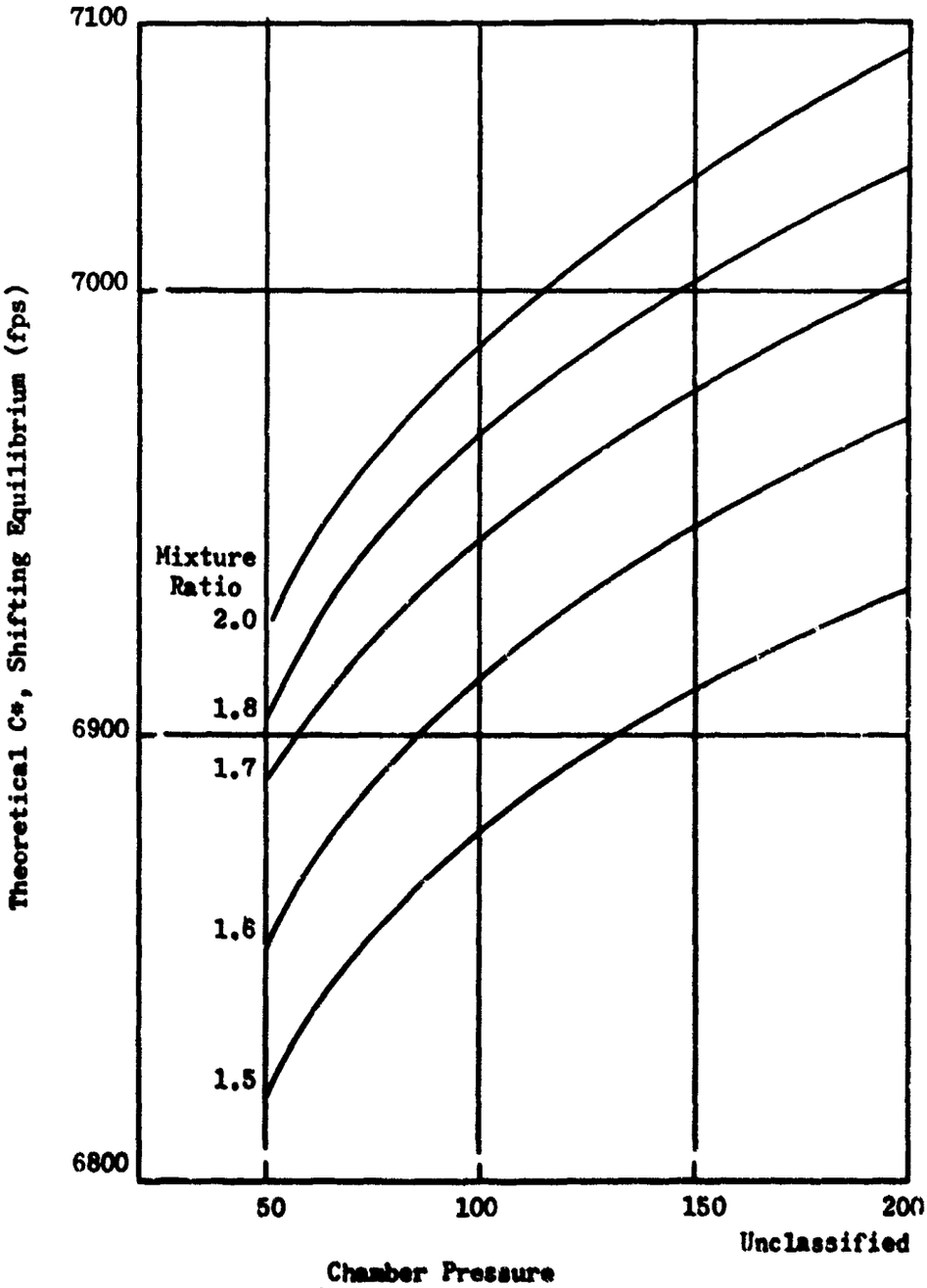

LF_2/N_2H_4 Blend Propellants

FIGURE 2 (U) Theoretical C* vs. Chamber Pressure

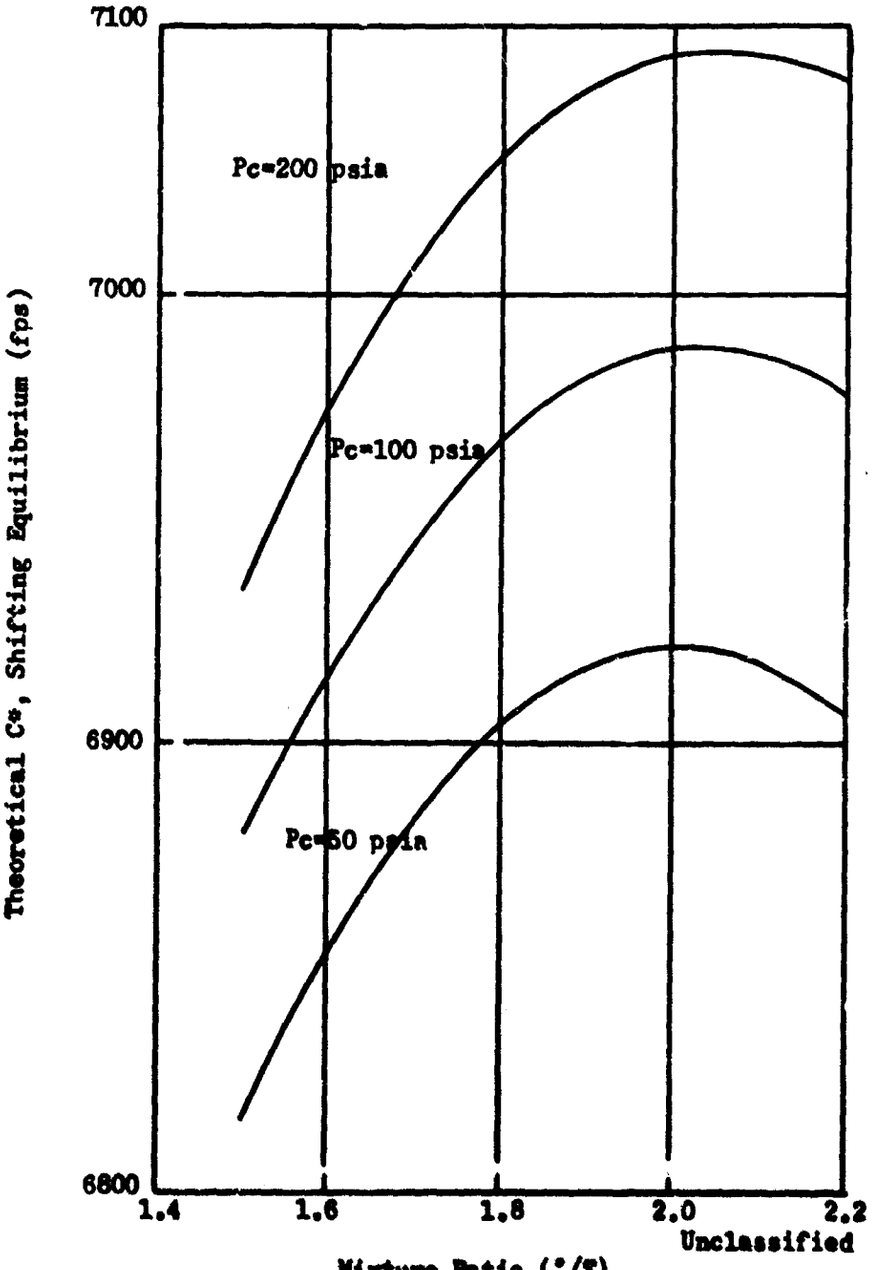

FIGURE 3 (U) Theoretical C* vs. Mixture Ratio

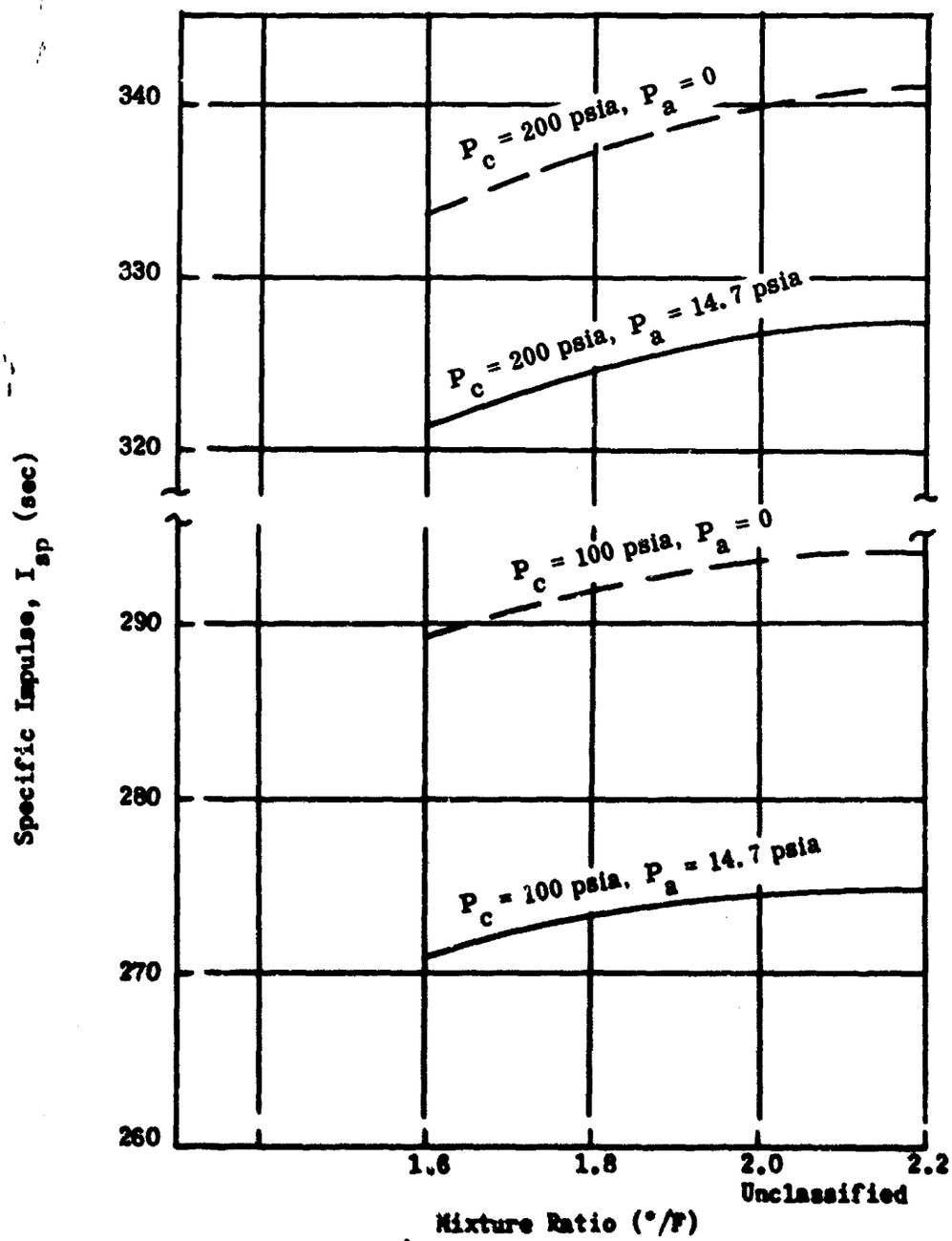

LF_2/N_2H_4 Blend Propellants

FIGURE 4 (U) Theoretical Specific Impulse

to an ambient pressure of 14.7 psia (TRW test facility pressure), will give a thrust of about 100 pounds. For design configurations tested at a chamber pressure of 150 psia, the throat area is 0.524 square inches. For thest calculations, the C* efficiency is assumed to be 96 percent.

(U) Knowing the throat diameter, exhaust gas characteristics, chamber pressure, and characteristic velocity; the heat transfer coefficient was calculated by the simplified Bartz equation. Also, by assuming a recovery factor of 0.9 with a C* efficienty of 96 percent, the adiabatic wall temperature is conservatively calculated as a function of area ratio. These results are shown in Figure 5.

b. Material Selection

(U) Results of the literature search indicated that the materials which would have the greatest resistance at high temperatures to attack by hydrogen fluoride, the primary combustion product constituent of the propellants under consideration, were graphite base materials, selected carbides--such as TaC--and tungsten. These predictions from the literature were confirmed by torch and static reactivity chamber tests utilizing hydrogen fluoride as the reactant.

(U) Based on the results of the laboratory testing of the various candidate materials to determine their relative resistance to high temperature reaction by hydrogen fluoride and information obtained from the literature concerning the performance of materials in fluorine-rich environments, materials for the subscale nozzle throat inserts and combustion chamber liners were selected. Table VIII lists the liner materials selected for the eight subscale units, as well as the material sources and fabrication methods employed.

(U) The all-graphite pyrolyzed plastic Carb-I-Tex 700, pyrolytic graphite, CGW molded monolithic graphite, hot bonded grafoil (PG foil), and reimpregnated pyrolyzed plastic grade PTB (PT-0145) were selected to represent graphitic materials in various physical conditions produced by different processing techniques. All of these materials were completely graphitic, with the exception of the PTB (PT-0145). This material had an all-graphite base which was subsequently impregnated with a resin to develop a partially ablative material.

(U) In order to provide a free-standing carbide throat insert with adequate thermal shock resistance, an arc-cast hypereutectic carbide material was selected. The insert was produced from a hypereutectic HfC - graphite material, since this material has one of the highest eutectic melting temperatures for a single carbide (next to TaC-C) and had been successfully produced and tested under severe thermal shock conditions. Hypereutectic TaC--although of higher melting temperature, and theoretically good resistance to very high temperature HF reaction--was not selected because of technical limitations existing at the time with facilities for producing the carbides. The high vapor pressure of carbon at the extremely high melting temperature of the TaC-C eutectic required pressurized furnace equipment (not available at the time) in order to prevent carbon "boil" or loss in the system.

(U) Opportunity for testing an essentially stoichiometric tantalum carbide throat insert was provided through the use of a prestressing approach developed by TRW Systems Group. The finished throat insert was fabricated from a pre-form of hot pressed tantalum carbide powder.

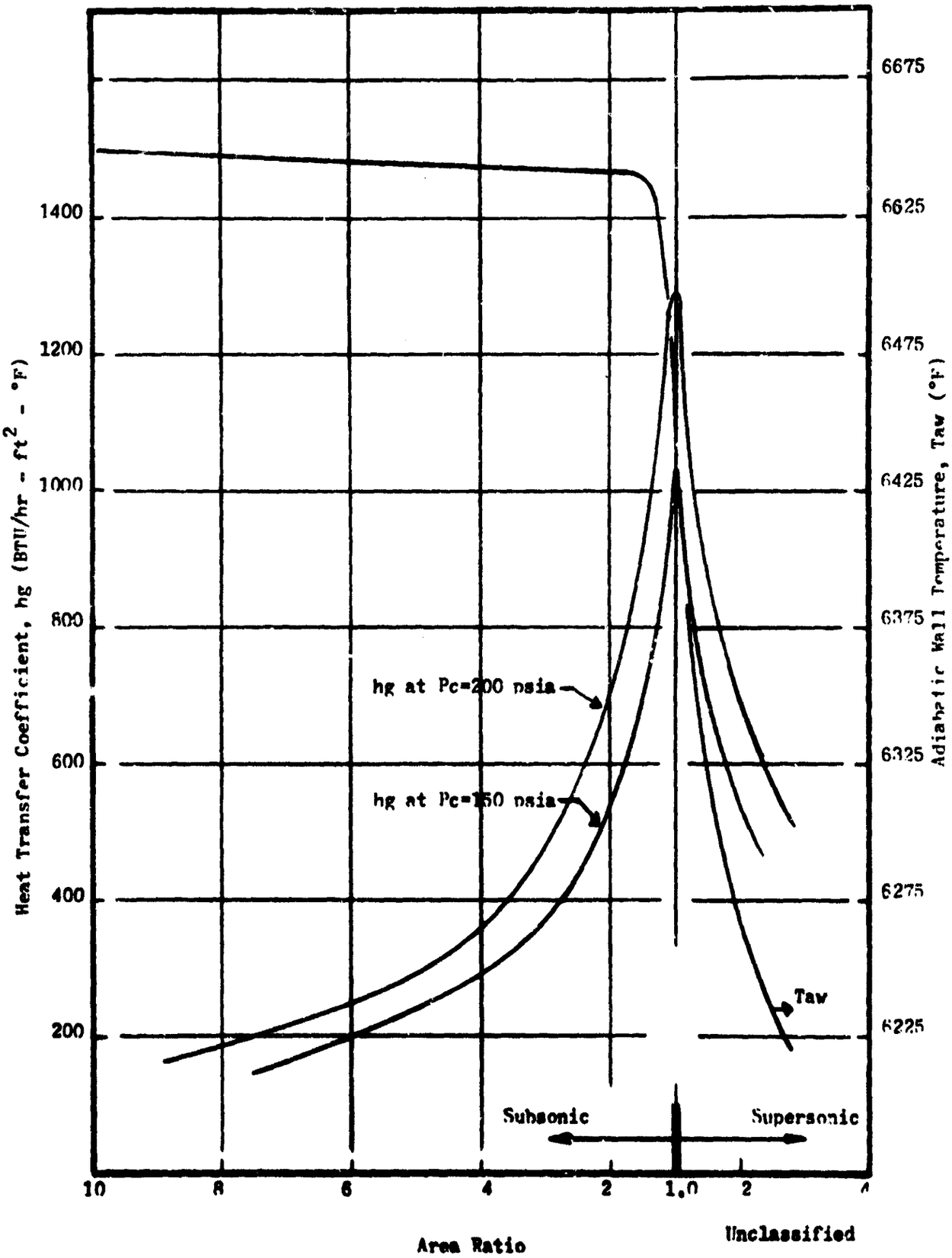

FIGURE 5 (U) Heat Transfer Coefficient and Adiabatic Wall Temperature; Subscale Thrust Chambers

TABLE VIII (U) Subscale Thrust Chamber Materials and Sources

Subscale Unit S/N	Location	Liner Material	Fabricated Conditions	Source
1	Chamber	Carbon Cloth Reinforced Phenolic Plastic	Molded and cured	TRW
	Throat	TaC (Pre-stressed)	Hot pressed	TRW Systems
2	Chamber	CGW Graphite	Molded monolithic	Union Carbide
	Throat	Hypereutectic HfC	Arc melted and cast	Battelle
3	Chamber	Carb-i-Tex 700	All-graphite, pyrolyzed	Carborundum (Carbon Prod. Division)
	Throat	Carb-I-Tex 700	All-graphite, pyrolyzed	Carborundum (Carbon Prod. Division)
4	Chamber	Pyrolytic Graphite	Pyrolytically deposited	Pyrogenics
	Throat	Pyrolytic Graphite	Pyrolytically deposited	Pyrogenics
5	Chamber	CGW Graphite	Molded monolithic	Union Carbide
	Throat	Tungsten-2% ThO_2	Isostatic powder pressed and sintered, extruded and forged	GE extruded TRW forged
6	Chamber	PTB (PT-0145)	All-graphite-pyrolyzed; resin impregnated	Union Carbide
	Throat	PTB (PT-0145)	All-graphite-pyrolyzed; resin impregnated	Union Carbide
7	Chamber	CGW	Molded monolithic	Union Carbide
	Throat	Hot Bonded Graphite	Hot pressed PG foil	Union Carbide (HTM)
8	Chamber	CGW Graphite	Molded monolithic	Union Carbide
	Throat	CGW Graphite	Molded monolithic	Union Carbide

Unclassified

(U) Tungsten, with 2% thoria addition, was selected for throat insert evaluation as a result of its good performance in the high temperature hydrogen fluoride laboratory environmental tests. The addition of 2% ThO provides several performance improvements, such as--higher elevated temperature strength, much higher recrystallization temperature, markedly greater resistance to gain growth at very high temperatures, and improved machinability. At elevated temperatures (above 4500°F), there is a significant improvement in strength. Also the recrystallization of tungsten is retarded with ThO_2 addition, resulting in a smaller grain size when recrystallization does finally occur. During another TRW program, tungsten was evaluated in a cyclic heating condition. A "germination effect" in unalloyed tungsten was observed during which cyclic heating and cooling under restraint caused a blow-up of the grains to a very large size. The addition of ThO_2 resulted in no grain blow-up. Although there is no data to indicate that one grain condition is definitely better than the other, it is generally conceded that a finer grain structure is more desirable in any refractory metal structure.

(U) Table IX lists available physical properties of the various materials selected for the subscale nozzle assemblies. Properties such as thermal conductivity, specific heat, and density are required to permit thermal analyses for predicting liner material temperatures and designing for proper support materials of adequate section thickness. In addition to these properties--material strength, modulus of elasticity, and thermal coefficient of expansion are necessary for stress analyses to predict insert performance (under stress) throughout a firing cycle, and thus permit development of proper insert designs. For certain materials and designs, accurate and reliable property data is more necessary. For example, materials of very high thermal conductivity (or very low, depending upon material and orientation; i.e.: pyrolytic graphite) can present critical design problems. High conductivities in the radial direction (perpendicular to nozzle axis) require characteristics in the support materials, such as--higher temperature capability, increased section thickness, and/or lower thermal conductivity. Conversely, lower thermal conductivity in the liner materials (radially) can mean excessive surface temperatures with consequent higher material loss rates due to high temperature reaction.

(U) For the prestressed design, accurate data for physical properites such as thermal coefficient of expansion, thermal conductivity, modulus of elasticity and strength were required to establish the proper stress balance between the throat insert and its supporting components at all times during a complete thermal cycle.

(U) In instances where throat inserts were designed with adequate ramp support angles for retention, and the insert material properties do not differ greatly from those of other supporting materials used in nozzle construction, accurate knowledge of physical properties and their variation with temperature is not critical. Also, some properties--such as density, and Poisson's Ratio--do not change significantly with temperature, so that knowledge of room temperature values is frequently sufficient. Indications of the variations and the relative reliability (estimated values where experimental data is not available) of the various physical properties for the materials utilized in the chamber and nozzle throat areas are indicated in Table IX.

Table IX (U) Typical Physical Properties of Liner Materials

Material		Density g/cc R.T.	Tensile Strength psi X 10^3 R.T.	5000°F	Mod of Elasticity psi X 10^6 R.T.	4000°F	Poisson's Ratio R.T.	Thermal Cond Btu-ft/ft^2/hr/°F R.T.	1500°F	Thermal Coef. of Expansion in/in/°F X 10^{-6} R.T.	2000°F	Specific Heat Btu/lb/°F R.T.	1800°F
CSW Graphite	With Grain	1.82	2	3.1 E*	1.75		--	65	30 E	1.2	2.0 E	.17 E	.42 E
	Across Grain		1.8	2.7 E	1.20			50	25 E	1.9	2.7 E		
Pyrolytic Graphite	"c" direction	2.2	0.4	0.2	--	--	0.24	0.54	0.72	7.2	13.6	.23	.48
	"a-b" direction		13	45	4.25	2.7		234	132	0.7	0.8		
Hot-Banded Grafoil	"c" direction	1.78	0.1	--	--	--	--	0.15	0.7	--	--	.23	.48 E
	"a-b" direction		2	--	0.55	--		234 E	110.0	--	--		
Carb-I-Tex 700	With Grain	1.44	5.5	--	1.3		--	1.67	2.5	0.6	--	.17 E	.42 E
	Across Grain		--	--	--		--	--	--	1.8	--		
FMI (FT-6145)	With Grain	1.56	8	--	0.9 E	--	--	--	--	0.6 E	--	.17 E	.42 E
	Across Grain		10	--	0.3 E	--		--	--	1.4 E	--		
Carbon Cloth Phenolic	With Flies	1.42	18	--	3.2	--	--	.33 (virgin)	0.27 (char)	6-11	--	.29 (virgin)	0.25 (char)
	Against Flies		1 E	--	--	--	--	.25 (virgin)	--	20-50	--		
TaC (Hot pressed)		14.4	30-50	--	55 E	--	0.17	12.8 E	22 E	3.5 E	3.7 E	.045	.06
Hypereutectic HfC (arc cast)		10.0	11	12 E	48	16	--	--	--	--	--	.186	.26
Tungsten - 2% ThO_2		18.8	110 E	3 E	60 E	37 E	--	75	70	1.5 E	2.4 E	.03 E	.03 E

Unclassified

* E - Estimated

c. Design Analysis

(U) The basic design employed in all subscale thrust chambers was a heat sink concept. The basic configuration is presented in Figure 6. The injector and thrust stand mounting flange are shown.

(U) The thrust chamber internal dimensions are sized for two chamber pressures 150 and 200 psia. The throat diameters are 0.817 and 0.707 inches respectively. The throat radius of curvature was approximately equal to the throat diameter. The nozzle convergence and divergence half angles are shown. The chamber diameter and length were sized based upon injector and performance considerations.

(U) Each of the eight thrust chamber designs fabricated is presented in Figure 7 through 14. Thermocouple location and designation is indicated in each figure. Materials designated by number in these figures are presented in Table X. Units S/N 1 through S/N 6 are designed for a chamber pressure of 150 psia. Units S/N 7 and 8 are designed for 200 psia chamber pressure.

(U) Units S/N 1 and 2 (see Figures 7 and 8) employed a chamber extension between the injector and thrust chamber. This section was added to the first two units tested to examine the affect on combustion performance of an increased chamber volume. Since it appeared that there was a negligible effect on combustion performance, the shortened chamber was used for all subsequent tests (see Figure 6).

(U) As presented previously, the basic intent of the subscale thrust chamber evaluation program was to examine liner material performance in rocket motor firings. For this reason, and for cost effectiveness, simple cylindrical or conical shapes were utilized where possible. The basic design for each unit employed a relatively simple heat sink design approach. Thus, the liner materials were designed to be installed in a conservatively sized insulator. The insulation, in each case, was silica phenolic, or a silica phenolic and carbon or graphite phenolic composite as required. Silica phenolic was utilized where it was assured that insulation temperatures would not exceed 3000°F, the approximate melting temperature of silica. Where insulation temperatures were predicted to exceed the melting temperature of silica, carbon of graphite phenolic insulation was provided.

(U) The steel shell was a cylindrical-shaped structure with bolted end plates at each end. The relatively simple design permitted the thrust chamber assemblies to be easily installed into the reusable steel. The heavy walled construction permitted thermocouple packing glands to be threaded into the wall.

(U) With the simplified design approach, a minimum of analysis was required for each design. These analyses are discussed subsequently. In most cases, only heat transfer analyses were performed to predict the insulation temperatures and the liner surface temperatures. Where excessive thermal expansion was predicted, expansion gaps were provided. Thermocouples were provided at selected locations to check the predictions. In the design of units S/N 1 and 4, analyses were more detailed because of heat sink design and structural considerations.

(1) Subscale Chamber S/N 1

(U) Subscale chamber S/N 1 incorporates a prestressed throat insert configuration. Prestressing expands the list of candidate materials to include

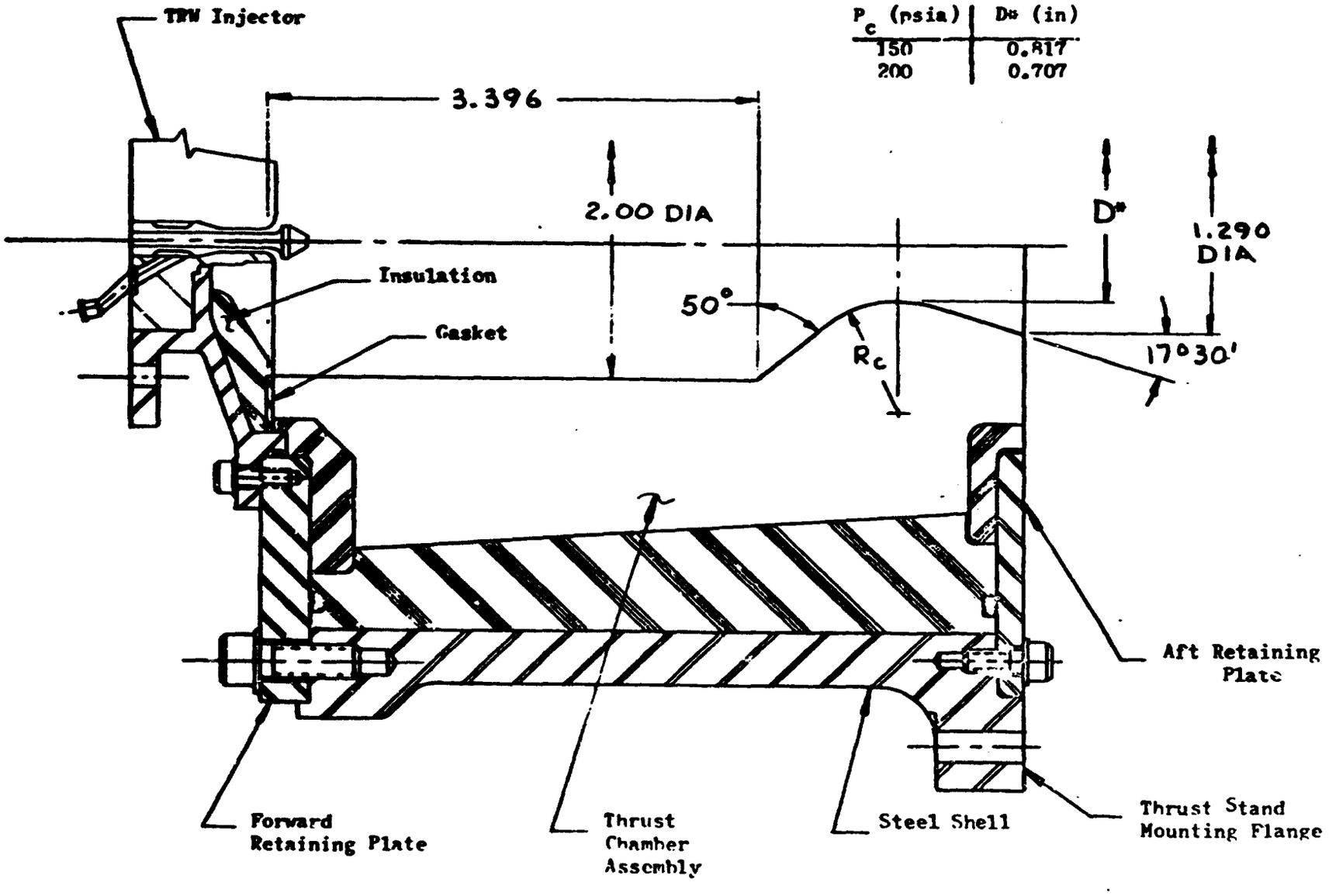

Unclassified

FIGURE 6 (U) Subscale Thrust Chamber Design

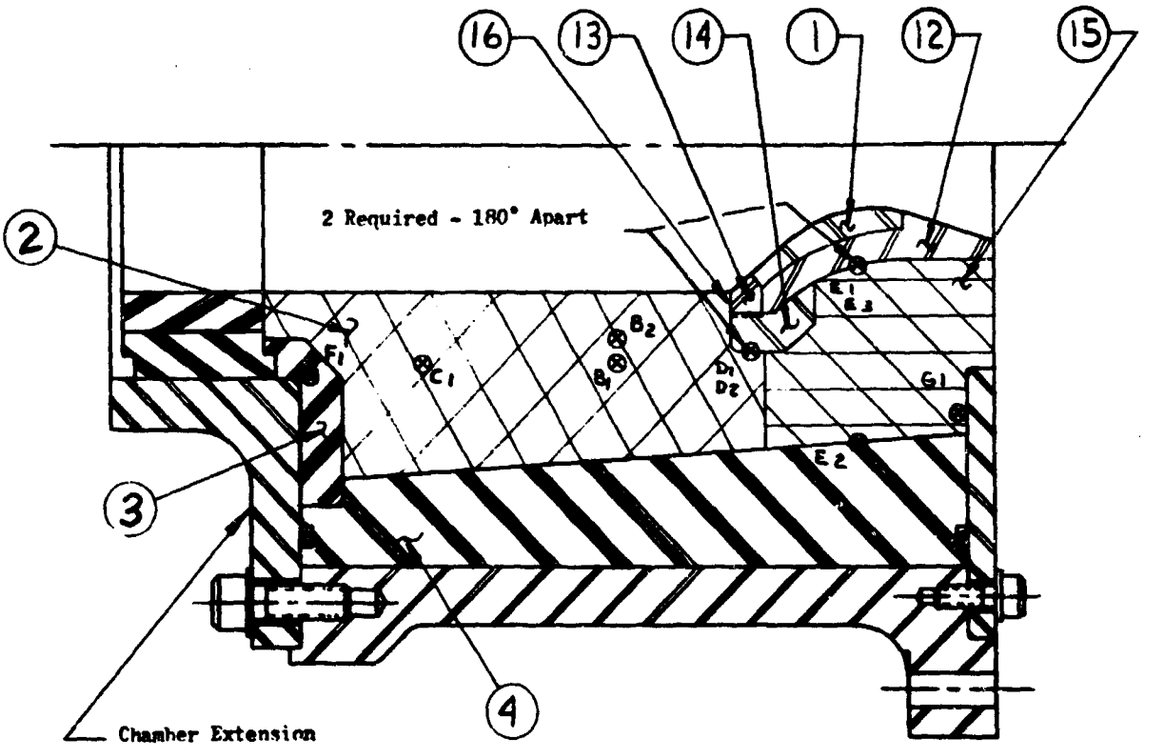

Unclassified

FIGURE 7 (U) Subscale Thrust Chamber S/N 1

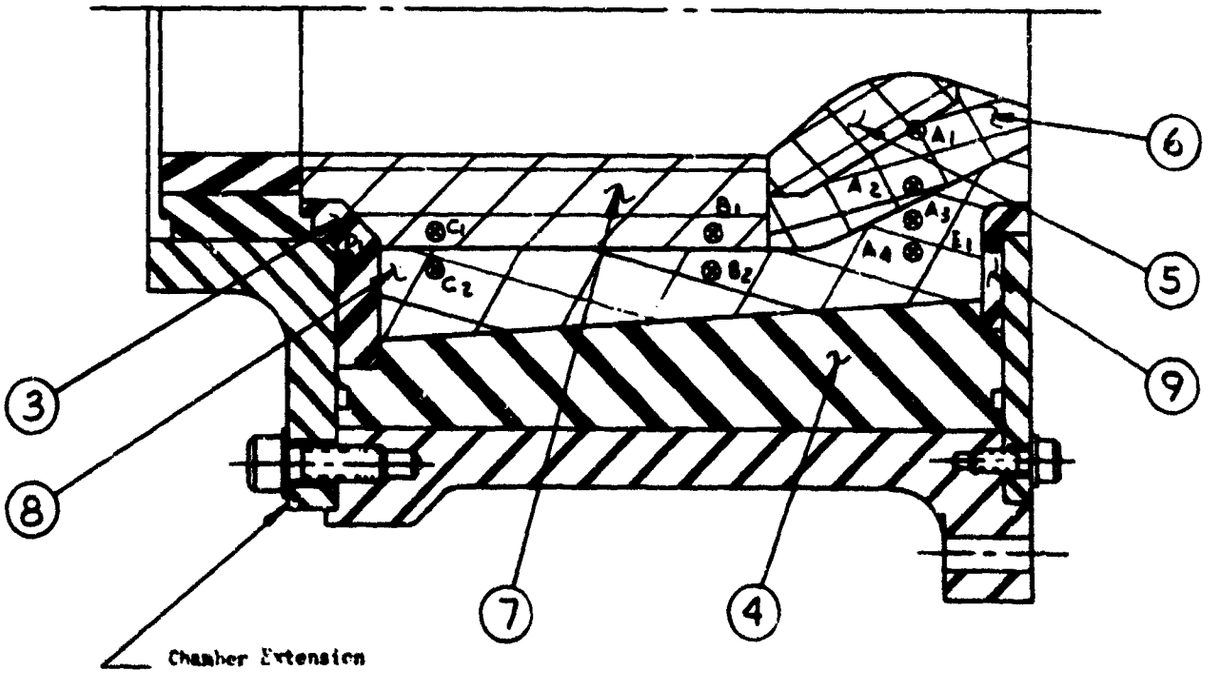

Unclassified

FIGURE 8 (U) Subscale Thrust Chamber S/N 2

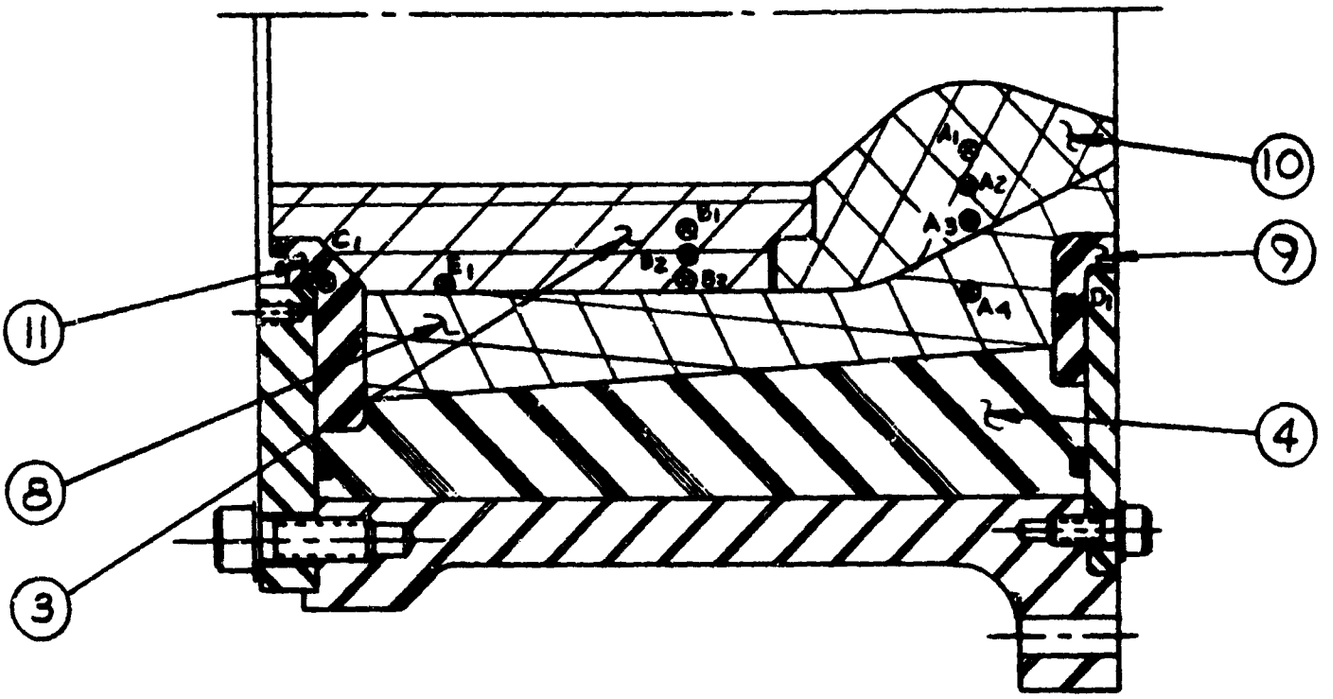

Figure 9 (U) Subscale Thrust Chamber S/N 3

Unclassified

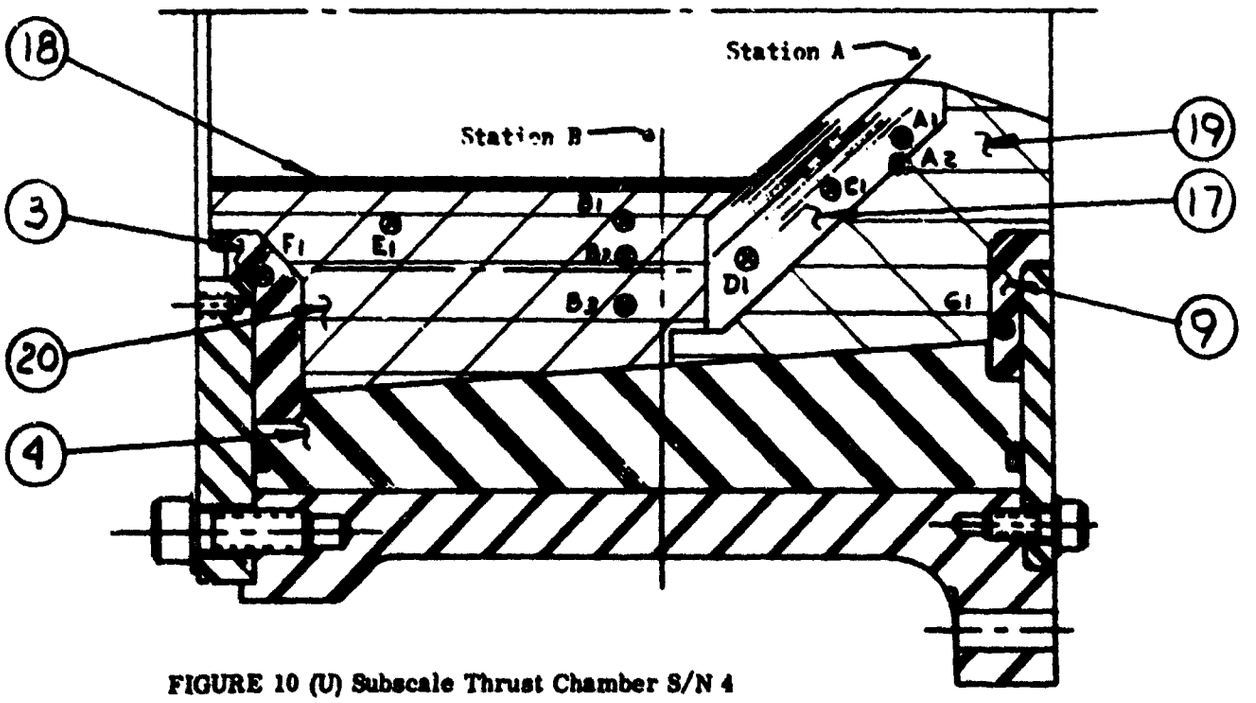

FIGURE 10 (U) Subscale Thrust Chamber S/N 4

Unclassified

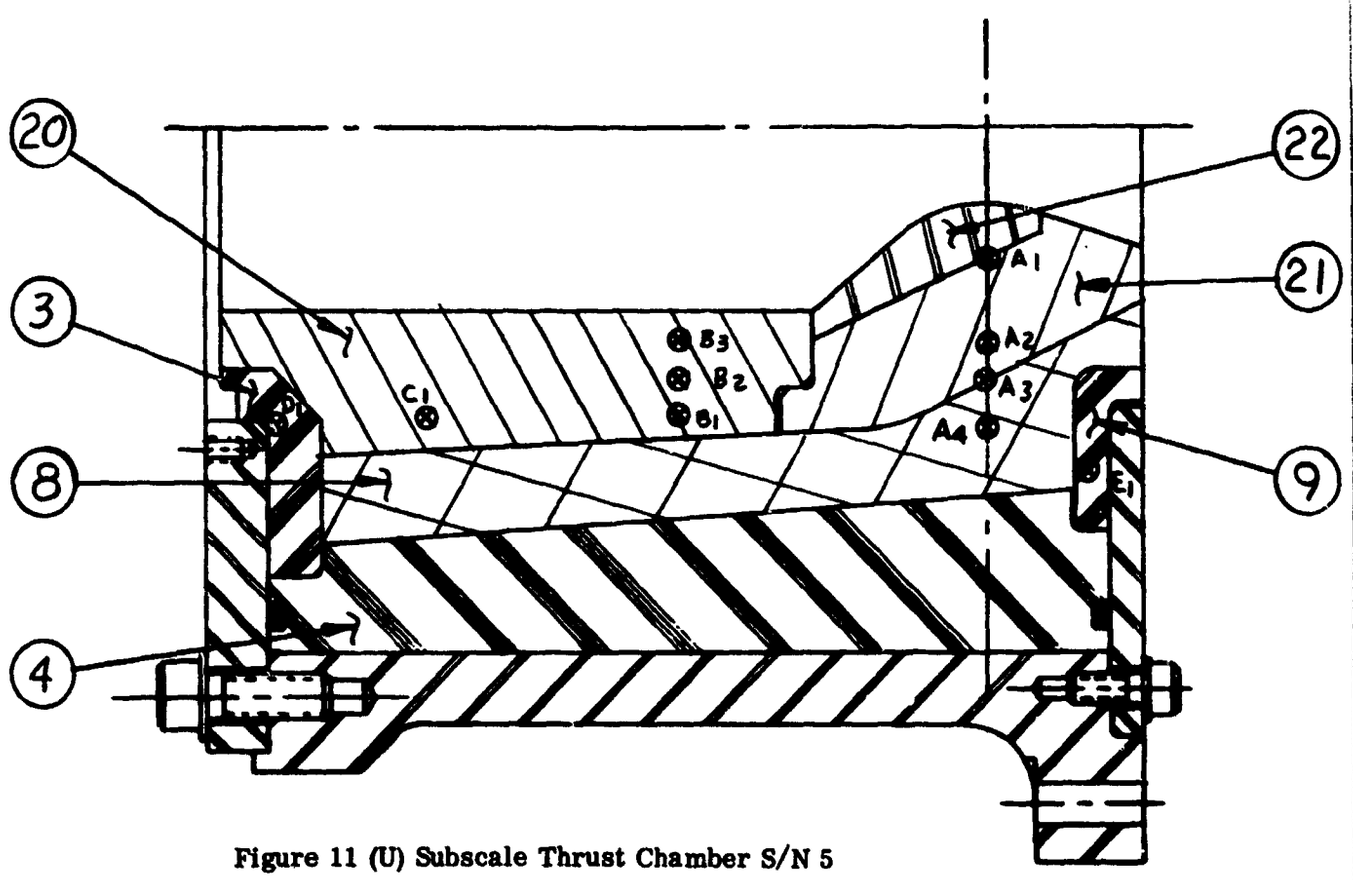

Figure 11 (U) Subscale Thrust Chamber S/N 5

Unclassified

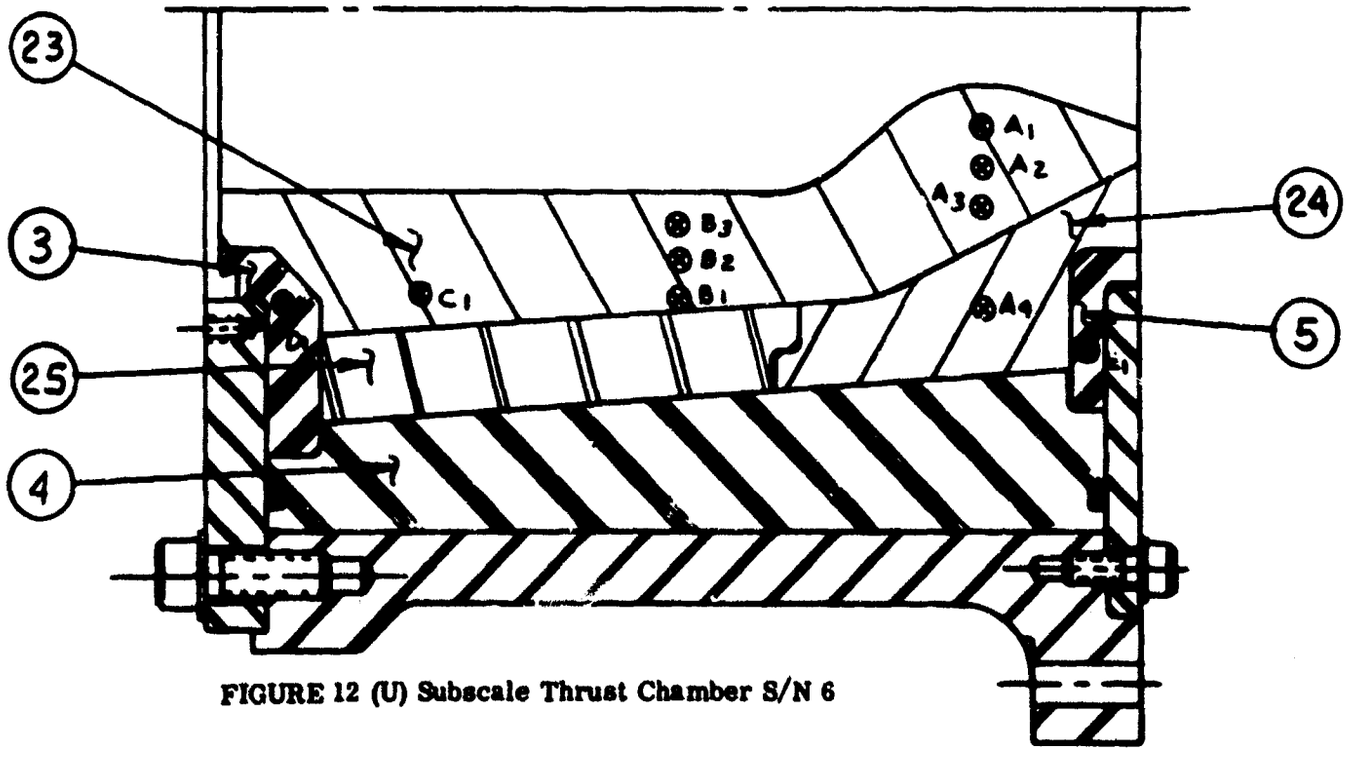

FIGURE 12 (U) Subscale Thrust Chamber S/N 6

Unclassified

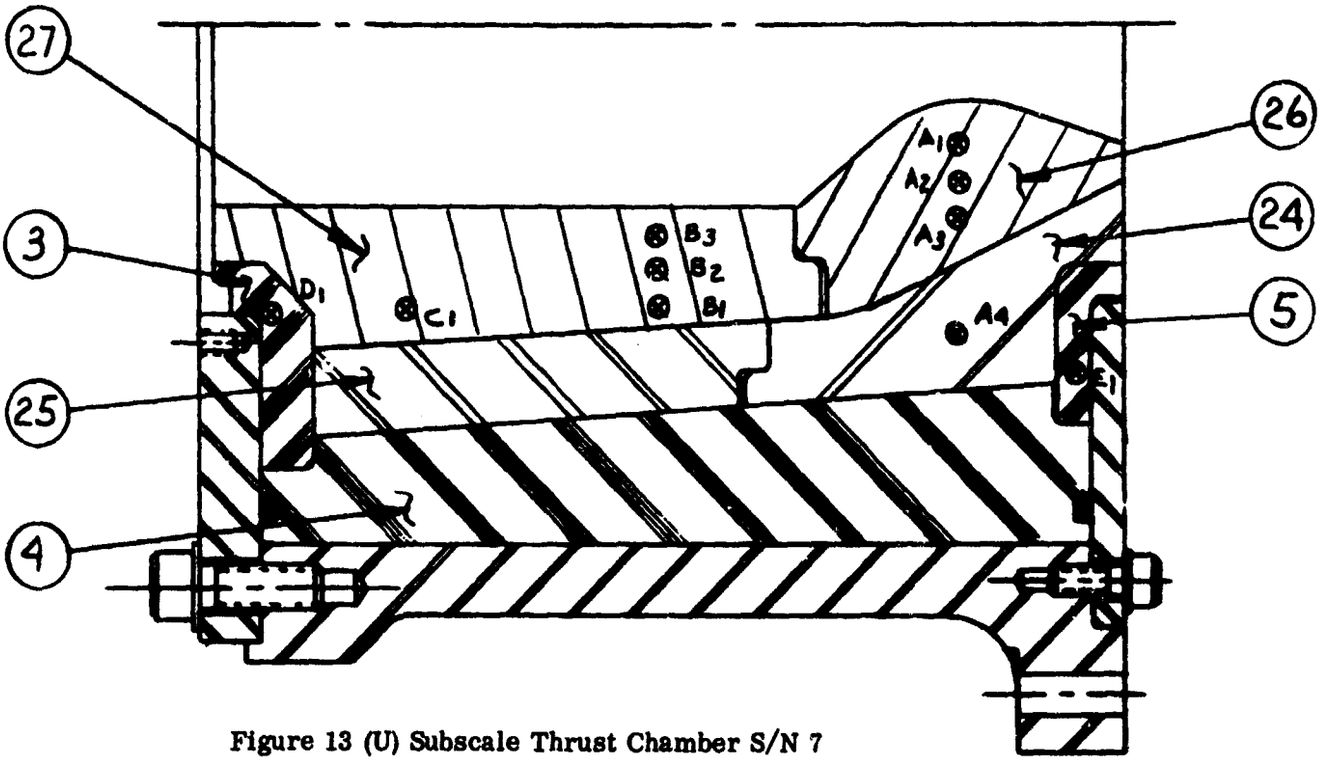

Figure 13 (U) Subscale Thrust Chamber S/N 7

Unclassified

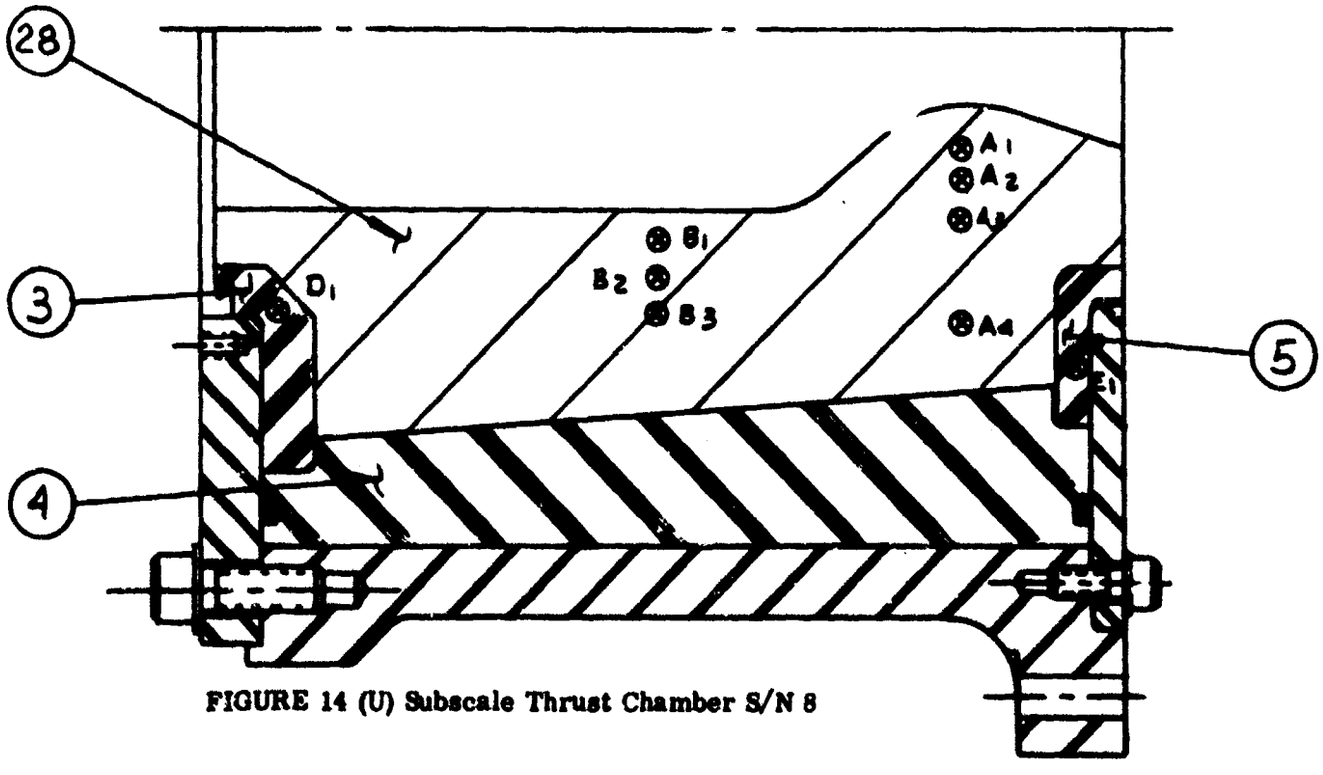

FIGURE 14 (U) Subscale Thrust Chamber S/N 8

Unclassified

TABLE X (U) Subscale Thrust Chamber Materials

Unit S/N	Throat Assembly	Chamber	Insulation
1	TaC throat insert (1) Tungsten prestressing ring (12) TZM axial insert retainer (13) Ta-10W axial insert retainer (14) Carbon brick support (15) Tantalum washer (16)	Carbon Cloth (2)	Forward insulation (3) and shell insulation (4) are silica cloth phenolic.
2	Hypereutectic HfC throat insert (5) ATJ graphite insert (6)	CGW graphite (7)	Chamber and throat liner support (8) are carbon cloth phenolic. Forward insulation (3), rear insulation (9) and shell insulation (4) are silica cloth phenolic.
3	Carb-I-Tex 700 prepyrolyzed composite (10) (Ply orientation perpendicular to centerline)	Carb-I-Tex 700 pyrolyzed composite (11) (Ply orientatation parallel to centerline)	Same as Unit S/N 2
4	Pyrolytic throat insert (17) KJB carbon brick support (19)	Pyrolytic sleeve (18) CGW graphite heat sink (20)	Same as Unit S/N 2
5	Tungsten with 2% ThO_2 (22) CGW graphite insert (21)	CGW graphite (20)	Same as Unit S/N 2
6	PTB Prepyrolyzed Graphite Phenolic (23)	Same as throat	Carbon Cloth Phenolic (24) Graphite Cloth Phenolic (25)
7	Grafoil (26)	CGW graphite (27)	Same as Unit S/N 6
8	CGW graphite (28)	Same as throat	Same as Unit S/N 1

Unclassified

Note: Numbers in ( ) refer to components presented in Figures 7 through 14.

not only those materials which are chemically attractive but also those that may be thermal shock sensitive. During t' e design analysis, four basic physical throat configurations were considered to determine the optimum design.

(U) Composite wall material combinations which were most promising included TaC, W, Ta - 10W, carbon, silica phenolic; and TaC, Ta - 10W SGS, Ta - 10W, carbon, silica phenolic. However, the latter combination could not be considered in the final analyses because the SGS (stabilized grain size) grade Ta - 10W could not be procured in time to meet the delivery schedule of the insert.

(U) Heat transfer and stress analyses were performed for the four cases at the throat. The heat transfer analyses were performed utilizing a TRW Systems computer program. This program is a transient conduction program capable of evaluating the temperature profiles in up to six integral components of different materials. Both cylindrical and flat plate geometries may be handled. Temperature dependent thermal properties (specific heat and thermal conductivity) are considered. Arbitrary heating conditions, including both radiation and convection, may be considered in both boundaries.

(U) The prestressing stress analyses were performed using a TRW Systems newly developed computer program. The analysis was initiated in company sponsored investigations and later defined and programmed under Contract AF 33(615)-1662, "Thermal Shock Characteristics of Refractory Materials." The stress analysis is described in detail in Air Force Report No. AFML-TR-65-363.

(U) Briefly, the stress program computes the stresses and strains induced in long hollow cylinders and thin hollow discs by arbitrary radial temperature gradients. Plastic as well as elastic materials behavior can be included, and the materials may be anisotropic in the r,θ, and z directions (cylindrical coordinate system). All of the materials properties may be temperature dependent. Internal and external pressures can be accommodated, and end forces or the axial stresses or strains can be specified in several different ways. The program will also handle two concentric cylinders of different materials. The latter features are utilized in computing the stresses of the prestressed insert and its prestressing elements.

(U) The design of the prestressed insert assembly is shown in Figure 7. With this configuration, three different throat assembly materials are exposed to the exhaust stream in locations representing three widely varying exhaust environments. A brief discussion is given in the following for justification of material selections and functional component requirements.

(U) Tantalum carbide was originally proposed for the throat insert and subsequently justified as a potential insert candidate based on its reactivity behavior. None of the other materials evaluated, which possessed superior corrosion resistance, would seem to warrant the attention of prestressing at this stage of development.

(U) Graphite, tungsten, tantalum, and other alloys have melting temperatures and strengths of the right order for use as prestressing elements (rings). Other considerations being comparable, tungsten was chosen in this application because it was the only material readily available in the proper size.

(U) The function of the axial insert retainer is to keep the TaC insert from moving forward along the contour of the tungsten prestressing ring. The parts are held together by the threaded joint as shown. Item 13 (Figure 7), the TZM axial insert retainer, which is held by the tapered section on the back side of Item 12, the prestressing ring.

(U) The threaded joint restricts the selection of retainer materials to only several refractory metals which can be threaded and have sufficent strength and ductility to insure mechanical integrity of the threads. The greatest restriction is imposed on Item 13 (Figure 7) which is exposed to the exhaust stream.

(U) The intermediate back-up material between the prestressed insert and silica phenolic liner is carbon brick. The insulative characteristics of this material make it suitable for use in this application to limit the I.D. surface temperature of the silica phenolic to 3000°F for firing durations up to 300 seconds.

(U) The temperature distributions for times up to 300 seconds are given in Figure 15. These data were obtained from a one-dimensional heat transfer analysis performed at the plane of minimum throat diameter. Figure 16 shows the circumferential stresses which occur at the inner and outer surface of the TaC insert. These stresses were calculated at the plane of minimum throat diameter, assuming the conditions of plane stress. The subscripts a and b represent the locations noted at the top of Figure 15. Three different geometric constraints are included for comparison to demonstrate the magnitude of reduction is stress gained by prestressing. σ_a and σ_b represent the circumferential stresses at radii r = a (compression) and r = b (tension) when the TaC insert is not prestressed. σ_a (p) and σ_b (p) are the resulting stresses when prestressing occurs from only the differential thermal expansion between the TaC insert and the tungsten prestressing ring. σ_a (p 0.0005) and σ_b (p 0.0005) represent the same stresses when an initial radial interference of 0.0005 inches is used.

(U) From Figure 16, it is seen that the maximum stresses occur between 1 and 5 seconds after engine start-up. Without prestressing, the maximum tensile hoop stress (σ_b) is 146 psi at 1.5 seconds which decreases rapidly to approximately 40 ksi at 20 seconds. With prestressing, the maximum tensile hoop stress σ(p 0.0005) is reduced to approximately 30 psi at 1.5 seconds. At times greater than 20 seconds, the influence of prestressing on the stresses in the TaC insert is very slight. Fortunately by this time, the large thermal gradient and resulting thermal stresses have decreased to levels where prestressing is not required.

(U) At longer times, the problem is to avoid plastic flow in the prestressing ring rather than to reduce tensile hoop stresses in the TaC. In Figure 16, σ_c (p 0.0005) denotes the tensile hoop stresses on the back side of the tungsten ring. Plastic flow starts to occur at about 5 seconds with a plastic component of strain of approximately 0.08 percent. Flow continues to occur during the remainder of the firing to a maximum plastic strain of approximately 0.4 percent.

(U) As a consequence of the plastic deformation in the prestressing ring, the part does not return to its original configuration after cool down, and therefore, may not be fired a second time with any assurance of success.

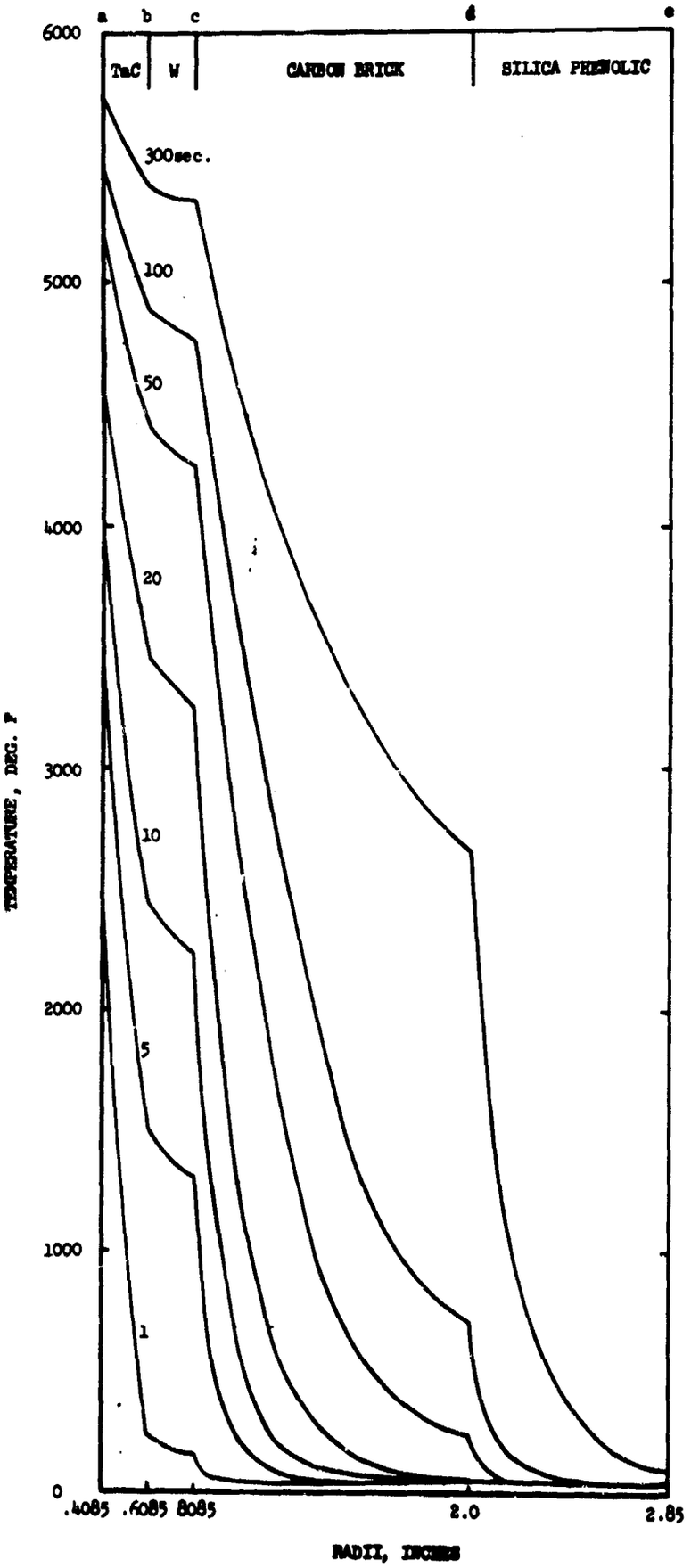

Unclassified

FIGURE 15 (U) Temperature Profile for Unit S/N 1

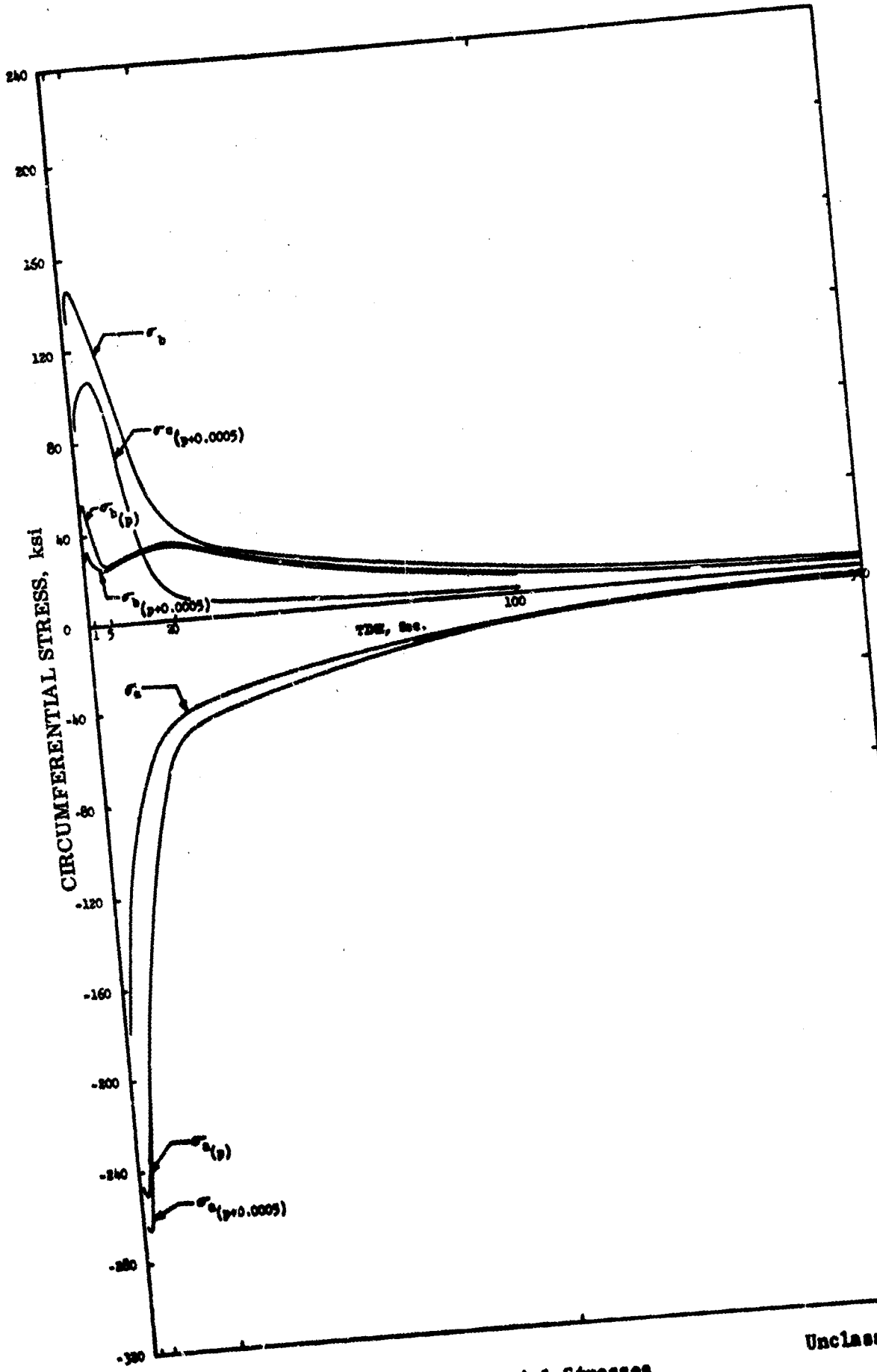

FIGURE 16 (U) Circumferential Stresses

(U) In the preliminary analyses, Ta - 10W SGS was considered for the prestressing ring. At the time noted above when tungsten begins to flow, the Ta - 10W had expanded away from the TaC and plastic flow did not occur. Thus, multiple firings could have been performed with this design.

(U) In the thermal stress analysis, the TaC is treated elastically since mechanical property data (stress - strain behavior) over the appropriate temperature range were not available. As it was, modulus of elasticity versus temperature had to be extrapolated from data at room temperature. For this reason, it was possible that the stresses in both the TaC and W would be less than predicted, which would increase the probability of a successful firing. The lack of property data for TaC was undoubtedly responsible for the greatest uncertainty in the thermal stress calculations.

(U) Both the elastic and plastic stress-strain behavior of the tungsten were considered in the thermal stress calculation of the insert. The property data used were taken from the literature and are shown in Figures 17 and 18. By accounting for the plastic behavior of tungsten in the thermal stress analysis, it was possible to predict the time during firing when plastic deformation of the prestressing ring would occur.

(U) Carbon cloth phenolic tape oriented 45° to the chamber centerline was used as the chamber liner. Insulation was silica phenolic.

(U) In view of the assumptions which were necessary in performing the thermal stress analyses and the uncertainties in fabricating perfectly mating parts (TaC/W), for the curved back design, it was decided that the insert be fired in a simplified duty cycle. Hopefully, answers to some of the questions which cannot be predicted by the analysis would come from the results of the post firing analysis of the insert. Thus it was desired to maintain the thermal history in firing as uncomplicated as possible. The single pulse firing duration of 100 seconds was planned.

(2) Subscale Chamber S/N 2

(U) Unit S/N 2, (shown in Figure 8) has a throat insert of hypereutectic hafnium carbide (0.375 in. thick) backed up by National Carbon ATJ Graphite (0.5 in. thick) and insulated with carbon phenolic and silica phenolic. Carbon phenolic was employed where insulation temperatures were expected to exceed 3000°F. Silica phenolic was used elsewhere. The chamber consists of National Carbon CGW graphite, insulated by carbon and silica phenolic. The predicted temperature distribution is presented in Figure 19 for this configuration at the throat location. A maximum duration of 175 seconds was determined to be acceptable (the planned test pulse duration). Predicted interface temperatures and char propagation in the insulation was sufficiently low that no structural difficulties were predicted.

(U) Temperature variations were calculated for this and subsequest designs using a TRW One-Dimensional Heat Transfer Program. This program has compiled in it a series of unique abilities. All heat transfer equations have been derived in cylindrical coordinates to permit investigation of circular sections varying in diameter from a fraction of inch to several feet in diameter. Temperature dependent thermal properties such as specific heat, density, and thermal conductivity have been incorporated for both materials of construction and propellant gases.

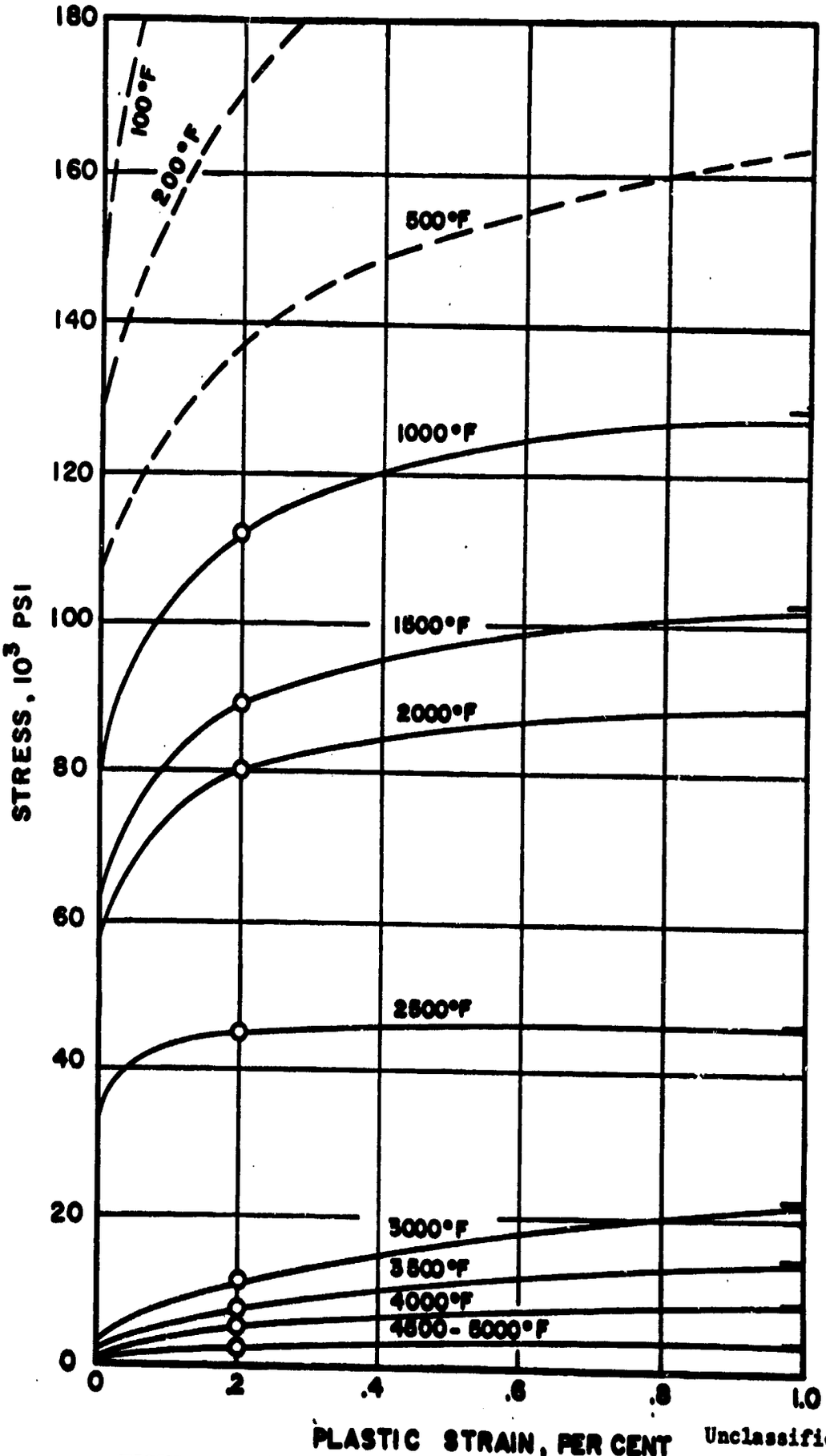

Unclassified

FIGURE 17 (U) Stress-Strain Behavior of Tungsten

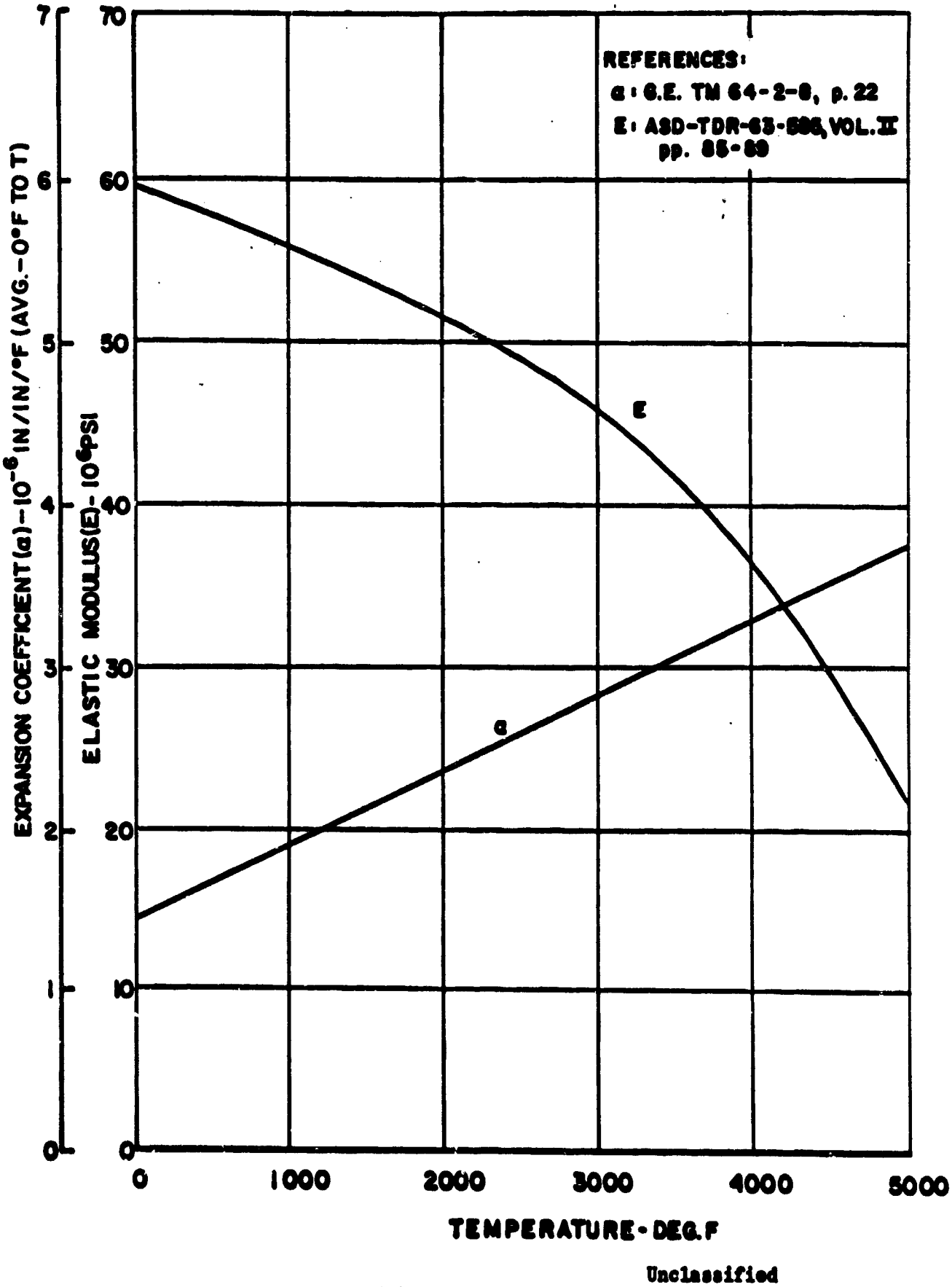

Unclassified

FIGURE 18 (U) Properties of Tungsten

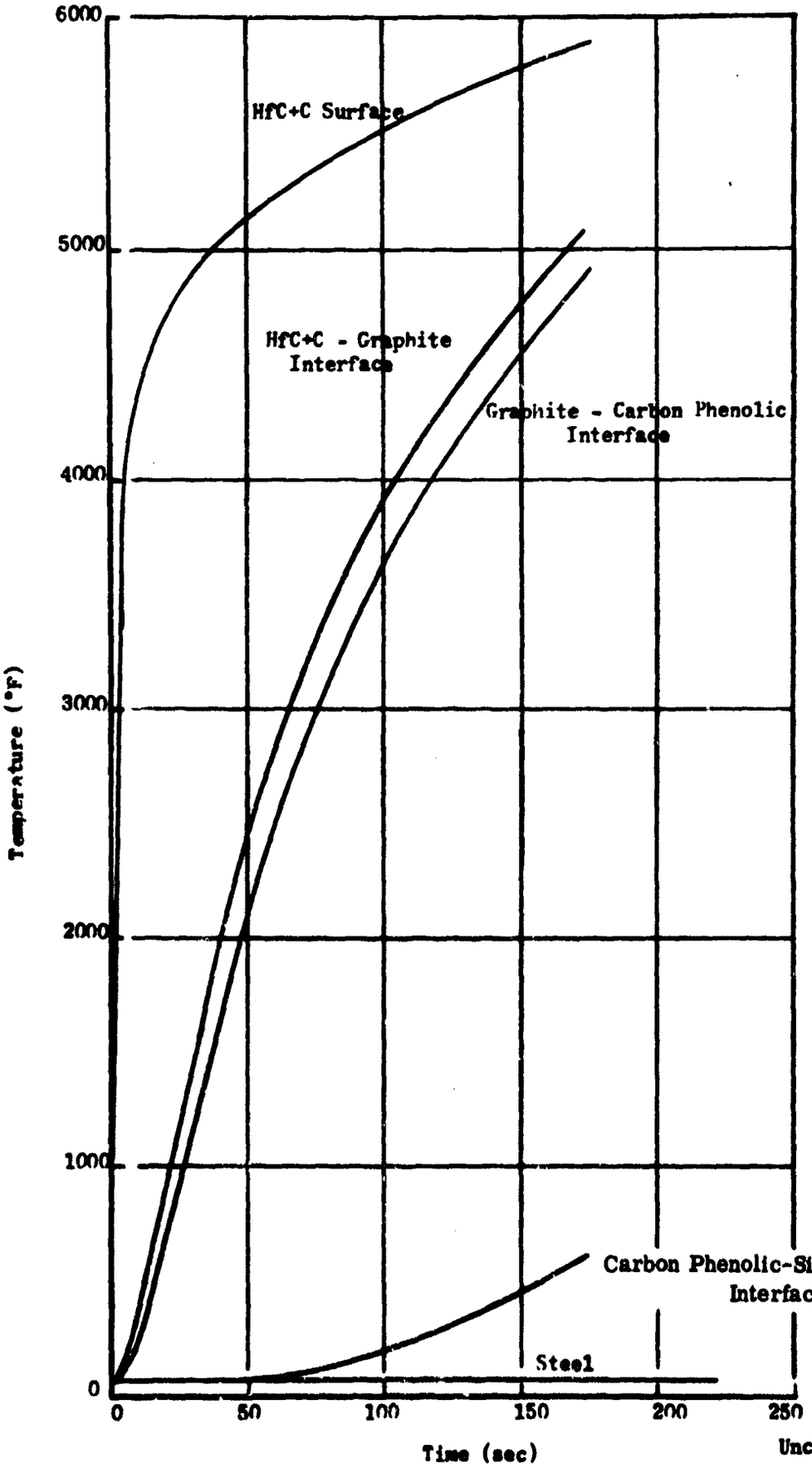

FIGURE 19 (U) Temperature Distribution at Throat for Unit S/N 2

(3) Subscale Chamber S/N 3

(U) The throat insert and chamber liner for unit S/N 3 were made from Carb-I-Tex 700 (see Figure 9). In the throat region, ply orientation was perpendicular to the nozzle centerline. In the chamber region, the planes of the Carb-I-Tex 700 were oriented 90° to that of the throat insert such that each plane is parallel to the chamber centerline.

(U) The predicted temperature history for the Carb-I-Tex 700 insert configuration at the throat location is shown in Figure 20. High inside surface temperatures were predicted for the 175 second firing pulse. Predicted interface temperatures and char propagation in the insulators is sufficiently low so that no structural difficulties were anticipated.

(4) Subscale Chamber S/N 4

(U) The configuration of subscale thrust chamber S/N 4 is shown in Figure 10. In this configuration, a pyrolytic graphite throat insert design was employed which utilized the anisotropic properties of the material to keep the throat surface temperature low. The a-b planes (planes of high thermal conductivity) are parallel to the throat inlet ramp. The chamber was lined with graphite to provide the heat sink for the throat insert. This configuration permits a much larger heat sink for a given thrust chamber envelope that one in which the more conventional graphite washers are employed in the throat region. The throat insert employed for this configuration was fabricated from bulk pyrolytic graphite. This material is a massive oriented pyrolytic graphite which can be fabricated in special shapes with thickness to radius ratios greater than 0.5. A thin-walled pyrolytic graphite tube (wall thickness approximately 0.040 inches) with the a-b planes parallel to the axis was employed to insulate the graphite heat sink from the combustion gases in the chamber.

(U) A one-dimensional heat transfer analysis was conducted for each station shown in Figure 10. The results of the analyses are presented in Figure 21 and 22. The heat sink analysis of the throat insert is shown in Figure 21. For this analysis, it was assumed that heat is conducted only in the direction shown in Figure 10 (Station A). As is shown, it is possible to keep the throat surface temperature below 5800°F for approximately 150 seconds of elapsed firing time. As discussed previously at wall temperature below approximately 5900°F, graphite appears to be more resistant to HF than many of the other refractory materials. The laboratory tests conducted firing this program have also indicated low HF reactivity with graphite. Thus, a heat sink design concept which would utilize a graphite material in the throat region and keep the throat surface temperature low is of interest for low erosion.

(U) Figure 22 presents a radial heat transfer analysis at Station B. This analysis was conducted to examine the insulating capabilities of the pyrolytic tube in the chamber. This analysis indicates that only a small amount of heat will be transferred to the chamber heat sink through the chamber wall.

(U) Although an exact prediction of temperature map for the design presented in Figure 10 is not possible by one-dimensional heat transfer analysis techniques, an order of magnitude was indicated. Since only a small amount of heat is transferred to the graphite heat sink through the chamber walls, it should provide a good heat sink for the pyrolytic graphite throat insert. The maximum temperature of the heat sink after a 175 firing pulse was expected to remain below 3700°F for the configuration shown.

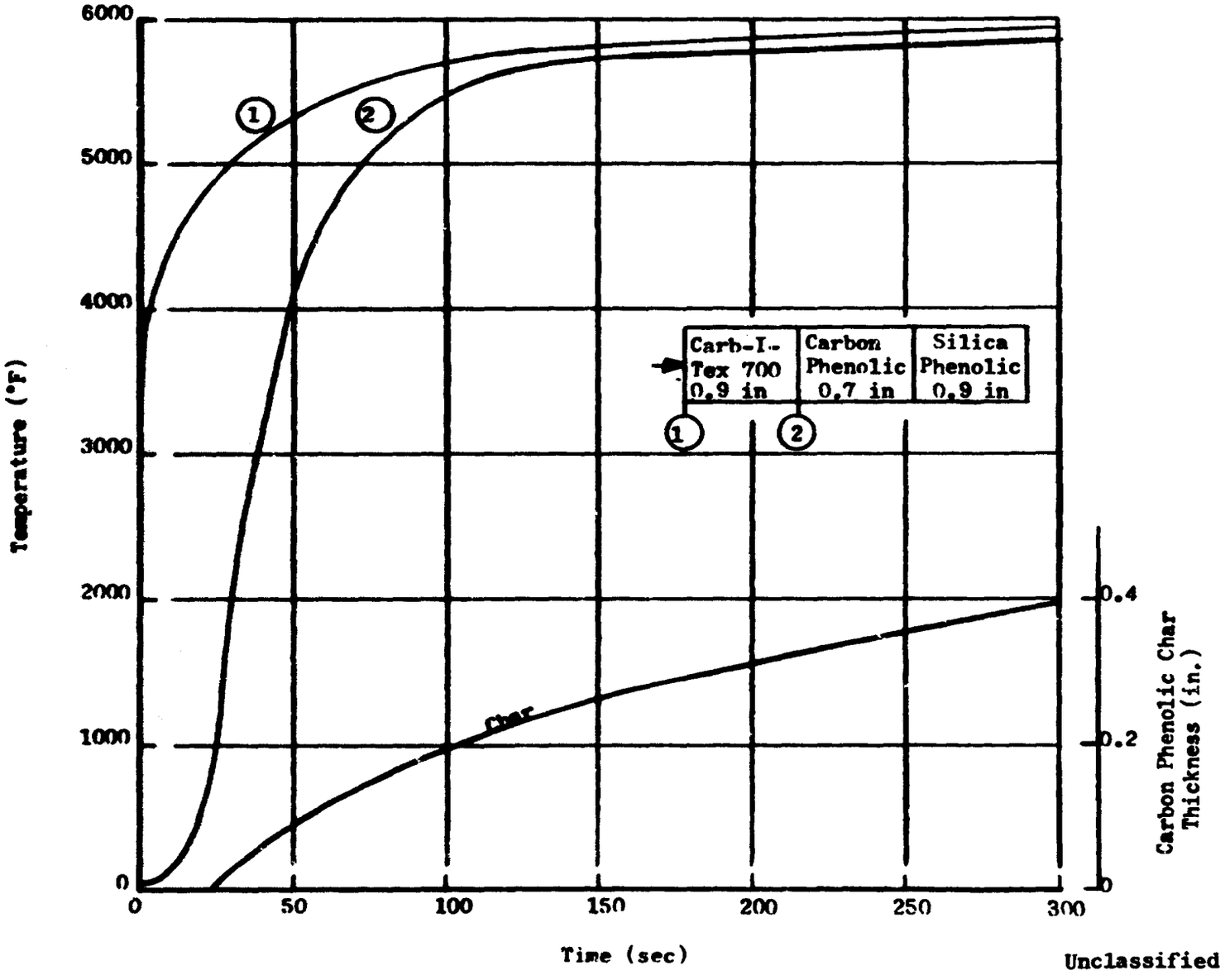

FIGURE 20 (U) Temperature Distribution at Throat for Unit S/N 3

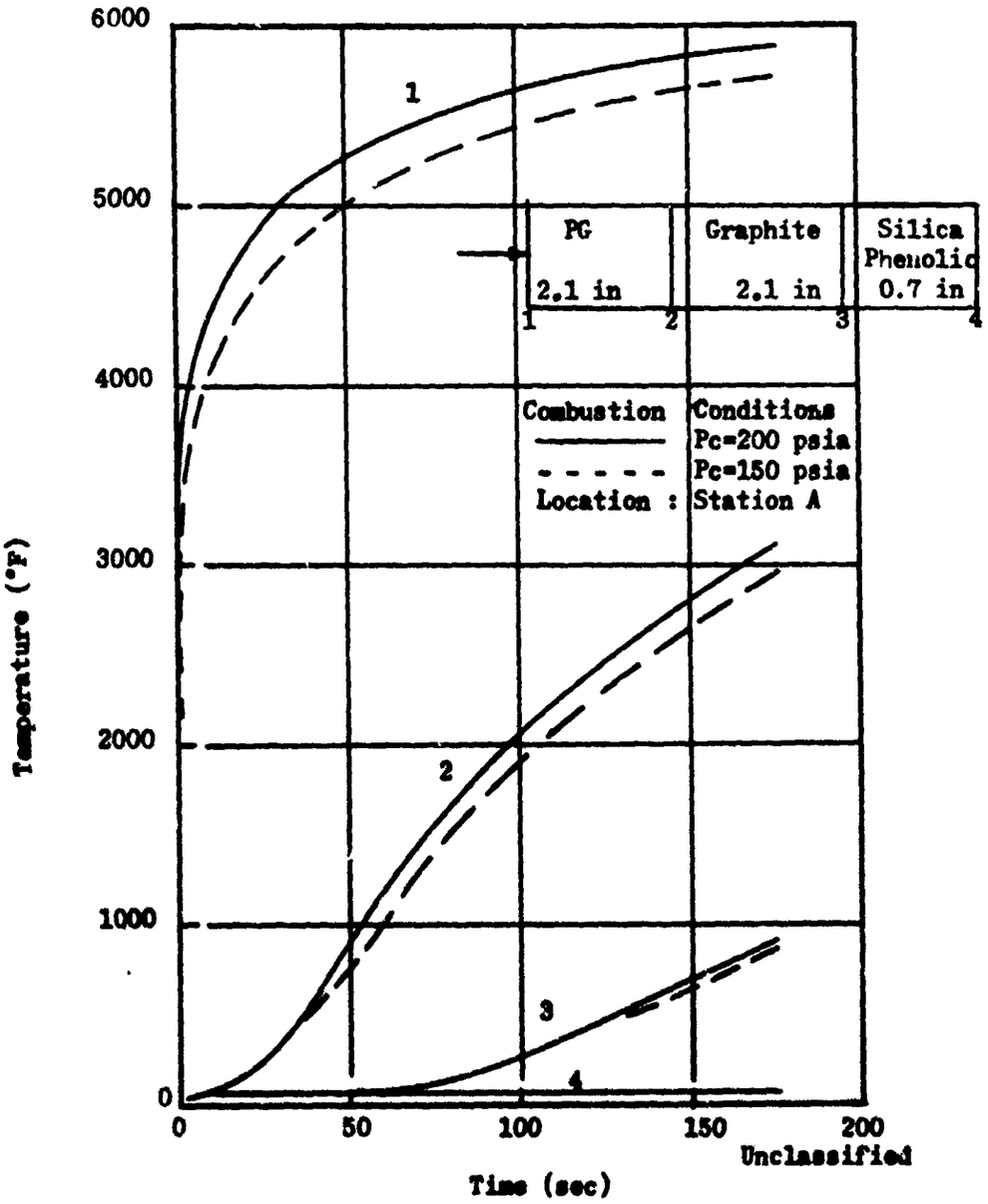

FIGURE 21 (U) Temperature Distribution at Throat For Unit S/N 4

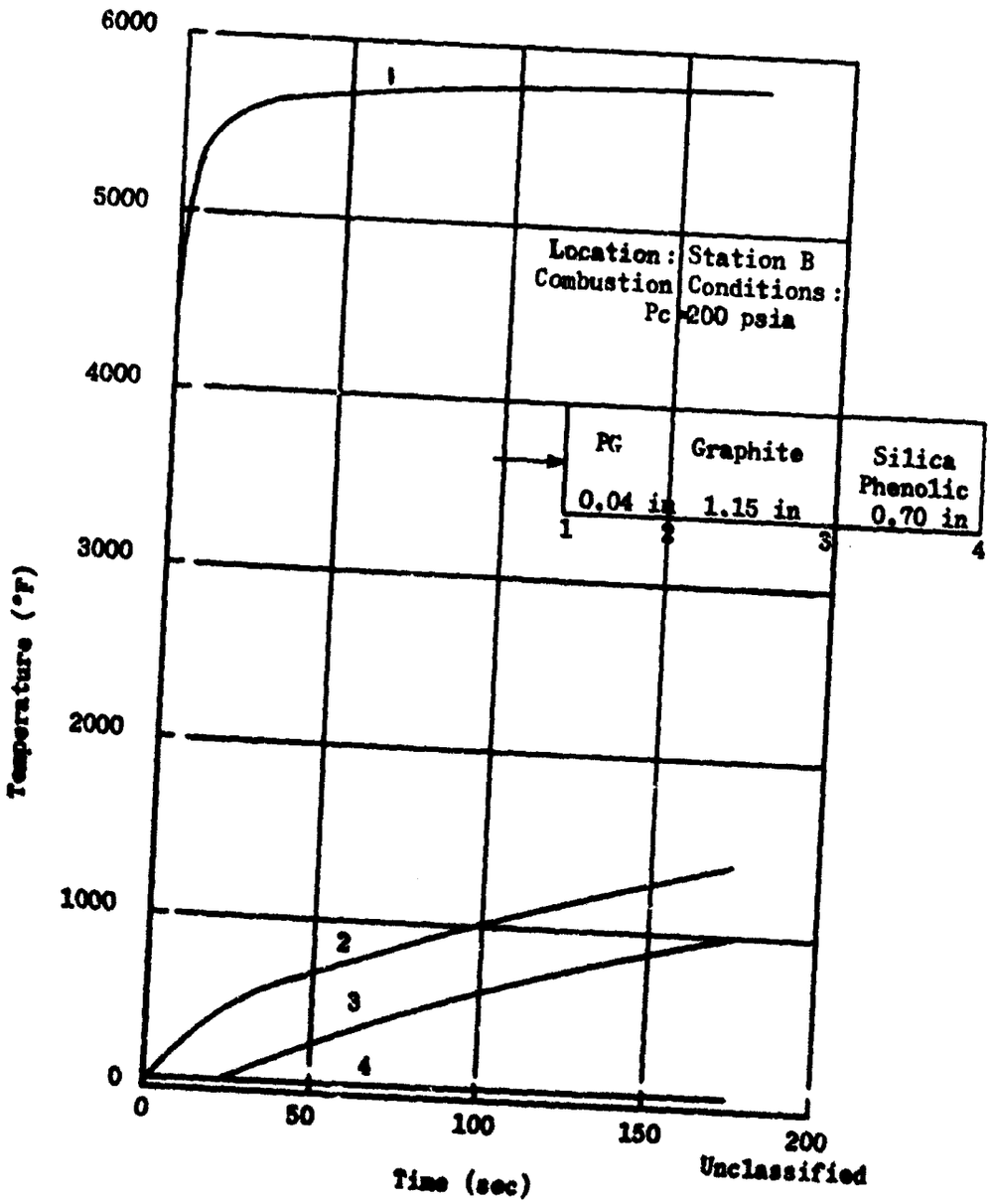

FIGURE 22 (U) Temperature Distribution in Chamber For Unit S/N 4

(U) A detailed stress analysis was performed at Station B (see Figure 16) to assure that stresses due to differential thermal expansion would nould not cause failure of the pyrolytic graphite sleeve. The TRW thermal elastic stress analysis computer program was used for the stress calculation. The maximum temperature gradient across the pyrolytic graphite sleeve was used for this calculation. The maximum temperature gradient was predicted to occur at approximately 10 seconds of elapsed firing time as shown in Figure 22. A maximum hoop compressive stress of approximately 24,000 psi was predicted by the elastic analysis at the inner surface of the pyrolytic graphite sleeve. This computed stress is greater than the allowable compressive stress for pyrolytic graphite in the a-b direction, (approximately 10,000 psi at 5000°F). However, the inner surface will be hot and ductile such that a material plastic flow will occur which will reduce the actual stress values below those computed on an elastic basis. These stresses computed on a plastic basis permit safe operation. All other values predicted by the elastic analysis (which is conservative) were well below the allowable stress for each material.

(U) The stability of the pyrolytic graphite sleeve was also investigated. A critical collapse (buckling) pressure of 460 psi was calculated at the maximum temperature gradient. The actual collapse pressure predicted by the thermal elastic stress analysis was 339 psi which is below the critical value. Again this is conservative, since the plastic yielding of the pyrolytic graphite sleeve at the inner surface will reduce the actual collapse pressure below that predicted by the thermal elastic analysis.

(5) Subscale Chamber S/N 5

(U) The configuration for subscale thrust chamber S/N 5 is presented in Figure 11. The throat insert material selected was tungsten with a 2% ThO_2 addition.

(U) A heat transfer analysis was conducted for the composite wall at the throat (see Station A, Figure 11). The results of the computation (150 psi, O/F - 2.0, steady state burst) are shown in Figure 23. Two different heat sink materials were used for the tungsten throat support in the computations. The first of these was bulk graphite (National Carbon CGW or ATJ); and the second pyrolytic graphite with a-b planes radial. With reference to Figure 23, it is apparent that their is no significant difference in expected surface temperature when using either material in this radial thickness range. The predicted tungsten insert temperature at times greater than 100 seconds is in excess of 5800°F (curve 1 and 4, and 2 and 5).

(U) The remainder of the cross section computation yields temperatures at the carbon-silica interface of 740°F at 175 seconds with the steel remaining at ambient temperatures (70°F). The carbon-phenolic will be almost completely charred under this condition.

(6) Subscale Chamber S/N 6

(U) Subscale thrust chamber S/N 6 incorporated National Carbon PTB pre-pyrolyzed graphite phenolic for the chamber and throat liner as shown in Figure 12. Carbon cloth phenolic, plies oriented 45 degrees to the chamber centerline, and graphite cloth phenolic were used as support materials in the throat and chamber regions respectively. Silica phenolic insulation was used

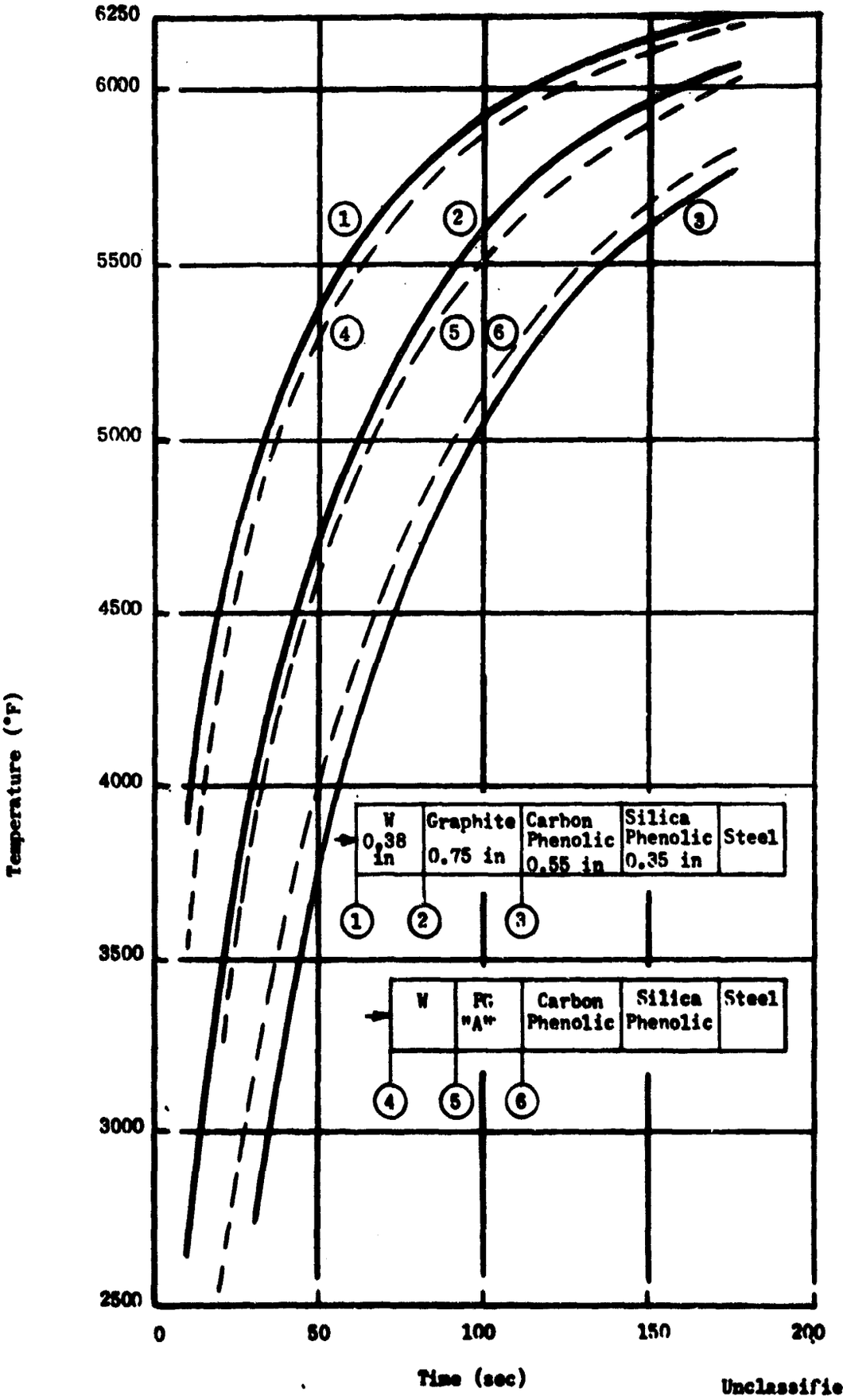

FIGURE 23 (U) Temperature Distribution at Throat for Unit S/N 5

between the support materials and the steel shell. The results of a heat transfer analysis conducted at the throat location is presented in Figure 24.

(7) Subscale Chamber S/N 7

(U) Unit S/N 7 was designed for a chamber pressure of 200 psia (see Figure 13). For this unit, a hot-bonded Grafoil tape structure fabricated by High Temperature Materials was used for the throat insert. Ply orientation, or a-b direction, was radial. High density graphite was employed for the chamber liner. The liner materials were supported in a manner similar to that employed in subscale thrust chamber S/N 6. Heat transfer analysis for the throat location was conducted and the results are presented in Figure 25.

(8) Subscale Chamber S/N 8

(U) Unit S/N 8 was designed for a chamber pressure of 200 psia to investigate the erosion characteristics of a high density monolithic graphite in the throat. A one-piece construction employing National Carbon Grade CGW graphite was used for the chamber and throat regions as shown in Figure 14. A heat transfer analysis was conducted for the throat location, The results are presented in Figure 26.

2. FABRICATION

(U) Fabrication of the subscale thrust chambers was accomplished in a similar manner for most designs. The insulation and, in most cases, the throat and chamber liner material were machined from a billet of the desired material which had been fabricated by TRW or supplied by a vendor. The various machined components were then bonded into an assembly, and the assembly bonded into the steel shell.

(U) The steel thrust chamber housing was conservatively designed for ease of fabrication and assembly. The housing consisted of a cylindrical shell with two end plates. Materials were heat treated 4140 steel for the cylinder and T-1 steel for the end plates. The steel components were reused during the program.

(U) The silica phenolic insulation in all chambers was designed to provide an adequate thermal barrier while minimizing the cost of fabrication. The forward and rear insulation components were fabricated from MX 2600 silica phenolic broadgoods (Fiberite Corporation). These laminates were flat pressed perpendicular to the billet centerline. The shell insulation was a cylinrdically wrapped billet of MX 2600 silica phenolic.

(U) The carbon and graphite phenolic insulation and liners were fabricated by two techniques. Fiberite Corporation's MX 4926 carbon phenolic and MX 2630A graphite phenolic materials were used. Insulators which were cylindrically oriented were tape wrapped and hydroclave cured. Liners and insulation components with ply orientation of 45° and 90° to the chamber centerline were close die molded.

(U) Following machining of the various components, thrust chamber assembly was accomplished by bonding the components into place. At composite interfaces which were conical, or gapped greater than 0.010 inches, Epon 913 (Shell

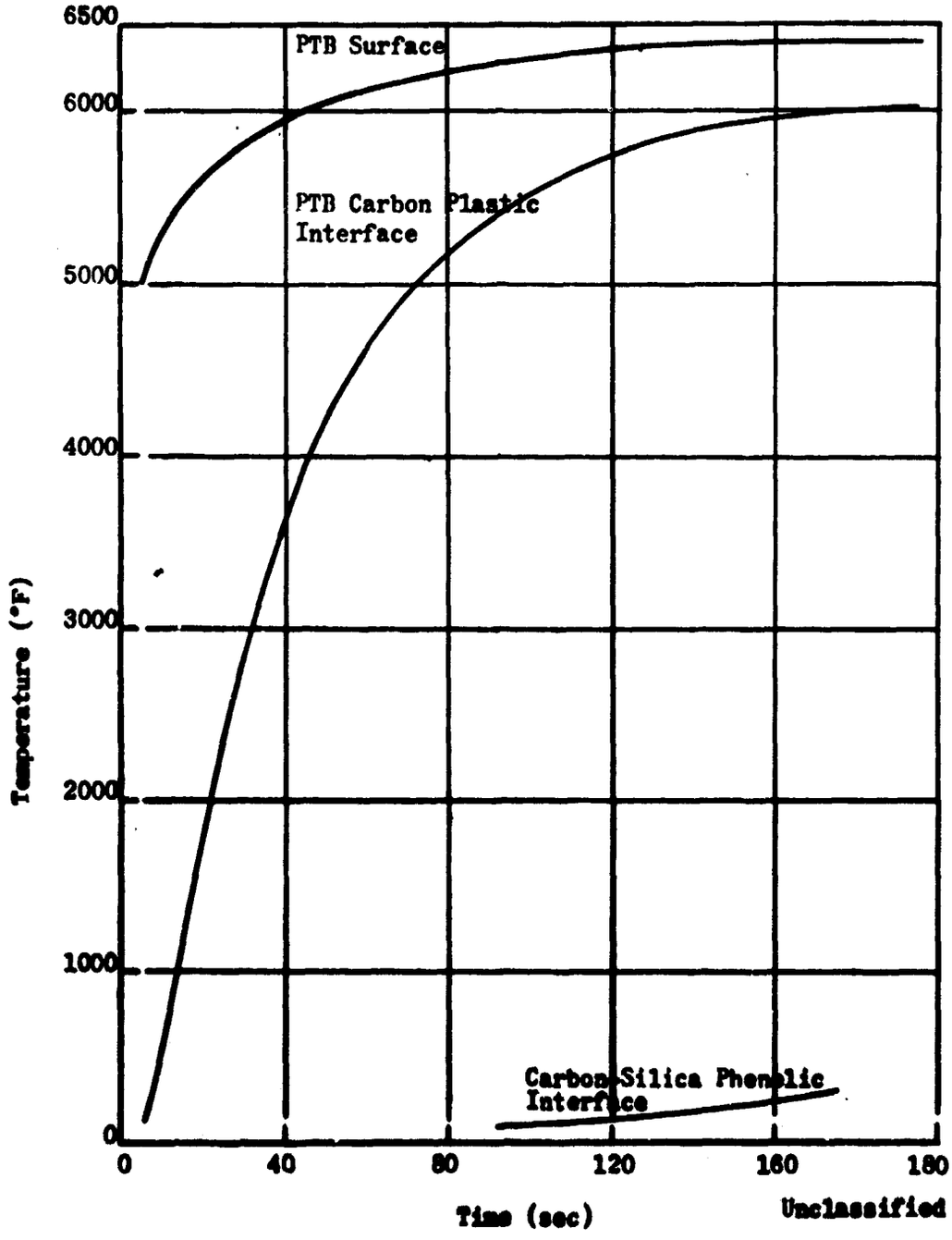

FIGURE 24 (U) Temperature Distribution at Throat for Unit S/N 6

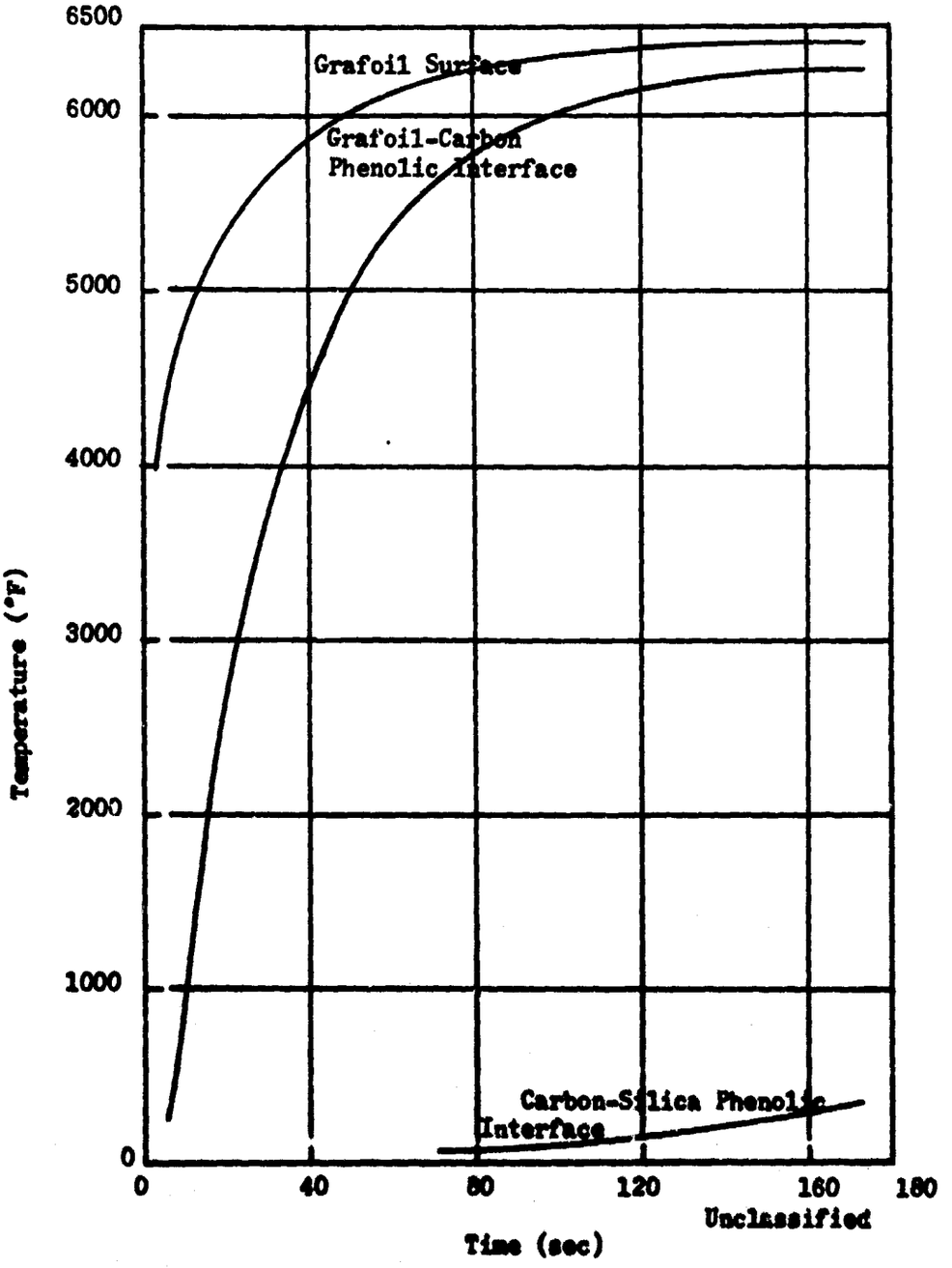

FIGURE 25 (U) Temperature Distribution at Throat for Unit S/N 7

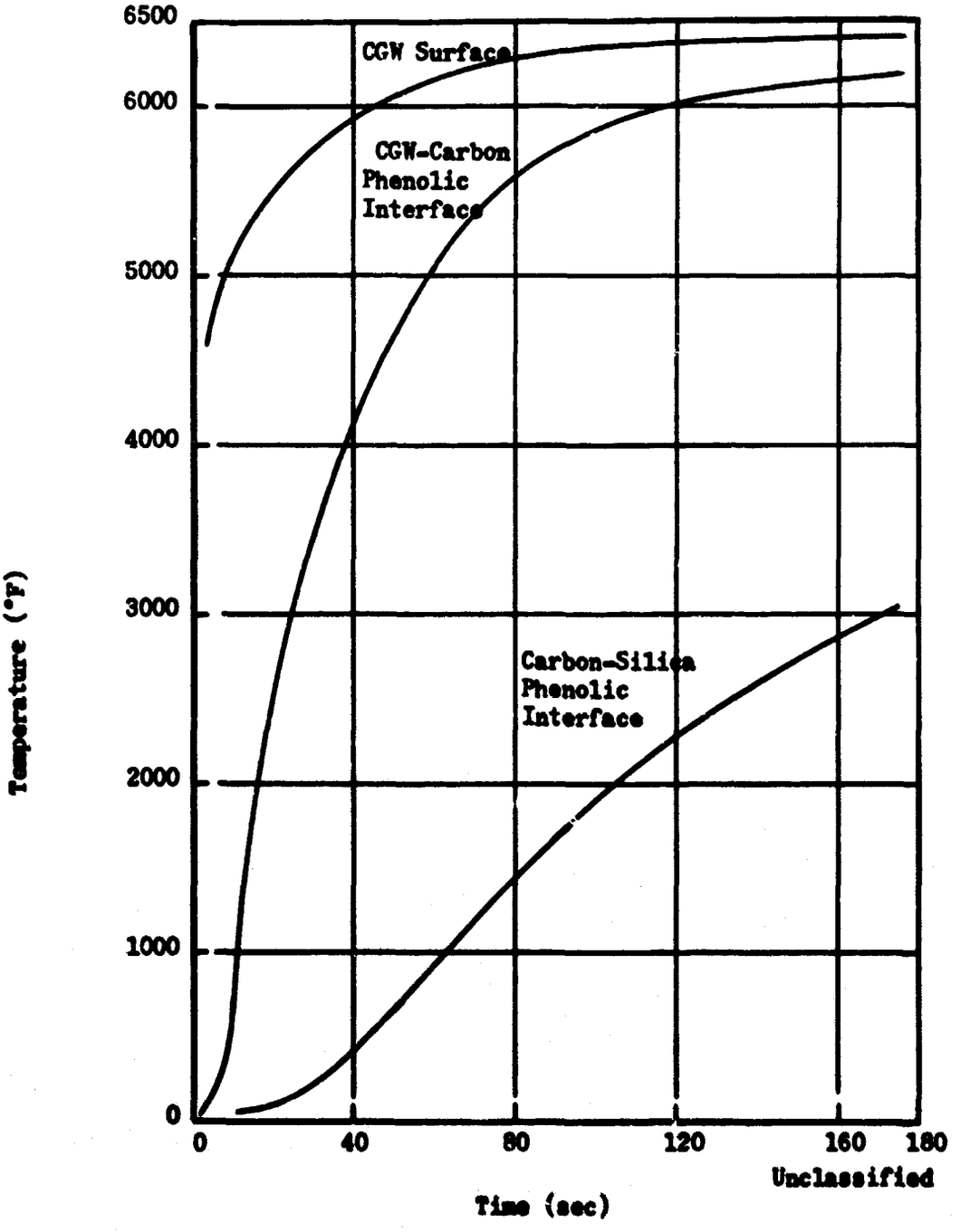

FIGURE 26 (U) Temperature Distribution at Throat for Unit S/N 8

Chemical Company) was used. Epon 919 (Shell Chemical Company) was employed at diametral interfaces and for small clearance gaps. Thermocouple holes were then drilled and the thermocouples installed. Two thermocouple combinations were used depdening upon the temperature to be measured--Tungsten/Tungsten 26% Rennium, and Chromel/Alumel. In some instances, this assembly procedure differed when dictated by design requirements.

a. Subscale Chamber S/N 1

(U) A hot pressed tantalum carbide compact was prepared from -325 mesh powder supplied by Wah-Chang Corporation. Approximately 500 ppm iron powder was added to the TaC to promote sintering and improve density of the final compact. After homogenization, the powder was loaded into the cavity of a 2-inch diameter graphite die and induction heated to 2100°C. An initial pressure of 1500 psi was applied to the die plungers until some compaction was noted (1400°C). Pressure was then increased to 3000 psi and maintained for the duration of the operation. Approximately 90 minutes were required to attain maximum temperature. The compact was held at 2100°C for 30 minutes and cooled slowly over a period of several hours. Density was 13.66 gms/cc or about 94.8% of the theoretical density.

(U) Metallographic examination revealed a uniform, isotropic fine-grained structure. In addition to the 5 volume percent voids, a dispersion of dark particles, predominantly in the grain boundaries, were evident. This is presumed to be free carbon which appears to persist in all refractory carbides despite their stoichiometric composition.

(U) The insert was machined using diamond grinding and lapping techniques. Stress relieving was done in vacuum before machining at 2000°C for one hour.

(U) The Ta-10W alloy used for the axial retainer ring was commercial grade material purchased from the Wah-Chang Corporation. The starting material was 3-inches in diameter by 1-inch long rod stock. Machining was performed by lathe turning using carbide tools.

(U) The starting material for the prestressing ring was 2-inch diameter commercially available pressed-sintered-extruded tungsten rod stock (4 to 1 reduction in area). The stock diameter was increased to 2½ inches by upset forging (approximately 50% reduction). Rough machining was done using diamond grinding. Stress relieving after rough machining was performed in air at 1850°F for 30 minutes. Oxides were removed by soaking in molten sodium hydroxide.

(U) The axial retainer was machined by lathe turning from wrought stock (2½ inch diameter) purchased from the Climax Molybdenium Company (Climax Specification CMX-WB-TAB-2). The material was stress relieved at 2350°F for one hour.

(U) The back-up ring was made from Speer Grade 787 carbon brick. The part was fabricated by turning from a cylindrical billet.

(U) Before final assembly all components of the insert except the back-up ring were ultrasonically rinsed in trichloroethylene, alcohol, and distilled water.

(U) The insert and the axial retainer were placed on the prestressing ring and an axial load of approximately 750 pounds maximum was applied to the assembly using a universal testing machine. Axial compressive strain in the TaC insert was monitored from three SR-4 type strain gages which were mounted on the I.D. surface of the TaC. The maximum strain observed was approximately 0.05% at 750 pounds load. The retainer ring was tightened using a band wrench while the load was applied.

(U) The finished prestressed insert is shown in Figure 27. The final assemlby of the combustion chamber is shown in Figure 28.

b. Subscale Chamber S/N 2

(U) A hypereutectic hafnium carbide throat insert was utilized for the throat insert. This material was arc cast and molded by Battelle Memorial Institute into a billet. The billet was subsequently machined to the finished dimensions as shown in Figure 29. Several casting flaws existed on the outside surface and two shrinkage voids appeared on the inside surface upstream of the throat.

(U) The chamber liner and throat support were fabricated from National Carbon CGW and ATJ graphite, respectively. The finished assembly, typical for all subscale units, is shown in Figure 30.

c. Subscale Chamber S/N 3

(U) The chamber liner and throat insert were fabricated from Carb-I-Tex 700 billets supplied by Basic Carbon (see Figure 31). This material is fabricated from graphite cloth and pyrolyzed to yield a completely graphitic structure. The details of the process are considered company proprietary by the vendor.

d. Subscale Chamber S/N 4

(U) The chamber liner and throat insert for unit S/N 4 were fabricated by Pyrogenics Incorporated, using their unique process for orienting the planes in pyrolytic graphite (Pyroid tradename). The chamber liner was a thin-walled tube; the throat insert a contoured heavy wall section. These components are shown in Figure 32. Radiographic inspection of the pyrolytic graphite components revealed both the throat insert and thin-walled chamber liner to be free of cross ply cracks. Circumferential delaminations in the throat insert, typical of pyrolytic graphite with a high section thickness to diameter ratio, were visible. The depths and extent of the delaminations were revealed by radiographic inspections performed on the throat insert. These delaminations were subsequently vacuum impregnated with National Carbon Grade C-9 carbonaceous cement.

(U) National Grade C-9 cement was also used to bond the complete assembly consisting of the pyrolytic graphite chamber liner backed by CGW graphite, and the Pyroid throat insert backed with Union Carbide's KJB-B insulating carbon brick. Following low temperature curing operations, the complete assembly was exposed to an 1125°F temperature (in vacuum) to carbonize the C-9 cement and thus prevent gasing during the test firing operations. National Grade C-9

Unclassified FIGURE 27 (U) Prestressed Insert

Unclassified FIGURE 28 (U) Unit S/N 1 Assembly

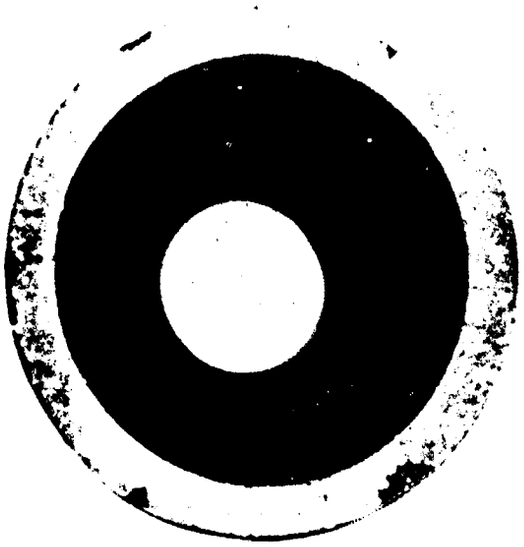

FIGURE 29 (U) Hypereutectic HfC Throat Insert for Unit S/N 2

Unclassified

FIGURE 30 (U) Unit S/N 2 Assembly

Unclassified

FIGURE 31 (U) Carb-I-Tex 700 Chamber and Throat Insert for Unit S/N 3

Unclassified

FIGURE 32 (U) Pyrolytic Graphite Chamber Liner and Throat Insert for Unit S/N 4

Unclassified

cement utilizes a carbon powder as a filler material and a resin as a binding agent. The graphite assembly was then bonded into the insulation.

e. Subscale Chamber S/N 5

(U) This unit had a tungsten -2% thoria throat insert. The tungsten material was initially formed from a powder mixture isostatically pressed and sintered into billet form. The billet was subsequently extruded (3/1 extrusion ratio), and the extrusion forged with a single blow (25% reduction) to produce an upset (pancake) forging. The extruded material was supplied by General Electric and then forged by TRW. Additional work, such as produced by back extrusion, was considered unnecessary--because of the apready very high as-sintered density of the 2% thoriated tungsten material prior to extrusion and upset forging, and the adequacy of thermal shock resistance in the tungsten material for the size and design of insert produced. The as-forged material had a density of 18.8 g/cc (approximately 99% of theoretical density). The forging was subsequently machined (see Figure 33) and the finished insert coated with 0.008 to 0.012 inches of tungsten-modified thoria to prevent melting reactions between supporting materials and contacting surfaces of the tungsten insert. The chamber liner and throat support were machines from CGW graphite.

f. Subscale Chamber S/N 6

(U) The liner material was National Carbon PTB prepyrolyzed graphite material (developed under contract AF 33(616)-6915). PTB is fabricated from a close die molded operation using mascerated carbon fibers and an organic resin. A billet is first pyrolyzed to form a graphitic structure. The raw billet is then impregnated and re-pyrolyzed to build up density and the resulting structure designated PTB (PT-0014). PTB is formed by reimpregnating PTB with a high hydrogen yielding resin which begins to out-gas at approximately 200°C; but with no subsequent pyrolysis. A billet of the material, supplied by National Carbon, was machined into a one-piece chamber and throat configuration. The liner and other chamber components are presented in Figure 34.

g. Subscale Chamber S/N 7

(U) A hot-bonded Grafoil tape structure was employed for the throat insert in this unit. Grafoil tape is a pure, flexible graphite material with highly directional properties similar to pyrolytic graphite. It is fabricated by High Temperature Materials, Inc. This unique material adds the advantage of flexibility to the thermal insulating properties of the anisotropic graphite, and, therefore, can be readily used to fabricate complex shapes where heat transfer control is desired. As in the case of conventional pyrolytic graphite, the thermal conductivity properties of hot-bonded Grafoil are anisotropic, i.e. low (insulative) in the "c" direction, and highly conductive in the "a-b" direction.

(U) Two methods of fabricating the Grafoil structures have been employed by High Temperature Materials with good success. One structure employs an adhesively bonded grafoil tape. A throat insert of this type has been previously tested in fluorine environments with good success.

(U) The hot-bonded Grafoil tape structure has a higher density (1.80 gm/cc) than the adhesively bonded structure. Fabrication is achieved by stacking

Unclassified

FIGURE 33 (U) Tungsten Throat Insert for Unit S/N 5

Unclassified

FIGURE 34 (U) Unit S/N 6 Components

the Grafoil material to the desired thickness, and hot pressing the structure at 4000 psi and 3000°C to form a dense billet. For unit S/N 7, a plane oriented, hot-bonded billet with the Grafoil plies perpendicular to the throat centerline was used.

(U) A billet, fabricated by High Temperature Materials, was machined to the desired configuration. During machining, the chips that were removed had a "flakey" appearance. However, the structure was sound and a good surface finish was obtained. A picture of the Grafoil insert installed in the carbon cloth insulation is presented in Figure 35.

h. Subscale Chamber S/N 8

(U) The throat and chamber liner for this unit was a one-piece construction employing National Carbon CGW graphite. Geometric configuration was similar to that of unit S/N 6 PTB liner insert. For this unit, the silica phenolic shell insulation of unit S/N 2 was reused. Only minor polishing was required to remove loose, charred material.

3. TEST PROGRAM

(U) The purpose of the subscale tests was to economically determine which of the selected materials would complete the required firing cycles. Additional information which was gained concerned the range of capability of the materials tested.

(U) TRW experience has indicated that propellant injection is a major factor in the life of engine materials. Therefore, it was necessary that a proven injector be employed for tests.

(U) To evaluate over-all rocket engine performance, it was necessary to measure thrust, propellant flow, chamber pressure, and temperatures. To measure thrust when the burst is several seconds in duration imposed no difficulty, since spurious forces due to test stand flexibility and component resonance are damped out. For this measurement, a standard load cell mounted on the engine centerline proved adequate. Force readout was automatically recorded.

(U) Combustion chamber pressure was measured by means of a pressure tap in the injector. Specific tests conducted on the SIVB Attitude Control Engines by TRW indicated no measurable difference in chamber pressure at the injector face and downstream, just ahead of the throat inlet section. Thus, for this program, it was assumed that chamber pressure measured at the injector face would be representative.

(U) Ten thermocouples were employed on each engine to permit plotting a temperature profile of the unit throughout the tests (eight thermocouples were used on unit S/N 8). Recording instruments were operative during the cool-down portion of the cycle to permit evaluation of heat soak back effects on the materials employed if required.

a. Facilities

(U) TRW Systems Group, under a company-funded development program, developed a 100-pound thrust (sea level) single element co-axial injector for the subscale

Unclassified

FIGURE 35 (U) Grafoil Throat Insert Assembly for Unit S/N 7

test program. The objectives of the program were to demonstrate an operable injector for use in the evaluation of thrust chamber materials and to complete and check out the liquid fluorine test stand complex at TRW Systems Capistrano Test Site in regard to instrumentation and operation procedures. All program objectives were accomplished; however, C* performance was lower than anticipated.

(U) The basic engine hardware configuration consisted of a 100 lb. thrust single element co-axial injector modified for liquid fluorine service and an ablative injector-face plate liner to provide thermal protection for the injector. Engine assembly was effected through a flanged plate. The "hot gas" seal at the injector-thrust chamber interface was a tongue-and-groove joint with a silicon rubber O-ring seal at the outside diameter of the tongue-and-groove joint.

(U) The 100 lb. thrust single element co-axial injector design utilized was a direct adaptation of the injector element developed by TRW Systems for the URSA-C-1 Engine (NASA Contract NASB-14019, Propellants: nitrogen tetroxide mixed hydrazine fuels). A cross section of the 100 lb. thrust liquid fluorine-hydrazine blend injector assembly set-up for oxidizer-center injection is presented in Figure 36. The liquid fluorine (LF_2) enters the injector sleeve through a drilled passage and flows into an annulus between the injector sleeve and the pintle guide where circumferential distribution of the LF_2 is accomplished. The LF_2 flow is then directed through an annulus bounded by the pintle shaft and the injector sleeve to the metering point, which is a gap between the pintle head and the injector sleeve and is normal to the injector centerline. The resultant oxidizer spray pattern is a concial sheet.

(U) The hydrazine blend (N_2H_4 blend) flow also enters the injector sleeve through a drilled passage and is directed into an annular plenum within the injector sleeve. The N_2H_4 blend then passes through a distributor plate (containing a ring of distribution orifices) into a pressure recovery and redistribution groove and is directed to the metering point, which is an annular gap between the injector body and the injector sleeve. The N_2H_4 blend flow, after leaving the metering point, attaches to the outer surface of the injector sleeve parallel with the injector centerline and produces a cylindrical sheet spray pattern which impinges with the conical oxidizer sheet. No film cooling provisions were employed.

(U) The pintle gap adjustment was accomplished by physically moving the pintle. The pintle was held in place by a locking collar and set screw arrangement. The unique design of the single element co-axial injector permitted complete injector disassembly and the ability to independently vary injector metering areas through simple adjustments. A photograph of the face side of the assembled injector is presented as Figure 37. The injector body and distributor plate were constructed of 17-4PH stainless steel. The injector sleeve, pintle, and pintle guide were fabricated from Nickel 200 (A-Nickel). The engine assembly technique and the general arrangement of test stand complex HB-2 at the TRW Systems Capistrano Test Site is illustrated in Figure 38.

(C) A total of 47 subscale liquid fluorine-hydrazine blend engine tests were conducted during the three injector check-out programs. Eight tests were conducted utilizing the fuel-center injector mode, and the remaining 39 tests were made with the oxidizer-center injection mode. The latter mode of operation demonstrated the higher C* performance. The majority of tests were conducted

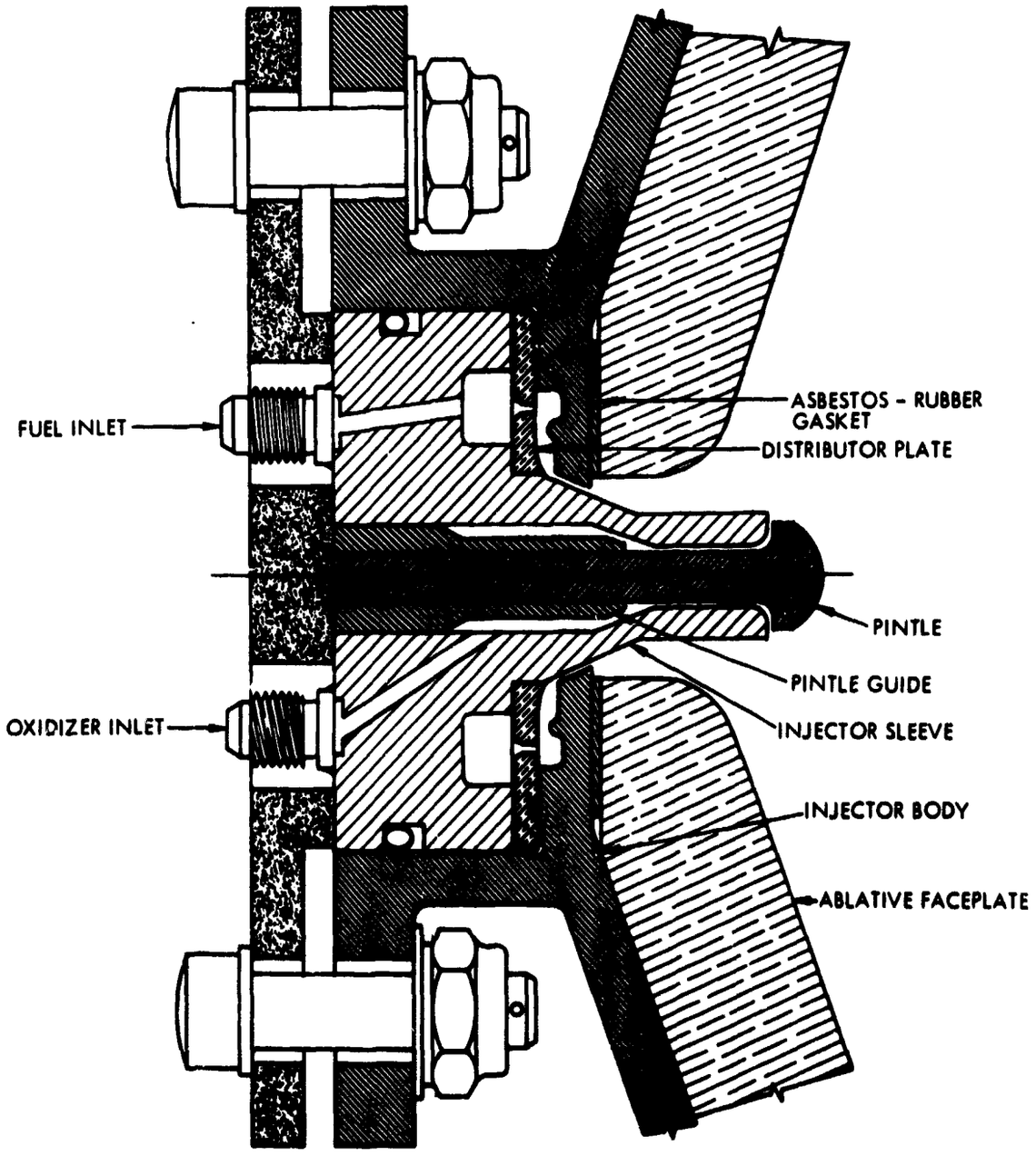

Unclassified

FIGURE 36 (U) Schematic of Single Element Coaxial Injector

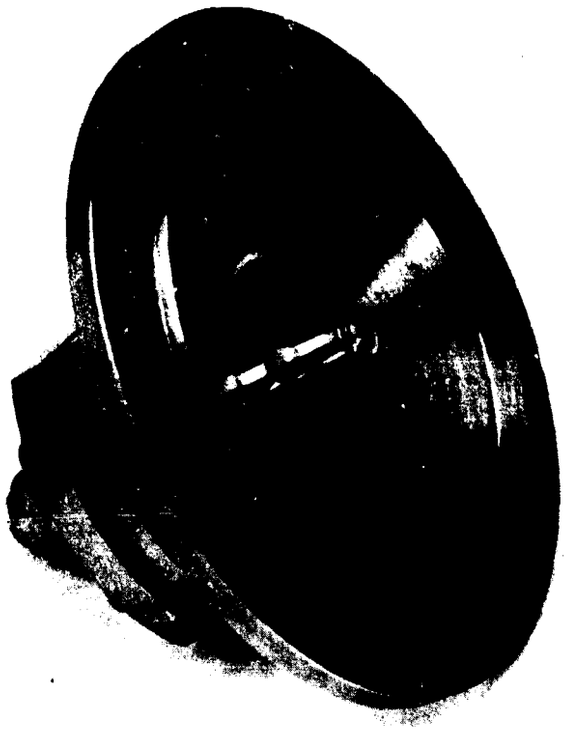

Unclassified FIGURE 37 (U) Injector Assembly

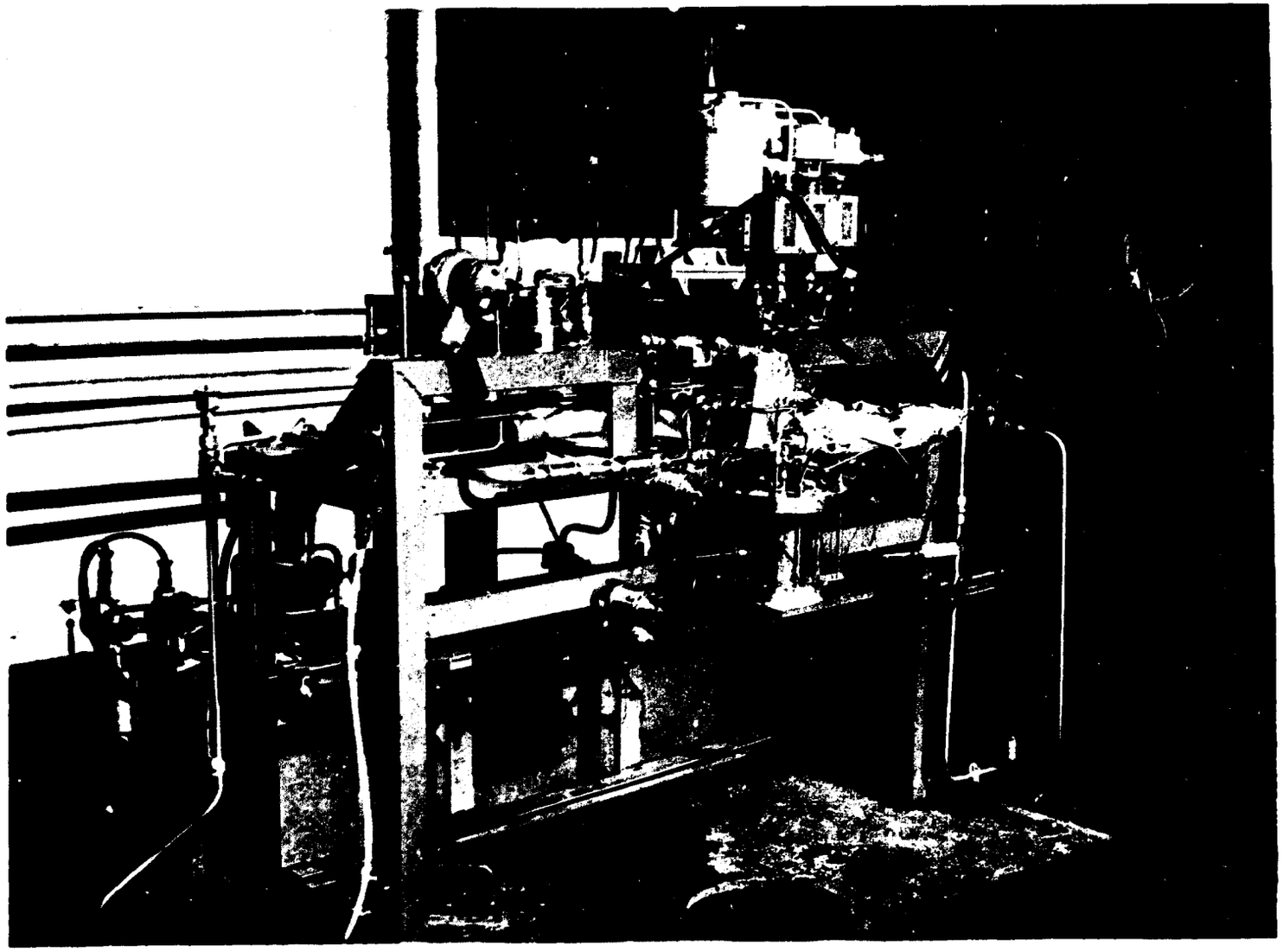

Unclassified

FIGURE 38 (U) Engine Assembly Installed on Test Stand

with a copper heat sink thrust chamber. Operating durations for these tests encompassed time periods up to 5 seconds. Single run durations of 30 seconds each were made with both a monolithic graphite heat sink thrust chamber and a monolithic random orientation molded silica-phenolic ablative thrust chamber. A mixture ratio range of 1.2 to 2.2 was encompassed with both fuel-center and oxidizer-center injection modes. In both cases C* efficiency decreased as mixture ratio was increased over the range considered. The results of the foregoing tests established nominal design conditions of 1.8 mixture ratio, total propellant flow rate of 0.42 lb/sec., C* efficiency of 90% of theoretical equilibrium performance (uncorrected for heat rejection), and a chamber pressure of 150 psia. The nominal thrust chamber L* was 40 inches. However, L* increases of 30% and 100% (with a constant throst diameter and constant constant contraction ratio) were evaluated and were found to only minimally influence delivered C*. The utilization of fixed-area cavitation venturis in both propellant feed systems were found mandatory to assure test-to-test repeatability due to variable pre-test chill down conditions introduced by variable atmospheric conditions.

b. Subscale Tests

(U) Following the preliminary test program to check out the test facility and verify performance predictions of the injector when used with LF_2/N_2H_4 blend propellants, the subscale test program was initiated. The duty cycle for the test program was selected based on the test information desired. Since the primary purpose of these tests was to determine chemical reactivity as a function of temperature and the maximum operating temperature for each material, long on-times were employed. Thus, a basic duty cycle was selected as follows:

Duty Cycle	On-Time	Off-Time
1	25 seconds	Cool to ambient
2	175 seconds	Cool to ambient
3	100 seconds	Cool to ambient

Total planned test time on all units was 300 seconds, except for unit S/N 7 which was 600 seconds.

(U) Following each duty cycle, the thrust chamber was allowed to cool to ambient to permit visual inspection of the chamber liner and throat insert. Duty cycle 1, a short pulse, was included to verify the chamber design and permit examination of the chamber liners and throat insert for thermal shock cracks. Duty cycle 2, a long steady pulse, was intended to bring the surface temperatures of the throat insert and chamber liner to a maximum and eliminate transient heating conditions. Duty cycle 3 was intended to determine the affects of reheating the insert and liner materials after a long pulse history had been experienced. Duty cycle 3 was subsequently revised to accumulate 100 seconds by pulsing during testing. The actual duty cycle of each test was altered from the basic duty cycle relative to design considerations or material performance as determined during the test. The actual duty cycle and test data for each unit is presented in Table XI.

(U) The results of each test are summarized in Table XI. This table presents the chamber and throat material for each unit, design chamber

Table XI (U) Subscale Tests Results

Unit S/N	Chamber Mat'l	Throat Mat'l	Nominal P_c, Psia	Date of Test	Run No.	Duty Cycle On-Time	Duty Cycle Off-Time	ΔD During Pulse	Net ΔD	C^*_{fps}/O/F	%C*	$I_{sp, vac}$ Sec	% $I_{sp\ vac}$
1	Carbon Cloth	TaC	150	11/8/65	050	100 seconds	Cool to ambient	0.020	0.020	6540/1.74	93	292	89
2	CGW	HfC + C	150	11/3/65	048	24 seconds	Cool to ambient	0.0025		6000/1.84	86	269	83
					049	138 seconds	Cool to ambient	0.0275	0.030	5980/1.83	86	279	85
3	Carb-I-Tex 700	Carb-I Tex 700	150	11/26/65	051	5 seconds	Cool to ambient	0.011		6300/1.64	90	258	78
				11/29/65	052	20 seconds	Cool to ambient	0.020		5600/1.53	81	233	71
				11/29/65	053	78 seconds	Cool to ambient	0.007	0.038	5450/1.69	78	240	73
				11/30/65	054	125 seconds	Cool to ambient						
4	PG Tube	PG (Pyroid)	150	12/1/65	055	25 seconds	Cool to ambient	0.010		6130/1.57	89	276	84
				12/2/65	056	175 seconds	Cool to ambient	-0.012		5960/1.77	86	267	81
				12/2/65	057	30 seconds	21 seconds	0.057	0.055	6250/1.80	89	283	86
						30 seconds	27 seconds						
						20 seconds	437 seconds						
						20 seconds	Cool to ambient						
5	CGW	W + 2% Th.	150	12/20/65	058A	5 seconds	Cool to ambient	0.030		5200/2.26	74	268	81
				12/20/65	058B	20 seconds	Cool to ambient	0.057	0.087	6000/1.83	86	250	76
				1/11/66	059	125 seconds	Cool to ambient						
6	PTB	PTB	150	1/21/66	063	15 seconds	Cool to ambient	0.032	0.032	5930/1.90	85	296	90
7	CGW	Graloil	200	1/24/66	064	7.5 seconds	Cool to ambient	0		5540/2.02	79		
				1/28/66	065	11.5 seconds	Cool to ambient	0		5930/1.97	84	288	85
				2/9/66	066	7 seconds	Cool to ambient	-	Failed	6340/1.87	90	282	83
8	CGW	CGW	200	1/13/66	060	10 seconds	Cool to ambient	0.001		6020/2.24	86	261	77
				1/13/66	061	10 seconds	Cool to ambient	0.0005		5830/1.77	83	268	78
				1/14/66	062	125 seconds	Cool to ambient	0.1605	0.162	6550/1.80	93	312	92

Confidential

CONFIDENTIAL

pressure, and test duty cycle. A summary of the throat insert erosion appears in the table. The maximum and minimum throat diameter is presented. The diameter change during the pulse is the average increase (or decrease) of the throat diameter and is based on measurements recorded prior to and immediately after the particular run. The net diameter change is the total diameter change. The effects of local streaking conditions are neglected in the diameter change during each pulse and the net diameter change data.

(U) The combustion performance of each test is presented in Table XI. Injector performance was evaluated for each run. At several time slices during each run, data were reduced to determine measured C* and specific impulse (Isp). Specific impulse is corrected to vacuum conditions. In each time slice, data were compared to the theoretical values at the measured O/F ratio. Theoretical C* and Isp as a function of O/F ratio were presented previously. For C* calculations, the throat area calculated from measurements taken prior to each run was used. Specific impulse has been corrected for vacuum and is compared to the theoretical vacuum specific impulse. Only, C* and Isp values at the beginning of each run are presented since degradation in parameters occurs with throat erosion. The results of each test run are discussed subsequently in order of test.

(1) Subscale Chamber S/N 2

(U) The planned duty cycle for unit S/N 2 included three pulses of 25, 175, and 100 seconds.

(U) Subscale thrust chamber S/N 2, the first unit tested, was fired on November 3, 1965. This unit was tested with a chamber extension (see Section V, Subsection 1c for discussion). During the first run, performance started out low, improved slowly, and stabilized by the middle of the run. Following the run, the injector was removed from the chamber. Chamber inspection revealed no significant erosion. Resin deposits on the injector face were removed, and the chamber was reassembled for the next run.

(U) The second run was a scheduled 175 second duration pulse. The test was terminated after 138 seconds due to visual leakage at the injector-chamber interface. Screws holding the injector to the chamber were loose and apparently yielded at high temperature during the test. The O-ring seal had failed. The graphite liner and ablative insulator in the chamber extension were severely eroded and several streaks were evident approximately ½ inch downstream of the injector. In one circumferential location, a deep gouge through the extension steel housing occurred which appraently caused the excessive temperatures.

(C) Measured C* was below 6000 fps. During the run, the oxidizer temperature decayed from -270°F to approximately -246°F at cut-off. This resulted in reduced oxidizer flow and a corresponding decrease in O/F ratio. The reason for this temperature variation is unexplained.

(2) Subscale Chamber S/N 1

(C) Subscale thrust chamber S/N 1 was tested on November 8, 1965. The duration of the test was 100 seconds. Run designation was 050. Again, the 1-inch chamber extension was used. Measured C* exceeded 6500 fps at the beginning of the test.

(U) Following the tests, the injector was disassembled from the chamber. Severe streaking and gouging prevelant in the previous long duration test (Run 049) was present in the chamber extension. The gouging and severe erosion occurred approximately 1/2 inch downstream of the injector chamber interface and was a local condition. It appeared that the test was completed just prior to the burn-through condition experienced in the previous run. Because of the local gouging condition, apparent in both longer runs to date, it was decided to eliminate the 1-inch chamber extension due to the apparent run duration limitation. Also, during preliminary injector testing, thrust chambers of different length were tested to determine the affect of the L* on performance. Only minor improvements in performance were obtained even with a doubled characteristic combustion length.

(U) An instrumentation problem was encountered during the first three runs.. Due to a limited number strip chart recorders, five thermocouples were recorded on tape and played back following the test. The windings in drive motor of tape recorder were defective causing random variation in speed. All tape was lost. This recorder was repaired prior to subsequent tests.

(3) Subscale Chamber S/N 3

(U) The planned duty cycle included four pulses of 5, 20, 175, and 100 seconds with a cool to ambient between each pulse. The first two pulses were incorporated to check performance and chamber integrity.

(C) The performance during run 051 was very low (C* of 3700 fps). Following the test, the injector was removed from the chamber. It was discovered that the pintle, which controls the oxidizer gap, has slipped causing poor injection characteristics. The oxidizer gap was corrected. The injector was water flowed and the pattern looked good.

(C) Ignition during run 052 was slow. During the first 12 seconds of the run, a C* of about 6300 fps was realized; however, it dropped to about 5000 fps at 15 seconds of elapsed firing time.

(U) It was noted that the oxidizer temperature rose during the latter portion of run 052 causing a decrease in the density of the liquid fluorine. Since the volumetric flow rate is held constant by a cavitating venturi in the oxidizer propellant supply line, mass flow rate decreased with a corresponding decrease in O/F ratio. This accounted for the performance deterioration. No reason was found for the increase in oxidizer temperature.

(C) Run 053 was scheduled for 175 seconds. This run was terminated at 78 seconds due to an excessive rise in the temperature of the steel retaining plate at the upstream end of the thrust chamber (over 2000°F). Characteristic velocity during this run varied from 5600 to 5300 fps. The O/F ratio was 1.53. Upon disassembly of the injector from the thrust chamber, several deep gouges in the chamber walls were revealed beginning approximately 0.5 inches downstream of the injector covering approximately 180 degrees of the circumference. Only slight evidence of the streaking was apparent on the surface of the throat insert. The injector was cleaned, rotated 180 degrees with respect to the chamber, and installed for the next run.

(U) Due to the deep gouges in the chamber wall at the upstream end, it was decided to revise the final test on unit S/N 3 to a 125 second duration

pulse. Ignition was good during this run. Chamber pressure was low (110 psia average). This was due to prior throat erosion.

(4) Subscale Chamber S/N 4

(U) The planned duty cycle for subscale thrust chamber S/N 4 was accomplished. The third run was a pulsed duty cycle to investigate affects on material performance. One of the cool-down cycles in the third run (Run 057) was longer than originally planned. General performance during the test series was good.

(U) The unit was fired for 25 seconds (Run 055). Performance dropped off rapidly during this run. Following this test, the injector was water flowed and found to have a ragged pattern. The injector was then disassembled and cleaned, and the pintle polished in an effort to boost performance for the subsequent runs. The appearance of the thrust chamber was good.

(U) During the 175 second run, performance was good. Chamber pressure rose from 151 to 160 psia. Following the test, the injector was removed from the thrust chamber for examination. Deep local erosion through the pyrolytic graphite chamber sleeve approximately 0.5 inches downstream of the injector was observed. The pyrolytic graphite sleeve was entirely gone in this region. The downstream portion of the cylindrical sleeve (chamber wall) was intact and in good condition with some streaking evident in the throat region. The carbon brick material, downstream of the throat insert, was badly cracked and eroded.

(U) Following run 056, the injector was water flowed indicating some slight streaks. The injector was then cleaned and polished prior to the next run.

(C) During run 057, a pulsing duty cycle was employed accumulating 100 seconds of actual firing time. The duty cycle is presented in Table XI. A chamber pressure in excess of 160 psia was measured during the first pulse of this run. Performance was good (C* about 6250 fps). Following a 21 second cool-down, the chamber was fired for 30 seconds. Characteristic velocity during the second pulse was about 5720 fps. Following a 27 second cool-down, the chamber was fired for 20 seconds with an average characteristic velocity of 5870 fps. Due to the shortage of recording paper on one recorder, the cool-down period was extended to 437 seconds to permit reloading of an oscillograph paper magazine. The last 20 second test was accomplished during which the characteristic velocity was approximately 5330 fps. The over-all decay in the measured characteristic velocity during this run reflects erosion of the throat insert as the calculation was based on the average throat diameter prior to this run.

(5) Subscale Chamber S/N 5

(U) The planned duty cycle for subscale thrust chamber S/N 5 included tests of 5, 20, 175, and 100 second duration with a cool to ambient between each test. The last test was a planned pulsing duty cycle.

(C) The first two runs were for pulses of 5 and 20 seconds. Performance was low during the tests with C* valves of about 5200 fps. The O/F ratio was high (2.0 to 2.26) due to a lower temperature of the fluorine propellant. The

lower temperature caused the density of the fluorine to increase and the mass flow to increase. Chamber pressure during the first run was 161 psia, and during the second run varied from about 161 to 140 psia. An average diametral erosion of 0.030 inches was observed at the throat of the tungsten throat insert.

(C) Run 059 was 125 seconds in duration. Chamber pressure varied from 130 to 135 psia during the test. Characteristic velocity was 6000 fps. The O/F ratio during the test increased from 1.6 to 1.9 due to a drop in the oxidizer temperature. This characteristic has been discussed in conjunction with previous subscale thrust chamber tests. An average diameter erosion of 0.057 inches occurred during this run. Since throat insert performance was poorer than that experienced on the other units, it was felt that additional testing would yield little information. Therefore, no additional tests were conducted.

(6) Subscale Chamber S/N 8

(U) Subscale thrust chamber tests on unit S/N 8 deviated from the planned duty cycle. In addition to chamber materials evaluation, a secondary objective of the test was to examine injector performance at a chamber pressure of 200 psia.

(C) The first run was a 10 second check-out firing. Visually, the tests looked good. Chamber pressure and characteristic velocity during Run 060 were 188 psia and 6020 fps respectively. Due to the higher chamber pressure (above 150 psia as for previous tests), the fuel cavitating venturi dropped out of cavitation changing the flow. The mixture ratio increased to 2.2. As a result, it was decided to increase fuel tank pressure for subsequent tests.

(U) During Run 061, performance was lower due to a bi-stable injector flow condition. The pintle was cleaned and polished following this run.

(C) A 125 second firing was conducted on the unit. The test was very good. Initial characteristic velocity and chamber pressure were 6550 fps and 209 psia respectively. Chamber pressure dropped off to 146 psia at 125 seconds due to throat erosion. Post firing examination revealed severe gouging in the injector end of the chamber and throat. As a result, it was decided to terminate testing at this point since comparative material preformance data had been obtained.

(7) Subscale Chamber S/N 6

(C) Subscale thrust chamber S/N 6 was scheduled for a duty cycle similar to that for unit S/N 4. The run number was 063. This unit was tested for 15 seconds. The intended duration was 25 seconds. Characteristic velocity and O/F ratio were 5930 fps and 1.9 at the beginning of the run respectively. Initial chamber pressure was 145 psia; however, it dropped off rapidly to approximately 90 psia at 15 seconds when the test was terminated. Visually, a sparking was observed in the exhaust plume during the test.

(U) Post test exarination revealed severe erosion at upstream end of the chamber and an erratic erosion in the throat region. Due to the severe erosion of these materials, no additional tests were conducted.

(8) Subscale Chamber S/N 7

(C) The first run was planned for 25 seconds duration. Two attempts to accumulate this time were made, but terminated at 7.5 and 11.5 seconds respectively due to rapid chamber pressure decrease during the runs. Initial chamber pressures were 180 and 200 psia respectively but dropped to approximately 120 psia by the end of each run. Characteristic velocity was below 6000 fps.

(U) The reason for the poor performance during these runs is not clear. Water flow test patters on the injector following each run were good. However, a discoloration of the injector metering annuli was discovered. The injector was disassembled and polished to remove discoloration. The thrust chamber was in excellent condition with no signs of erosion.

(U) For Run 066, the planned test duration was 175 seconds at a chamber pressure of 200 psia. The test was terminated after approximately 7 seconds due to rapid decay in chamber pressure and a poor visual appearance of the exhaust plume. Examination of the thrust chamber following the test indicated the throat insert had failed.

(C) Analysis of the data of Run 066 indicates a normal engine start occurred. For about 1.25 seconds, the engine operated smoothly with a measured characteristic velocity of 6340 fps. All operating parameters such as propellant weight flow, mixture ratio, and pressure drop across the injector were normal. At 1.25 seconds, the chamber pressure dropped abruptly from in excess of 200 psia to about 60 psia within a few milliseconds. During the remainder of the 7 second test, chamber pressure decayed to approximately 40 psia. Review of all data indicates performance of the injector and supporting facility was normal during this test.

(U) Upon examination of the throat insert, it was evident that the Grafoil had defoliated and leaf-like sections had been expelled. An examination of the downstream back-up support for the insert showed no signs of excessive material loss indicating axial containment was still provided. The chamber portion of the unit was sound with minor evidence of gouging or streaking.

4. POST FIRING EVALUATION

(U) This section includes a detailed post firing analysis of the subscale thrust chamber tests. A performance evaluation of liner material and design concept performance are presented. Liner materials are evaluated in detail to determine any significant characteristics.

a. Material Performance

(U) A post firing evaluation of each unit was made subsequent to the tests. A macroscopic evaluation is made of the data and sequence of events. Physical data and other pertinent information is presented. Throat diameter measurements are tabulated for each run in Table XI. Thermocouple data is discussed where pertinent to the interpretation of test results.

(U) Post firing evaluations of liner materials were intitated after necessary measurements were recorded for the chamber and nozzle components. The thrust chambers were disassembled and sectioned longitudinally to reveal the interior surfaces after exposure to the fluorine propellant gases during test firing.

Photographs were taken to record the surface conditions. Pertinent details of the surface conditions and other observations were recorded and are presented. A summary of the performance of these materials is presented in Table XII.

(1) Subscale Chamber S/N 1

(C) Unit S/N 1 was fired for a continuous 100 second pulse. Injector performance was good with C* efficiency greater than 93% of the theoretical value. Throat diameter after test varied from 0.830 to 0.850 inches, approximately a 3% area increase. Severe local erosion occurred in the chamber extension approximately 1/2 inch downstream of the injector (see Figure 39). An attempt to eliminate this severe local erosion condition was made; however, it appears that additional injector development would be required in order to completely resolve this condition. Since materials downstream of this position, including the throat insert, were not affected by this localized chamber wall erosion, it was felt that the objectives of the subscale test program could be accomplished if the subsequent units were designed to accommodate the local erosion condition.

(U) Unit S/N 1 employed a hot pressed tantalum carbide throat insert contained in a prestressed assembly, and a carbon cloth chamber liner. The prestressed insert assembly included a carbon brick backup ring, Ta-10%W retainer ring, TZM molybdenum axial insert retainer, tungsten prestressing ring, and the tantalum carbide throat insert.

(U) The carbon brick backup ring contained axial cracks at four circumferential locations after a single pulse test of 100 seconds. Although all four cracks ran the entire length of the part, it remained in one piece during its removal from the chamber. Three of the four cracks propagated through the holes drilled for thermocouple access to the insert. The part is shown in Figure 40.

(U) During a leak check of the chamber prior to testing, the porous carbon brick provided a leak path for gas around the insert. After firing, there was evidence of slight leakage through the part as noted by discoloration of the downstream end. However, the problems related to cracking and leakage in the carbon brick did not apparently degrade performance of the insert.

(U) The tantalum-tungsten retainer ring surface in contact with the carbon brick was darkened and a minor carbide reaction was apparent. The surface in contact with the tungsten was discolored with gold and black thin films. The gold areas were very hard and looked like TaC. The dark areas had the appearance of a tungsten oxide.

(U) The threaded portion of the part, in contact with TZM, was slightly reacted and discolored, but generally in good condition. Small fragments of reacted thread material flaked off during disassembly. This was also evident in a cross section of the part which was mounted for metallographic examination.

(U) A tantalum washer (0.007 inches thick) was situated forward of this part to limit the carbon-molybden reaction in an adjacent part. The tantalum washer was carburized from contact with the carbon cloth phenolic, and also fused to the retainer ring in several places. The washer was fragile (embrittled) and broke apart as it was pried loose from the retainer ring.

Table XII (U) Summary of Liner Material Performance

Subscale Engine S/N	Nozzle Throat Material	Chamber Material	Degradation of Material: Nozzle Throat	Degradation of Material: Chamber	Performance of Nozzle Throat Material
1	Tantalum Carbide Prestressed	Carbon Cloth	Insert cracked, but remained in place. Some erosion, uneven due to injector streaking.	High erosion near injector head. Material charred to 1/2 inch depth. Some small cracks in char layer, along plies.	Good
2	Arc-Cast Hypereutectic Hafnium Carbide	CGW Graphite	Uneven throat erosion due to injector streaking. Also, carbide-graphite eutectic eroded faster than graphite flakes.	Major erosion near injector head.	Good
3	Carb-I-Tex 700	Carb-I-Tex 700	Small radial cracks along plies - little change in contour - minimal areas of localized, high erosion.	Axial crack full length of chamber along plies. High erosion near injector.	Good
4	Pyrolytic Graphite	CGW Graphite + PG Chamber Liner	Major delamination of PG insert. Localized guttering of insert. No apparent catestrophic material loss due to delamination of the PG.	PG chamber liner gone. Large axial crack in CGW. High erosion near injector.	Good
5	Tungsten-2% Thoria-Gorged Material	CGW Graphite	Uneven throat erosion with several severe, localized high erosion areas. Material recrystallized with some grain growth. Erosion due to chemical reaction - no melting observed.	High erosion near injector. Liner material eroded through at this location	Fair
6	PTB - Ablative material - single piece construction		Localized erosion plus some porous deposits. Small radial cracks.	Radial cracks and large areas of erosion. Deposites of ablative material residue. Discolored.	Poor
7	Hot-Bonded Graphite (Graphoil)	CGW Graphite	Insert delaminated and delaminated sections collapsed due to pressure. Delaminated material near exit lost due to structural weakness.	Essentially no erosion. Chamber liner and insulating backup pushed forward by 1/8 inch.	Failed Mechanically
8	Monolithic Graphite Grade CGW - Single Piece Construction		Several high erosion areas on the nozzle throat section. Some general erosion and contour change evident.	High erosion near injector. Some localized washing or erosion. No cracking.	Good

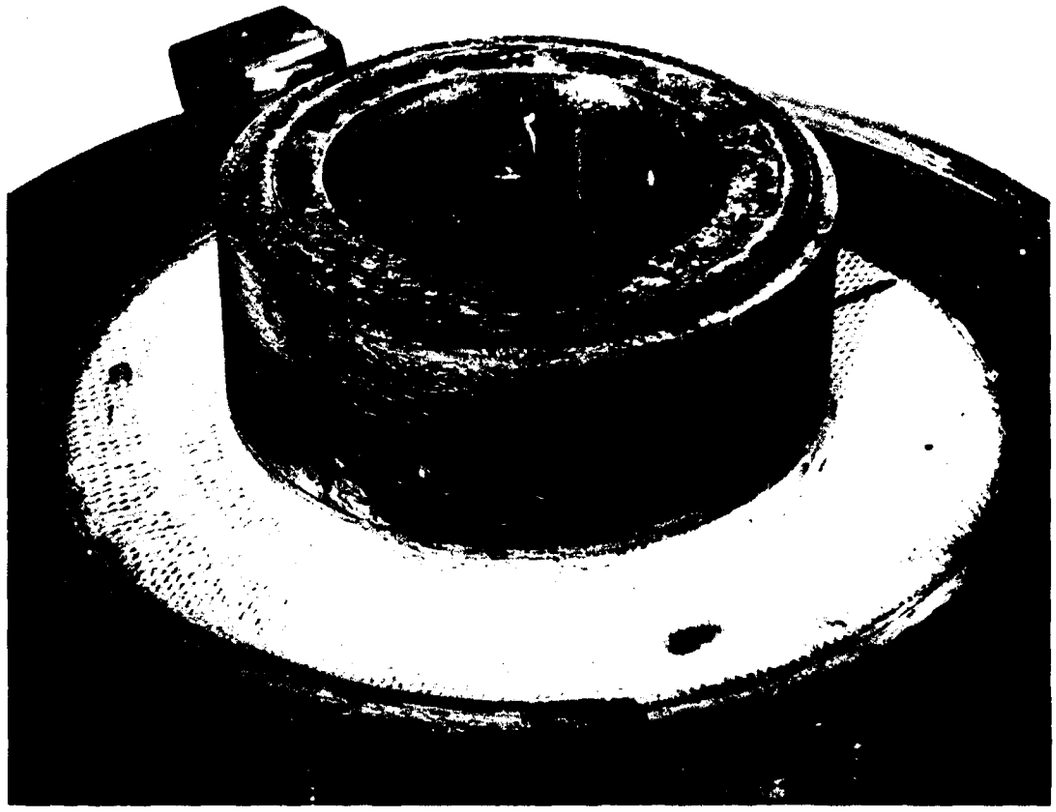

Unclassified FIGURE 39 (U) Inlet of Unit S/N 1 After Test

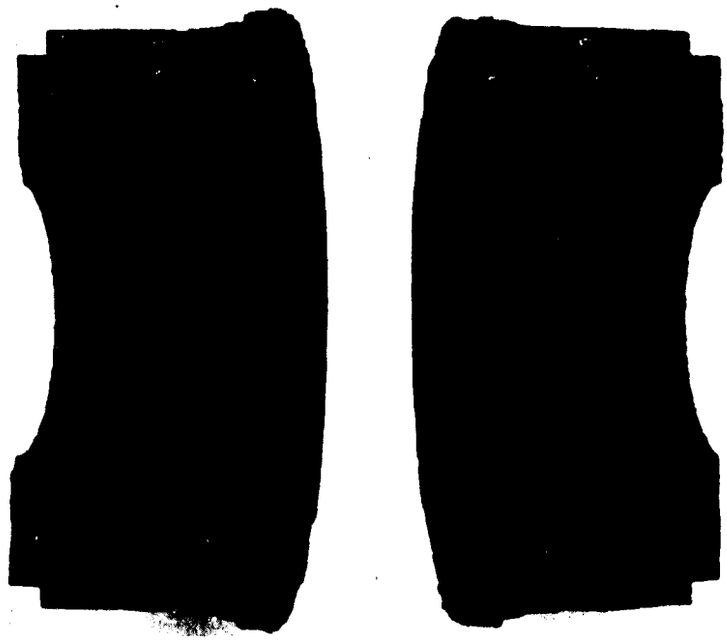

Unclassified FIGURE 40 (U) Unit S/N 1 Carbon Brick

(U) Based on both chemical (compatibility) and structural considerations the retainer ring and washer performed satisfactorily for the application. The TZM axial insert retainer withstood the combustion environment very well, as is seen from the photograph of Figure 41. Only slight erosion was apparent, except at one circumferential position where streaking had occurred. At this circumferential station, evidence of streaking was visible in all of the interior components of the combustion chamber.

(U) Exposure of the TZM part to the combustion environment resulted in a fully recrystallized structure. A slight refinement in the grains occurred adjacent to the machined surfaces, but in general a uniform structure was observed throughout the part.

(U) A gold-colored deposit, probably TaC, was observed on the mating surface with adjacent components. The coating was barely visible in the cross sections of metallographic samples.

(U) The tungsten prestressing ring was exposed to the propellant exhaust stream downstrem downstream of the throat insert. This portion of throat suffered practically no dimensional change. Some oxidation of the exposed tungsten occurred after engine shut down, since the normal nitrogen purge duration was shortened to minimize thermal shock during cool down. Thus, oxidation resulted from exposure to ambient air.

(U) Considerable grain growth was observed in the tungsten in the area back of the TaC. At the extreme aft end of the tungsten part, the grain structure remained fine and apparently unaffected by the firing duty cycle. This was the only portion of the insert which radiated directly to the ambient surroundings, and would account for the part being cooler during testing. Intermediate between this area and the throat extremely large grains were observed. Apparently this area of the part remained hottest for the longest period of time. The calculated temperature for the tungsten at 100 seconds after ignition was approximately 4800°F, and at this temperature considerable grain growth would be expected.

(U) Evidence of a reaction at the interface between the tungsten and the tantalum carbide was seen in the sectioned parts. The thickness of the reacted interface was small (several microns) and not continuous. A very probable reaction between W and TaC would involve the formation of Ta_2C and W_2C, since both of these compounds have a hexagonal structure very close to the same size. The bond formed from the reaction at the interface fractured intermittently through the reacted zone and the TaC.

(U) Predicted temperatures (4800°F at 100 seconds) in the tungsten would be expected to result in the formation of tungsten carbide (approximately 4500°) at the tungsten/carbon interface. However, no evidence of the reaction was observed, indicating that the back side temperature stayed below 4500°F, or there was insufficient time for the solid state diffusion necessary for the formation of the carbide phase.

(U) Several dimensional checks in the constant diameter section of the tungsten piece showed measured variations in the range of 0.001 to -0.003 inches on the 1.560 inch diameter. The diametral increases were observed at 90 degrees from the decreases, indicating out of roundness.

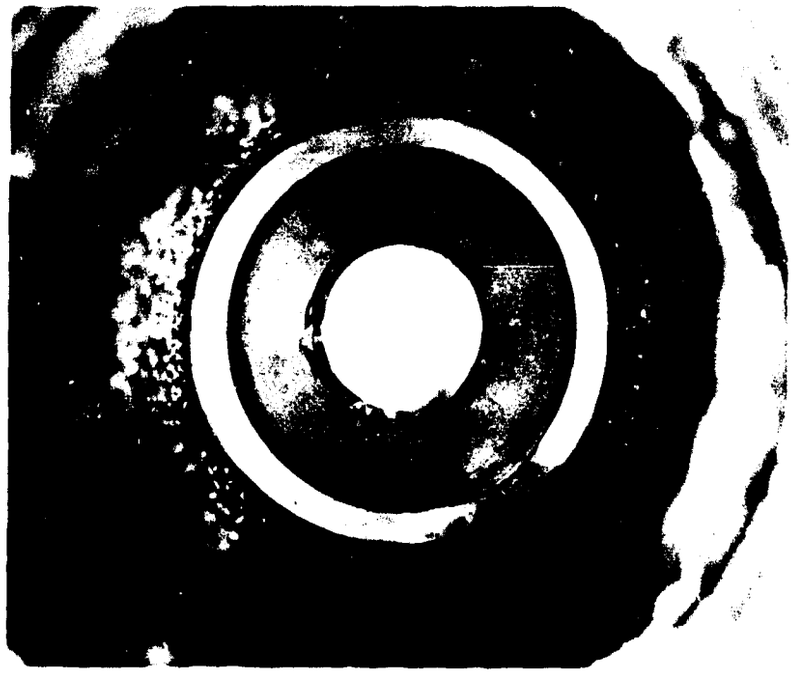

Unclassified

FIGURE 41(U) Upstream End of Prestressed Throat Insert Assembly After Test

Unclassified

FIGURE 42 (U) Axial Section of Prestressed Throat Insert Assembly After Test

A slight increase (approximately 0.47%) in the diameter was expected due to the plastic flow predicted by the thermal stress analyses.

(U) A crack approximately one-half inch from the upstream end of the insert ran the entire circumference. An axial crack from the terminus of the circumferential crack intersected the forward edge of the part (see Figure 42 and Figure 43). Both cracks propagated intergranularly and appeared to have occurred at fairly high temperatures. Figure 44 is a photomicrograph of the tungsten showning the circumferential crack. A positive basis is not available for determining the time or temperature at which cracking occurred. The maximum hoop stress calculated for the tungsten occurred at approximately 5 seconds after ignition. Plastic flow was predicted to occur at this time and continue for the duration of the firing cycle. A similar behavior would be expected for the stress-strain behavior in the axial direction, i.e., for a long cylinder (plane strain) the axial and circumferential thermal stresses would be similar in magnitude.

(U) Erosion of the TaC throat insert was moderate, as is seen in Figure 42. The TaC suffered greater recession than either the TZM or W, as seen at the appropriate interfaces in this figure. However, direct comparison may not be completely justified because of the differences in the thermal histories of the various components. Surface temperatures of the components at adjoining interfaces could be widely different, although the exhaust environment would be the same. The erosion pattern was slightly egg-shaped with the major perturbation in line with the streaking path which ran the length of the chamber. The maximum diameter was 0.858 inches measured from this point. A minimum diameter of 0.830 inches was measured at 45 degrees from the maximum.

(U) The TaC insert cracked in both the circumferential and axial directions. The major crack was circumferential and followed the path of the circumferential crack in the tungsten prestressing ring. A large number of smaller hairline cracks ran parallel with and close to the main crack. The number of cracks decreased towards both ends of the insert. Cracks in the axial direction were mainly hairline, and many were superficial originating at the I. D.

(U) In general, cracks propagated intergranularly. The true character of the cracks in this brittle material is difficult to illustrate in a metallographic specimen, since fragments (grains) of the crack structure are broken loose and are lost during polishing.

(U) Some erosion developed in the carbon cloth chamber liner, with the most severe erosion occurring near the injector head. However depth of erosion was not severe enough to puncture through the upper part of the chamber liner, as was the case for other engines of long duration firing. Charring of the carbon cloth, as evident in the cross section, was uniform and approximately 1/2 inch deep measuring from the chamber inner wall. Several very fine cracks were noticeable along the plies (at a 45° angle to the wall), but these cracks did not extend beyond the char layer and, thus, did not influence performance.

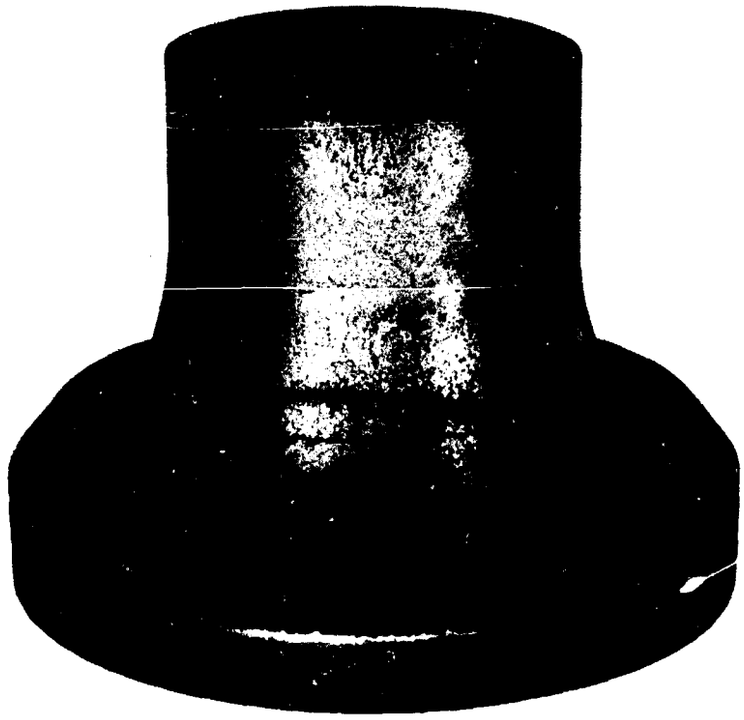

Unclassified

FIGURE 43 (U) Back Side of Prestressed Throat Insert Assembly

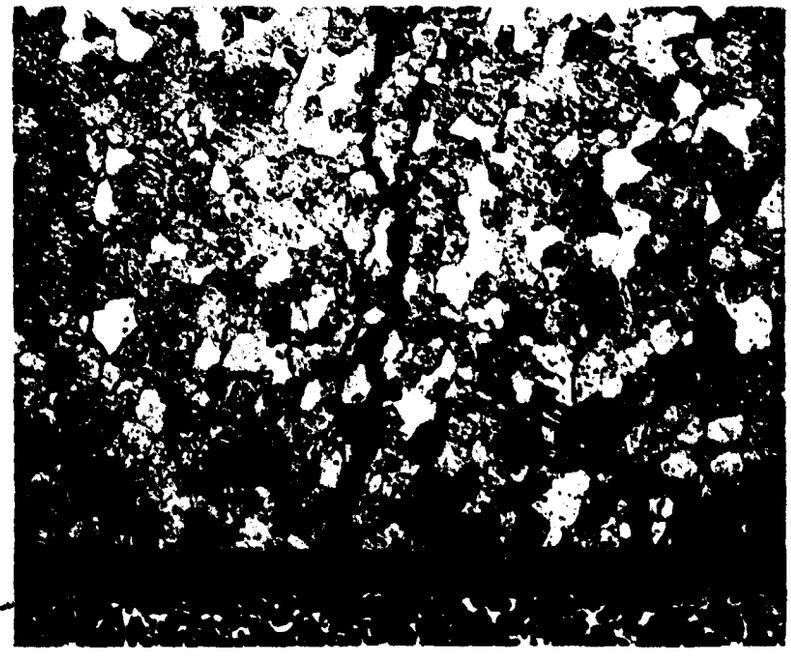

Unclassified

FIGURE 44 (U) Photomicrograph of Crack in Tungsten Prestressing Ring: 100X

(2) Subscale Chamber S/N 2

(U) Unit S/N 2 was fired for 25 and 138 second pulses for a total time of 163 seconds. Between each pulse, chamber components returned to ambient temperature. Severe erosion of the chamber extension was experienced similar to that described in conjunction with unit S/N 1.

(U) Unit S/N 2 contained a throat insert machined from arc-cast, hyper-eutectic hafnium carbide, and a CGW graphite chamber liner.

(U) After the initial 25 second burst the motor was allowed to cool to ambient temperature for visual examination. No cracks were observed in the throat insert, indicating good thermal shock resistance. A single streak pattern was evident on the insert surface covering an angle of approximately 45°. The C-9 graphite cement used to fill in several casting defects in the I. D. surface of the throat insert was essentially intact.

(U) After a second firing of 138 seconds (for a total time of 163 seconds), the throat insert was removed from the thrust chamber for complete examination. Careful inspection under 10X magnification did not reveal any cracks in the insert, thus confirming the good thermal shock resistance of the cast hyper-eutectic carbide. The streaking observed after the initial 25 seconds burst was still evident. Void areas originally covered up with the graphite cement were exposed due to the loss of this material. A comparison of the visual appearance before and after firing is illustrated in Figure 45. The throat erosion pattern was uneven, and resulted from streaking by the injector.

(U) Careful examination of the throat insert surface showed that flakes of free graphite projected above the surface. Figure 46 attempts to illustrate this condition. A cross-section of the insert was prepared for metallographic examination and selected areas are illustrated in Figure 47 and 48. Figure 47 clearly shows the projection of graphite flakes from the surface in an area upstream of the throat insert where the mechanical erosive (shear) effect of the propellant gases is relatively low. Graphite flakes do not project beyond the eutectic HfC matrix in the throat area, probably because the graphite flakes are relatively weak and are mechanically eroded away by the high velocity of the propellant gases. Projection of the graphite flakes in the relatively low propellant gas velocity areas does indicate that the chemical corrosion rate of the eutectic hafnium carbide-carbon (graphite) matrix is greater than the erosion rate for graphite. This is consistent with laboratory reactivity studies indicating graphite to have a resistance to reaction by hydrogen fluoride superior to that of hafnium carbide.

(U) During handling of the throat insert, it was noted that a carbonaceous material rubbed off the surface. However, subsequent visual and metallographic examinations did not reveal any evidence of deposits or reaction products on the exposed surfaces. Thus, the carbonaceous material which rubbed off undoubtedly came from the exposed graphite flakes.

(U) The CGW graphite chamber liner developed extensive erosion, particularly near the injector head. However, the erosion did not pierce the chamber liner. Streaking by the injector, which was observed on the nozzle throat insert surface, was also evident on the chamber liner.

(U) The throat erosion pattern was uneven with measured maximum and minimum throat diameters of 0.885 and 0.869 inches, following the test. This

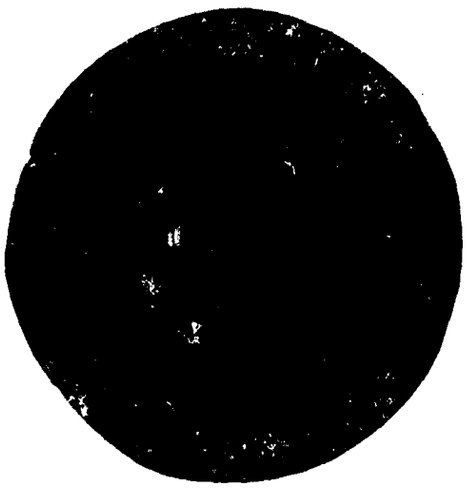

a) As Cast and Machined.

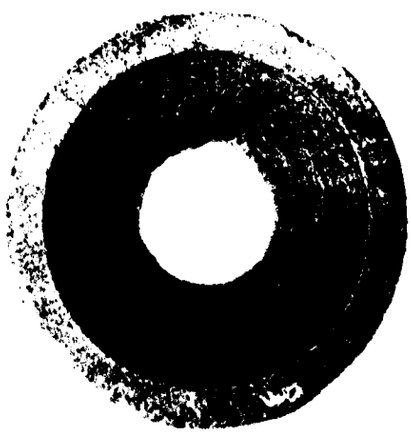

Approximately 1X

b) After 163 Seconds of Test Firing.

FIGURE 45 (U) Appearance of HfC-C Before and After Test

Unclassified

3X

Unclassified

FIGURE 46 (U) Surface of HfC•C After Test

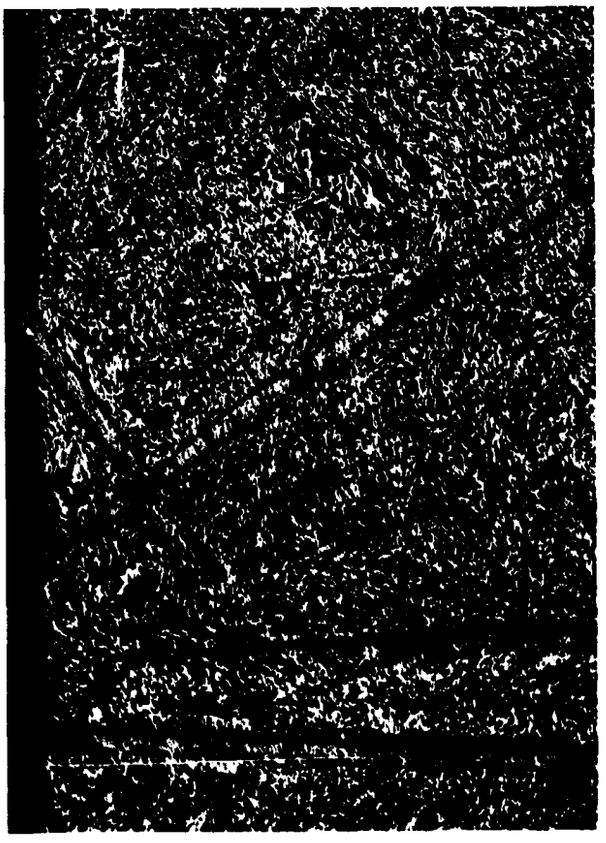

Unetched 100X Magnification

Unetched 100X Magnification

Unclassified

FIGURE 47 (U) Cross-section of HfC•C Upstream of Throat

up stream

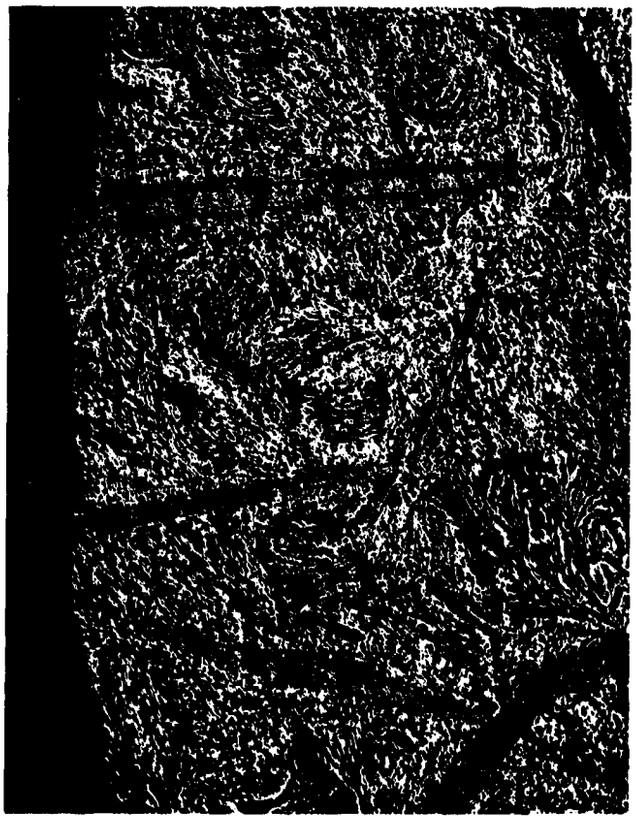

down stream 100X Magnification

Unclassified

FIGURE 48 (U) Cross-section of HfC•C at Throat·

uneven throat erosion resulted from streaking by the injector. The average radial erosion was 0.030 inch. No cracks were observed.

(3) Subscale S/N 3

(U) Subscale thrust chamber S/N 3 was tested for an accumulated time of 228 seconds. After removing the thrust chamber from the steel housing, unit S/N 3 was sectioned axially (see Figure 49). A close-up view of one section is presented in Figure 50.

(U) The Carb-I-Tex 700 material performed well both as a chamber liner and a nozzle throat insert. Erosion of the chamber liner near the injector inlet, while visibly extensive, did not penetrate through the liner. This greater erosion is attributed to impingement by unreacted fluorine. The reaction of graphite materials by fluorine has been determined to be more severe than that of HF (see Appendix). Slight axial delaminations along the length of the chamber were developed during firing. These delaminations occurred only between the plies of the Carb-I-Tex 700 and there were no visible indications of detrimental effects from the cracks--such as high localized erosion, spalling, or failure of the back-up insulation material. Figure 50, a half section, illustrates the minor nature of the delaminations and the fluorine reaction problem. In this photograph, the plies of the chamber liner material are normal to the plane of the photograph and are axial (along the length of the chamber). Locally increased erosion in line with the upstream injector end gouging is apparent. Whether the erosion resistance in the chamber section is better when the plies are parallel to the surface, or at right angles to the surface (as in the throat) is not certain. Logically, however, it would be expected to be better if the ply are oriented as in the throat.

(U) The nozzle throat insert had some radial cracks between the plies, but again these did not appear to be detrimental. Areas of localized erosion were not as deep as those observed in other thrust chamber materials tested. Very little over-all change occurred in the throat contour, although the surface roughness indicated some general erosion. Erosion appeared to be the result of chemical reactivity with the propellant gases or, a result of downstream projection of the injector gouging pattern. There was no visible indications of material loss either by spalling or by melting.

(U) The carbon cloth support material was charred through approximately 1/2 of its section behind the throat insert. The carbon cloth char depth was greater in the chamber region. The silica insulation between the steel shell and the carbon cloth was not charred. This agrees with the predicted thermal analysis results.

(C) Characteristic velocity during the test, except for a portion of Run 052, was below 6000 fps. An erosion of 0.011 inches was measured following Runs 051 and 052. Erosion during the third and fourth runs, Runs 053 and 054, was 0.020 and 0.007 inches respectively. The rate of erosion on the last two runs was less than that of the first two runs. This is probably due to the fact that performance and chamber pressures were lower during these runs.

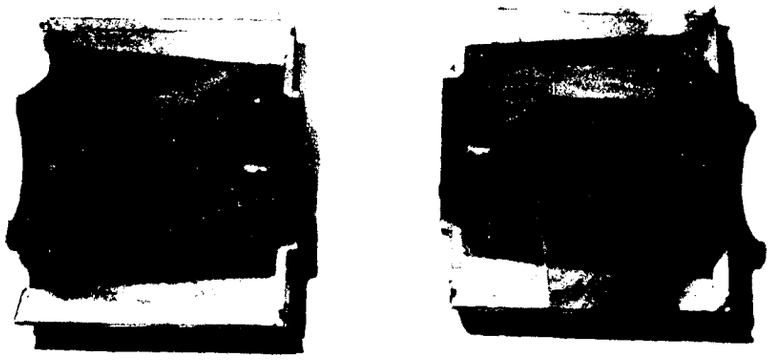

FIGURE 49 (U) Sectioned Unit S/N 3 After Test

Unclassified

FIGURE 50 (U) View of Sectioned Unit S/N 3 After Test

Unclassified

(4) Subscale Chamber S/N 4

(U) Subscale thrust chamber S/N 4 was tested for an accumulated time of 300 seconds. This unit was sectioned similarly to unit S/N 3 and views of these sections are presented in Figures 51 and 52.

(U) The pyrolytic graphite sleeve in unit S/N 4 was completely gone following the test. Severe erosion occurred at the chamber just downstream of the injector as had been experienced in previous tests. During the last run (Run 057), a burn-through to the steel occurred. The pyrolytic graphite sleeve was in tact following the first pulse (Run 055). Following the second pulse (run 056), it was observed that the upstream portion of the sleeve (adjacent to the injector) was entirely eroded away. During the last run (Run 057), the combustion gases apparently flowed behind the sleeve causing it to erode and/or break-up. If finite pieces of the sleeve did pass through the throat, they were quite small as no large blips in the chamber pressure trace were observed.

(U) Appearance of the pyrolytic graphite nozzle throat insert, illustrated in Figure 52, is deceptive. Although the insert delaminated extensively and showed high erosion on the convergent surface, the actual throat diameter did not increase markedly. Some of the areas of high erosion on the convergent surface were due to streaking of the injector. However, pyrolytic graphite acts as an insulator in the "c" direction (which was normal to the inlet surface) such that material surface temperatures could thus become very high leading to increased erosion tendencies. Material underneath this surface ("a-b" planes parallel to the surface contour) leading to the throat section are protected by the insulative nature of the surface material, thus reducing the maximum temperature which this material might otherwise experience. Thus, failure by layers is logical, and visibly, is what occurred in the convergent section. At the throat location, the visible erosion pattern was an uneven, scalloped effect. Distinct local areas of increased loss were apparent, although these did not necessarily line up with injector end chamber local areas.

(U) The carbon brick support material behind the throat insert developed numerous fractures. Sections of the carbon brick forming the exit cone either suffered severe erosion, or fractured and spalled off. Superior insulative characteristics, however, were evident.

(U) Over-all combustion performance during the test of unit S/N 4 was good. Throat erosion during Run 057 accounts for the lower calculated characteristic velocity values following the first pulse since calculations are based on the initial throat area. The silica insulator between the internal chamber components and the steel shell was approximately 80% charred in the chamber region and less severely charred in the throat region. This char is greater than that predicted. However, the loss of the pyrolytic graphite sleeve in the chamber permitted greater heating of the graphite heat sink and this would account for the increased char.

(5) Subscale Chamber S/N 5

(C) Subscale thrust chamber S/N 5 was tested for an accumulated time of 150 seconds. Basically, the design incorporated a tungsten -2% ThO_2 throat insert and a CGW high density graphite chamber liner. During the first two pulses, Runs 058A and 085B, a diameter change in the throat of 0.030 inches was observed for a total firing time of 25 seconds. Visually, the throat insert looked good and there was no evidence of streaking or surface melting. However,

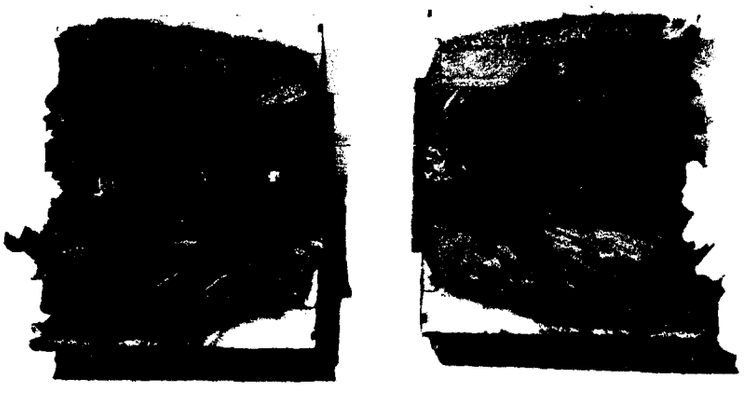

FIGURE 51 (U) Sectioned Unit S/N 4 After Test

Unclassified

FIGURE 52 (U) View of Sectioned Unit S/N 4

Unclassified

measurement indicated that the throat was oval-shaped. During these runs, characteristic velocity was below 6000 fps.

(C) The final pulse on unit S/N 5 was rescheduled for 125 seconds as a result of the throat diameter change. It was felt that if erosion would continue at the present rate, the throat insert would be lost during a longer test pulse. During this pulse, Run 059, characteristic velocity was 6000 fps. An average erosion of 0.057 inches was realized for a net diameter change of 0.087 inches. No further tests were conducted on this unit.

(U) Erosion developed in the chamber liner, Figure 53, punctured through the liner in one section and burned into the insulating plastic. A streaking pattern, developed in the chamber liner, was typical of streaking patterns developed in other CGW graphite chamber liners. Erosion of the tungsten alloy throat at this location was particularly severe, as illustrated in Figure 54. Because of this, the erosion pattern tended to be eccentric and deeply penetrated in localized areas. At an area 180° from the streak, dimensional loss was high, but uniform. No deposits were found on the insert surface, and the only discoloration was a slight darkening of the surface. Appearance and feel of the eroded areas were very smooth, indicating chemical rather than melting attack.

(U) Metallographic examination of the tungsten - 2% thoria insert, at both the throat location and several areas of high erosion, revealed no apparent change in the surface of the insert, as illustrated in Figure 55, a and b. Since there was not evidence of surface melting or mechanical failure of the tungsten alloy, the erosion mechanism is believed to be associated entirely with chemical reaction--either with the propellant gases (primarily HF), or unreacted fluorine in the streaked areas. Compounds formed by reaction of tungsten with fluorine are volatile at the engine operating temperatures, and the reaction products would be blown out with the exhaust gases, thus accounting for the lack of deposits on the insert surface.

(U) Grain structure of the tungsten - 2% thoria insert after test firing was compared to a sample machined from the insert prior to assembly, The fine cold worked structure of the as-machined material, Figure 55c, has been recrystallized during test firing, the some grain growth followed. While excessive grain growth is not desireable, the amount of grain growth experienced by the insert did not detract from its performance.

(6) Subscale Chamber S/N 6

(C) Subscale thrust chamber S/N 6 was tested for a duration of 15 seconds (Run 063) of a planned 25 second pulse. Unit S/N 6 was the final subscale unit designed for 150 psia chamber pressure operation. This unit incorporated a one-piece PTB throat insert and chamber liner. Characteristic velocity at the beginning of the run was 5930 fps. However, during the tests, chamber pressure dropped off rapidly and sparking was observed in the exhaust plume. Visual examination following the test revealed severe erosion in the chamber liner and erratic and severe erosion of the throat insert. Total average erosion was 0.032 inches, which is must greater erosion rate than other subscale units tested. No additional tests were conducted.

(U) Sectioning of the motor revealed several radial cracks and a heavy porous black deposit in addition to severe, localized erosion pits. The

08800-2 1X Mag. Unclassified

FIGURE 53 (U) Unit S/N 5 CGW Graphite Chamber After Test

08800-4 1X Mag. Unclassified

FIGURE 54 (U) Unit S/N 5 Tungsten Throat Insert After Test

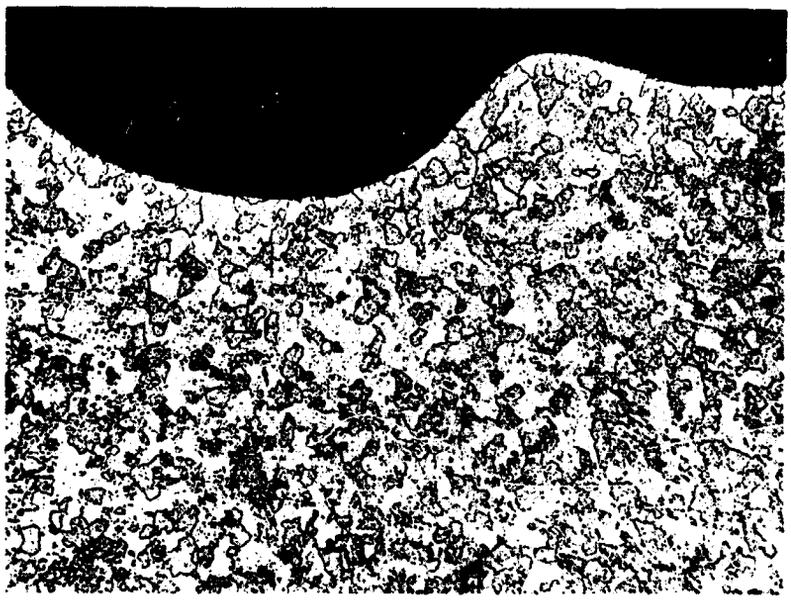

A-8083 75X Mag.

a) Surface Microstructure of W-2% ThO_2 Nozzle Throat Insert - High Erosion Area of Test Fired Insert.

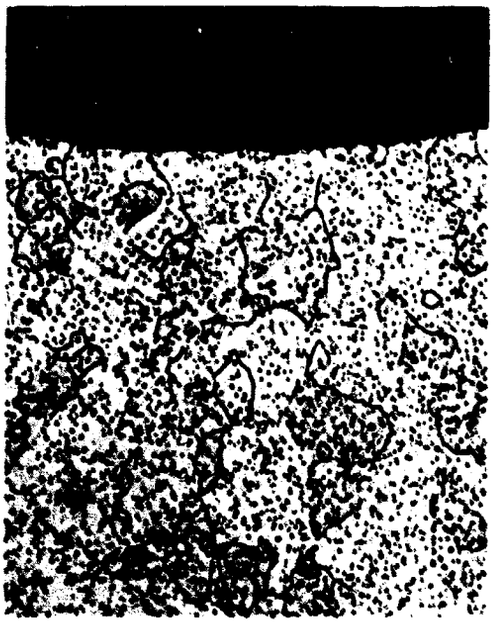

A-8082 250XMg.

b) Grain Structure - Test Fired Insert

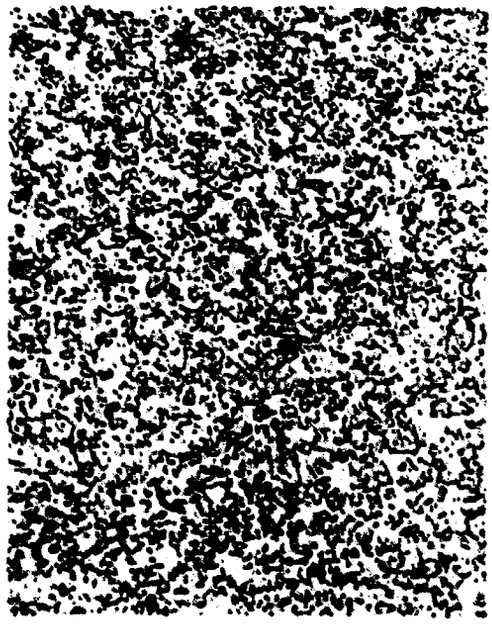

A-8084 250 X Mag.

c) Grain Structure - As Machined

Unclassified

FIGURE 55 (U) Microstructure of W-2% ThO_2 Throat Insert

largest amount of erosion occurred near the injector head, where the chamber liner burned through to the insulating plastic in one small area. Streaking by the injector resulted in extensive erosion of the chamber liner and deep erosion pits at the throat section, (see Figue 56). Radial cracking of the PTB and the porous black deposit are also evident in this photograph.

(7) Subscale Chamber S/N 7

(U) Unit S/N 7 was planned to accumulate a total duration of 600 seconds at a chamber pressure of 200 psia. The first two runs, somewhat abbreviated due to low combustion performance, were a 7.5 and 11.5 second duration respectively. No erosion occurred in the chamber or throat region during these pulses.

(U) During the third pulse, Run 066, the throat failed as reflected by a rapid drop in chamber pressure from approximately 200 psia to less than 100 psia at about 2 seconds of elapsed time. During this run, the Grafoil throat structure failed. Following the test, much of the Grafoil material was observed extending out of the nozzle exit cone as shown in Figure 57. This type of failure was unexpected, since two previous tests of 7.5 and 11.5 second durations had been conducted on this chamber with no throat erosion and no apparent damage.

(U) The throat insert was fabricated from hot-bonded Grafoil (hot pressed pyrolytic graphite foil) with the "a-b" planes oriented radially. The hot-bonded Grafoil delaminated, as illustrated in Figure 58, and the exit portion of the insert was blown away from the motor. Firing time on this motor was too short to develop significant erosion of the chamber liner or the nozzle throat insert. All of the material removed from the insert resulted from mechanical failure.

(U) Subsequent to the design and fabrication of this unit, mechanical property tests were performed on the hot-bonded Grafoil material. Tensile strength of the "c" direction (across the "a-b" planes) was found to be extremely low, less than 200 psi. Thus, while the hot-bonded Grafoil appears as a solid block, it is equivalent to very thin, stacked pyrolytic graphite sheets. Provision for support of the insert, similar to a "stacked washer" arrangement for a nozzle throat insert, would greatly reduce the possibility of mechanical failure, but this compromises the advantages of the flexible nature of this material; and performance would be less than, or certainly no better than, conventional plate pyrolytic graphite. However, this material has greater potential for fabrication in very large sizes than does conventional plate pyrolytic graphite.

(8) Subscale Chamber S/N 8

(C) Subscale thrust chamber S/N 8 was tested at a chamber pressure of 200 psia. Three tests accumulating a total firing time of 145 seconds were conducted. This unit incorporated a one-piece CGW high density graphite chamber liner and throat insert. During the first two pulses, Runs 060 and 061 characteristic velocities of 6020 and 5830 fps respectively, were observed. Total erosion of 0.0015 inches was observed. During the last pulse, Run 062, an initial characteristic velocity of 6550 fps was realized. Chamber pressure, initially 209 psia, dropped off to 146 psia at 125 seconds reflecting throat erosion. An average throat diameter erosion during this pulse of 0.1605 inches was observed. Two erosion streaks in the throat insert were observed reflecting

08871-8 1.7X Mag. Unclassified

FIGURE 56 (U) Unit S/N 6 Sectioned PTB Chamber and Throat Assembly

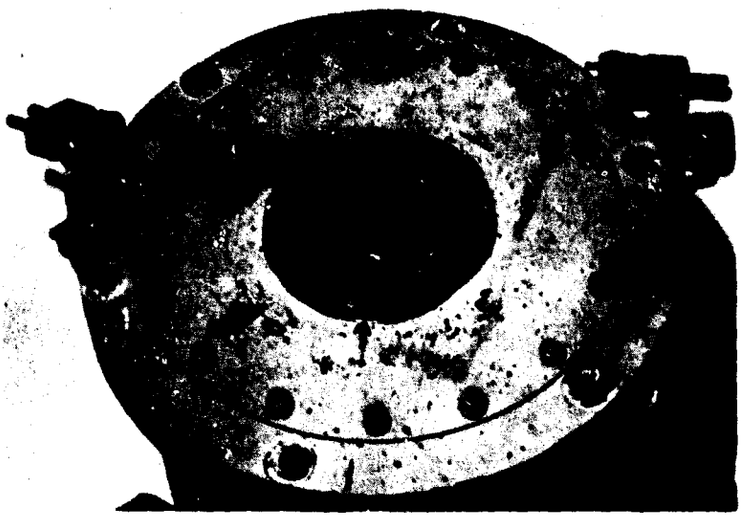

Unclassified

FIGURE 57 (U) Exit of Unit S/N 7 After Test

08871-4 1.8S Mag.

Unclassified

FIGURE 58 (U) Unit S/N 7 Sectioned Hot-Bonded Grafoil Throat Insert After Test

08871-2 0.7X Mag.

FIGURE 59 (U) Axial Section of Unit S/N 8 After Test Unclassified

injector streaking. No additional tests were conducted on this unit since severe erosion of the upstream end of the chamber occurred similar to that discussed previously.

(U) The chamber liner and nozzle throat survived test firing without cracking. Half-sections of this motor illustrating the post-fired condition are shown in Figure 59. Near the injector area, extensive erosion resulted in puncturing the chamber liner and burn through of the insulating plastic. Streaking of the injector was evident for localized areas of high erosion on the lower sections of the chamber liner and the nozzle throat section. Some changes in the throat contour and localized erosion areas were observed.

(U) Except for the erosion, there were no other changes evident in the CGW subsequent to test firing. The exposed surfaces were free of deposits or marked discoloration. Condition of the surfaces suggests that erosion was due to chemical reaction and that the reaction products were volatile at engine temperatures, or removed by the propellant gases.

b. Design Concept Performance

(U) The design approach employed in most subscale thrust chamber configurations was to simply (1) install the liner components into a heat sink structure, (2) provide adequate support for the liner materials, (3) consider thermal expansion by providing gaps where necessary as predicted based upon heat transfer and stress analysis, and (4) provide adequate insulation for the steel housing. This approach was used for units S/N 2, 3, 5, 6, 7, and 8. In these designs except for unit S/N 7 (see Subsection 4a), design concept performance was adequate. Design concept performance of units S/N 1 and 4 are discussed subsequently.

(U) Thrust chamber S/N 1 employed a prestressed tantalum carbide throat design concept. The intent was to match thermal expansion of the throat insert with the support structure thus eliminating thermal shock failure of the throat insert during transient heating. However, due to the complexity of the insert and large number of integral components and corresponding inter-reactions, it is difficult to positively identify the source of fracture.

(U) Most evidence leads to the conclusion that cracking in the TaC insert in unit S/N 1 occurred as a direct result of the circumferential fracture in the tungsten. It is believed that fracture occurred late in the firing, at probably about 50 seconds after ignition. The several facts which support this conclusion are (1) the erosion was extremely slight around cracks in TaC which intersected the I. D. and (2) the crack in the tungsten was characteristic of a high temperature failure. It is also probable that a more catastrophic fracture of the TaC would have occurred at lower temperatures when the thermal stresses were higher.

(U) Fifty seconds after ignition the calculated thermal hoop stresses in the TaC insert in unit S/N 1 have decreased about 30% to a level where the support from the prestressing ring is not very important. At this time prestressing provides only a 10% reduction in the stresses. However, the sudden loss of this prestress by failure in the tungsten would undoubtedly cause fracture in the TaC.

(U) Thrust chamber S/N 4 was designed to take advantage of pyrolytic graphite's high thermal conductivity, as discussed previously. During Run 055, there was a temperature drop in the "a-b" plane direction (see Figure 60) as expected. Temperatures at sections B-B and E-E in the chamber (see Figure 60) were at the approximate level expected (see Figures 10 and 22). The uniformity of the temperatures at B2 and B3 reflect the effect of heat conduction from the throat insert as expected.

(U) During Run 056, the second test of unit S/N 4, thermocouple A1 appears to have malfunctioned early in the test (see Figure 61). The measured value of C1 (approximately 4000°F) is inconsistant with the theoretical predictions (see Figure 21). Temperature data at Section B-B (B2 and B3) however, were greater than predicted by analysis (Figure 21). This was due to the bi-directional heating of the CGW graphite heat sink.

(U) During the third test of unit S/N 4 (Run 057), temperatures at locations B and in the throat were approximately the same (see Figures 62 and 63). This reflects the loss in the pyrolytic graphite sleeve in the chamber thus affecting the heat sink characteristics. The results of the first tests (Runs 055 and 056), however, indicated the success of the design approach.

(U) The desire to observe temperatures at several locations in each unit were two-fold: (1) to monitor the test and to provide some insight into modes of failure should a major failure occur, and (2) to provide a thermal gradieny in a given material so that thermal properties could be evaluated. The latter case, however, could not be evaluated for any of the tests since random failure of thermocouple probes prevented observation of sufficient data.

c. Throat Insert Erosion

(U) To evaluate the relative erosion characteristics of the throat insert materials for rocket thrust chambers, several materials were tested. While adequate thermal protection is necessary to provide structural integrity during a specific duty cycle, erosion of the nozzle throat is a strong determinent of thrust level variations and losses during a mission. For those applications in which maintenance of thrust level is of paramount important in performing a certain mission, materials are required which suffer minimum surface degradation when exposed to the elevated temperature of the propellant gases. Surface degradation may occur by either reaching the melting or subliming temperature of the material, or by chemical reaction of the specific material with the species of the propellant gases.

(U) An attempt was made to correlate erosion as a function of temperature and pressure by reducing the test data to a comparable form. To do this, the following assumptions were made:

A. The surface temperature of the various materials was obtained by extrapolating measurements of thermocouples installed near the surface by means of an IBM computer heat transfer program. Specifically, the combustion efficiency, chamber pressure, and temperature, from which the adiabatic wall temperature and convective heat transfer coefficient were calculated, were obtained from test results. The adiabatic wall temperature, convective heat transfer coefficient, and material thermal properties were used to obtain temperature gradients through the wall. Agreement of the predicted and measured thermocouple temperature was used at a reasonable assurance that the predicted surface temperature was close to the actual surface temperature.

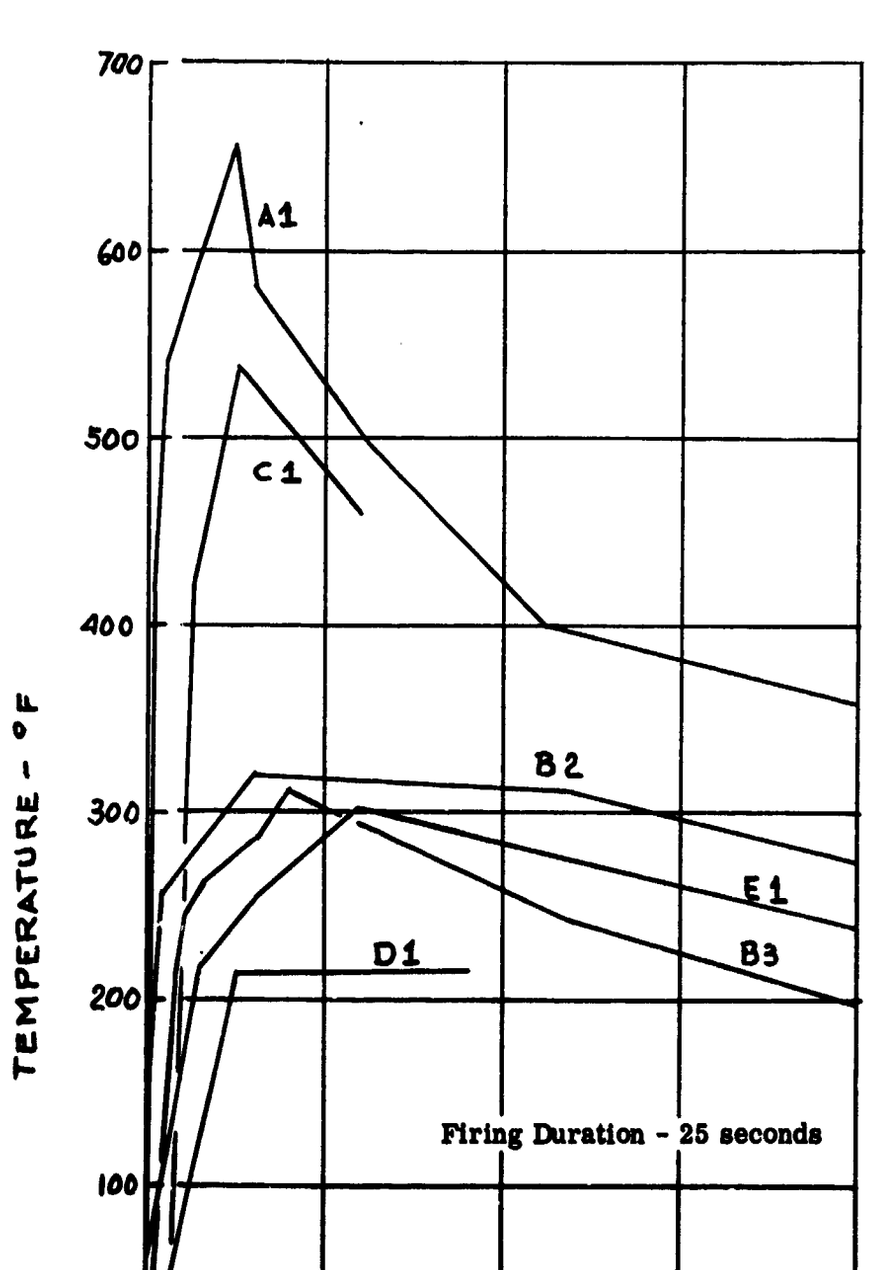

FIGURE 60 (U) Thermocouple Data, Run 055

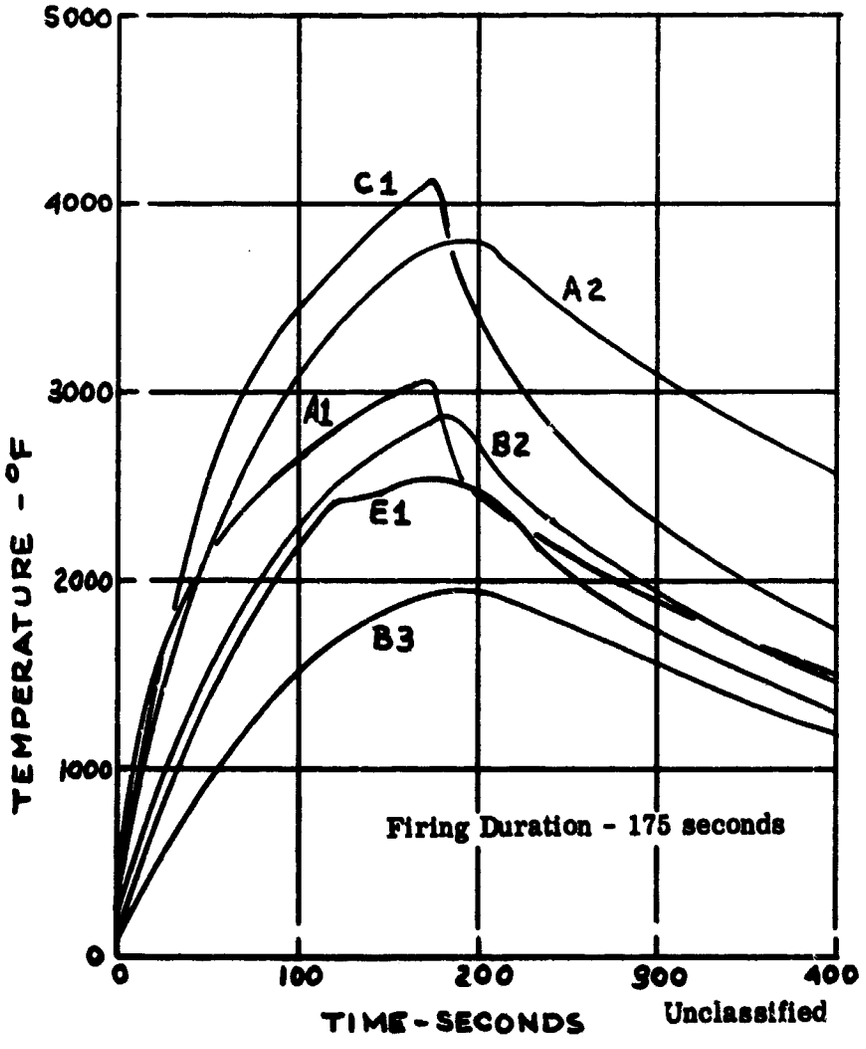

FIGURE 61 (U) Thermocouple Data, Run 056

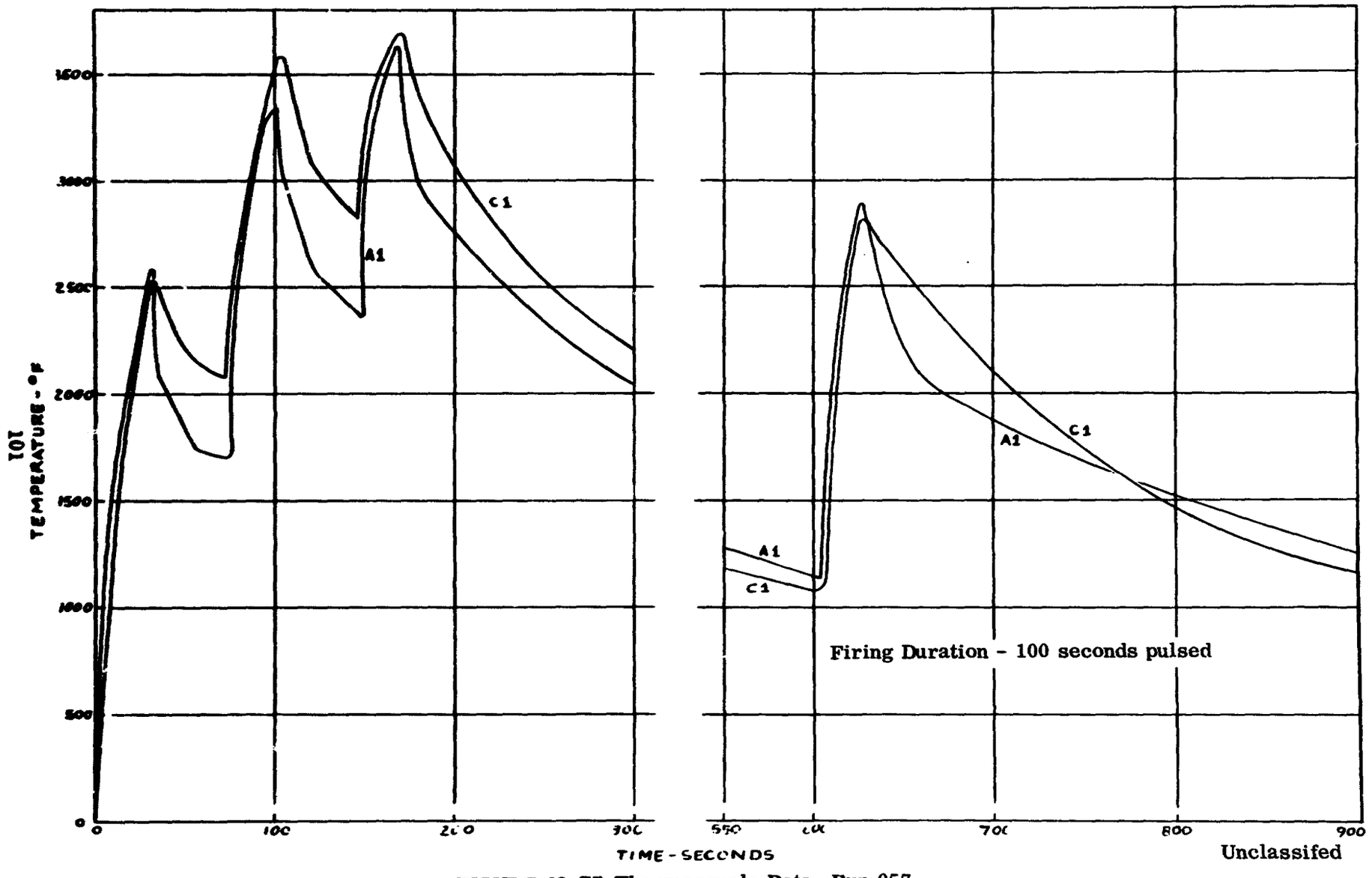

FIGURE 62 (U) Thermocouple Data, Run 057

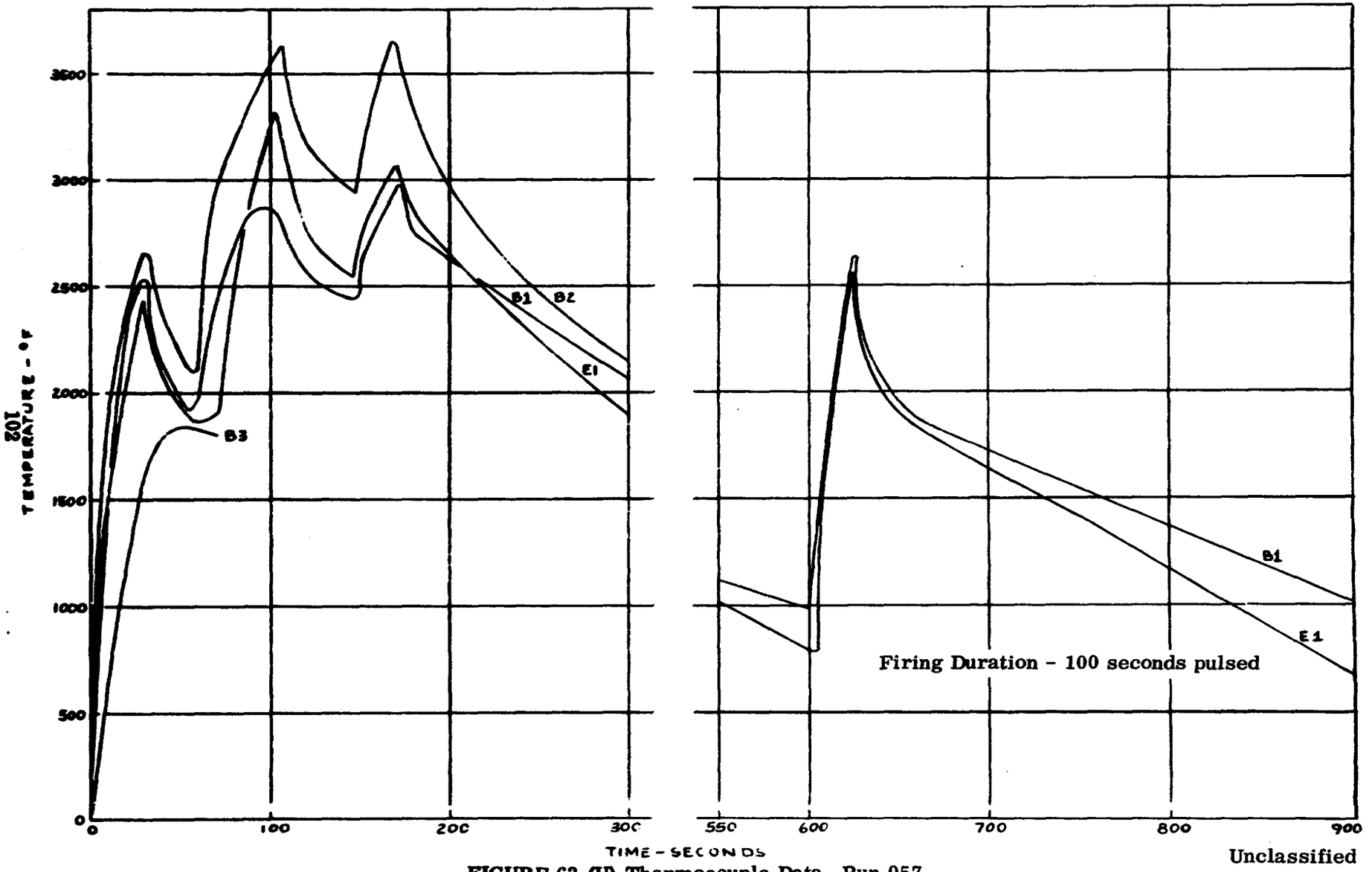

Unclassified

FIGURE 63 (U) Thermocouple Data, Run 057

B. The erosion rate was calculated using the variation in throat diameter which in turn was calculated from instantaneous thrust level and chamber pressure.

(U) The instantaneous throat erosion was calculated by using the thrust equation:

$$F = C_F A^* P_c$$

where F = thrust
C_F = thrust coefficient
A^* = throat area
P_c = chamber pressure

(U) For a perfectly expanded nozzle, the throat coefficient can be defined as:

$$C_F = Cf(\gamma)\left[1 - \left(\frac{Pa}{Pc}\right)^{\frac{\gamma-1}{\gamma}}\right]^{\frac{1}{2}}$$

where C = constant
$f(\gamma)$ = function of γ
γ = ratio of gas specific heat
P_a = ambient pressure, 14.5 psia

(U) At the relatively low chamber pressure considered in these tests, the affects of small variation in γ due to changes in combustion have negligible influence. Thus, letting γ equal 1.30, the thrust equation reduces to:

$$F = C\left[1 - \left(\frac{14.5}{Pc}\right)^{0.231}\right]^{\frac{1}{2}} A^* P_c$$

(U) The simplified thrust equation was used to calcualte throat diameter change during each test run as follows:

A. Calculate C for a given test run using A* measured prior to run, and P_c and F after start-up transients die out (approximately 3 seconds). This assumes that no change in throat area occurs in 3 seconds.

B. Calculate A* and thus, throat diameter, for other times during the test run using C determined at 3 seconds, and the instantaneous F and P_c observed at the desired time.

(U) The variations in throat diameter D*, chamber pressure P_c, and throat surface temperature Tw are given in Figure 64 through 67 as a function of time for the various subscale thrust chambers considered. (Only data which yielded reasonable results were considered). For comparison purposes, the variations in throat diameter during firing for the units S/N 1, TaC; S/N 2, HfC + C; S/N 6, PTB; and S/N 8, CGW, are plotted in Figure 68 as a function of time for certain runs.

(U) The results indicate the carbides experienced lower erosion than did the graphite materials. The significance of this results is discussed in detail in the Discussion of Results section (see Section VII).

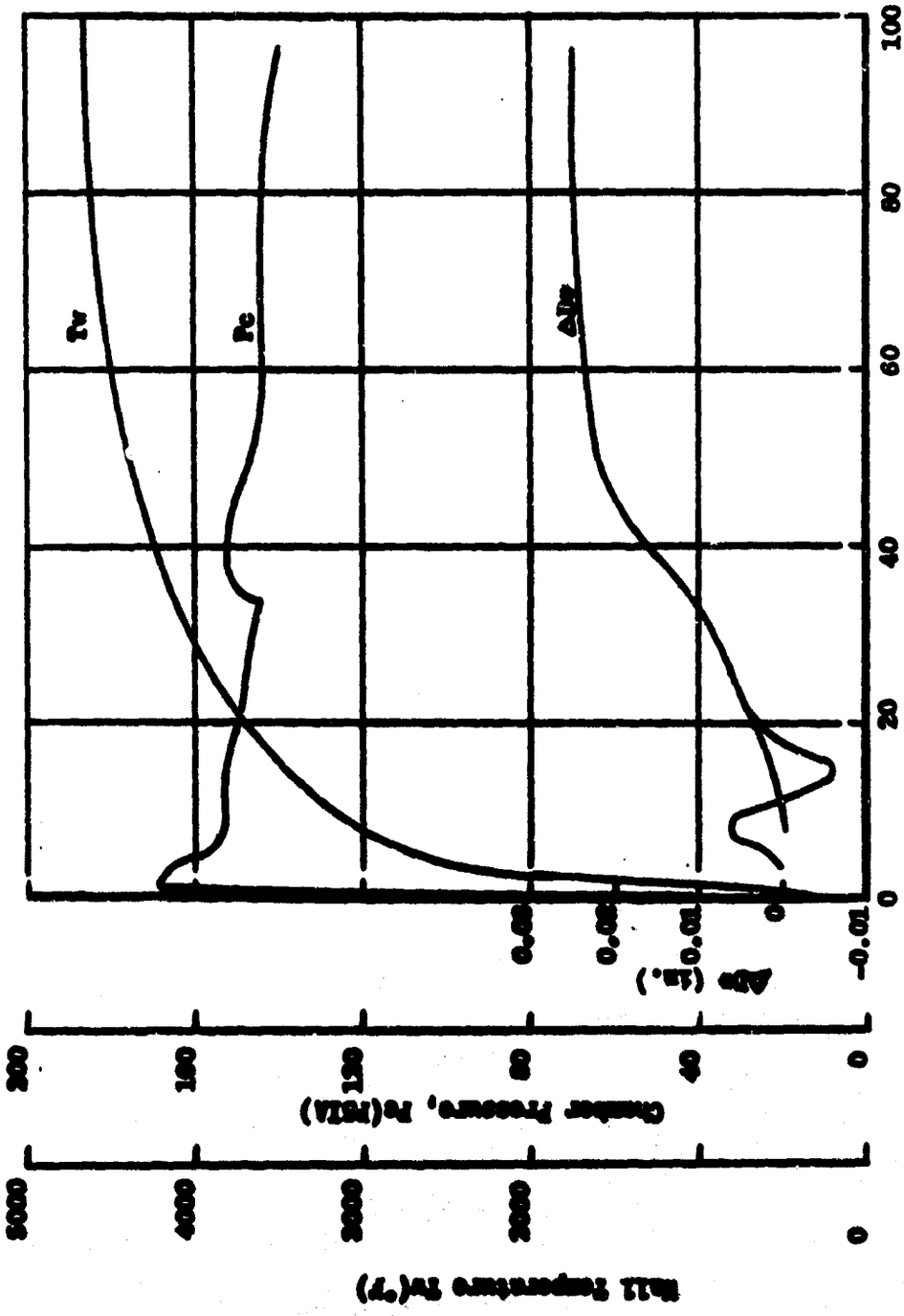

FIGURE 64 (U) Unit S/N 1 Data: Run 060

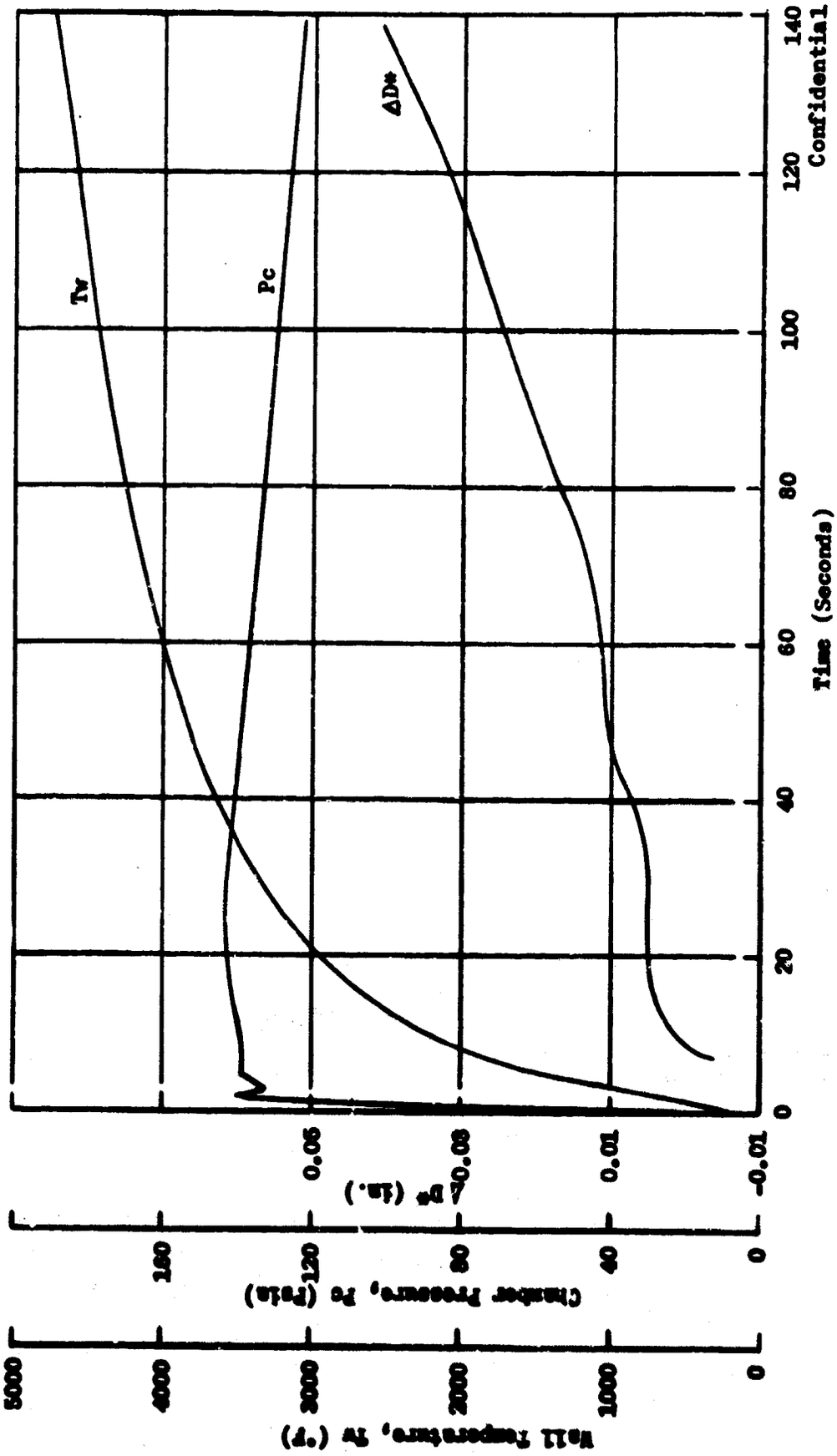

FIGURE 65 (U) Unit S/N 2 Data: Run 049

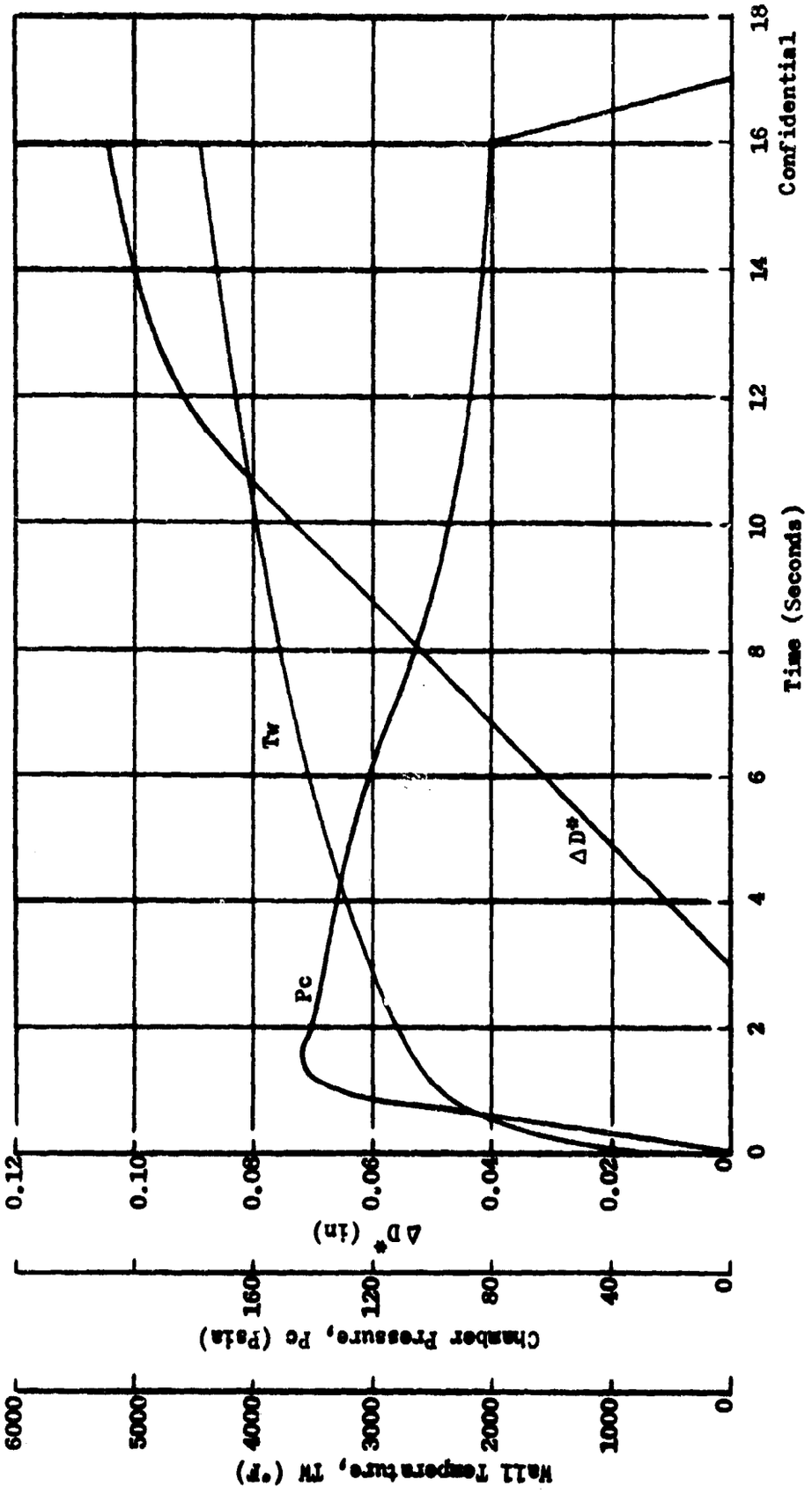

FIGURE 66 (U) Unit S/N 6 Data: Run 065

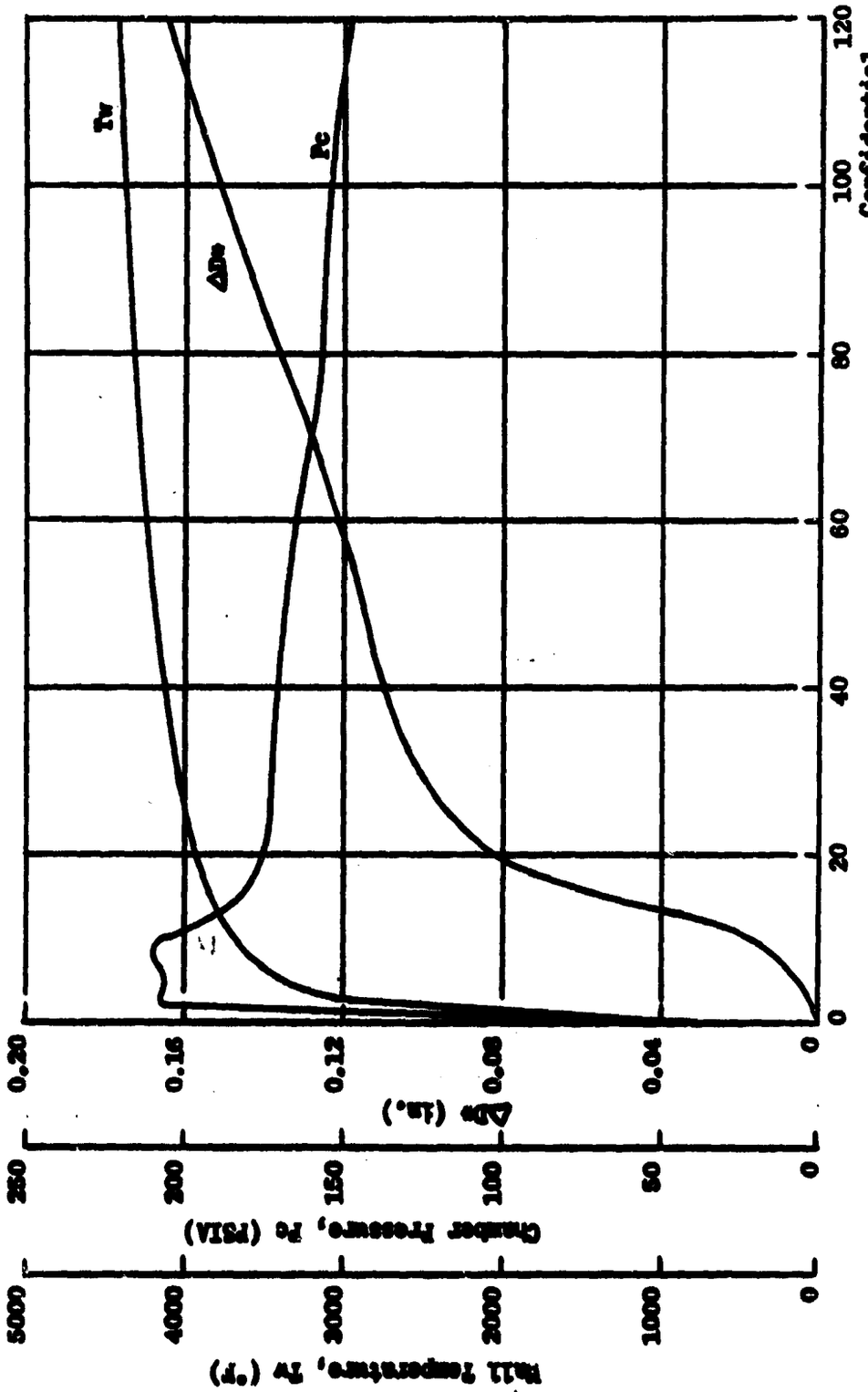

FIGURE 67 (U) Unit S/N 8 Data: Run 062

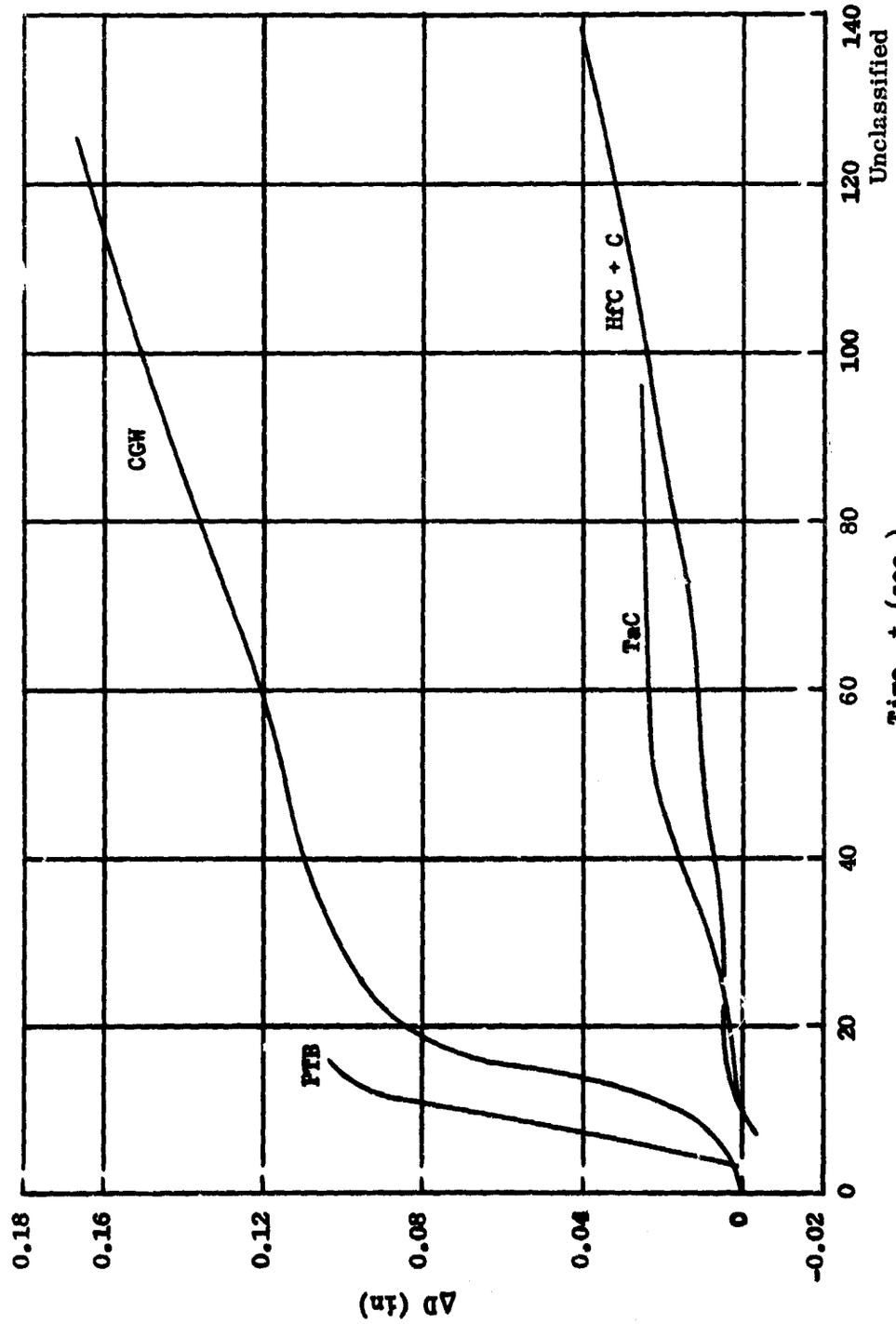

FIGURE 68 (U) Comparison of Diametral Erosion

SECTION VI

FULL SCALE THRUST CHAMBER EVALUATION

(U) The full scale thrust chamber evaluation activities incorporated the results of the materials survey and subscale thrust chamber evaluation into the design and fabrication of three full size thrust chambers. Post firing evaluation was performed following tests at the Air Force Rocket Propulsion Laboratory. The details of the thrust chamber concept evaluation are discussed in this section.

1. DESIGN AND FABRICATION

(U) The design requirements were specified to be compatible with available injectors and test facilities at the Air Force Rocket Propulsion Laboratory. Materials for the first two full scale thrust chambers were selected based upon the results of the Phase I technical activity and the present state-of-the-art for the design and fabrication of the material and design concepts examined. Thompsine Tape was selected for the third full scale unit to demonstrate its advantages as an engineering material in ablative designs.

a. Requirements

(U) Design requirements of the full scale chamber evaluation program were specified by the Air Force Rocket Propulsion Laboratory. The propellant combination and operating goals were the same as those of the subscale thrust chamber concept evaluation activity except for the thrust level. Full scale units were designed for a thrust level of 3750 pounds. The performance properites have been presented previously in Section V, Subsection 1a. The duty cycle specified for the full scale designs is presented in Table XIII.

(U) For a chamber pressure of 200 psi and a mixture ratio of 2.0 and an ambient pressure of 13.2 psia, the throat area of 13.9 square inches in a perfectly expanded nozzle will give a thrust of approximately 3750 lbs. This calculation assumes a thrust coefficient which is 97% of the ideal thrust coefficient. The exit area to throat area ratio for perfect expansion is approximately 3.4 inches, thus the nozzle exit area is 43.0 square inches. The characteristic chamber volume is 40 inches.

(U) Knowing the throat diameter, exhaust gas characteristics, chamber pressure, and characteristic velocity, the heat transfer coefficient was calculated by the simplified Bartz equation. Also, by assuming a recovery factor of 0.9 with a C* efficiency of 96%, the adiabatic wall temperature is conservatively calculated at a function of area ratio. These results for the full scale thrust chamber design are presented in Figure 69.

b. Material Selection

(U) Materials for the first two full scale thrust chamber designs were selected based upon the results of the Phase I technical activity and the present state-of-the-art for design and fabrication of the several materials and design concepts examined. As a result, Carb-I-Tex 700 was selected as a throat insert material for the first full scale unit based upon its good performance and design simplicity. The chamber liner material selected was carbon cloth phenolic, tape wrapped at 30° orientation to the chamber centerline.

(U) Pyrolytic graphite incorporated into a heat sink design was selected as a throat insert material for the second full scale unit. A concial "a-b"

Table XIII

Full Scale Test Duty Cycle

Test Duration (Seconds)	Cooldown Period
10	Cool to ambient
60	Cool to ambient
240	Cool to ambient
100	Cool to ambient
12	20 seconds
15	15 seconds
8	Cool to ambient
120	30 seconds
35	Cool to ambient

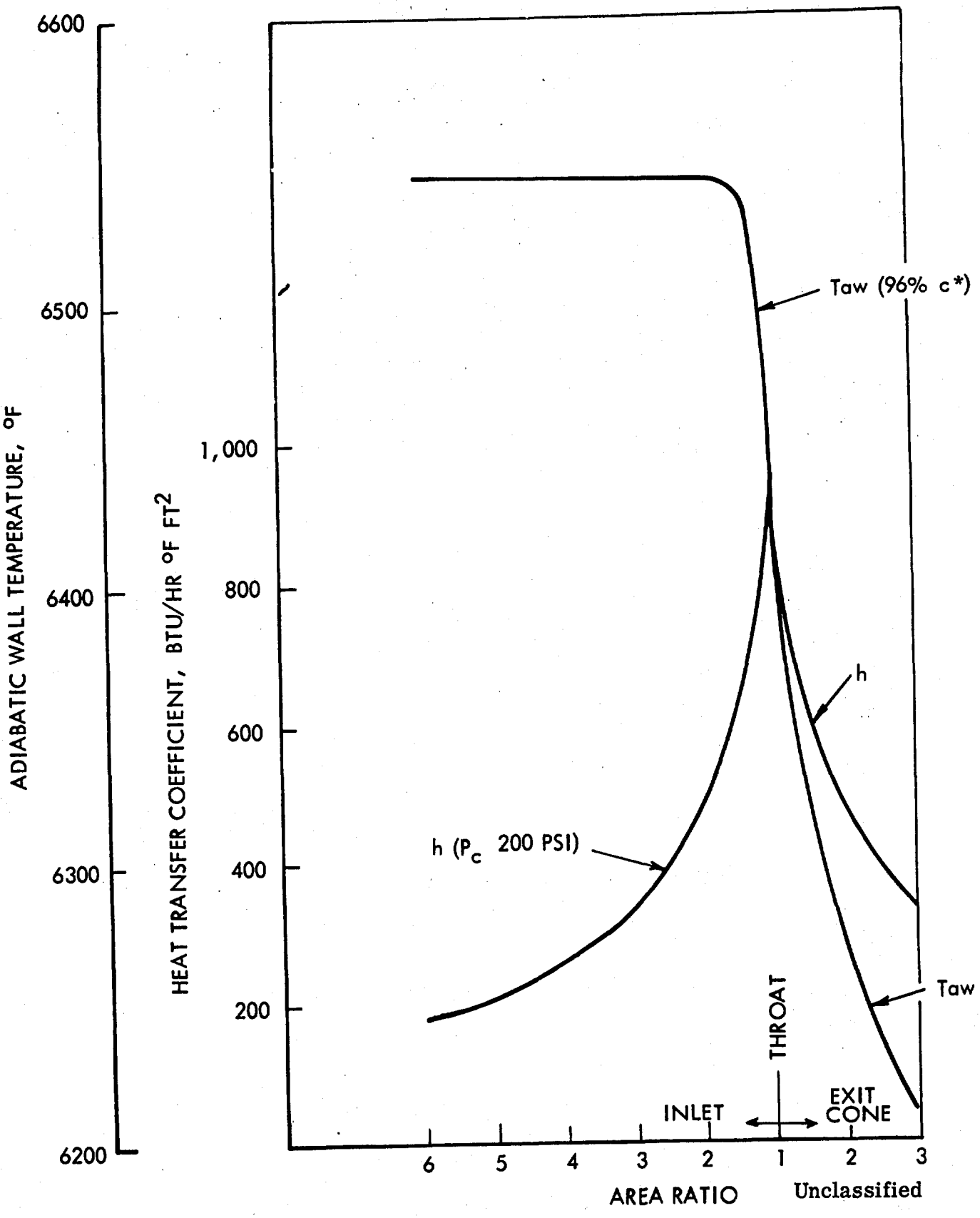

FIGURE 69 (U) HEAT TRANSFER COEFFICIENT AND ADIABATIC WALL TEMPERATURE FULL SCALE DESIGN

plane orientation was used to take advantage of the anisotropic properties of pyrolytic graphite to minimize the surface temperature of the throat insert.

(U) In keeping with the major objective of material and design performance evaluation, the third full scale unit was designed using Thompsine Tape. Thompsine Tape is a material developed by TRW which incorporates a uniquely constructed reinforcement for ablative plastics. The uniqueness of the material lies primarily in the elimination of the need for interface bond lines between the exposed material (gas side) and the insulative material (shell side). This is done by mechanically weaving the two materials together prior to resin impregnation and cure. The two sections are thus an integral part upon curing. Besides giving a much stronger interlaminar integrity, fabrication set-up costs are reduced in half. Secondary advantages which are built into the tape weave permit attainability of high dimetral wrap ratios. This design was selected to provide information relative to both the performance of a non-conventional reinforcement weave pattern and the interface integrity, and to provide broader scope knowledge to the performance of ablative materials in an LF_2/N_2H_4 blend environment.

(U) Material properties used design of the full scale thrust chambers are presented in Table IX. Thompsine Tape properties are reported in conjunction with the design details.

c. Chamber Design

(U) The basic design for all full scale units was an ablative or heat sink design concept. The basic configuration is presented in Figure 70, the design drawing for full scale unit S/N 1. The injector-thrust chamber interface was designed to mate with AFRPL injector.

(U) The chambers were designed with an 8-inch inside diameter for a length of approximately 9.3 inches. The throat diameter was 4.2 inches. The exit diameter was 7.42 inches. The throat convergence and exit cone half angles were 40 and 15 degrees respectively. A compound throat radius of curvature was employed to yield a smooth contour transition at this location. Over-all thrust chamber length was 19.5 inches.

(U) The three full scale thrust chamber designs are presented in Figures 70 through 72. Radial thermocouple positions are shown in each figure. Materials are also presented in these figures.

(1) Full Scale Chamber S/N 1

(U) The details of the full scale unit S/N 1 design are shown in Figure 70. The chamber liner material was a carbon cloth phenolic oriented 30 degrees to the chamber centerline. The throat insert material was Carb-I-Tex 700 prepyrolyzed graphite cloth oriented perpendicular to the chamber centerline. The nozzle exit cone material was carbon cloth phenolic oriented 40 degrees to the chamber centerline. A 0.25 inch thick carbon cloth phenolic insulation was provided on the outside surface of the throat insert. Silica phenolic insulation was provided between the chamber components and the steel shell.

(U) A one-dimensional heat transfer analysis was conducted at the throat location. The results of this analysis are presented in Figure 73. For a 240

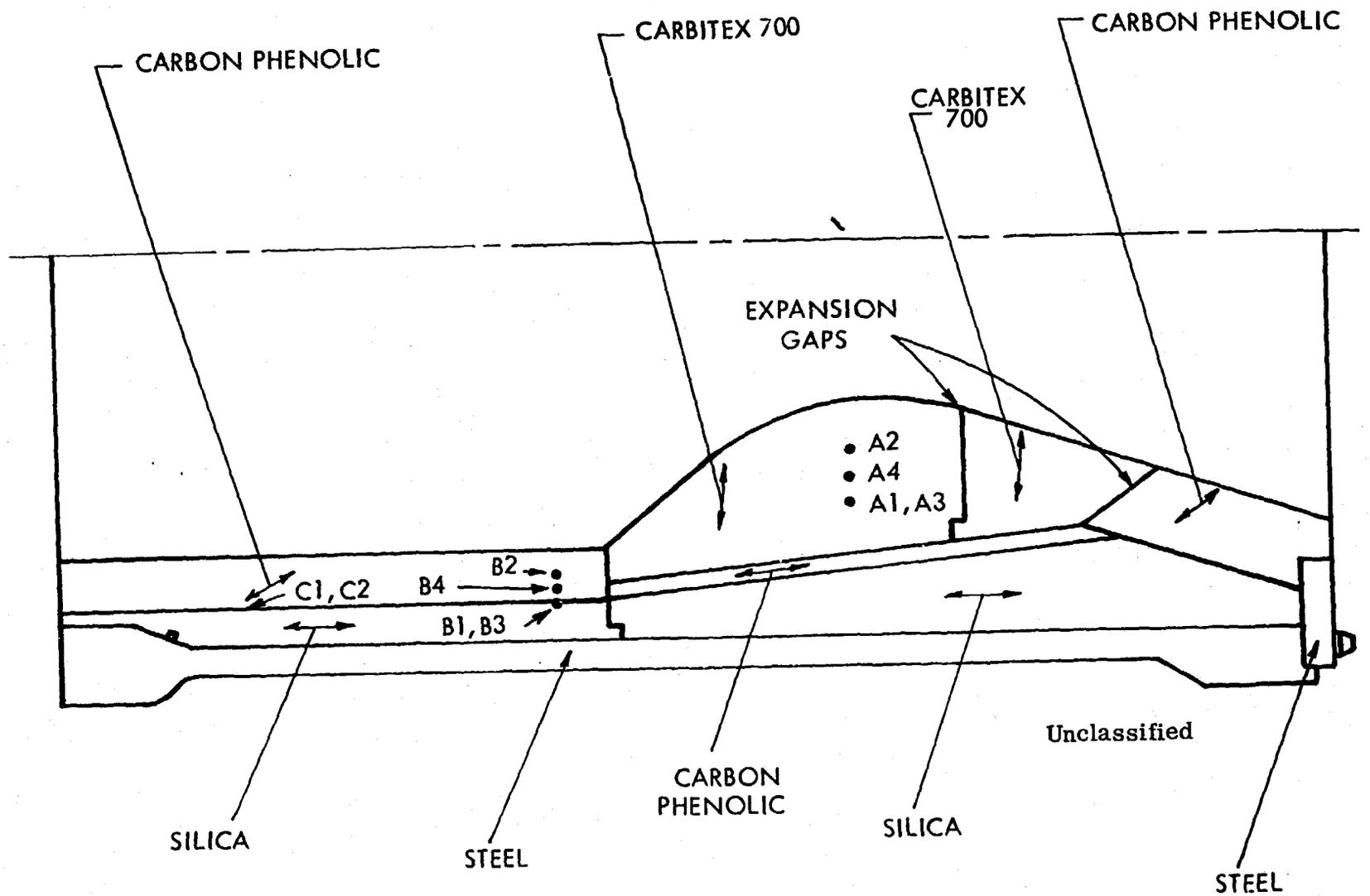

FIGURE 70 (U) FULL SCALE THRUST CHAMBER S/N 1

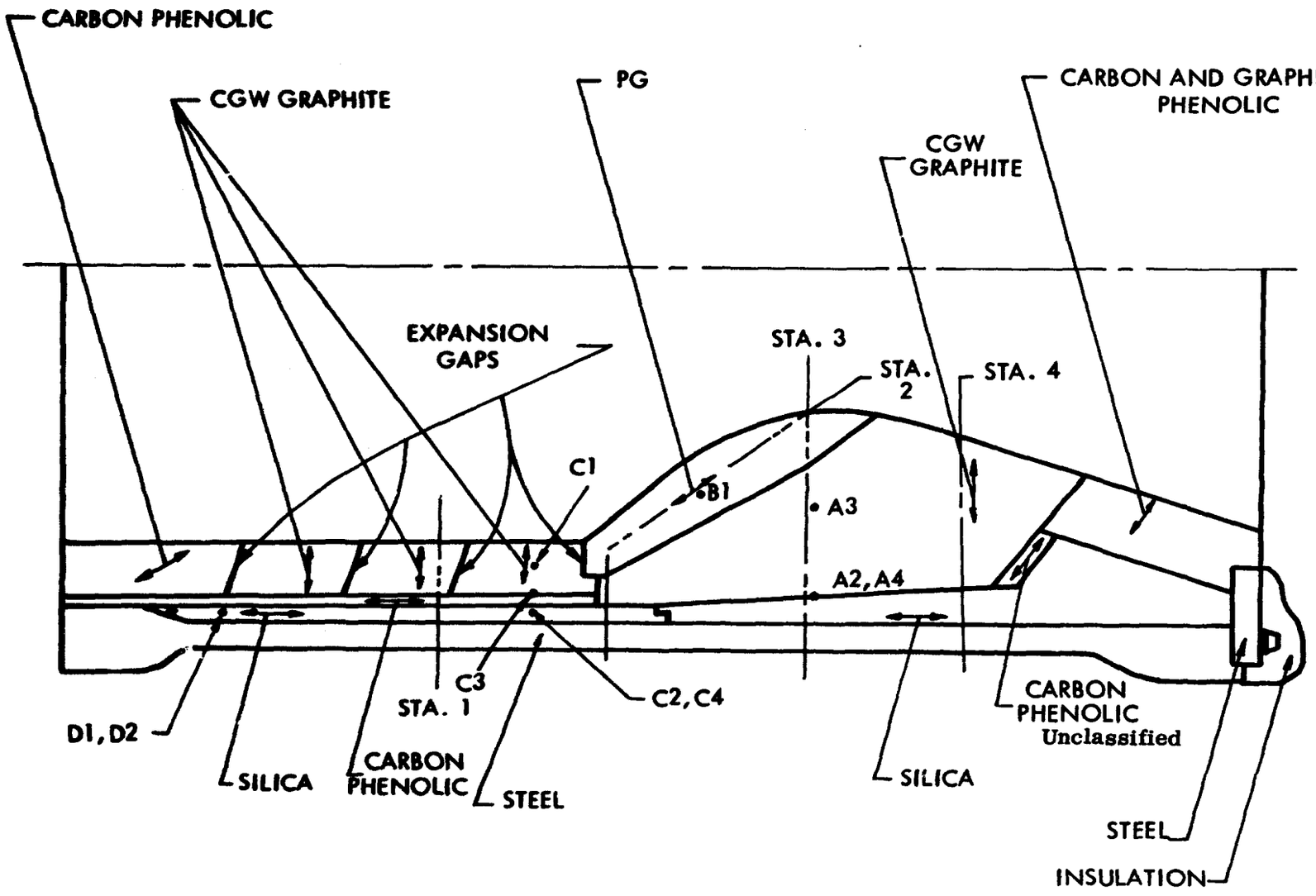

FIGURE 71 (U) FULL SCALE THRUST CHAMBER S/N 2

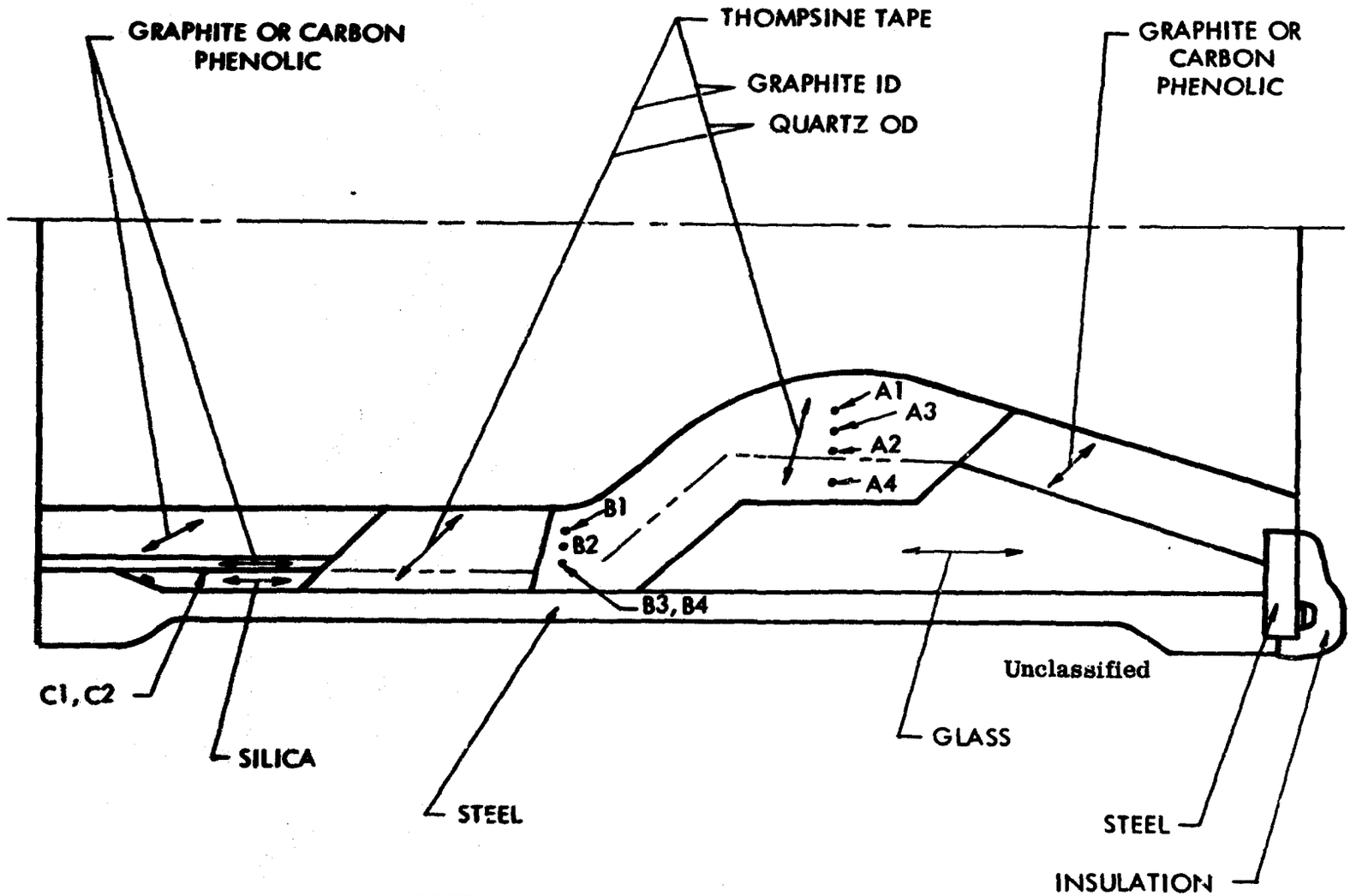

FIGURE 72 (U) FULL SCALE THRUST CHAMBER S/N 3

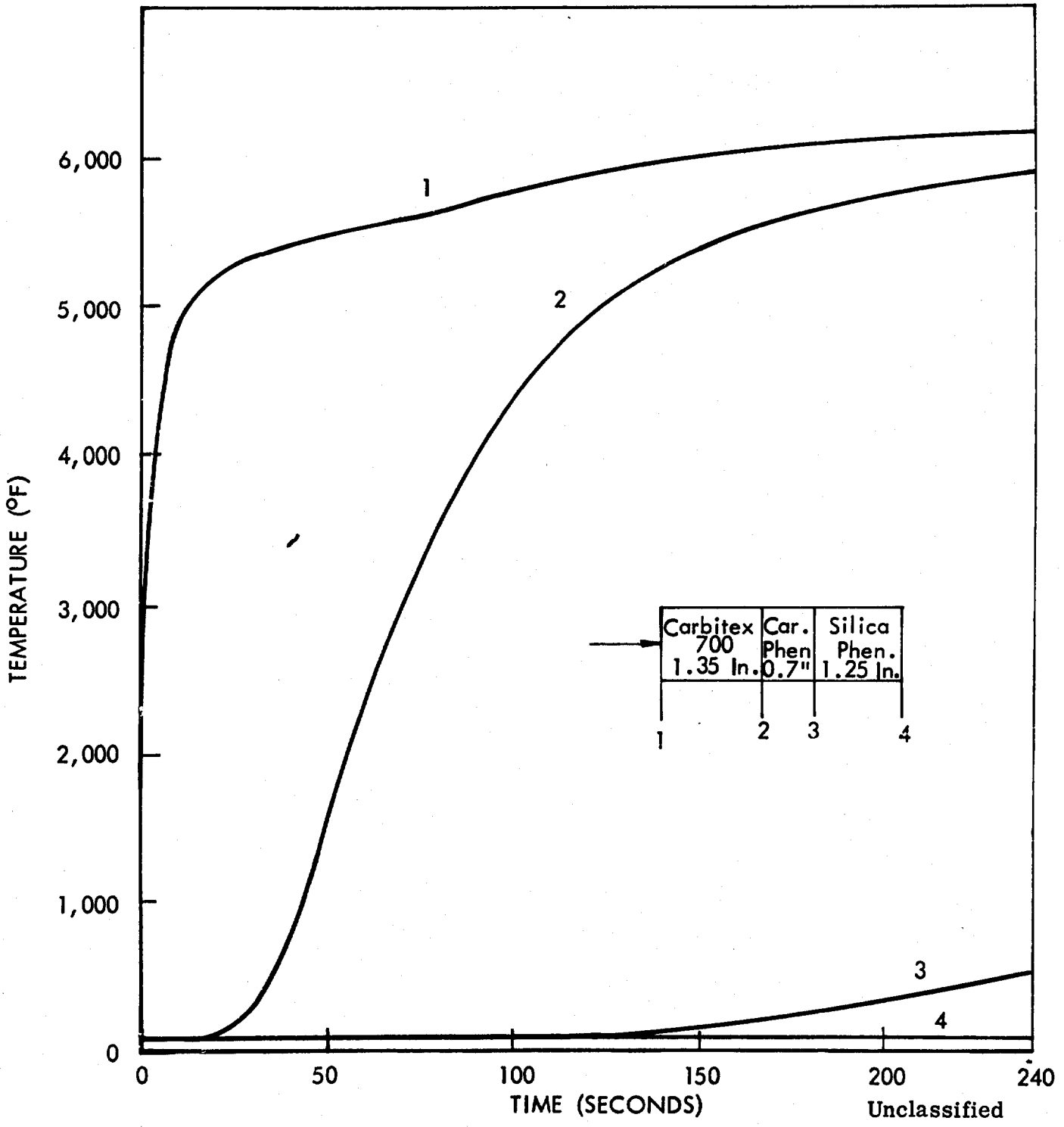

FIGURE 73 (U) PREDICTED TEMPERATURE DISTRIBUTION AT THROAT FOR UNIT S/N 1

second pulse, the maximum predicted temperature of the steel is less than 400°F. Since 240 seconds was the maximum time for any run (including pulsing duty cycles), the steel structure was predicted to maintain its low temperature characteristics. Also, after the first pulse the insulation char will reduce the heat transfer to the steel. Phenolic insulation was greater in the chamber than at the throat locations, therefore, is deemed adequate for the proposed duty cycle.

(U) Thermal expansion of the throat insert was calculated for the mean temperature of the Carb-I-Tex 700 insert at 240 seconds. Total axial expansion of 0.041 inches was predicted. A total axial gap for thermal growth of 0.038 inches was provided in the design and is shown in Figure 70. A lap joint was utilized between the two throat insert pieces. The carbon cloth exit cone was designed to incorporate a mechanical retention at the aft end. Although thermal expansion gaps were provided, the thrust chamber components were conservatively sized to carry all predicted thermal loading for the design with no expansion gaps.

(U) Thermocouples locations are also shown in Figure 70. The approach was to monitor temperatures at the throat location and two chamber locations. Ten thermocouples including four tungsten/tungsten 26% rhenium and six chromel alumel thermocouples were utilized.

(2) Full Scale Chamber S/N 2

(U) The basic thrust chamber configuration is presented in Figure 71. Thermocouple locations were selected to verify predicted heat transfer characteristics and are shown. This design incorporated a pyrolytic graphite throat insert similar to that employed in subscale unit S/N 4. However, a slightly different technique was employed to heat sink the throat. The concially shaped "a-b" planes were designed so that a graphite heat sink located behind the throat insert was utilized.

(U) During the fabrication of the throat insert, the a-b plane orientation in the pyrolytic graphite was modified. The "a-b" planes of pyrolytic graphite were conical near the inside surface of the throat and turn upstream towards an axial orientation near the outside diameter of the part (see Figure 74). This configuration resulted from manufacturing considerations and did not affect the over-all concept performance.

(U) The thrust chamber liner was a composite structure of CGW graphite and carbon cloth. Carbon cloth was employed at the injector-thrust chamber interface to minimize heat transfer to the injector.

(U) The thickness of the carbon cloth inlet was increased over that employed in unit S/N 1 to accommodate erosion based on the test results of unit S/N 1, a similar chamber inlet design. In unit S/N 1, the carbon cloth liner was almost entirely eroded in approximately 373 seconds of elapsed firing time.

(U) The CGW graphite chamber liner was designed in three pieces to minimize the tendency to crack during test. Split line gaps were provided to accommodate thermal expansion of the chamber and throat components. These gaps were sized based upon the maximum expected mean temperature of each graphite component at 240 seconds of elapsed firing time. For these

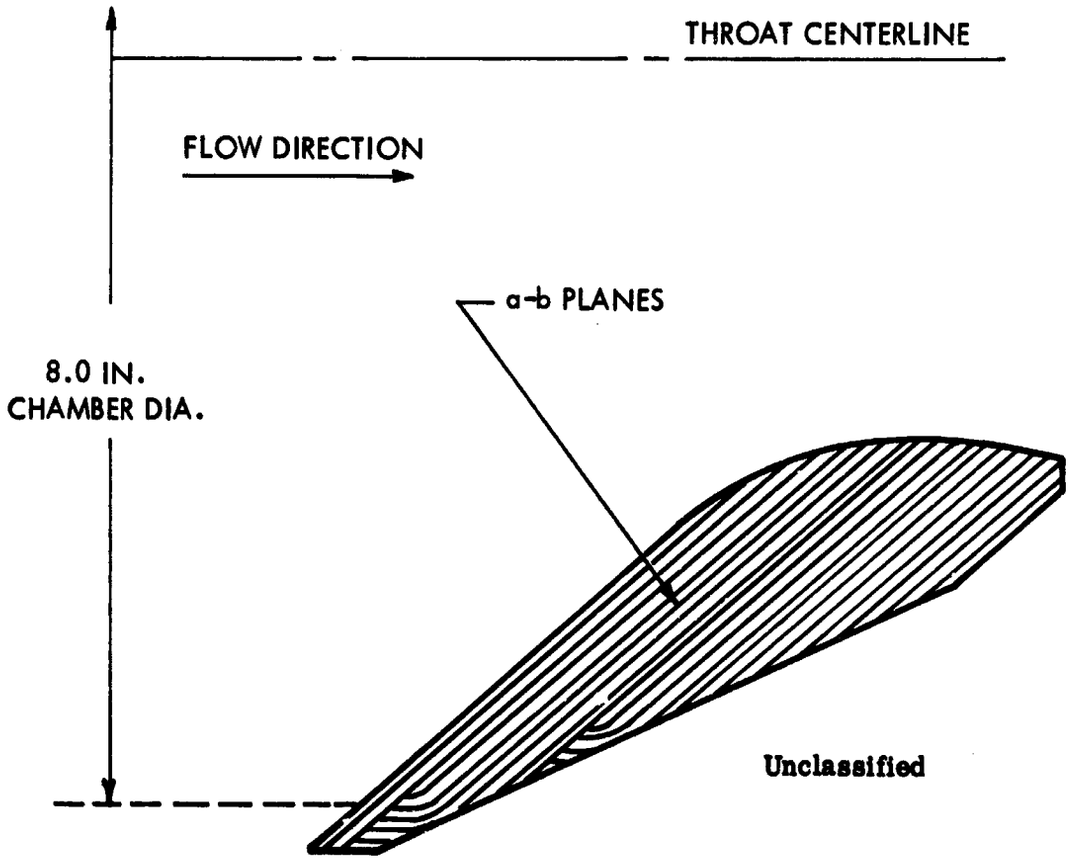

FIGURE 74 (U) PYROLYTIC GRAPHITE THROAT DESIGN FOR UNIT S/N 2

calculations an allowable compressive stress of 9000 psi in the graphite components was used as a design criteria. The gaps were filled with a low modulus material compatible with the design criteria.

(U) The exit cone incorporated alternate carbon and graphite cloth segments to evaluate relative erosion resistance. Each segment was approximately 3/4 inches long.

(U) Silica phenolic insulation was used between chamber line components and the steel shell. In areas where predicted insulator temperatures were in excess of 3200°F (approximate melting temperature of silica), a thin layer of carbon cloth phenolic insulation was employed.

(U) One-dimensional heat transfer analyses were conducted at four locations in the thrust chamber. The location of the composite wall for each analysis is presented in Figure 71 (denoted by Stations 1, 2, 3, and 4).

(U) The results of heat transfer analysis at Station 1, a chamber location, are presented in Figures 75 and 76. The analysis considers a total test time of 240 seconds. Interface temperatures are deemed adequate for this design. As shown, the silica insulation-steel shell interface is predicted to rise to approximately 600°F at 240 seconds which is adequate structurally. The analysis, however, does not consider the heat sink characteristics of the steel shell and, therefore, is conservation.

(U) The heat transfer analyses were run in the throat region to evaluate the heat sink characteristics of the pyrolytic graphite throat and CGW graphite throat support. A one-dimensional heat transfer analysis was conducted at Stations 2, 3, and 4 (Figures 77 through 82 respectively). The run at Station 2 represents heat transfer from the throat in the high conductivity "a-b" plane direction to the CGW heat sink. Stations 3 and 4 are heat transfer analyses in the radial direction at the throat and downstream of the throat insert. The predicted thermal gradients (at Stations 3 and 4, Figures 80 and 82) are almost identical at times of 5, 60, 100 and 240 seconds. This implies that there will be little tendency for axial heat conduction between these two stations. The thermal gradient implies that heating of the CGW graphite structure becomes significant at approximately 60 seconds. The axial gradient in the CGW between the stations is quite small at a given radius for all times. Thus, the predicted surface temperature of the pyrolytic throat as shown in Figures 77 and 79 should be close to the actual temperatures and the heat sink characteristics of the design will be realized. Thermocouple locations were selected such that a comparison with predicted temperatures could be made.

(3) Full Scale Chamber S/N 3

(U) Full scale unit S/N 3 was designed to evaluate and demonstrate the advantages of Thompsine Tape as an engineering material. The design for unit S/N 3 is presented in Figure 72. The design incorporates the steel shell previously used on full scale units S/N 1 and 2. Thermocouple locations are shown.

(U) The design utilized Thompsine Tape and conventional phenolic materials in all ablative thrust chamber configuration. The upstream portion of the thrust chamber (adjacent to the injector) utilized a liner of graphite phenolic tape oriented 30 degrees to the thrust chamber centerline, and subsequently

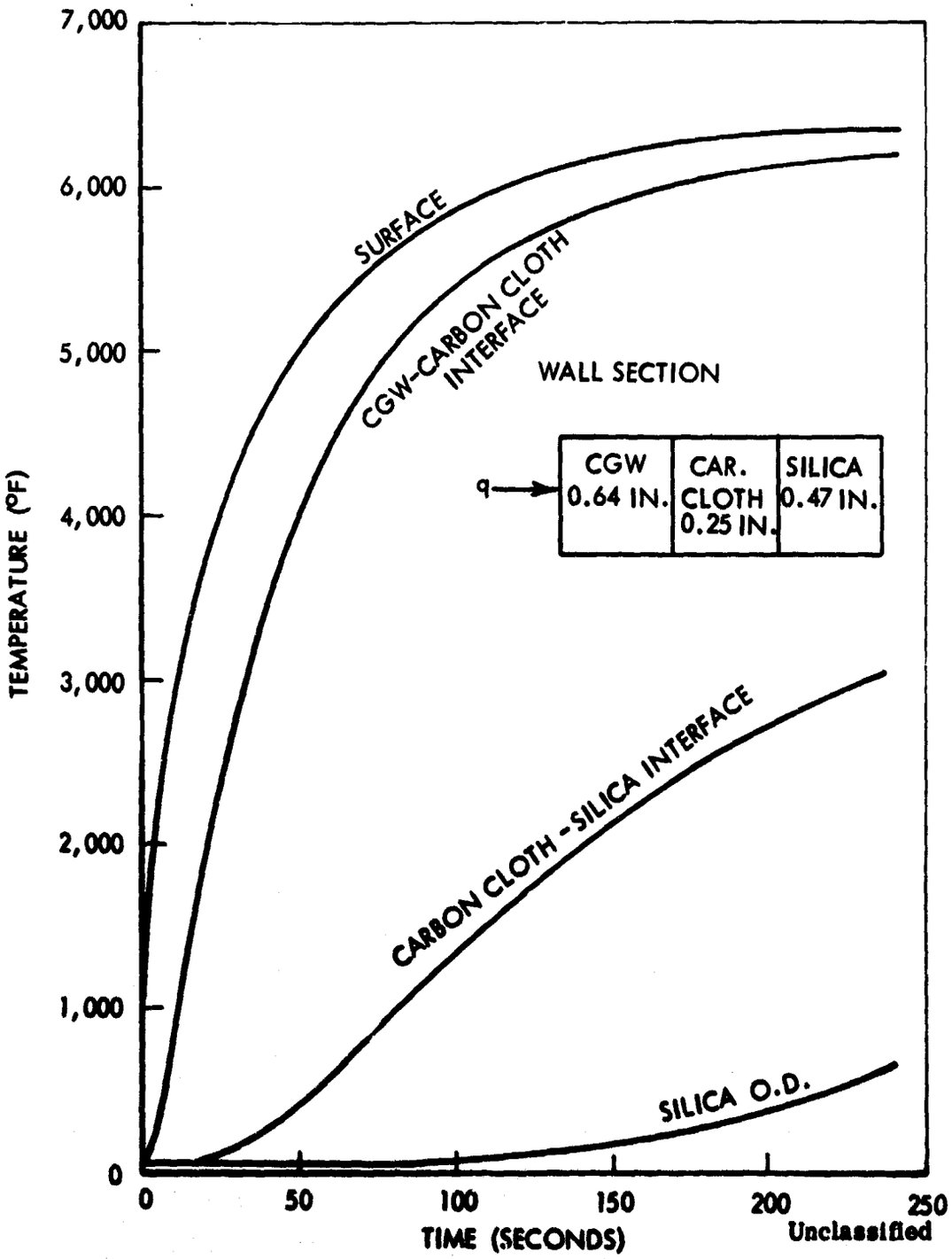

FIGURE 75 (U) PREDICTED TEMPERATURE DISTRIBUTION AT STATION 1 FOR UNIT S/N 2

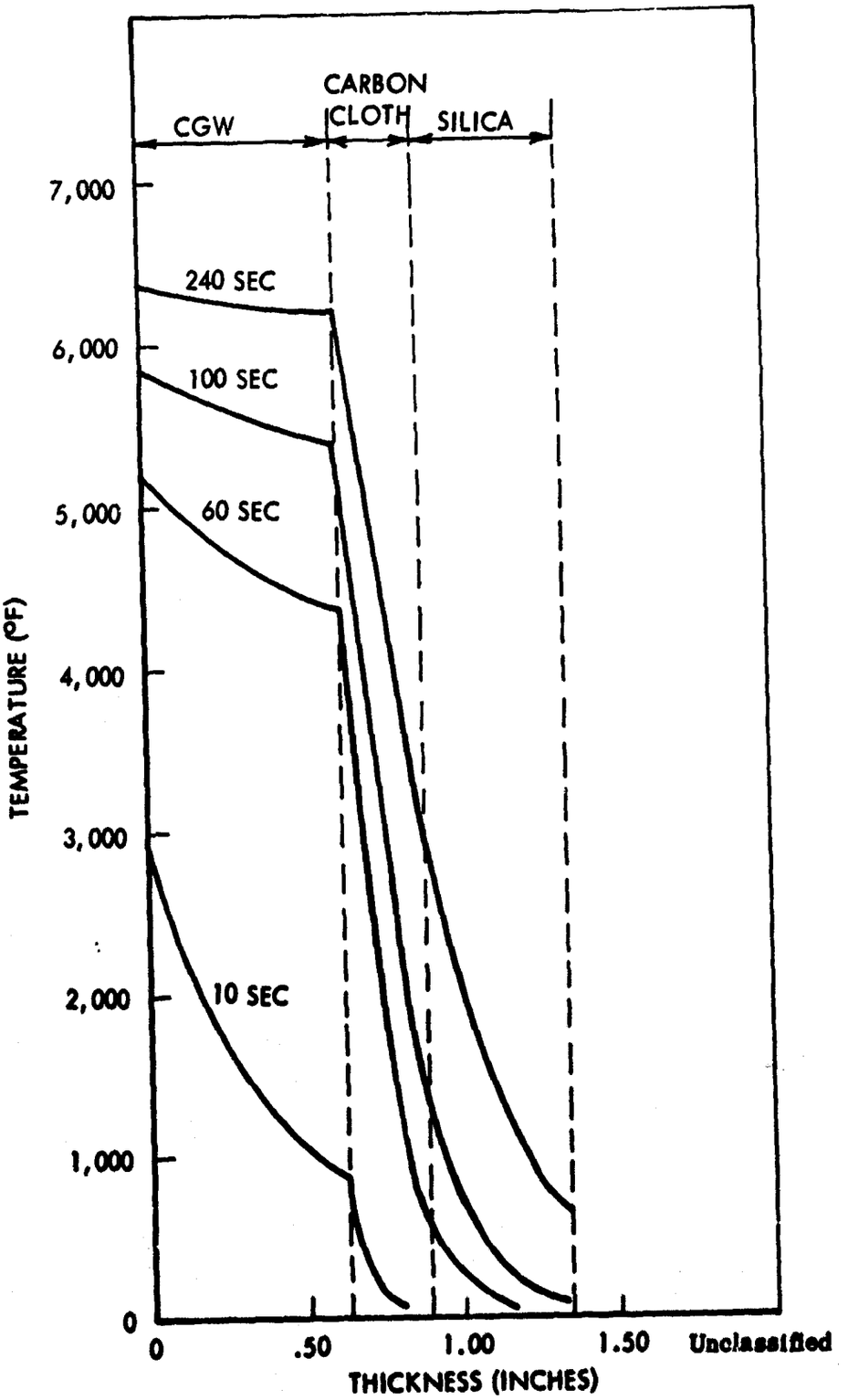

FIGURE 76 (U) PREDICTED TEMPERATURE PROFILE AT STATION 1: FULL SCALE UNIT S/N 2

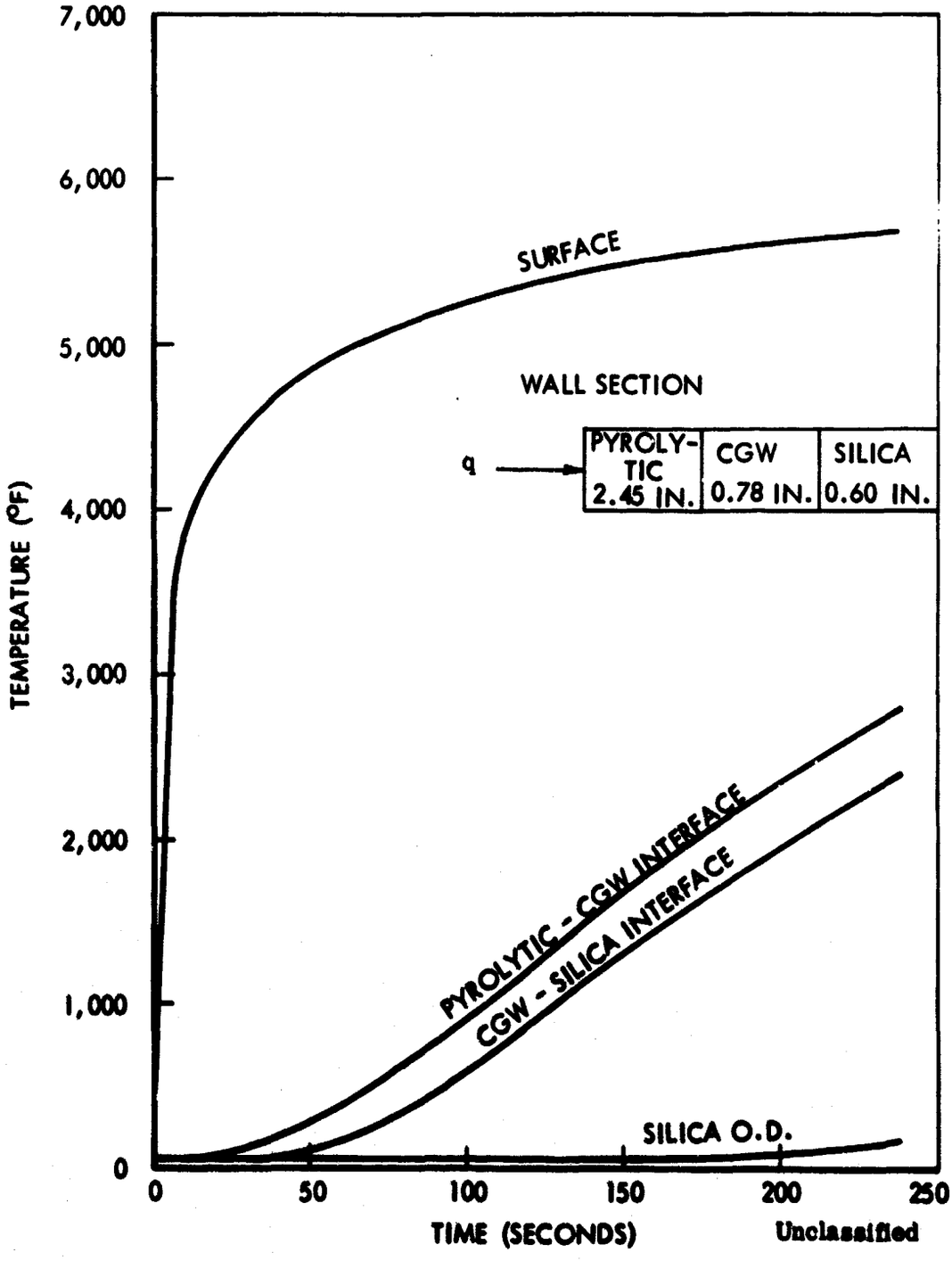

FIGURE 77 (U) PREDICTED TEMPERATURE DISTRIBUTION AT STATION 2: FULL SCALE UNIT S/N 2

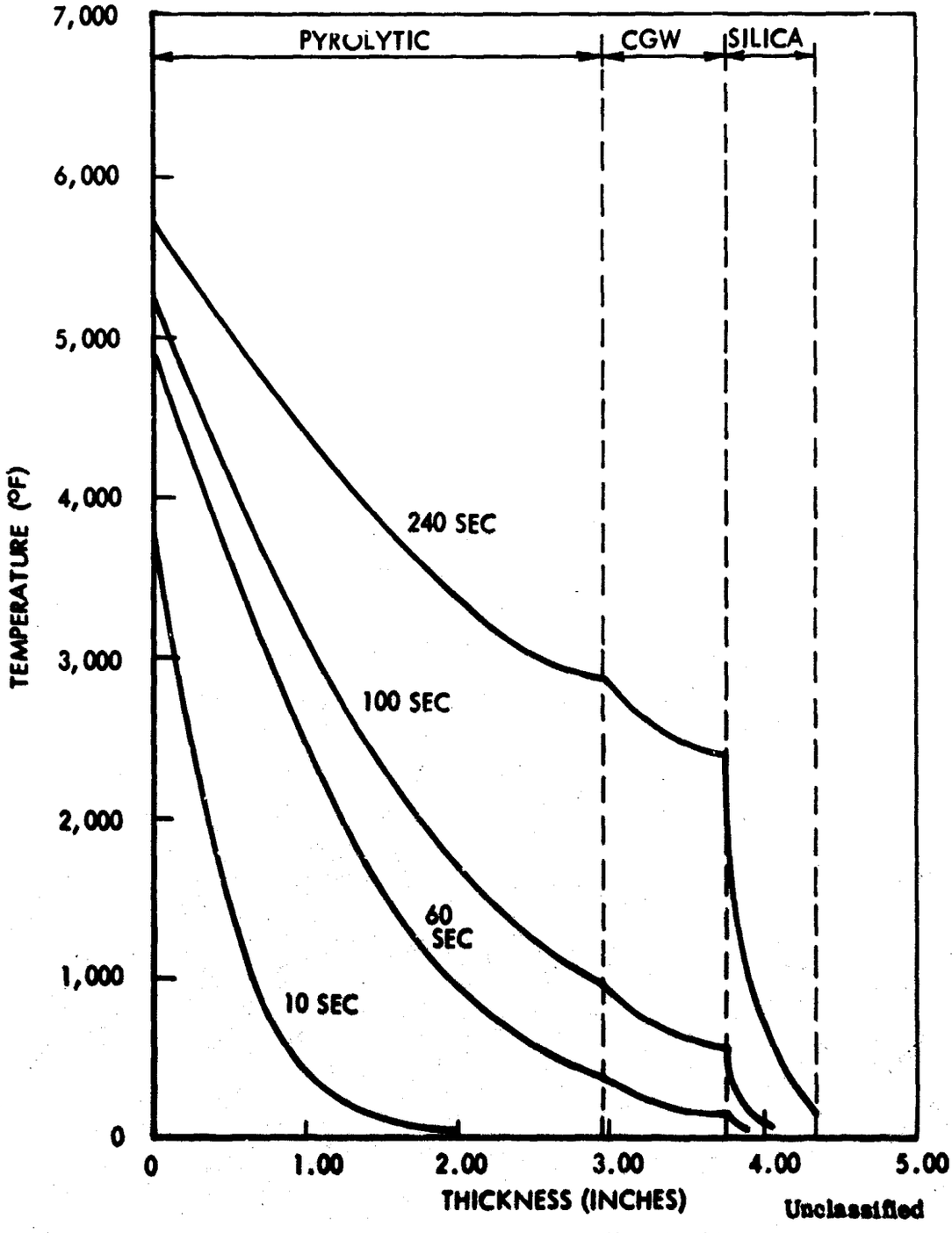

FIGURE 78 (U) PREDICTED TEMPERATURE PROFILE AT STATION 2: FULL SCALE UNIT S/N 2

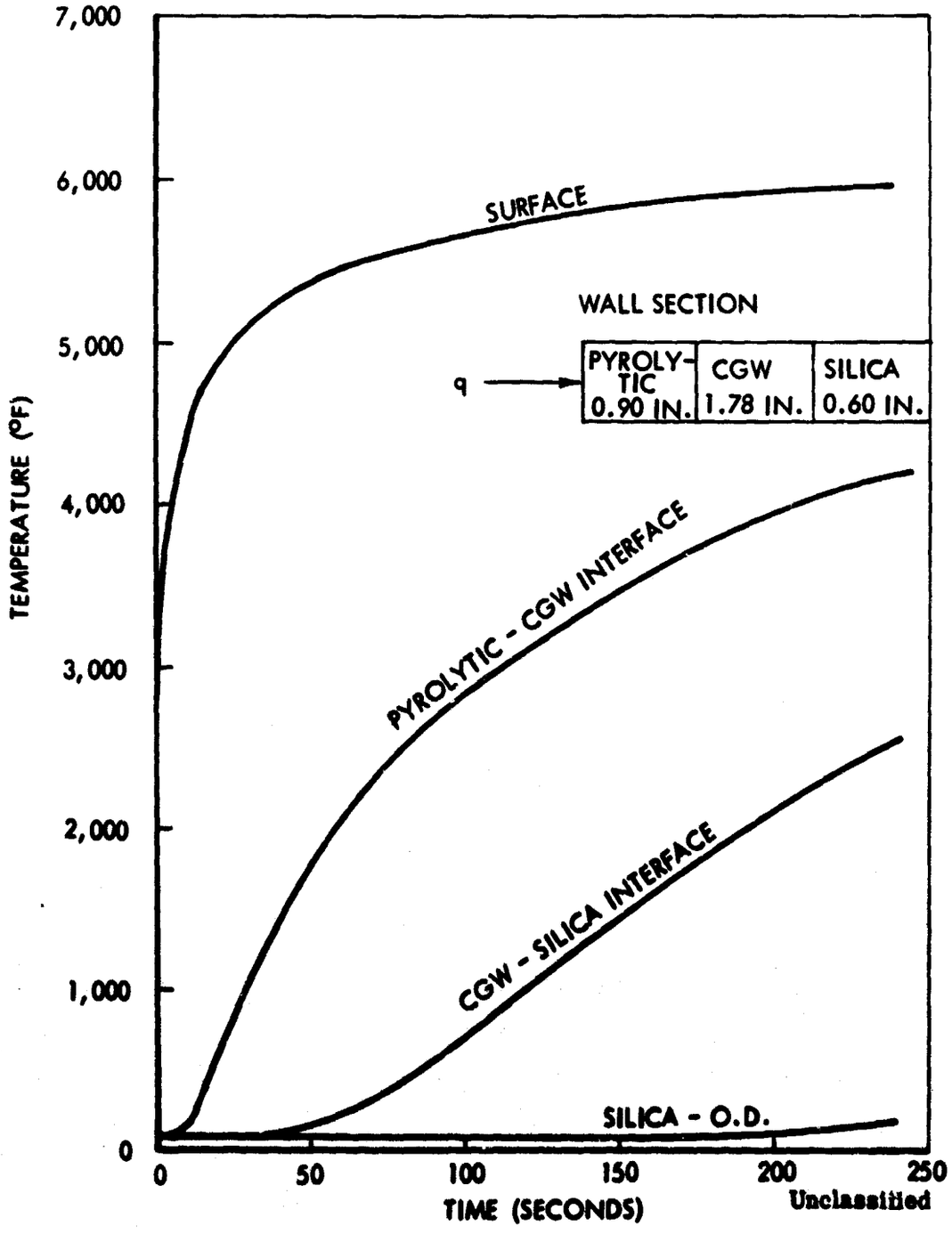

FIGURE 79 (U) PREDICTED TEMPERATURE DISTRIBUTION FOR STATION 3: FULL SCALE UNIT S/N 2

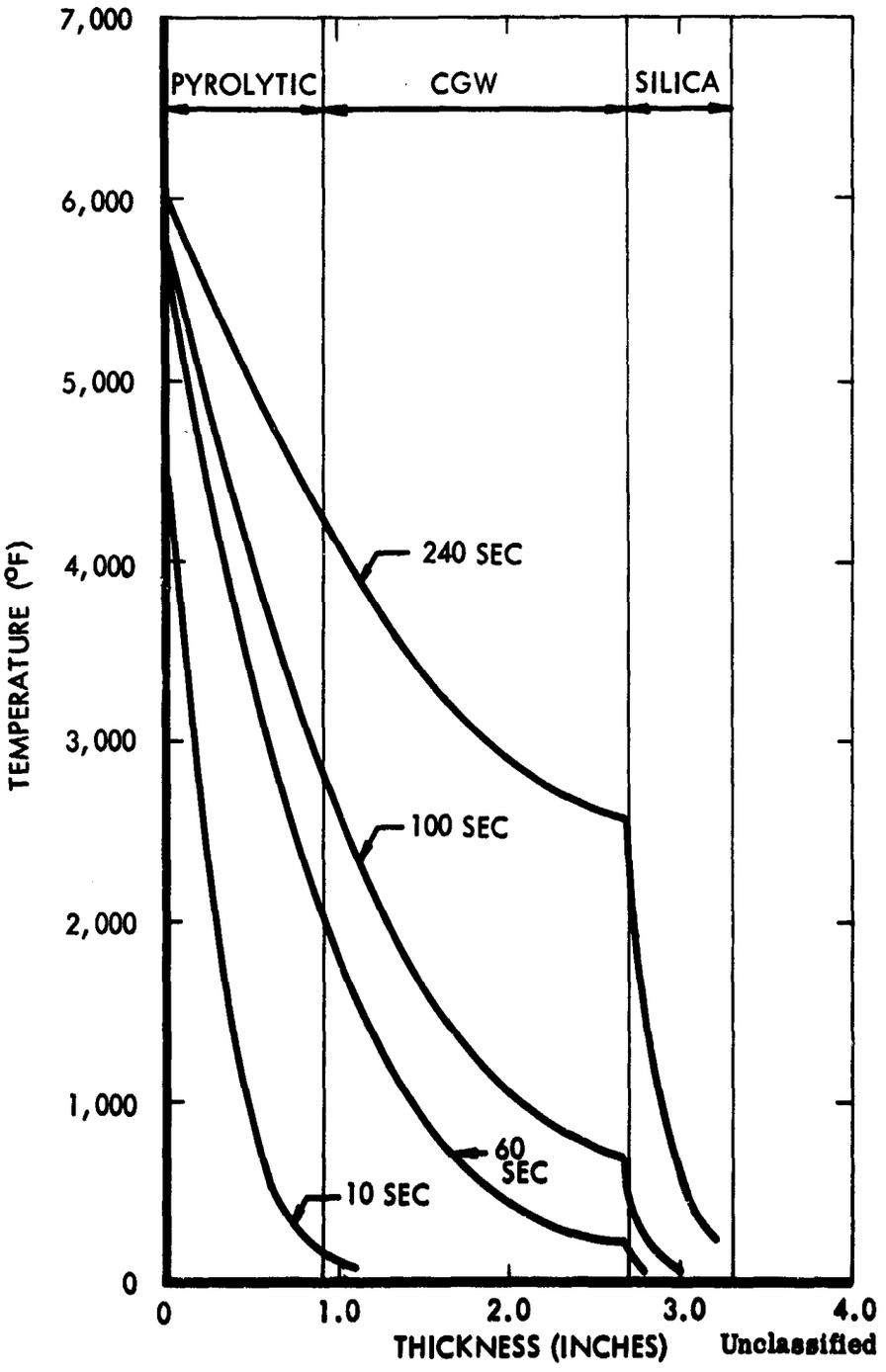

FIGURE 80 (U) PREDICTED TEMPERATURE PROFILE AT STATION 3: FULL SCALE UNIT S/N 2

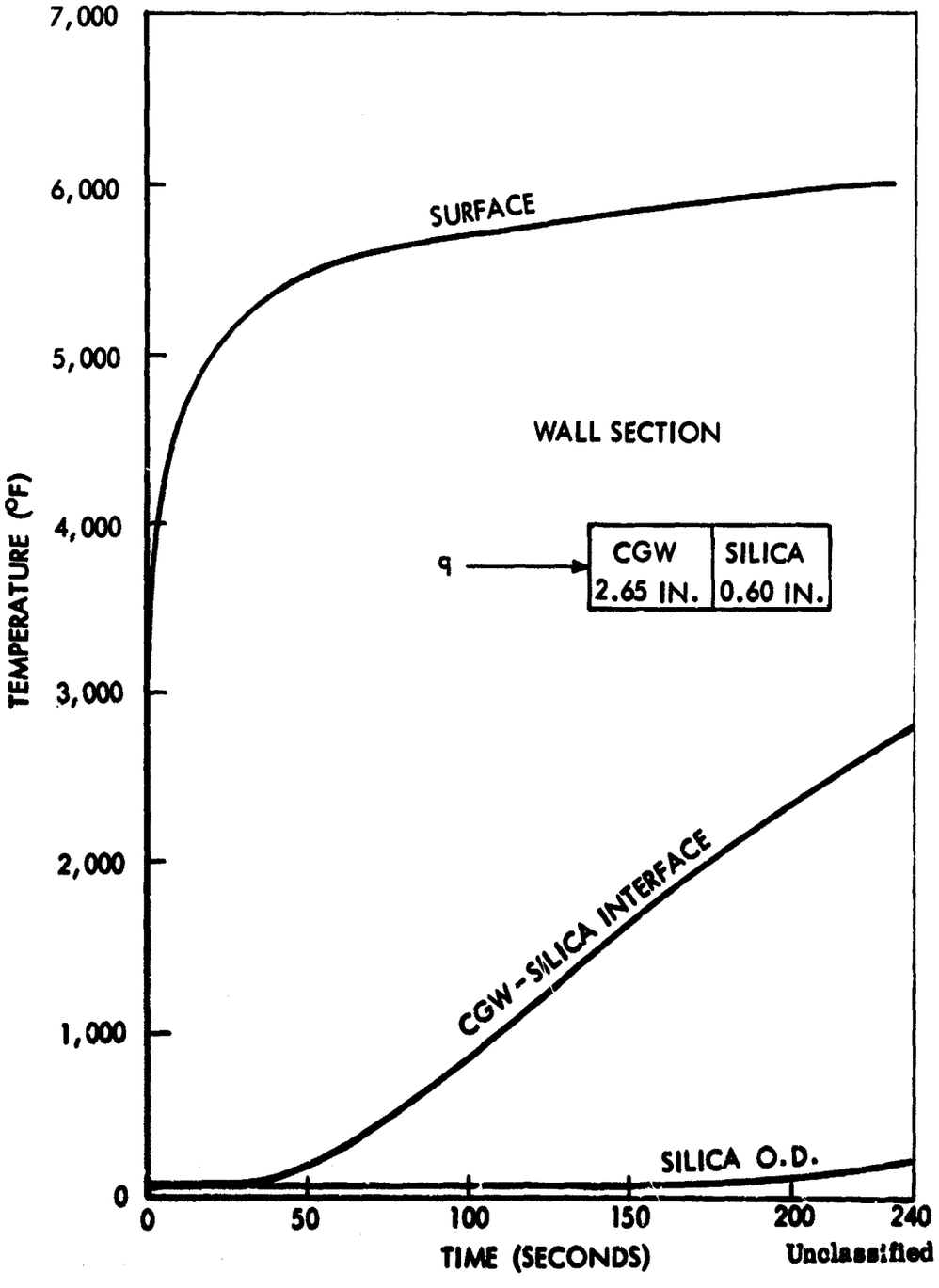

FIGURE 81 (U) PREDICTED TEMPERATURE DISTRIBUTION AT STATION 4: FULL SCALE UNIT S/N 2

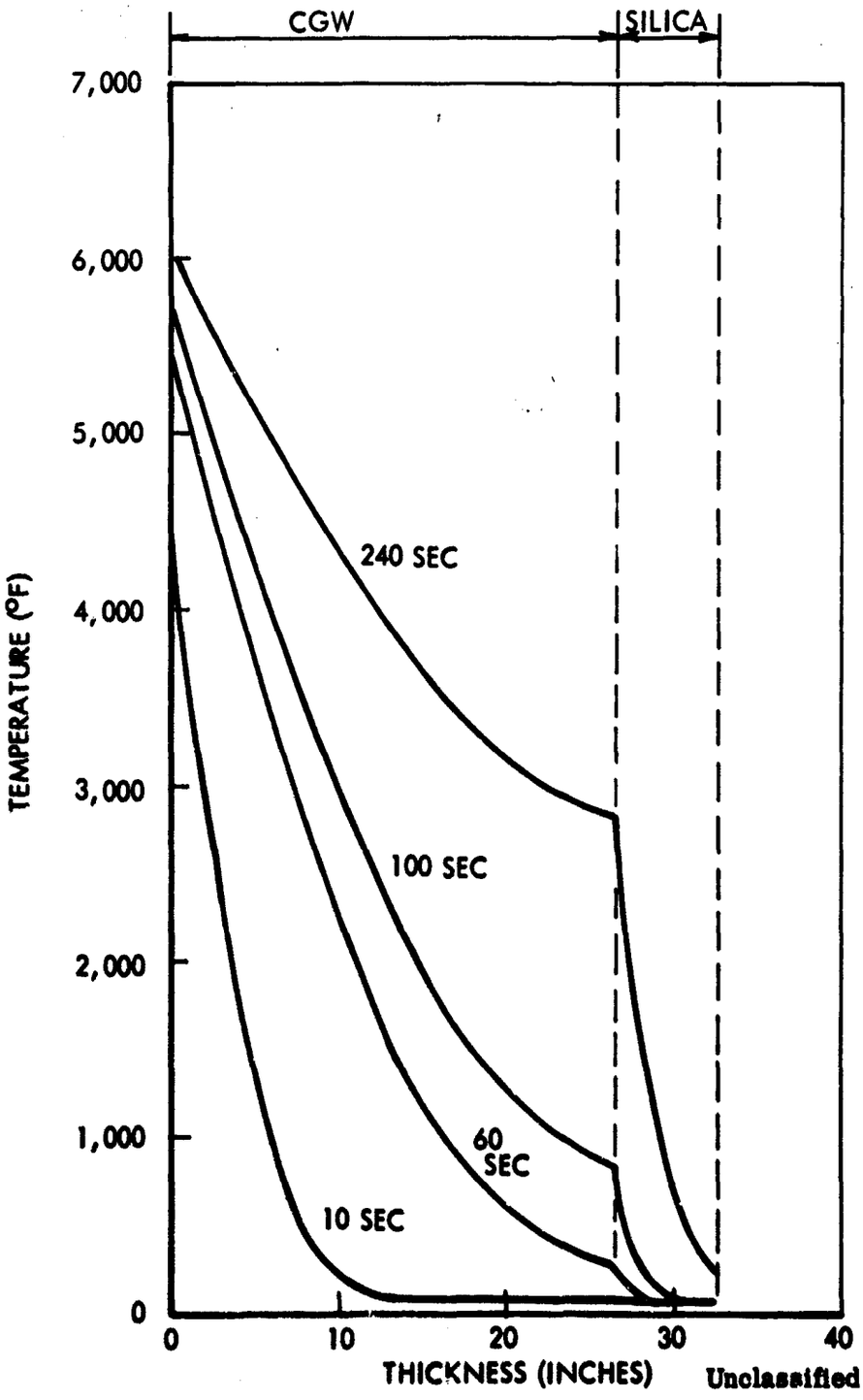

FIGURE 82 (U) PREDICTED TEMPERATURE PROFILE AT STATION 4: FULL SCALE UNIT S/N 2

overwrapped with carbon and silica phenolic parallel to the centerline. This configuration is similar to that employed in units S/N 1 and 2.

(U) The downstream portion of the thrust chamber liner and throat incorporated Thompsine Tape. The Thompsine Tape was duplex material thus eliminating the need for an interface bond line between the exposed graphite material (gas side) and the insulative quartz material (steel side). This was done by mechanically weaving the graphite and quartz materials into a single tape structure prior to resin impregnation. The two sections were thus an integral part upon curing. The tape orientation in the chamber and throat sections was 45 and 75 degrees respectively. Details of the Thompsine Tape configuration are included in the appendix.

(U) The nozzle exit cone utilized a carbon phenolic cloth wrapped at a 45 degree orientation. The exit cone and throat sections were overwrapped with glass phenolic parallel to the thrust chamber centerline to provide an integral structure.

(U) One-dimensional heat transfer analyses were conducted at two locations in the thrust chamber, at the throat and in the chamber upstream of the throat. The location of the composite wall for each analysis is presented in Figure 72 (thermocouples sections A-A and B-B). Thermal conductivity characteristics for the Thompsine Tape were estimated. The thermal properites were expected to be comparable with the conventional graphite and silica phenolic materials due to the similarity in basic materials (graphite and quartz yarns). Thus, the conventional material properites were used for the heat transfer calculations.

(U) The results of the heat transfer analyses are presented in Figures 83 and 84. Figure 83 presents the temperature distribution at the throat section A-A. Figure 84 presents the temperature distribution in the chamber at section B-B; and these results should be similar to the expected temperature distribution at section C-C. In all cases, adequate insulation was provided and no signigicant change in the structural shell temperature was predicted. Thermocouple locations were selected to compare predicted temperature distributions with actual test results.

d. Fabrication

(U) Fabrication of the full scale thrust chambers was accomplished similarly to the subscale thrust chambers fabrication technique. The insulation and in most cases the throat and chamber liner materials were machined from billets of the desired material which had been fabricated by TRW or supplied by a vendor. The various machined components were then bonded into an assembly.

(U) The steel thrust chamber housing was conservatively designed for ease of fabrication, assembly, and for reusability. The housing consisted of a cylindrical shell with an end plate. The shell was fabricated from low carbon steel. All sections were itentionally overdesigned to permit drilling and tapping for thermocouple installation. Steel components were reused during the full scale thrust chamber evaluation program.

(U) Following machining of the various components, thrust chamber assembly was accomplished by bonding the components into the steel shell. Bonding techniques were similar to those used in the subscale evaluation. Thermocouples

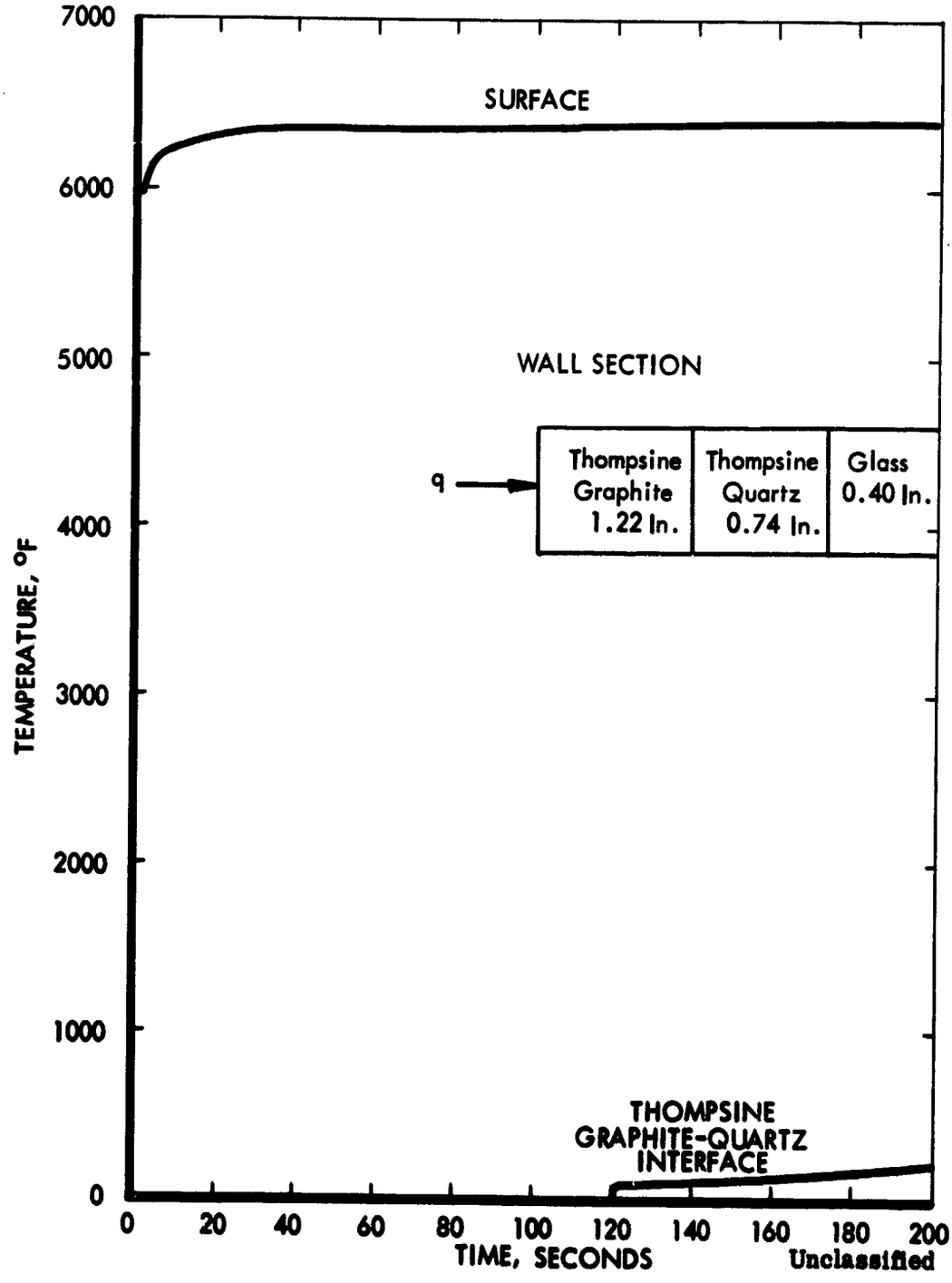

FIGURE 83 (U) PREDICTED TEMPERATURE DISTRIBUTION AT THROAT FOR UNIT S/N 3

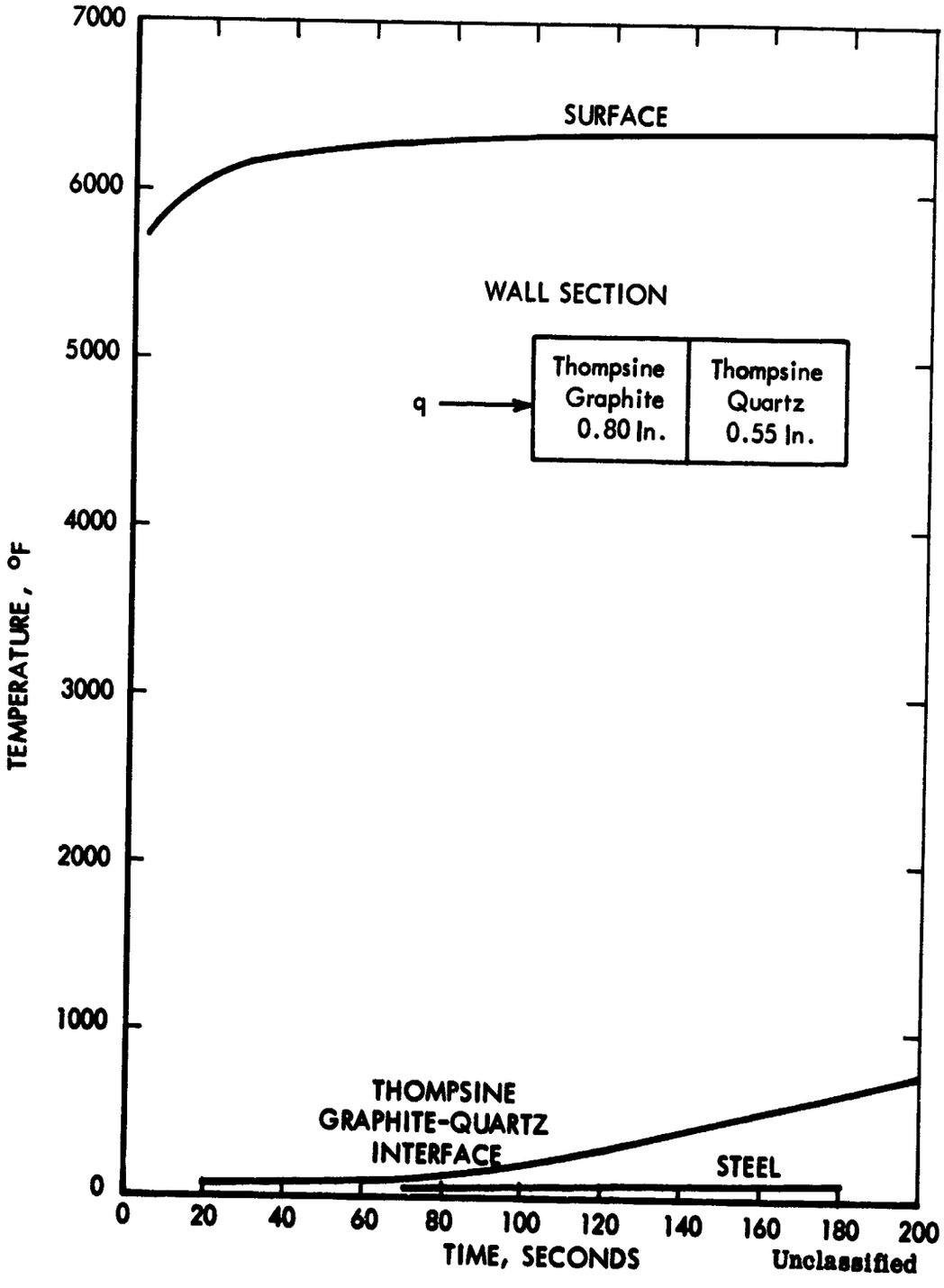

FIGURE 84 (U) PREDICTED TEMPERATURE DISTRIBUTION IN CHAMBER FOR UNIT S/N 3

holes were then drilled, and thermocouples installed. Thermocouple combinations used were tungsten-tungsten 26% rhenium and chromel alumel depending on the expected temperature.

(1) Full Scale Chamber S/N 1

(U) Unit S/N 1 incorporated a two-piece Carb-I-Tex grade 700 throat insert. The material was made by Graphite Specialities, Sanborn, New York, (a division of Carborundum). The material was a fully graphitized composite with a ply orientation perpendicular to the throat centerline. The specific gravity was in excess of 1.4 for both pieces. Both throat pieces were 100% x-rayed and determined to be free of cracks.

(U) The chamber liner was fabricated by tape wrapping. The carbon cloth phenolic (U. S. Polymeric FM 5055) liner was wrapped first and hydroclave cured. Following a clean up cut on the OD surface, the liner was overwrapped with silica cloth phenolic (Fiberite MX 2600).. The liner and insulation composite was then autoclaved cured.

(U) The throat support and exit liner assembly were fabricated concurrently. Carbon cloth and silica cloth phenolic materials were used for this structure. The construction sequence was: (1) tape wrap the carbon cloth exit cone, (2) tape wrap the carbon cloth throat support, and (3) overwrap the structure with silica cloth phenolic. The assembly was then hydroclave cured as a unit.

(U) Finish part properties including specific gravity residual volitales, and acetone extractables were evaluated for the ablative materials. The specific gravities of the chamber liner carbon cloth and silica were 1.47 and 1.72 respectively. The specific gravities of the throat exit assembly were 1.46 and 1.72 for the carbon cloth and silica respectively. The degree of polymerization of the silica for the throat and chamber insulation was 93.05% and 99.49% respectively. All properties were within acceptable limits. A view of the finished chamber assembly from the upstream and is presented in Figure 85.

(2) Full Scale Chamber S/N 2

(U) Full scale unit S/N 2 incorporated a pyrolytic graphite throat insert. The material for the throat insert was fabricated by Pyrogenics, Inc., Woodside, New York. The configuration of the throat which included a conical oreintation of the a-b planes was produced on an ID mandrel in three furnace runs. The furnace used to manufacture the part would accommodate a maximum part diameter of 8½ inches and as a result the a-b planes curved towards an axial orientation near the outside surface of the part as shown in Figure 74. This tendency, however, did not affect the integrity or the performance of the part.

(U) Difficulty was experienced during the fabrication of the pyrolytic graphite throat insert. The throat as originally delivered to TRW was visually inspected which revealed several hair-line cracks on the inside conical surface. Radiographic inspection revealed internal delamination and some internal cracks. It was felt that the internal defects would cause no performance difficulties. However, the inside conical surface cracks could effect the integrity of the part since it was desirable, if not necessary, to have the inner pyrolytic graphite surface crack free. The throat insert was subsequently returned to

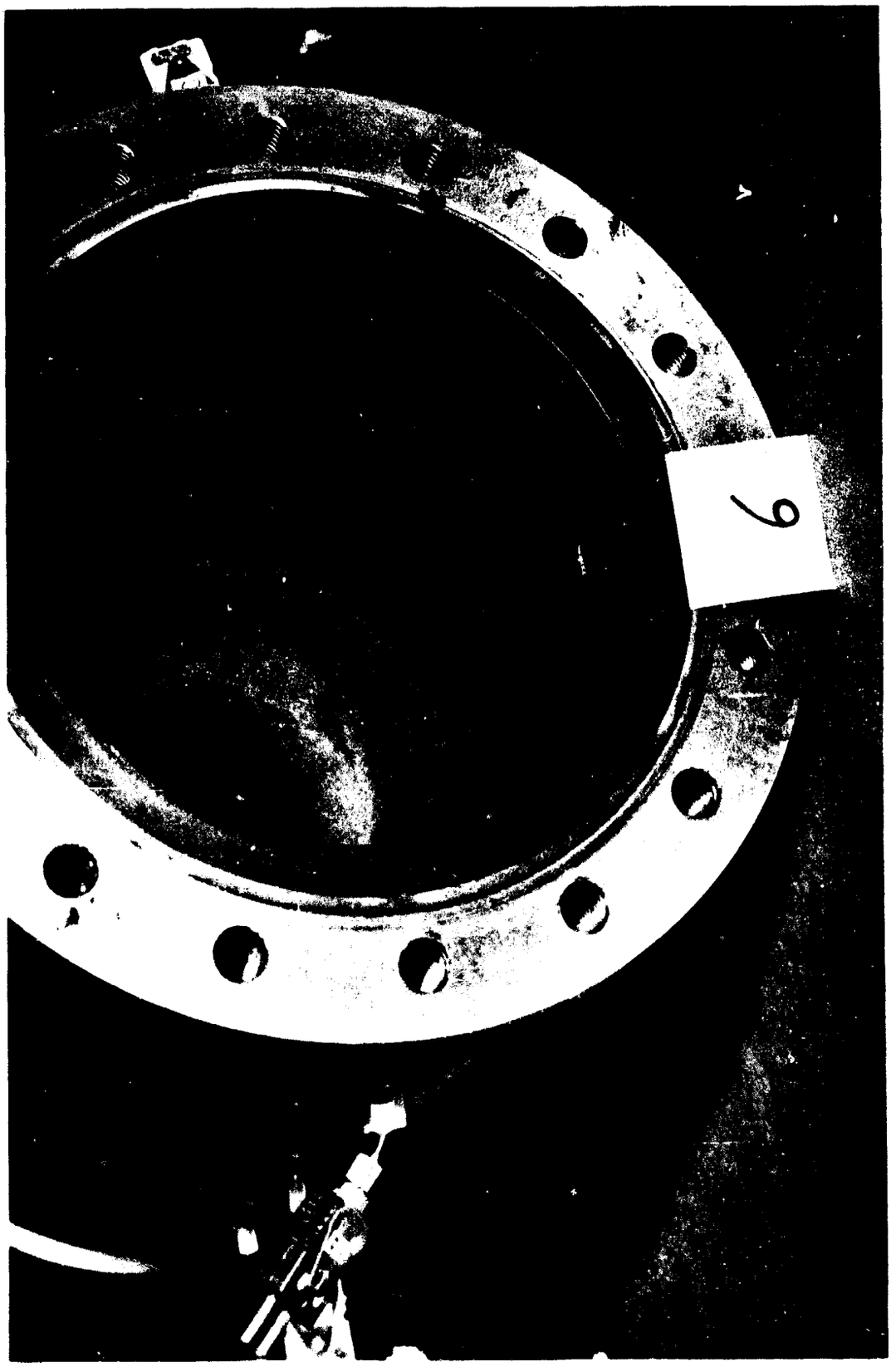

Unclassified **FIGURE 85(u) Full Scale Unit S/N 1 Assembly**

the vendor for rework which consisted of deposition of an additional layer of pyrolytic graphite on the inside surface.

(U) Following rework the pyrolytic billet was retruned to TRW. Visual inspection of the throat insert revealed the inside conical surface was crack free except for two small cracks at the smallest diameter. These cracks, however, cleaned up during final machining to contour.

(U) During the machining of the pyrolytic graphite, a slight out of round condition was noted on the inside conical surface. The inside diameter at the origin of the conical throat (adjacent to the chamber liner) was less than 8 inches. As a result the chamber liner contour was modified at the downstream end to provide a smooth transition to the throat approach surface. The finished machine throat insert revealed no inside surface cracks. Delaminations between the layered "a-b" plane edges were exposed in the throat region. These delaminations were subsequently filled with National cement Grade C9 (Union Carbide Corporation), a carbonatious cement.

(U) The throat support was machined to shape from a CGW graphite billet. The pyrolytic graphite throat insert was then bonded into the throat support with National Grade C9 cement. The throat assembly was subsequently cured similarly to subscale unit S/N 4.

(U) The chamber assembly was fabricated as an integral structure. The carbon cloth phenolic chamber liner (Fiberite MX 4926) was wrapped on a mandrel with a 30° orientation using bias tape. The carbon cloth liner was hydroclave cured. The carbon cloth component was subsequently machined and then the three machine CGW graphite components were bonded into place on a mandrel with the established thermal expansion gaps. The assembly was subsequently overwrapped with carbon and silica cloth phenolic and autoclave cured. The inside diameter of the chamber was then machined to size.

(U) The throat insulation assembly incorporated the exit cone. Fabrication was accomplished by wrapping the exit cone and the carbon cloth insulator on a mandrel. The exit cone utilized alternate sections of graphite and phenolic tape (Fiberite MX 2630A and MX 4926, respectively). These components were hydroclave cured.

(U) The silica insulation in the throat insulation assembly was machined from the insulation utilized in unit S/N 1. This insulation was only slightly charred following the tests of unit S/N 1. When machined to the unit S/N 2 configuration, all charred material was removed. The exit cone component and the carbon cloth throat insulator were then bonded into the silica insulation.

(U) The steel shell and retaining plate unit of S/N 1 were reused. A hot spot was located on the steel shell as a result of the unit S/N 1 test. Inspection of the steel indicated that this was a local condition. No structural problems were anticipated as a result of this condition. The three major subassemblies, chamber, throat, and throat insulation were subsequently bonded into the steel housing. Thermocouple holes were drilled. A view of the finished assembly looking downstream toward the throat is presented in Figure 86.

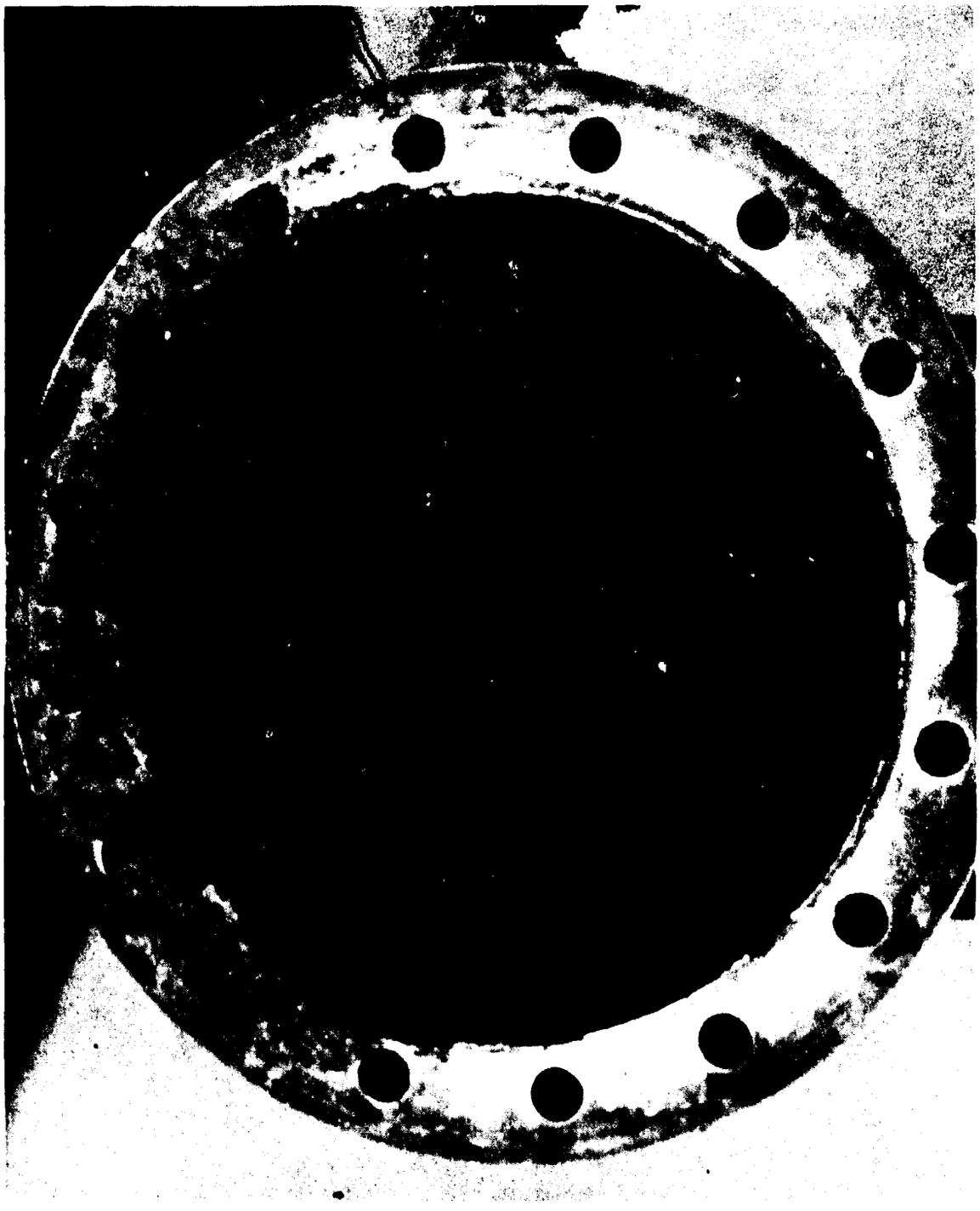

Unclassified FIGURE 86(U) Full Scale Unit S/N 2 Assembly

(3) Full Scale Chamber S/N 3

(U) Full scale unit S/N 3 was fabricated utilizing Thompsine Tape. The intent of the program was to utilize Thompsine Tape as it was currently known to TRW with minor improvements based on previous experience. As a result of configuration of the Thompsine Tape was modified slightly, and a preliminary laboratory evaluation was conducted prior to fabrication of full scale unit S/N 3. A brief discussion of the fabrication is presented in this section. Details of the Thompsine Tape fabrication are presented in the Appendix.

(U) The design requirements for the Thompsine Tape configuration were established in a mutual agreement between the weaving vendor and TRW. Although it was not the purpose of this program to develop improved versions of Thompsine Tape, it was felt that limited changes could be made to the tape to improve both processing and performance. Two major improvements were made. 1) An increase in yarn density (more yarns per inch of the tape growth) provided an increased body, greater ease of impregnation, and fewer wraps during fabrication and, 2) an additional thread on each salvage edge was provided to lower extensibility during the impregnation and hence maintainence of the elasticity of the tape width.

(U) Since it was desired to fabricate unit S/N 3 as an integral chamber, the unit was tape wrapped and cured in stages with subsequent wraps being made directly on the previously cured parts. The tape wrapping was initiated with the injector end of the chamber. The first wrap consisted of a 30° oriented wrap of graphite phenolic, which was overwrapped consecutively with carbon and silica phenolic parallel to the cernterline. The multiple wrap was bagged and hydroclave cured. The cured part was subsequently machined to provide a starting point for the Thompsine Tape wrap.

(U) The 45° oriented Thompsine Tape was then wrapped in the chamber region up to the throat approach. The 75° interface was then machined on the as wrapped Thompsine Tape billet to form a starting ring for the 75° oriented wrap in the throat approach and throat region. Considerable difficulty was encountered in starting this wrap (see Appendix for details). However, the 75° oriented Thompsine wrap was accomplished. Diametral wrapping ratio attained in the throat area was approximately 2.3 to 1. Following tape wrapping the part was hydroclave cured.

(U) Following machining on the surfaces to be overwrapped, the final tape wrapping activities took place. This consisted of a 40° oreinted carbon cloth exit cone and a parallel to centerline glass phenolic overwrap. The part was bagged and hydroclave cured. The subsequent part was finish machined, X-rayed, and assembled into the steel shell. Thermocouple holes were drilled prior to shipment. X-ray films of the Thompsine Tape chamber indicated slight delaminations in the convergent section to the throat. However, these delaminations did not extend through to the inside surface. No delaminations were noted in the chamber wrap area (45° oriented Thompsine Tape). A view from the inlet end of the finished assembly is presented in Figure 87.

2. TESTING

(U) The test facilities and test results are presented in this section.

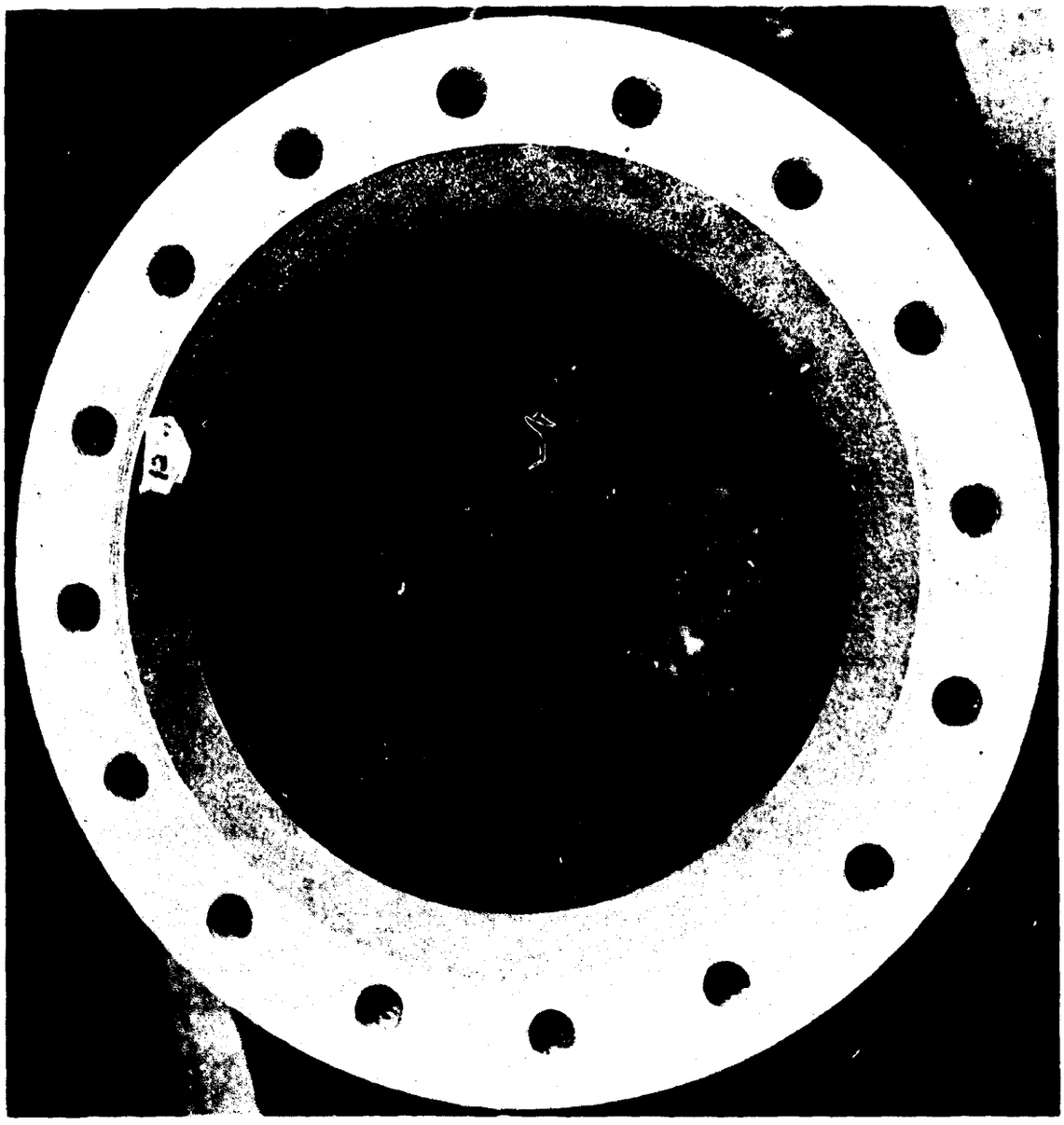

Unclassified FIGURE 87 (U) Full Scale Unit S/N 3 Assembly

a. Facilities

(U) All testing performed under Phase II of this contract was conducted at Air Force Rocket Propulsion Laboratory located in Edwards, California between March 1966 and April 1967 using the liquid fluorine hydrazine blend propellant test facilities. All tests were conducted with nozzle exhausting to ambient conditions (approximately 13.2 psia).

(U) The RPL designed injector No. 12 was used for all Phase II testing in this program. Thrust chamber evaluation was conducted at approximately 200 psia chamber pressure and 3750 pounds of thrust. This injector has a long and impinging unlike doublet pattern consisting of three concentric rows of oxidizer orifices on the outer periphery of the injector with matching fuel orifices located on the injector dome face.

b. Test Results

(U) Full scale thrust chamber tests were planned to evaluate the design requirements for each unit. The planned duty cycle, except for unit S/N 3, was as presented in Section VI, Subsection 1a. Actual duty cycles were different from the planned duty cycle as a result of test difficulties and/or as a result of erosion or liner material degradation. The planned duty cycle for unit S/N 3 consisted of several shorter pulses since the ablative structure was not expected to perform as well as the pyrolyzed composite or pyrolytic graphite throat employed in units S/N 1 and 2.

(U) Table XIV contains a summary of the three full scale non-regeneratively cooled combustion chambers tested at AFRPL in the Phase II portion of this program. This summary includes the AFRPL test identification, date, test conditions, performance duration, and remarks. Single test durations ranged from 6 to 201 seconds. Accumulated durations for the three full scale thrust chambers were 373, 358, and 206 seconds for units S/N 1, 2, and 3 respectively.

(U) Table XIV presents the chamber and throat materials. The diameter change during each pulse is the average increase (or decrease) of the throat diameter and is based upon measurements recorded prior to and immediately after each run. The net diameter change is the total diameter change. The effects of high local erosion are neglected in the diameter change during each pulse and the net diameter change. Erosion is also presented in terms of percent of throat area change.

(U) The combustion performance of each test is also presented. At several time slices during each run, data are reduced to determine measured characteristic velocity (C*) and specific impulse (Isp). Specific impulse is based upon expansion to ambient conditions. Data are compared to the AFRPL theoretical values at the measured O/F ratio. Only C* and Isp values at the beginning of each run are presented since degradation in these parameters occur with throat erosion.

(1) Full Scale Thrust Chamber S/N 1

(U) Full scale thrust chamber S/N 1 was tested for durations of 11, 61, 100, and 201 seconds. Nominal chamber pressures for the four tests were 218, 210, 204, and 190 psia respectively.

TABLE XIV (U) FULL SCALE TEST RESULTS

Unit S/N	Chamber Material	Throat Mat'l	AFRPL Run No.	Test Date	Test Cycle, Sec.	Cooldown Period, Sec.	Total Test Time, Sec.	Throat Dia. Change During Pulse	Net ΔD	% Area Change During Pulse	% Isp., Sec.	Nominal Pc, psia	O/F	Remarks
1	Carbon Cloth Phenolic	Carb-I-Tex 700	279	3/21/66	11	A*		0.001 in.		0	90.4	218	1.82	
			280	3/31/66	61	A		-0.008		-0.4	90.1	210	1.84	
			281	4/1/66	100	A		0.016		0.8	89.0	204	1.89	
			285	4/7/66	201	A	373	0.677	0.686	34.8	91.8	190	1.68	Test terminated prematurely due to test facility difficulties
2	Carbon Cloth Phenolic and CBF Graphite	FO	298	6/3/66	9	A		0.069		3.3	98.8	202	1.49	
			299	6/17/66	39	A		0.080		3.8	92.4	203	1.64	
			302	6/23/66	60	A		0.099	0.158	0.4	91.8	206	1 79	Unit returned to TRW for rework
			308	8/12/66	72	A		0.014		0.7	92.8	179	1.37	Test terminated prematurely due to test facility difficulties
3			309A	8/18/66	150	350					93.2	180	1.42	
			309B	8/19/66	28	A	358	0.036	0.050	G1.7	93.2	180	1.42	
4	Graphite Cloth	Thompson Tape	333	12/6/66	6	A		0.004		.0.2	97.7	166	1.01	Test terminated prematurely due to injector failure
	Phenolic and Thompson Tape		338	1/9/67	19	A		-0.044		-2.1	91.2	201	1.71	
			340A	1/23/67	9	195					96.9	208	1.63	
			340B	1/23/67	9	A		0.059		2.8	96.0	205	1.67	
			341A	1/24/67	19	174					95.5	208	1.69	
			341B	1/24/67	19	307					95.2	206	1.72	
			341C	1/24/67	20	413					94.8	199	1.73	
			342D	1/24/67	20	325					95.2	198	1.76	
			342E	1/24/67	20	A		0.380		18.9	95.0	190	1.76	Unit returned to TRW for rework
			347	4/7/67	15	A		0.558		31.0	99.0	222	1.35	
			348	4/11/67	55	A	206	0.424	1.381	20.1	95.7	194	1.61	

*Gaseous cool to ambient conditions

Confidential

(U) Following the first test, inspection of the thrust chamber indicated that the Carb-I-Tex 700 throat insert and the carbon cloth chamber liners were in excellent condition. A small piece of Carb-I-Tex, however, was expelled during the run from the Carb-I-Tex component downstream of the throat. The circumferential groove which resulted from the expulsion of the Carb-I-Tex piece was subsequently filled with silicon rubber which was available at AFRPL prior to subsequent testing.

(U) Two tests of 61 and 100 seconds in duration were conducted. Following the 61 test test, the unit was in good condition and the previously mentioned circumferential groove caused no problem during the test. Following the 100 second test (Run 281), the injector dome failed resulting in pieces being expelled through the thrust chamber. Two gouges were observed in the throat approach region in the Carb-I-Tex material following the run. It is believed that these gouges were caused by the failure of the injector dome and subsequent expulsion of the pieces through the throat.

(U) The last run (Run 285) was scheduled for 240 second duration. This test was terminated at 201 seconds due to a failure of the fuel line at the injector inlet. Chamber pressure degraded approximately 30 psi during the test. Inspection of the chamber following the last run indicated severe erosion in the chamber region, with a local burn through to the steel just upstream of the throat convergent section. As a result no further tests were conducted and the unit returned to TRW for post-firing evaluation.

(2) Full Scale Thrust Chamber S/N 2

(U) A total of five tests were conducted on unit S/N 2. Durations of 9, 39, 60, 72 and 178 seconds were realized for a total accumulated test time of 358 seconds. The unit was cooled to ambient conditions between each test. The last test was fired for 150 seconds with a 350 second cool down and then refired for 28 seconds.

(U) During the first three test runs, Runs 298, 299 and 302, some cracks occurred in the conical convergents surface of the pyrolytic graphite. During test run 302, pyrolytic graphite pieces in the throat region were expelled leaving a portion of the pyrolytic graphite planes in the throat convergent section unsupported (see Figure 88, viewed looking upstream through throat). However, the throat area was maintained. Accumulated erosion during the three tests was quite high (0.158 inches on the diameter), but only 0.009 inches was observed during the last run. The greater erosion during Runs 298 and 299 was attributed to the surface material cracking and chucking in the throat region.

(U) TRW recommended that a further test (a longer duration run) was necessary to fully evaluate the pyrolytic graphite material and design concept in demonstrating a low throat erosion. Prior to subsequent testing, however, the throat insert was repaired by bonding graphite pieces into the gaps in the throat region with National Grade C-9 cement to provide adequate support.

(U) Following the thrust chamber repair (see Figure 89), the unit was scheduled for a 240 second test. The test was terminated at 72 seconds due to test facility difficulties. Unit S/N 2 was in good condition following the run. Throat erosion during this run was greater than expected due to the erosion of the less erosion resistant C-9 cement on the throat surface following the repair.

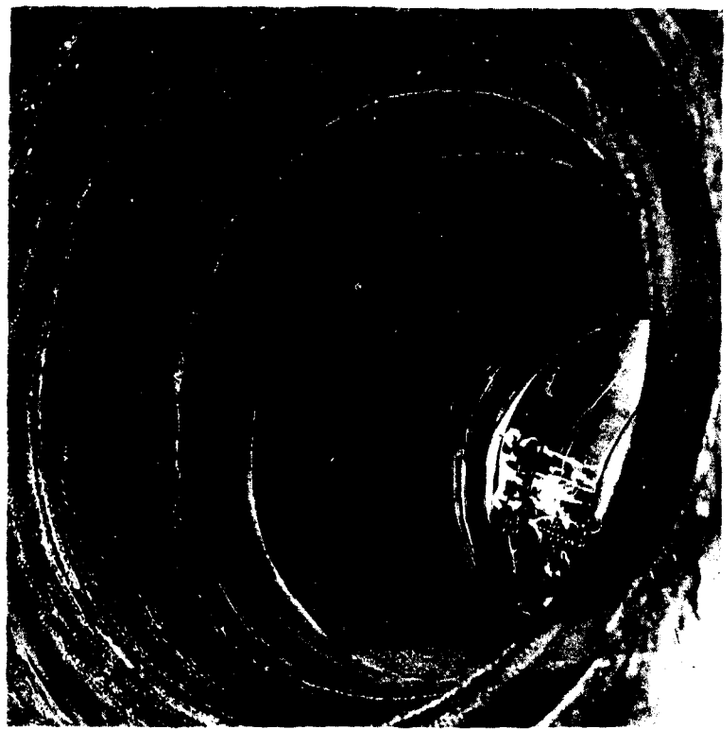

Unclassified FIGURE 88 (U) View of Unit S/N 2 After Test Run 302

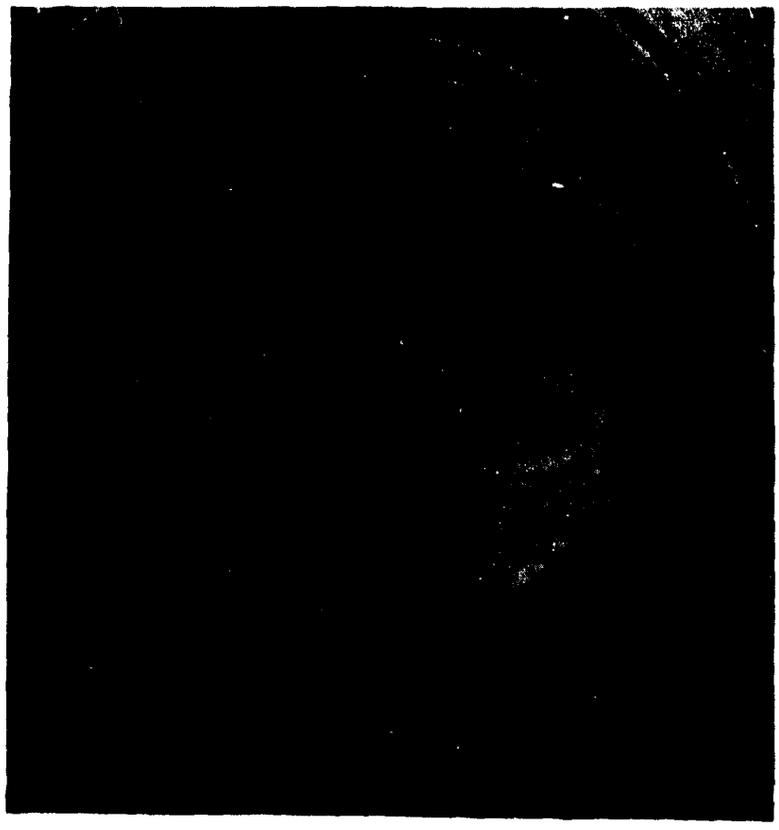

Unclassified FIGURE 89 (U) View of Unit S/N 2 After Test Repair

(U) A second run was scheduled for 180 seconds with a short cool-down period after the first 150 seconds. The test was successful. The motor was run for 150 seconds, shut down for 350 seconds and then was restarted for an additional 28 seconds. Post firing analysis indicated that the chamber was in good condition following the test sequence. Some evidence of flaking of the pyrolytic graphite material was noted in the throat region. No additional tests were conducted as it was felt that the test objective had been satisfied.

(3) Full Scale Thrust Chamber S/N 3

(U) Six tests were conducted on Unit S/N 3. Durations of 6, 19, 18, 98, 10, and 55 seconds were realized for a total accumulated time of 206 seconds. Both the 18 and 98 second tests were the accumulation of several test pulses. Test run 333, a scheduled 20 second run, was terminated prematurely. Approximately 7 seconds into the run, the injector face failed with the result that injector fragments were expelled through the chamber. A minor gouge was observed in the throat approach section following the test which was attributed to the injector failure. Other than this, the throat chamber was in excellent condition.

(U) Test runs 338 and 340 were accomplished without difficulty. Inspection of the unit after test run 340 revealed a slight streak in the throat. Erosion was slight and the chamber was in good condition.

(U) At the end of the fifth pulse of test run 341, it was observed that material was being expelled from the thrust chamber. Inspection of the unit following cool-down revealed severe local erosion in the throat approach at the three o'clock position, viewed from the exit plane looking toward the injector. The severe local erosion was in the same general location as the streak previously noted in the throat following test run 340.

(U) Unit S/N 3 was then returned to TRW in Cleveland for inspection. Except for the severe local gouges in the throat approach, the chamber was in excellent condition. Nominal radial erosion in the chamber was 0.031 and 0.054 inches in forward and aft positions, respectively. There were several uniform streaks, approximately 0.050 inches deep, in the convergent section and throat. These streaks were similar to those observed on the previous units tested (Units S/N 1 and 2). Only two very slight delaminations were observable in the thrust chamber--one in the graphite phenolic chamber liner and one in the Thompsine Tape section (throat approach and throat).

(U) Nominal and uniform erosion was observed in the throat and exit plane locations (except for the local gouging) of approximately 0.255 and 0.075 inches, respectively. Typical ply line delaminations occurred in the carbon cloth phenolic exit cone material.

(U) The severe local gouge was closely examined for signs of material failure. The gouge was somewhat irregular and extended axially, undercutting the material in the throat to a limited degree (see Figure 90). The gouge was approximately 2.5 inches wide and had a maximum depth of approximately 2.1 inches. No signs of spalling, interface (insulator-to-liner) failure, or material unraveling were evident in the vicinity of the gouge. No reason to suspect a highly local material failure was observable, nor was there any unusual characteristics noted in the inspection of the cured part and processing cycles during the fabrication process. A second much smaller local hole was also observable

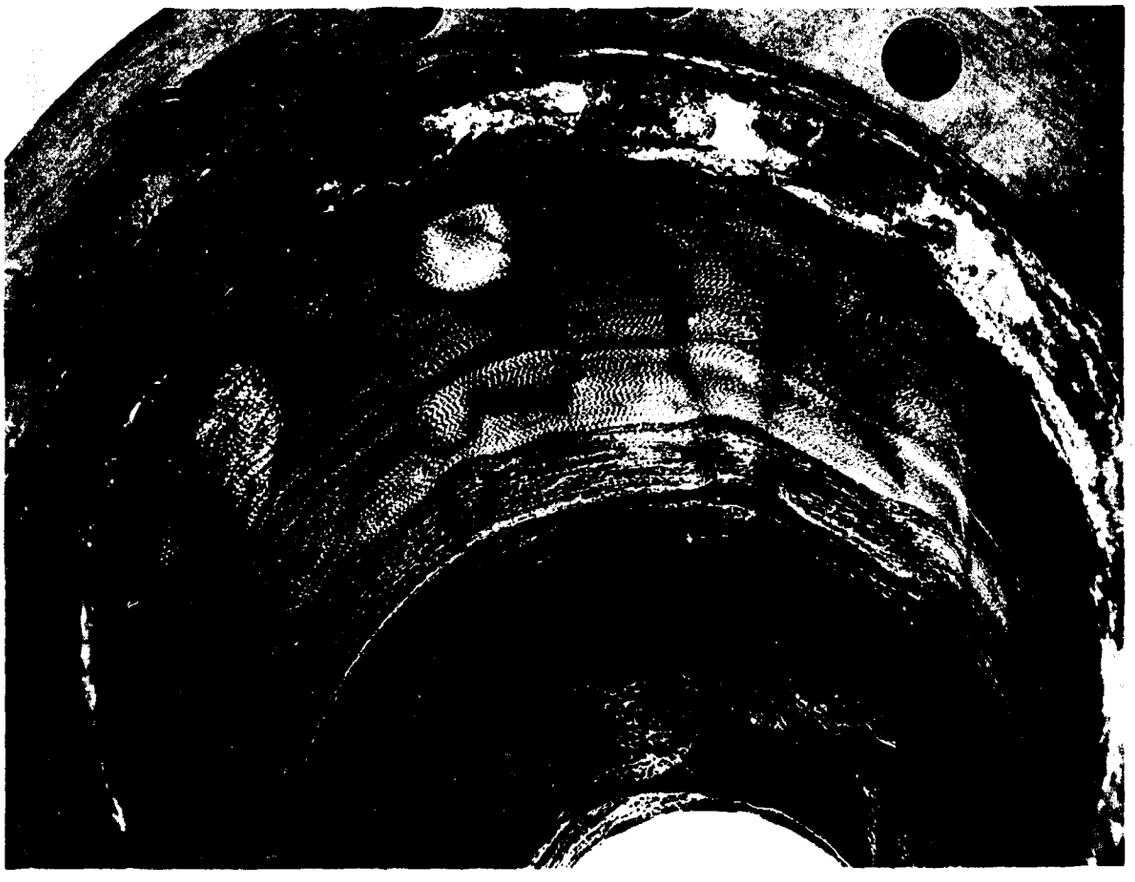

Unclassified FIGURE 91 (U) View of Unit S/N 3 After Repair

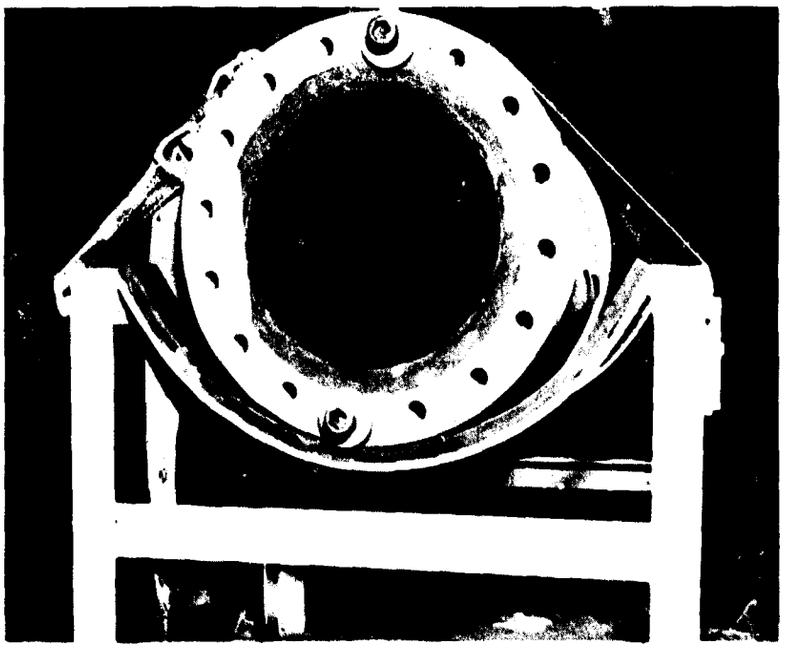

Unclassified FIGURE 90 (U) View of Unit S/N 3 After Test Run 341

at the eleven o'clock position (approximately 1/8 dia. x 1/2 deep). The reasons for these unusual characteristics were subsequently discovered during post-firing evaluation.

(U) The complete test duty cycle as originally planned was not completed since a long duration pulse was to follow test run 341. The purpose of this pulse was to demonstrate dissimilar material interface integrity under actual operation conditions after the char front has propagated across this interface. Although there was some question as to whether the char front has propagated through the interface at the throat based upon the thermocouple data, there was no doubt that the interface was charred in the chamber and throat approach locations. In order to permit additional testing on unit S/N 3, the gouged areas in the throat were repaired. A trowelable compound was used which consisted of Epoxy-Novolac/NMA resin containing graphite fibers and powder. Figure 91 shows a view of the unit following repair.

(U) The unit was then returned to AFRPL for two additional tests. Run 347 was a 10 second check-out run to verify repair material integrity. Considerable erosion occurred during Run 347, but this was essentially the trowel-on material used to repair Unit S/N 3. Run 348 was a 55 second run. Testing was terminated at this point since the test objectives had been accomplished.

3. POST FIRING EVALUATION

(U) Performance of the full scale thrust chambers was evaluated with respect to material performance and design concept performance.

a. Design Concept Performance

(U) The design concept performance for each full scale unit was evaluated in terms of the over-all structural performance, the thermal considerations (predicted versus actual temperature distribution), and erosion (specifically erosion of the throat).

(U) Erosion of the various throat materials was examined as a function of time in a manner similar to that used in the subscale thrust chamber evaluation (see Section V, Subsection 4c for description). For a single representative test run for each full scale unit, throat diameter change, chamber pressure, and throat insert surface temperature were plotted as a function of elapsed firing time. The specific test runs were selected to include long firing pulses with no throat material loss due to structural failure of the material. These results for units S/N 1, 2, and 3 are presented in Figures 92, 93, and 94 respectively. Significance of these results will be presented in Section VII of this report.

(1) Full Scale Unit S/N 1

(U) The design employed in unit S/N 1 consisted of an ablative chamber and a heat sink throat design. The configuration used simple geometric shapes to minimize design complexity. No difficulty was experienced relative to the structural performance of the unit except for the combustion chamber sections which experienced a severe erosion of the carbon cloth phenolic chamber liner.

(U) Predictions of temperatures in the Carb-I-Tex 700 throat insert material did not agree with the thermocouple data. This was not unexpected as the thermal

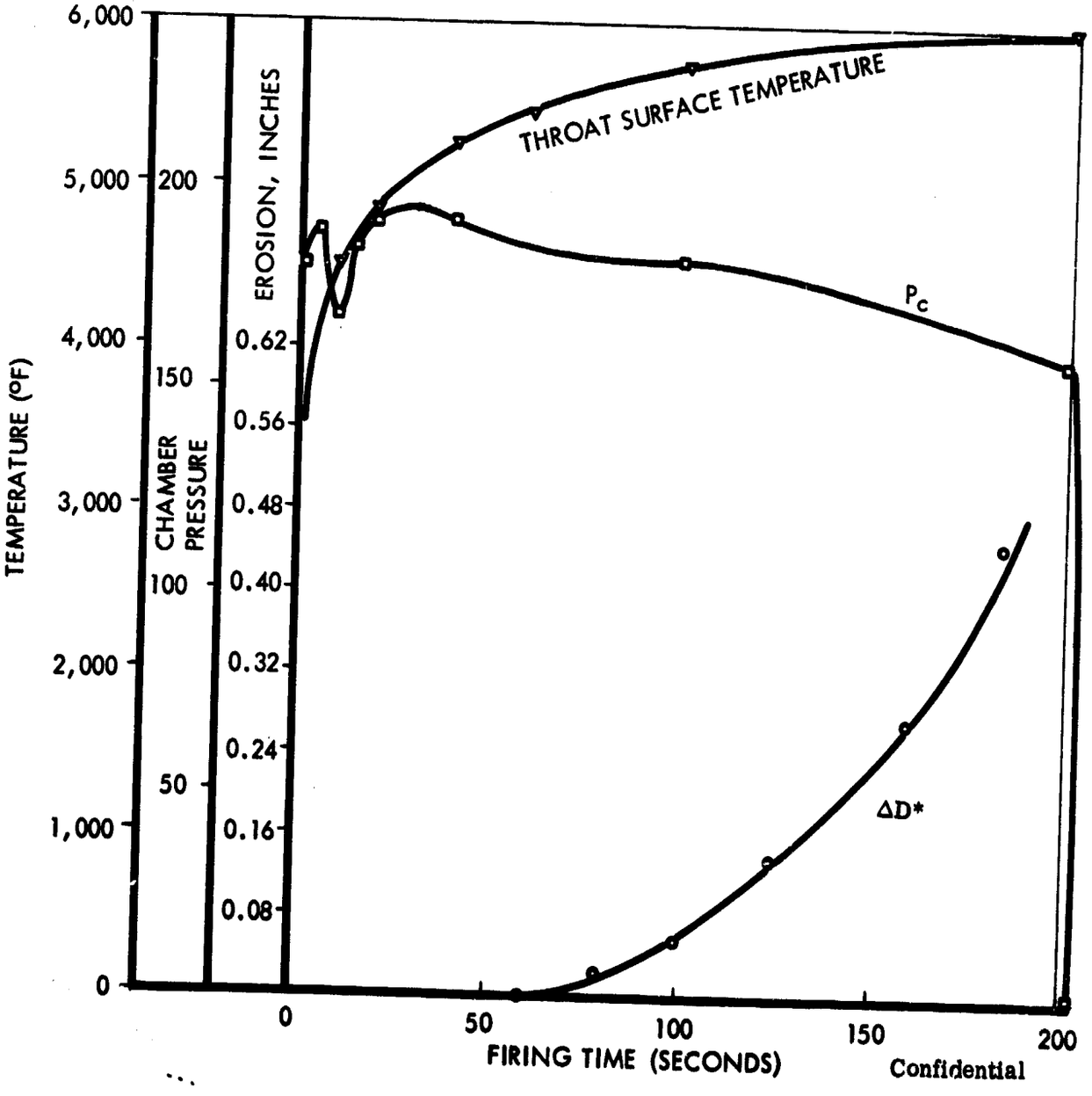

FIGURE 92 (U) UNIT S/N 1 DATA: RUN 285

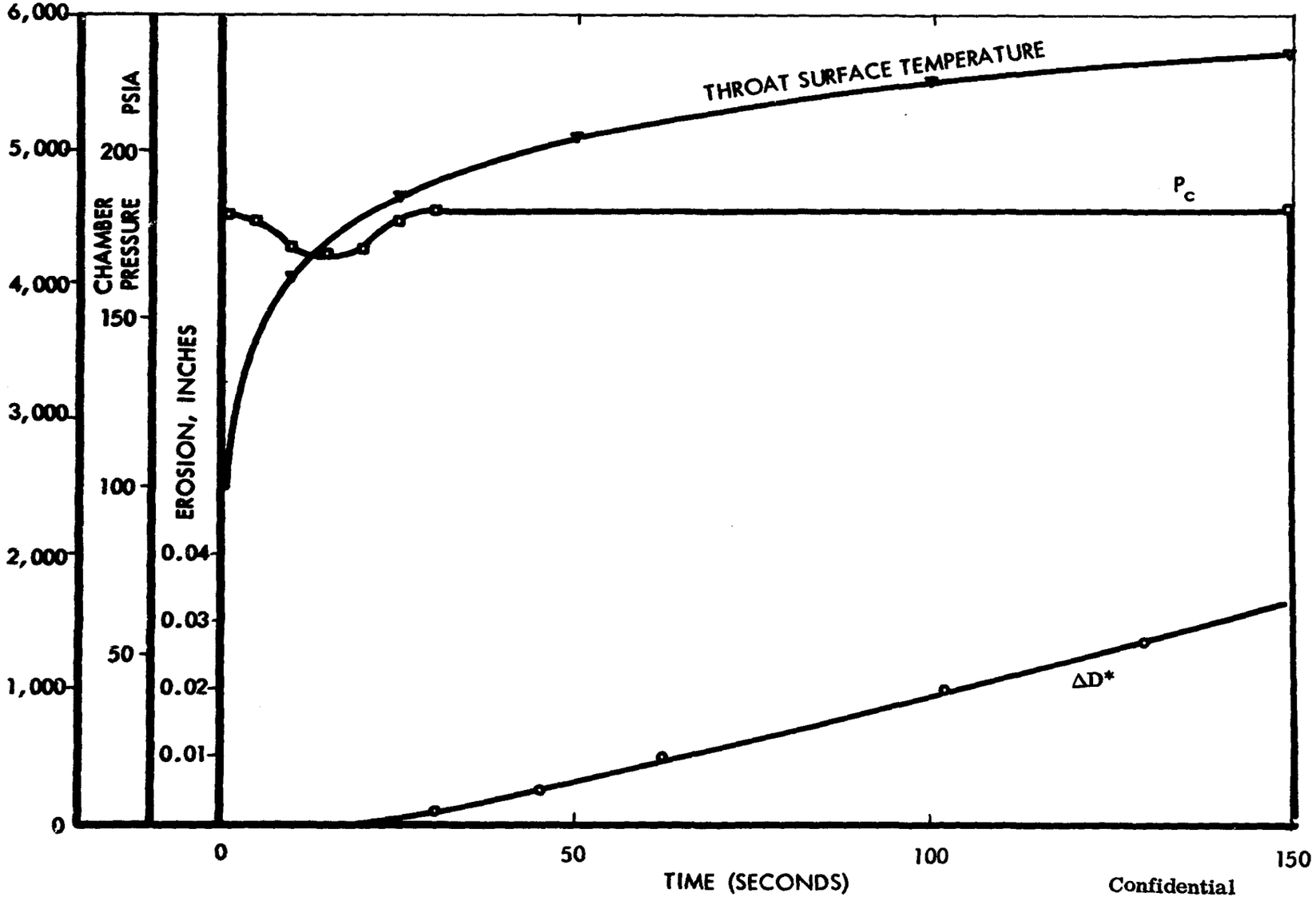

FIGURE 93 (U) UNIT S/N 2 DATA: RUN 309

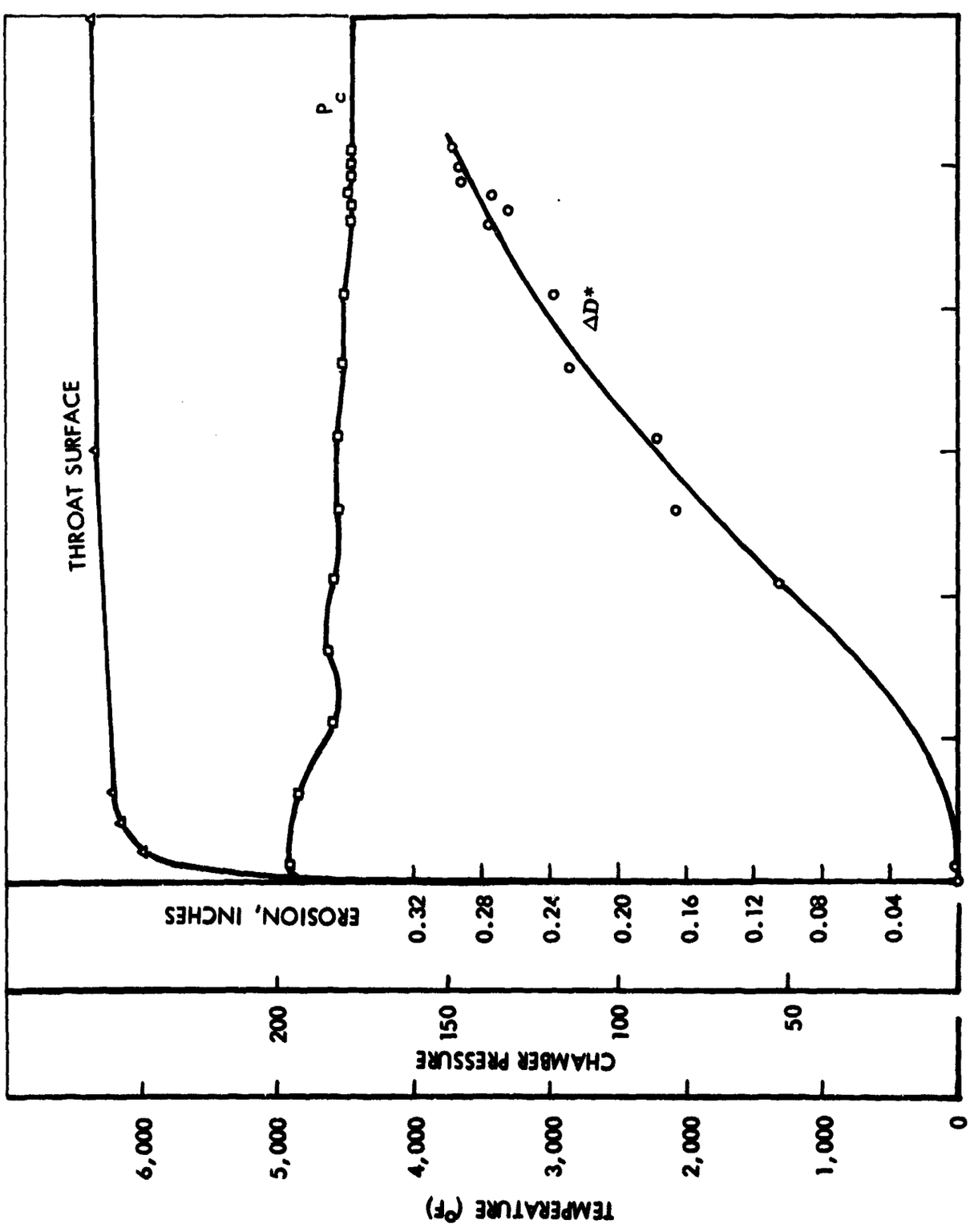

FIGURE 94 (U) UNIT S/N 3 DATA: RUN 348

properties of this material are vague and, in most cases, are engineering estimates only.

(U) In order to improve the estimate of the thermal properites, an iterative computer analysis was performed. The technique employed was to estimate the thermal diffisivity as a function of temperature and performance, perform a one-dimensional computer analysis using this data, compare predicted temperatures with the thermocouple data, revise the thermal diffusivity estimate, and repeat the process. For this analysis the data from test runs 280 and 281 in thermocouple section A-A were used. The results of the best computer analysis are presented in Figure 95. Also shown in Figure 95 are the actual thermocouple data. Using the density of Carb-I-Tex 700 and the specific heat for graphite materials, the thermal conductivity was calculated as a function of temperature and is presented in Figure 96. Although additional analyses could be performed to exactly match the computed temperature data with the experimental results, the results of the analysis would at best yield only estimated values for thermal conductivity due to possible inaccuracies in the temperature measurements.

(2) Full Scale Unit S/N 2

(U) Full scale unit S/N 2 was examined for structural performance, erosion, and thermal performance of the unique pyrolytic graphite throat insert design concept. Structurally, no difficulty was experienced except as previously discussed with respect to the pyrolytic graphite throat insert.

(U) Prior to disassembly, internal dimensions were recorded to evaluate over-all erosion. The following is a list of the average erosion recorded at each location excluding the throat.

Location	Change in Diameter during Test
Carbon cloth chamber liner	0.399
CGW graphite forward piece	0.358
CGW graphite center piece	0.188
CGW graphite aft piece	0.133
Nozzle exit cone exit plane	0.245

It was interesting to note that erosion in the graphite chamber liner decreased toward the throat.

(U) Alternate sections of carbon and graphite phenolic (about 0.75 inches long) were utilized in the nozzle exit cone to see if any significant performance differences existed. Examination of the sectioned exit cone indicated no significant difference existed in this region.

(U) The thermocouple data in Section C-C were compared with the predicted temperatures for this location. The correlation appeared reasonable thereby verifying the temperature predictions at the location in the thrust chamber. No additional analysis of these data were conducted.

(U) A detailed evaluation of the thermocouple data in Sections B-B and A-A was conducted and compered with the predicted values. The one-dimensional heat

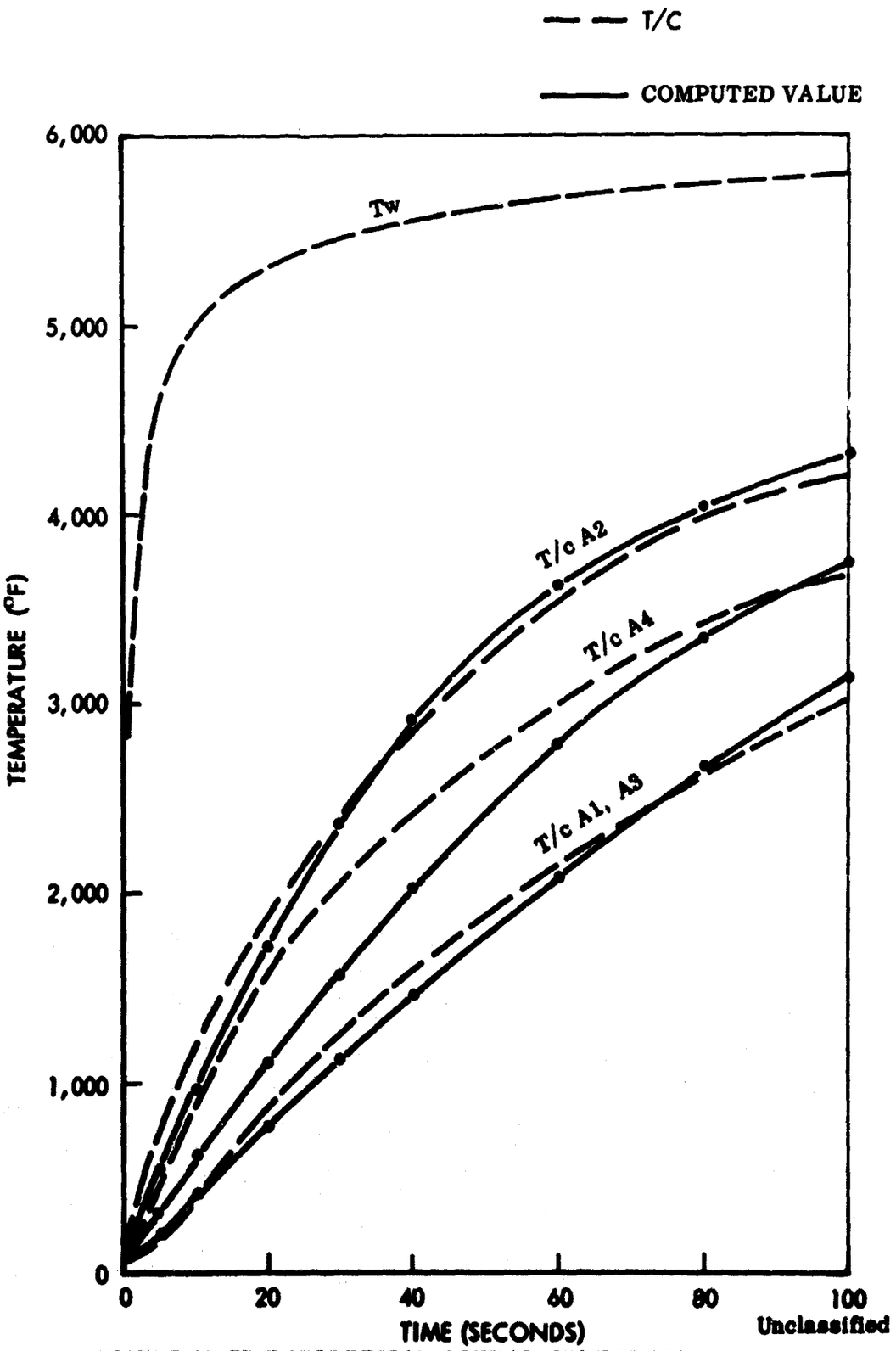

FIGURE 95 (U) THEORETICAL ACTUAL TEMPERATURE COMPARISON FOR UNIT S/N 1: RUN 281

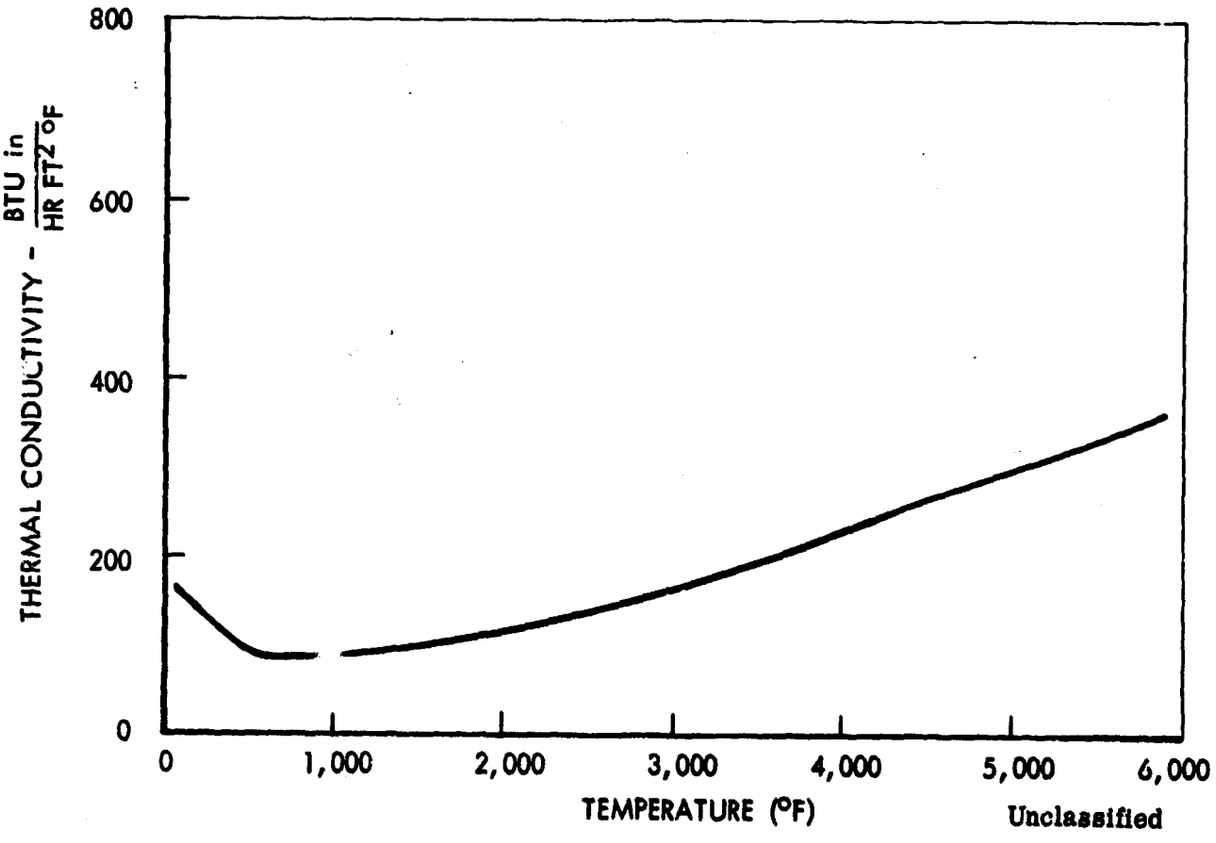

FIGURE 96 (U) THERMAL CONDUCTIVITY VERSUS TEMPERATURE FOR CARB-I-TEX 700

transfer analyses which were conducted at the throat location in conjunction with the design at Stations 2 and 3 (see Figure 71) were used. The run at Station 2 represents heat transfer from the throat surface in the high conductivity "a-b" plane direction to the CGW heat sink. Station 3 is a heat transfer analysis in the radial direction at the throat. The throat surface temperature predicted by each of the previous analysis techniques is presented in Figure 97. (data previously presented in Figures 76 and 78).

(U) The test results of Runs 299, 308, and 309 were compared to predicted temperature values. Thermocouple B-1 was compared with the predicted values for Station 2 analysis. The results of the comparison, presented in Figure 97, were good. Similar results were obtained when comparing the temperature of the thermocouple A-3 with predictions of the Station 3 analysis (see Figure 97). Within the experimental accuracy of the temperature data, the analytical approach was verified. Although neither of the one-dimensional heat transfer analysis techniques exactly describes the actual two-dimensional heat transfer condition, the predicted results bracket the actual throat surface temperature. The estimated value of surface temperature based upon this analysis is presented in Figure 97.

(3) Full Scale Unit S/N 3

(U) The general performance of unit S/N 3 is discussed with regard to the material performance (see Section VI, Subsection 3b). No detailed thermal analysis was performed as there was insufficient data to evaluate thermal properites.

b. Material Performance

(U) This section includes a detailed performance analysis of the full scale thrust chamber materials.

(1) Full Scale Unit S/N 1

(U) Figures 98 and 99 present a view of the thrust chamber inlet and exit of full scale unit S/N 1 following test respectively. Figure 100 presents several of the component parts following disassembly of the thrust chamber. The components, as viewed from left to right in Figure 100, are the chamber liner and insulation (sectioned), the throat insert, the throat extension, and the carbon cloth throat support. The silica insulation in the throat region and exit cone are not shown in Figure 100.

(U) The carbon cloth phenolic chamber liner was missing for an axial length of approximately two inches aft of the injector face, except for approximately a 15° arc as shown in Figure 98. Since there was little erosion of the silica phenolic overwrap in this area, it was concluded that the carbon liner was eroded or ejected from this area in the last few seconds of the firing. There was evidence that the liner broke up and was ejected since the material was separated at laminate ply interfaces.

(U) For an axial length of approximately 1½ inches upstream of the throat, the carbon cloth liner was missing (downstream portion of the chamber liner). The silica insulation behind the chamber liner was burned severely indicating the carbon cloth liner in this region was lost somewhat earlier in the firing

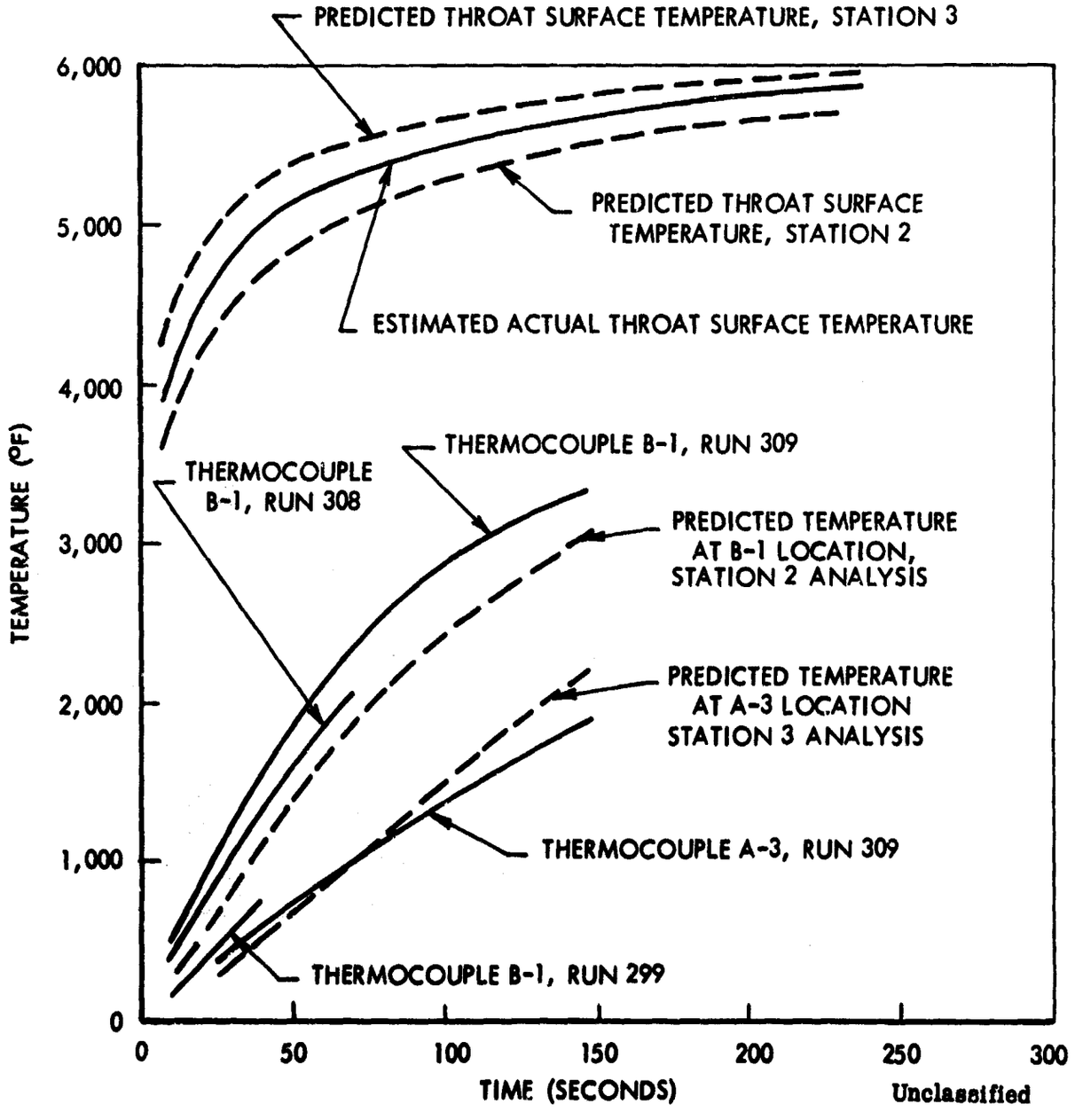

FIGURE 97 (U) TEMPERATURE CORRELATION DATA FOR UNIT S/N 2

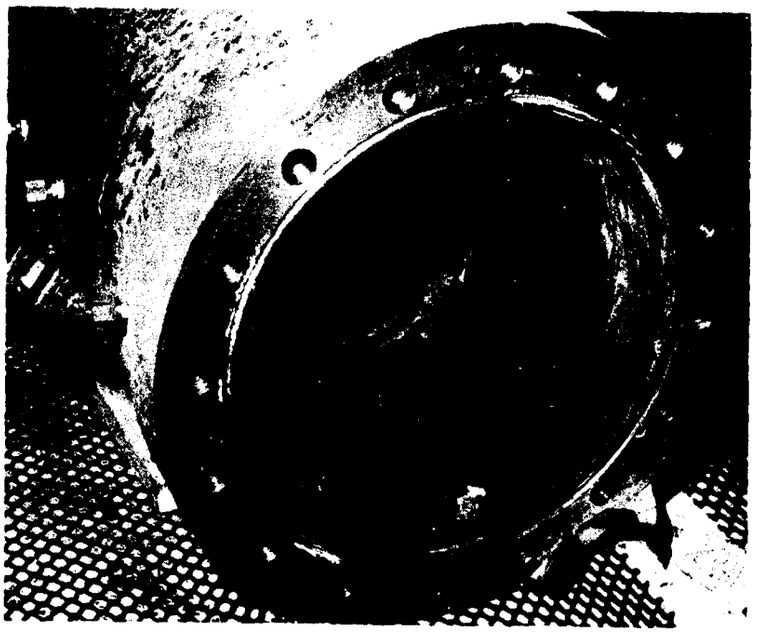

FIGURE 98 (U) Chamber Inlet of Unit S/N 1 After Test

Unclassified

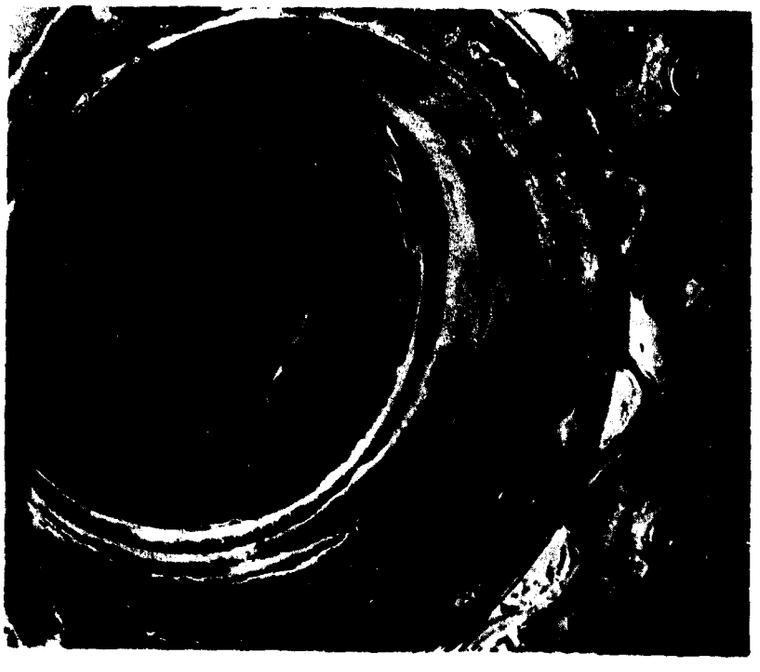

FIGURE 99 (U) Exit Cone of Unit S/N 1 After Test

Unclassified

Unclassified FIGURE 100 (U) Unit S/N 1 Component Parts After Test

than the portion of the liner at the upstream end of the chamber. In one location, a burn-through to the steel occurred.

(U) Injector streaking, noted by wide, deep, smooth erosion paths, was visually observed on the inside surface of the salvaged carbon cloth liner. Several "worm holes" were seen in the carbon near the aft end of the liner on the inside surface. The "worm holes" appeared to follow the tape orientation from the I.D. of the chamber liner to the O.D. of the liner. Several cracks, some wide, deep, and completely through (I. D. to O. D.) were observed. The entire remaining portion of the liner was separated from the silica chamber insulation indicating the need for greater integrity between the dissimilar materials of the liner and back up insulation. Figure 101 shows the two halves of the sectioned liner. The conditions described can be seen here. Figure 102 is a close-up view emphasizing the "worm hole" condition. It is significant to note that no "chunking" or spalling occurred on the chamber liner during firing.

(U) The silica phenolic chamber liner insulation was severely charred (Figure 103). Only a very thin section at the O. D. surface was identified as virgin silica. The inside surface of the insulation reflects an erosion pattern in areas where the carbon cloth liner was expelled. The silica insulation adjacent to the throat region was gouged severely, and deep pits into the silica were evident. On sectioning the liner insulation; deep, wide delaminations were seen in the thickness. Figure 103 shows these conditions. A photomicrograph, 2X magnification shows the delaminations, ply orientation, and general condition of the inlet insulation wall (see Figure 104).

(U) The Carb-I-Tex 700 throat insert was delaminated in several locations. Separation of the delaminated sections occurred at the inlet end of the throat insert and signs of flow in the delaminations were evident. The delaminations observed in the throat extension were slight. It was further noted that erosion of the throat and extension was quite irregular. Figure 105 shows the delaminations in the insert and the irregular erosion pattern in the extension. The view in Figure 106 shows more clearly the delamination of the insert and the separated delaminated sections at the forward end of the throat component.

(U) The reason for the irregular throat erosion is not clear. The throat diameter varied from 4.8 to 5.2 inches. As discussed previously, two gouged areas were observed in the throat insert just upstream of the throat plane following the 100 second test. It was believed that failure of the injector dome could have caused the gouges. During the last test, the irregular surface of the throat insert could have aggrevated the flow conditions causing non-uniform erosion.

(U) The carbon cloth phenolic throat support was completely charred (pyrolyzed) and separated from the silica insulation. The brittleness and fracture lines displayed by the liner indicates that the liner did not crack until it was pyrolyzed.

(U) A yellowish-green powder-like material was found on the O. D. of the liner. Some small amount of the silica reinforcement appeared to have adhered to the carbon cloth surface. However, these fibers appeared to be decomposed or degraded so that no fiber integrity remained although there was no evidence of silica melting. In the loose, sponge-like powdery coating on the liner could

Unclassified FIGURE 101 (U) Unit S/N 1 Chamber Inlet Liner After Test

FIGURE 102 (U) View of Unit S/N 1 Chamber Inlet Liner After Test
Unclassified

FIGURE 103 (U) Unit of S/N 1 Chamber Inlet Insulation After Test

Unclassified

FIGURE 104 (U) Cross-section of Chamber Inlet Insulation Wall, Unit S/N 1

Unclassified

FIGURE 105 (U) Unit S/N 1 Throat Insert and Throat Extension

Unclassified

FIGURE 106 (U) View of Unit S/N 1 Throat Insert and Throat Extension

Unclassified

be seen, under high magnification, minute crystall like particles which may have resulted from chemical reaction of the carbon and silica or between the silica and fluorine propellant species. No analysis of the material was made. The carbon exit cone remained intact with the overwrapped silica insulation. Visual observation showed some circumferentail cracking and erosion.

(U) The silica insulation overwrap on the carbon throat liner and the carbon exit cone was still intact. The forward edge of the silica (adjacent to chamber liner) was charred through. A burn through occurred at the interface. Virgin silica phenolic existed downstream of this location. As a result, the silica insulation was reused in unit S/N 2.

(U) The steel shell was in excellent condition following the test except for one hot spot. The inside surface of the shell was melted locally near thermocouple B-4. This melting condition, however, was not severe and as a result, the shell was reused for unit S/N 2.

(U) Although many of the components appear severely deteriorated, the total of 373 seconds firing duration at a chamber pressure of 200 psia represents an extremely severe environment. Under these conditions, the materials and design can be considered reasonably successful. It was shown that Carb-I-Tex 700 is a thermally shock resistant material with excellent erosion resistance for test duration up to 100 seconds, and fair erosion resistance for longer single pulse durations. It was shown also that oriented carbon cloth moldings can be fabricated which do not spall or chunk during firing. The need for integrating inner and outer liners by mechanical locking or materials integration was demonstrated by separation at all interfaces except in the exit cone where the char front did not apparently transgress the interface between carbon and silica. The knowledge obtained from this experiment will be most helpful in selecting materials and designs for subsequent fluorine propellant rocket motors.

(2) Full Scale Unit S/N 2

(U) Unit S/N 2 was in good condition following the test sequence. Evidence of flaking of the pyrolytic graphite throat insert material was noted in addition to the cracks previously discussed. The throat insert, however, was intact and the throat geometry retained (except for slight erosion, see Figure 107). Although the thrust chamber would have sustained additional testing, it was felt that little additional performance information could be obtained.

(U) Injector streaking noted by deep scallops approximately 1" to 1½" wide at the chamber inlet and smooth erosion paths was observed on the inside of the chamber components. The scallop like affect decreased in severity in the downstream direction towards the throat (see Figure 108).

(U) The carbon cloth inlet was charred through approximately 70% of the section. There were also radial cracks in the char layer in two places approximately 90° apart.

(U) In the forward and center sections of the CGW graphite liner, a scallop affect was observed. The aft CGW graphite liner was broken in three pieces. Part of C_4 thermocouple was still imbedded in the graphite ring. One break in in this aft chamber component was very close to the C_4 thermocouple and the other breaks were approximately 90° on each side of the C_4 thermocouple. Erosion was

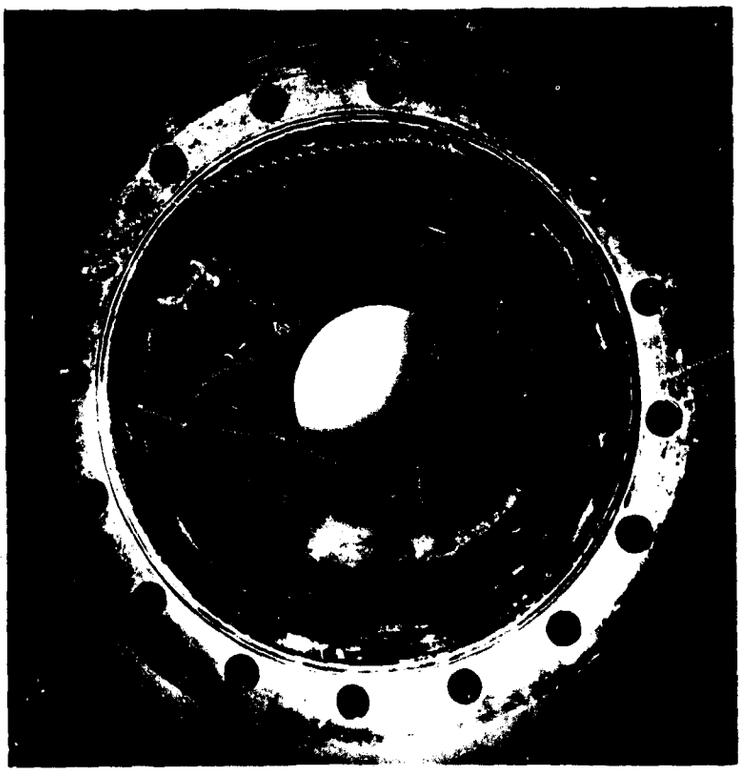

Unclassified FIGURE 107 (U) Unit S/N 2 After Test

Unclassified FIGURE 108 (U) Unit S/N 2 Inlet After Test

[illegible] rough in this place. No erosion or signs of gas flow were observed in the [illegible].

([illegible]) The silica phenolic chamber liner insulation was severely charred. Only a [illegible] section of the I. D. surface of the liner nearest the throat was identified as virgin silica. The carbon cloth phenolic was also severely charred. The I. D. of the carbon cloth phenolic was radially cracked in five places for a distance of approximately 3 inches. There was one noticeable separation approximately 2 inches upstream of the throat; however, this caused no difficulty.

([illegible]) The pyrolytic graphite throat insert was installed in a [illegible] graphite support. Severe local erosion was observed about 90° from the T_1 thermocouple. This area was about 45° in width. It is suppositioned that cracks in the surface layer of the pyrolytic graphite permitted this layer to break up and be expelled during testing. The pyrolytic graphite separated into 6 pieces when removed from the throat support. There were several radial cracks in each piece. The T_1 thermocouple was still partially imbedded in the throat. Each section appeared to be silvery in color. The throat was adequately bonded to the throat support. There were approximately 12 radial cracks equally spaced on the I. D. of the ATJ graphite throat support.

([illegible]) The silica insulation on the graphite throat support was still intact. The exit portion of the insulator was charred through. Virgin silica phenolic remained in the section directly around the throat area.

([illegible]) A white powder-like substance was found in the exit cone. There was one large circumferential crack approximately 3/8 inch downstream of the throat support. There was also one slight radial crack in this same area. These cracks, however, were only in the char layer. Visual observation shows very slight erosion.

([illegible]) The steel shell was in excellent condition following the test and was reused for unit S/N 3.

([illegible]) Although the pyrolytic graphite throat appeared quite fragile and displayed considerable local loss of material, throat area erosion was low if the effects of the structural failure are not included. During the first, second, and fourth test pulses (Runs 298, 299 and 308), throat surface material loss was abnormally high due to cracking and chunking, or erosion of the carbonaceous C-9 cement used during the repair of unit S/N 2 (see Subsection 2b for discussion). However, during Runs 302 and 309 when material failure did not effect the throat area, total diametral erosion of 0.009 and 0.036 inches was observed for accumulated pulse durations of 60 and 178 seconds respectively.

([illegible]) The reasons for the poor structural integrity were explored with the fabrication vendor. The vendor (Pyrogenics) felt that significant improvement in the part integrity could be realized with minor deposition process variations. Another approach to improve the final part would be deposite three conical pyrolytic components of the same configuration except with only 1/3 of the wall thickness, machine O. D. and I. D. surfaces, and subsequently bond the components together with National grade C-9 cement. With either fabrication approach, it is felt that the structural problems encountered with this throat insert could be eliminated.

(3) Full Scale Unit S/N 3

(U) Figure 109 shows unit S/N 3 from the injector end following the test. All the ablative material was found to be intact and erosion relatively smooth. Near the injector end, slight channeling was seen in the graphite-phenolic portion of the chamber but was smoothed out in the Thompsine Tape section. Only one or two delaminations were observed in the graphite-phenolic wrapped barrel section. The most significant observation is the retention of large amounts of the refurbishment material. Although seemingly loosely adherent, it was surprising that this much material remained after two starts of the motor. Erosion of the refurbishing material, although somewhat greater than the parent material, was not excessive.

(U) Figure 110 is a view from the aft end in which the carbon phenolic exit cone portion is the primary material visible. Considerable delamination of the carbon phenolic was apparent and several hoop tensile failures were noted as indicated in the circled areas of Figure 110. A small amount of the refurbishing material near the throat can be seen in the twelve o'clock position.

(U) It was noted that at 180° from the large refurbishment location slightly higher erosion occurred indicating, perhaps, slight channeling due to injector effects. As a result of the deep gouging in the first series of firings which resulted in the refurbishment of that area, the motor was rotated approximately 180° for the final firing series. The slightly higher erosion in the 180° position thus indicates a minor problem with the injector but does not account for the very series gouging on the first run.

(U) Upon receipt at TRW the assembly was oven heated and the ablative liner pressed from the steel shell. Some damage to the forward end was experienced from the disassembly operation and as a result some small amount of ablative material was lost. The liner was sectioned in half and the open faces are shown in Figures 111 and 112. The slight channeling of the graphite phenolic wrap near the injector is plainly visible. It will be noted that very little delamination occurred in this 30° graphite phenolic wrap, but some separation is apparent between the inner liner and the parallel to centerline overwrap which was carbon cloth. The Thompsine portion indicated very little delamination also, although the photographs indicate a very discontinuous fiber orientation. This was expected from the difficulties experienced in the tape wrapping operation due to the inadequately staged prepreg material (see Appendix for discussion).

(U) Several small holes were visible in the Thompsine portion which might be described as "worm holes." These were in the range of 1/16 and 1/8 inch diameter and occurred generally in the center of a delamination. The arrows in the figures indicate the location of some of these openings. It was noted that a small pointed tool could be inserted in these holes to some depth.

(U) The general outline of the char front can be seen. Beginning in the forward portion of the Thompsine Tape wrap, the char has penetrated approximately half-way through the quartz strata of the wall. Further aft in the throat approach section where the quartz was very thin, char has progressed through the Thompsine portion and well into the glass phenolic overwrap. At the throat and just aft of the throat the char has not penetrated the full

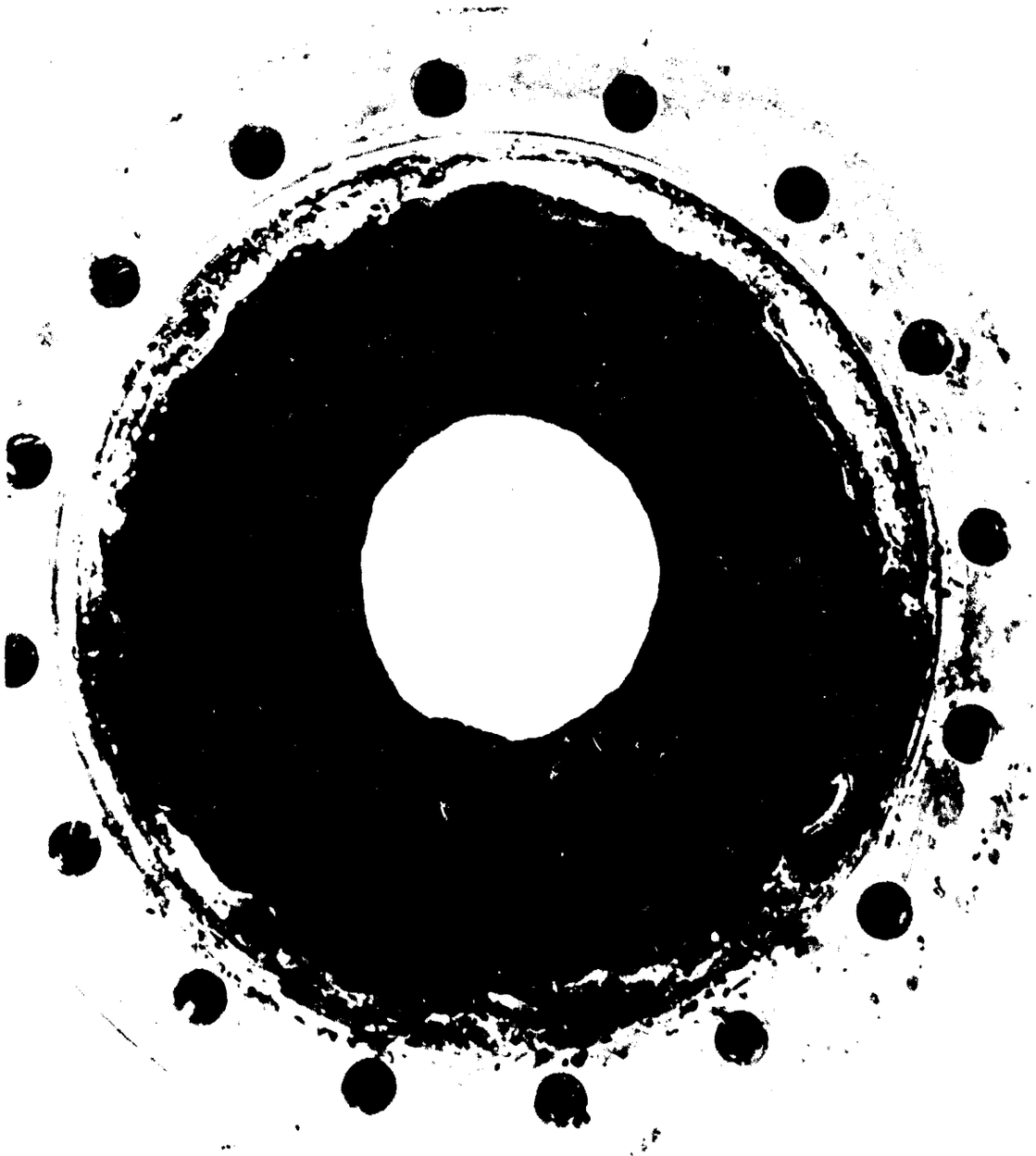

Unclassified FIGURE 109 (U) Unit S/N 3 Inlet End After Test

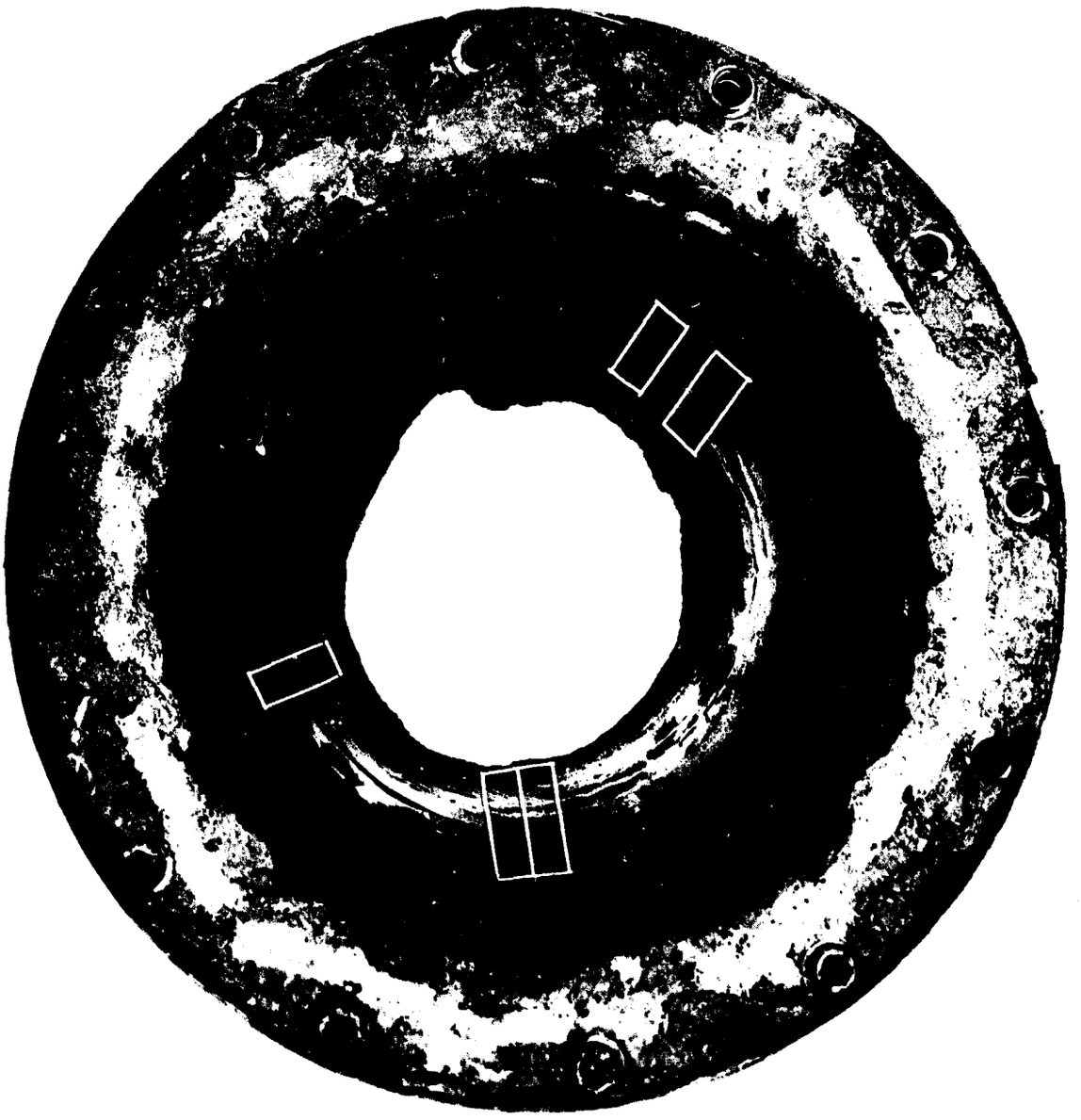

FIGURE 110 (U) Unit S/N 3 Aft End After Test

Unclassified

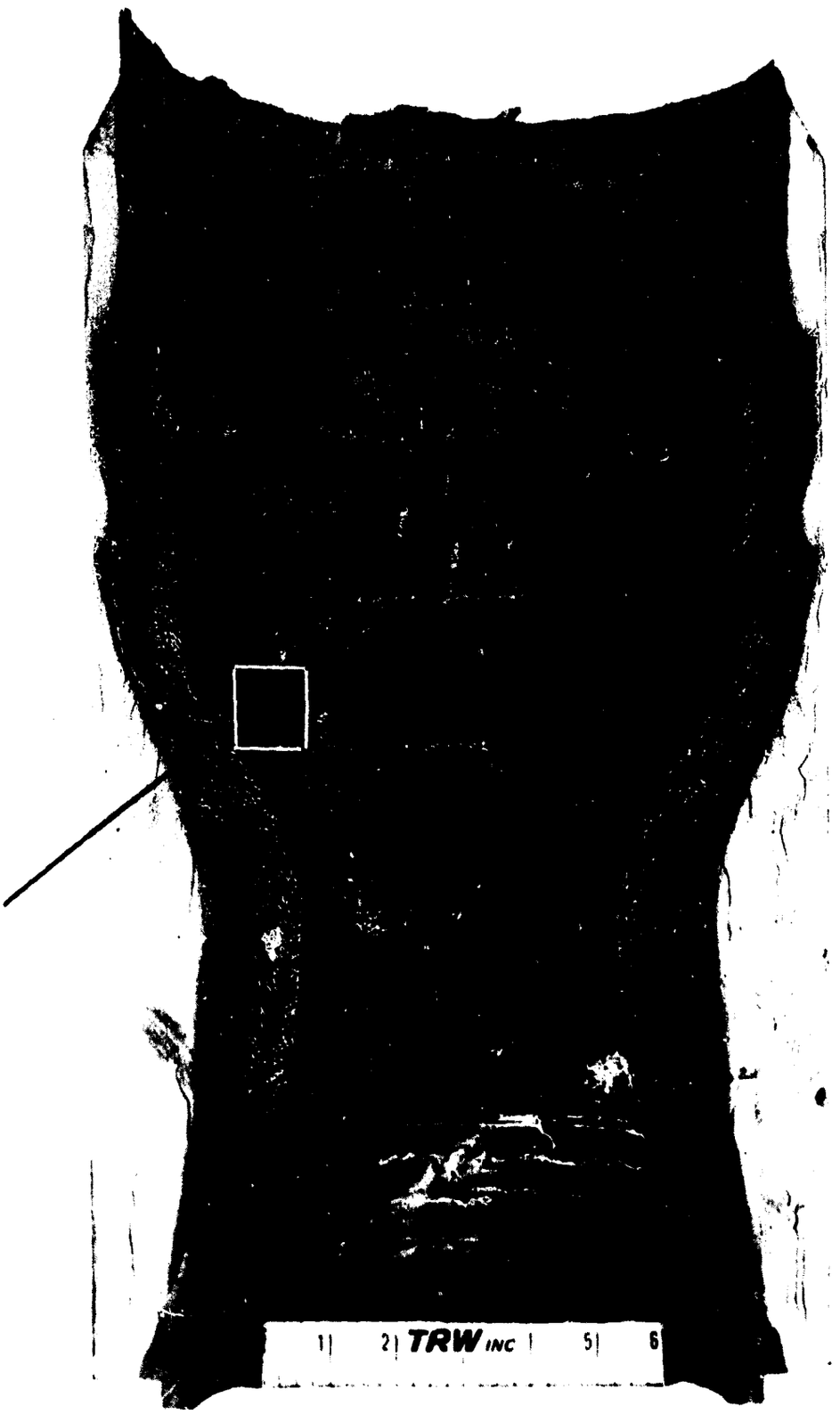

Unclassified

FIGURE 111 (U) Unit S/N 3 Sectioned

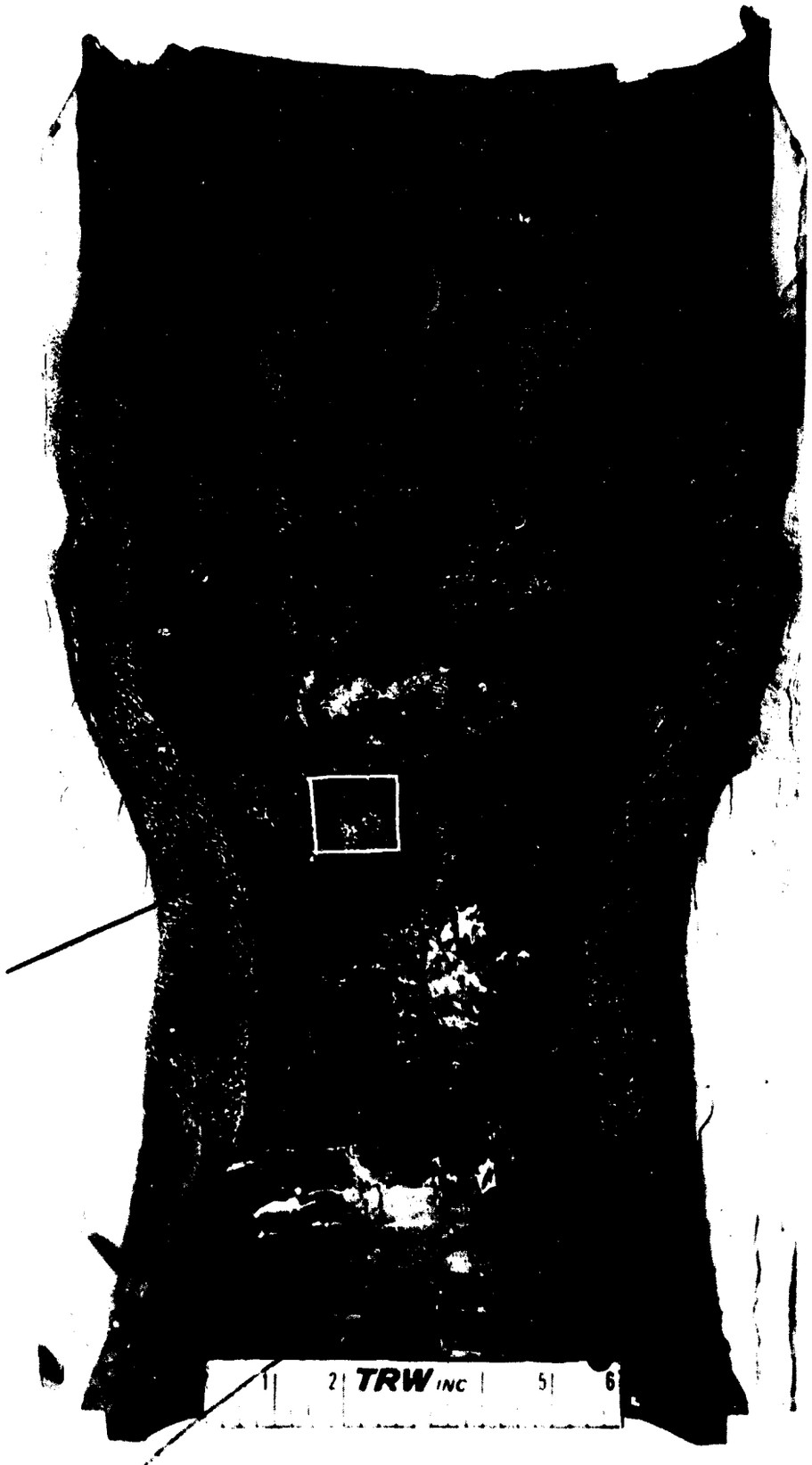

Unclassified

FIGURE 112 (U) Unit S/N 3 Sectioned

thickness of the Thompsine Tape. The most significant factor is the fact that char in all areas progressed through the interface between the graphite and quartz portions with no indication of separation or loss of integrity whatsoever. This, of course, is one of the primary advantages of the Thompsine Tape construction.

(U) The extensive delamination in the exit cone portion is visible in both Figures 111 and 112 and many of these delaminations extend through to the outer wrap where a substantial separation has occurred. The char front has completely penetrated the carbon phenolic and has progressed into the glass overwrap approximately 1/4 inch except for the last inch or so of the exit cone area. It is significant to note that severe delaminations are present in the glass overwrap material well below the char affected area.

(U) A section was made through one of the "worm holes," as shown in Figure 113. It was surprising to note a large cavernous area beheath the surface which was not evident from the surface. It was noted that the silica material was almost completely gone in this area leaving the ragged edges of the graphite fibers intact. A simple explanation to the phenomenon was soon formulated. It is obvious that the fluorine containing exhaust gases had penetrated through the delamination and had severely attacked the quartz substructure. A review of the physical chemicstry of the reaction explains somewhat the severity of the attack. The chemical reaction between propellant and quartz can be shown by the following equation:

$$4HF + SiO_2 \longrightarrow SiF_4 + 2H_2O$$

This reaction occurs with a theoretical reaction flame temperature of approximately 7770°F. The products of the reaction are both volatile and include water and SiF_4 which has a boiling point of -85°F. Evidence of the highly exothermic reaction are obvious from the pools of melted silica in the cavity which are vaguely apparent in the figure. An additional "worm hole", close to the one sectioned through, is circled on the photograph giving a better indication of the appearance of these openings. It is felt that this particular "worm hole" leads also to the same cavern as seen in the figure. It must be concluded that the "worm holes" could be caused by the rapid evolution and erosion of the high temperature reactants from the cavity.

(U) It is now possible to explain the severe gouging experienced in the first series of firings. Obviously, a burn through or a penetration of exhaust gases to the quartz part of the Thompsine construction caused subsurface attack and undermining and subsequent expulsion of a substantial chunk of the inner graphite fiber liner. It may be concluded that in any subsequent designs, very careful attention must be given to insure exclusion of the propellant specie from subsurface areas containing siliceous materials.

(U) Figure 114 is another section through a worm hole showing two additional highly reacted areas, one of which shows a pool of melted silica. In this case no worm hole was present although very slight delaminations can be seen leading to the reaction zone.

(U) A section through the primary refurbishment area is illustrated in Figure 115. The severe undercutting of the gouged area prior to repair is plainly visible. The refurbishment material was generally intact and shows

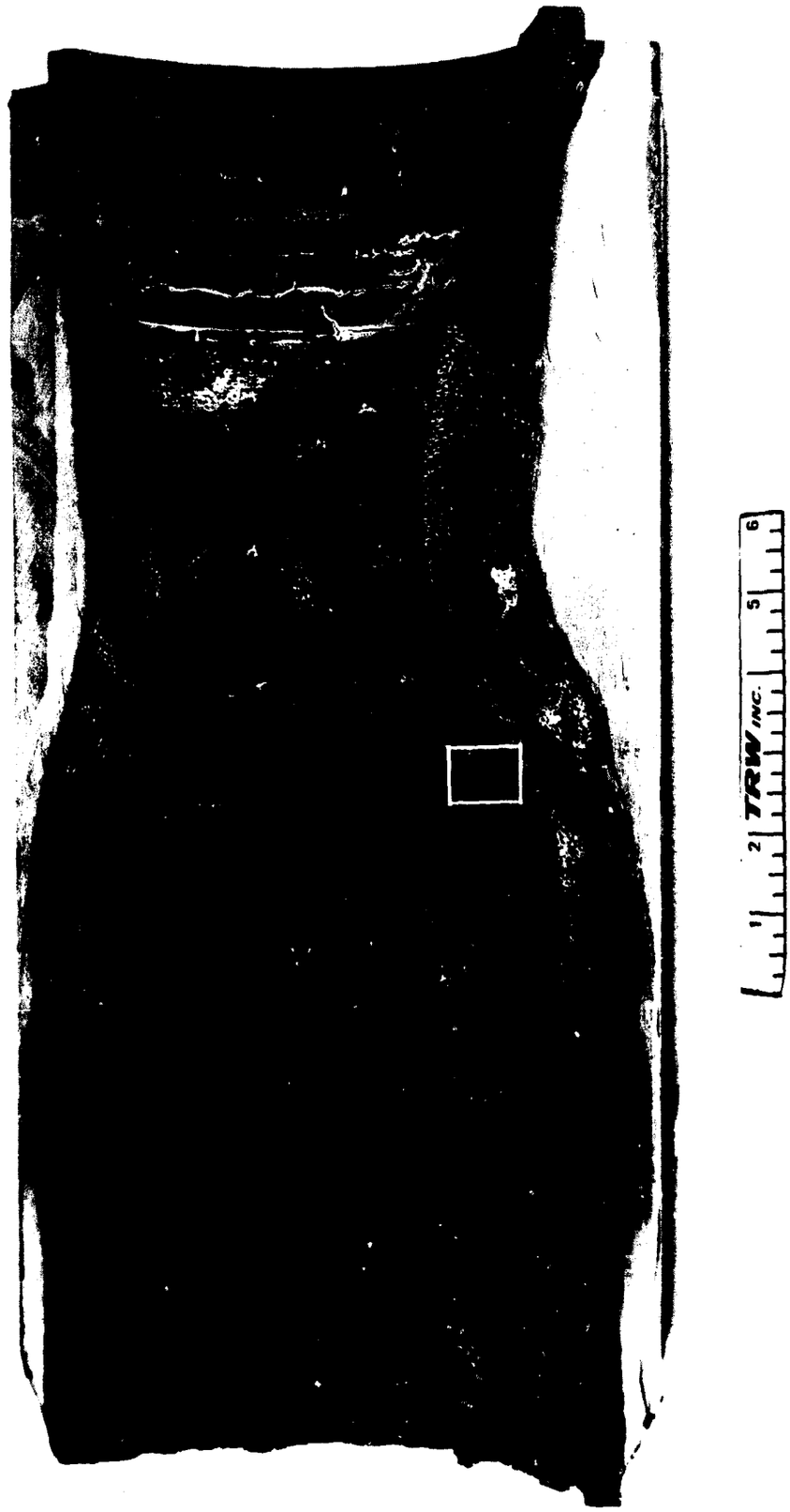

Unclassified FIGURE 113 (U) Unit S/N 3 Sectioned

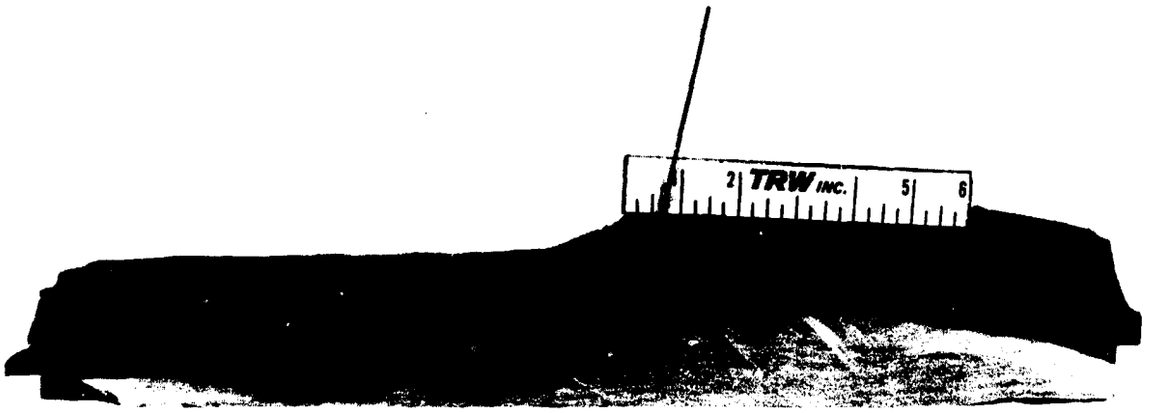

Unclassified

FIGURE 114 (U) Unit S/N 3 Axial Segment

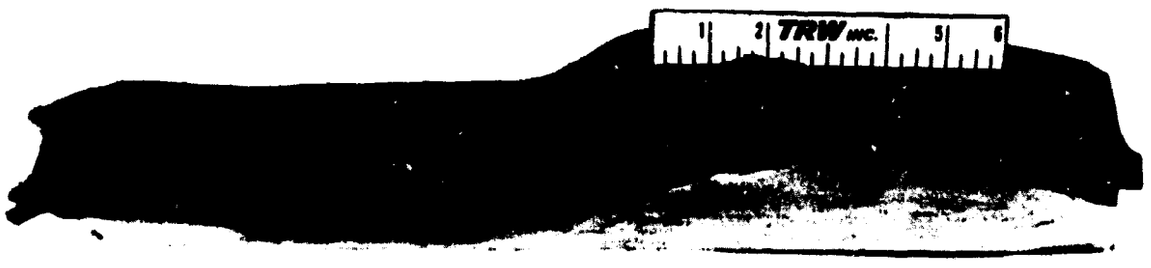

Unclassified

FIGURE 115 (U) Unit S/N 3 Axial Segment, Repaired Area

only minor cracking. Several small voids were visible, although not extensive. Considering the material was hand trowelled in a relatively awkward location, the degree of compaction achieved is excellent. No pressure was used during the cure of this material. A distinct char line in the material is visible. It is felt that such a formulation can be used successfully in subsequent repairs. Some separation is noted in the base of the refurbished material and a slight amount of char is noted in the glass overwrap which occurred in the initial firing sequence when burn-through occurred. An indication in Figure 112 is also given as to the erosion resistance of the refurbishing material which appears to be only slightly less than that of the Thompsine Tape.

(U) A thin slice was taken through a portion of the liner, sectioned into small pieces and impregnated with epoxy resin for more thorough investigation of the char characteristics. A reassembly of this section is shown in Figure 116. A macrophotograph of about 3X magnification is shown in Figure 117, taken in the cylindrical portion of the chamber at the graphite phenolic-Thompsine Tape interface. A careful examination reveals the ragged graphite-quartz interface in the Thompsine layer and shows no sign of loss integrity. The char front, although somewhat less apparent, is shown near the glass overwrap. In this area no loss of integrity is seen between the Thompsine and glass overwrap. It would be expected, however, that separation would have occurred if char had progressed to this location.

(U) One of the techniques used for evaluating ablative material char structures has been hardness measurements through the char section into the virgin composite. One of the primary advantages of such an analysis is the location of the char front particularly on carbonaceous reinforced materials where the coloration differences between char and virgin material are many times so subtle as to make positive location difficult. Another outcome of such an analysis is an indication of the size of the insipient heat affected zone where the material may be referred to as immature char.

(U) Such an analysis was conducted on unit S/N 3 on an axial cross section of the motor. A total of six stations were inspected including one station each in the graphite cloth chamber portion and carbon cloth exit section and four stations in the Thompsine Tape composite as depicted in Figure 118. Hardness measurements were made in 0.10 inch increments using a Shore D hardness tester starting 0.05 inch from the inside surface and progressing through to the O. D. surface. A minimum of three readings were taken at each test location and the values averaged. These values have been plotted for each axial station (Figure 118) on an enlarged scale of wall thickness with the various materials identified. Several observations of these data are significant.

(U) The hardness of the virgin materials were found to be in the 80-90 Shore D range while true char ranged from 30 to 50. At all stations of the Thompsine Tape minimum hardness char was not at the surface but was located from 0.35 inch to approximately 0.65 inch below the eroding surface. This observation is consistent with those of others reported in the literature and can be explained by one of the mechanisms of the ablative process. It has been learned that as organic resin is decomposed at the char front and low molecular weight gases percolate through the porous char layer toward the surface, a further degradation occurs and pyrolytic deposition of carbon is found in the very high temperature areas at and near the surface. An excellent

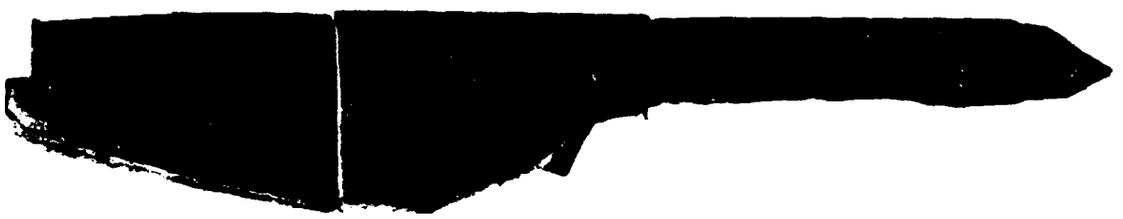

Unclassified

FIGURE 116 (U) Unit S/N 3 Axial Segment

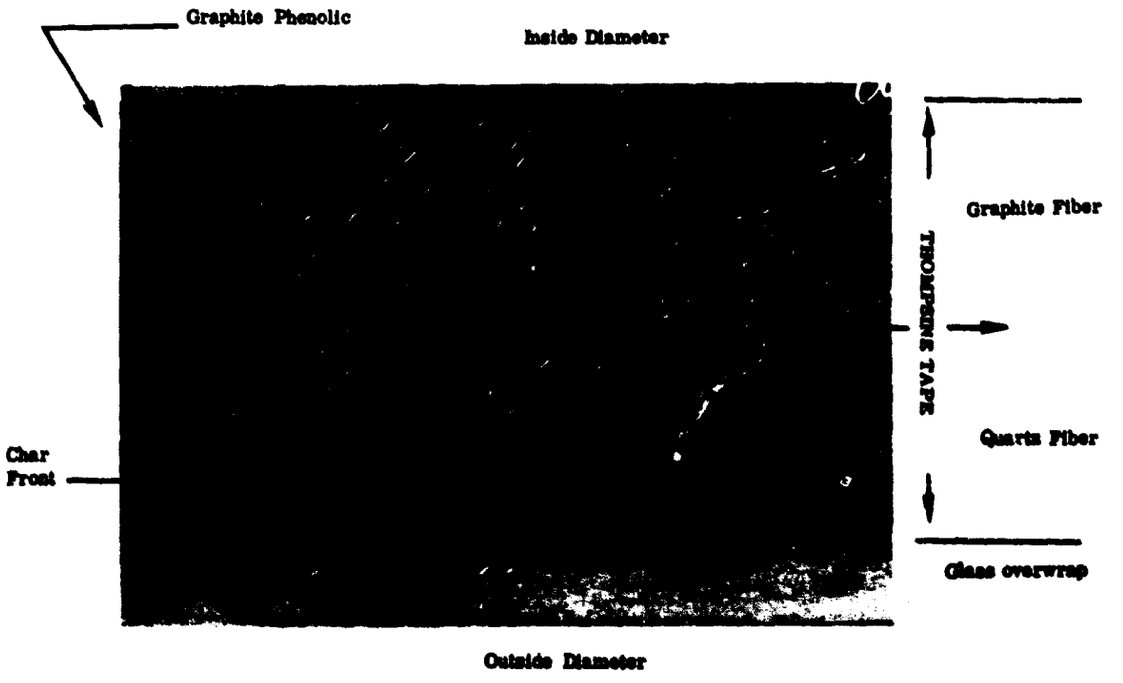

FIGURE 117 (U) 3X Magnification of Chamber Section: Graphite Phenolic - Thompsine Tape Junction.

Unclassified

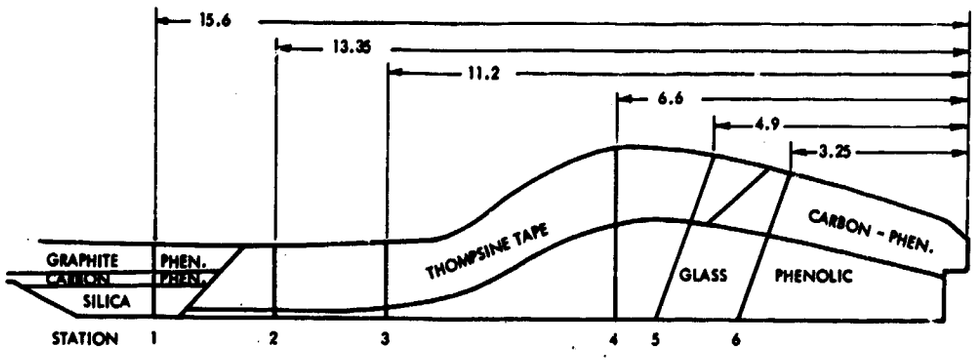

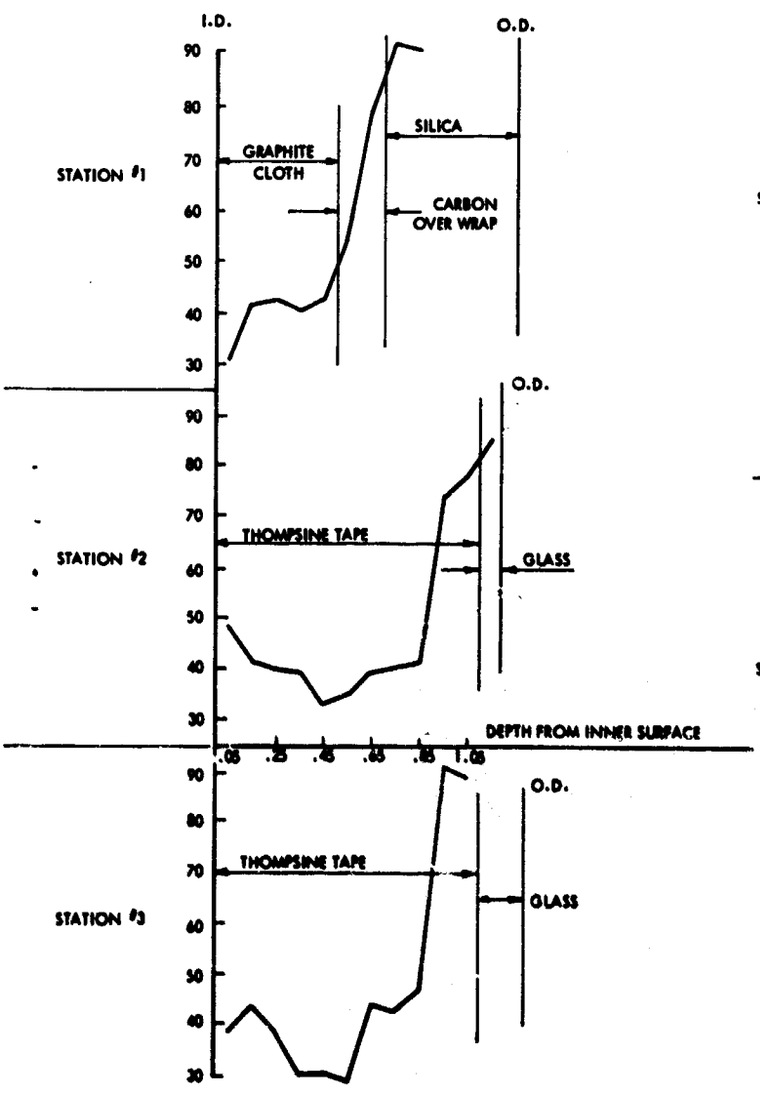

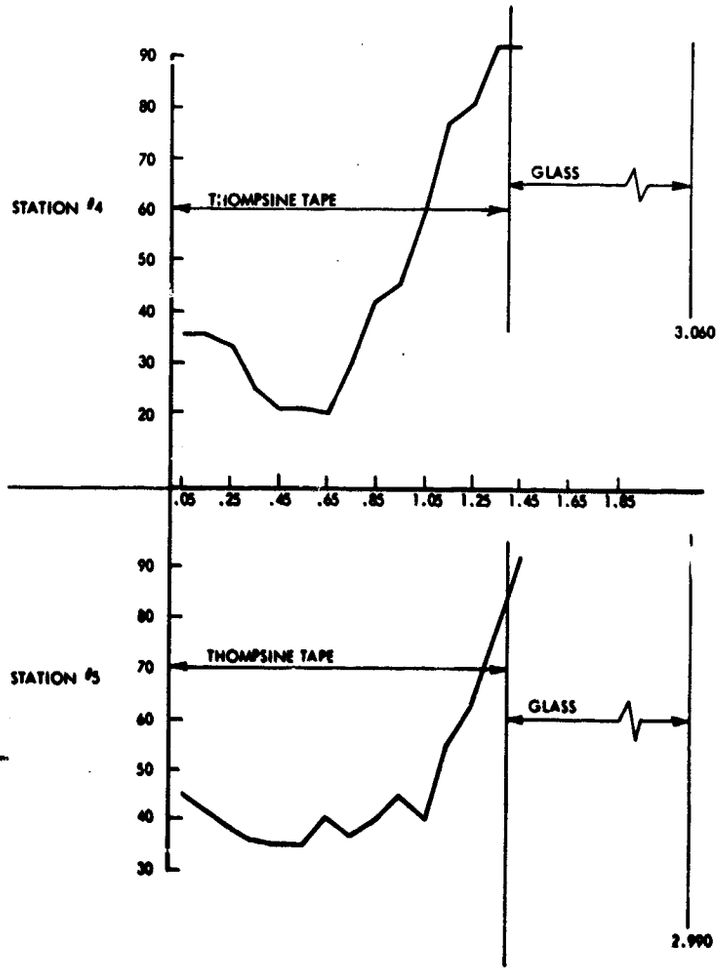

FIGURE 118 (U) CHAR HARDNESS TEST STATIONS

identification of pyrolytic graphite deposits has been made by Boeing in a study of ablative chars (1)[1]. The net result of these deposits is a higher density and thus greater hardness of the char in this region. This effect was not observed, however, in the carbon and graphite composite materials.

(U) At most axial stations a narrow band of perhaps 0.100 inch separated the fully charred material from virgin composite (e.g. Stations 1, 2, 3 and 6). However, at Stations 4 and 5 in the Thompsine Tape, a more gradual increase in hardness is observed indicating a larger incipient damage area. It will be noted also that at Station 6 in the carbon cloth composite, the char is considerably harder than that of the other materials even with very extensive delamination and axial cracking of the material. It will be noted here also that the char has progressed through the carbon into the glass overwrap material.

(U) It is felt that the hardness analysis has added considerably to the over-all understanding of the mechanism involved and the location of char front, which in most cases, was closer to the eroding surface than determined by visual observation.

(U) From the review of the design and construction of the motor and from the observations made in the post firing evaluation several conclusions can be drawn.:

A. Thompsine Tape can be fabricated in thicknesses and at diameters not possible with conventional bias tape construction.

B. Complete integrity is maintained between graphite and quartz strata of the Thompsine construction.

C. Extreme care must be taken in subsequent designs of Thompsine or conventional materials to insure exclusion of exhaust gases from silica containing overwrap materials.

D. The concept of refurbishment has been shown to be feasible and the erosion characteristics are nearly comparable to parent material.

(U) It is felt that the basic concept of Thompsine Tape and its advantages in the construction and performance of a liquid propellant rocket motor have been demonstrated.

[1] Numbers in parentheses refer to References

SECTION VII

DISCUSSION OF RESULTS

(U) Material performance during the thrust chamber tests can be separated into two major areas: mechanical behavior and erosion resistance. Interpretation of the materials performance in both categories is aided by the laboratory test results and information gathered from the literature, leading to the basis for selection of materials for testing in both subscale and full size engines tested during the program.

1. MECHANICAL BEHAVIOR

(U) High temperatures developed by the F_2/N_2H_4 blend propellant combination result in a severe thermal shock potential, principally for the nozzle throat. Although the chamber liner receives less of a thermal shock potential, injector streaking, thermal growth, and thermal fatigue are predominant design problems for this region, particularly where thin sections are employed for weight reasons.

(U) For the subscale tests, grade CGW graphite worked reliably as a chamber liner without any evidence of cracking or spalling. However, it was in a fairly massive state. None of the other chamber liner materials survived the mechanical strains of engine testing as well as the CGW, however, only one chamber liner material actually failed during testing. This was the thin pyrolytic graphite sleeve chamber liner, which was observed to have cracked after the 25-second pulse and was completely lost during the second pulse, exposing the CGW graphite backup material. Where the material was uncracked, superior resistance was noted. Cracks which developed in the carbon cloth chamber liner and delamination of the Carb-I-Tex 700 liner were not serious, but do indicate areas of potential concern for scale-up. Since all cracks formed in the carbon cloth terminated within the char zone, this type of mechanical failure presents a less serious threat to chamber liner integrity than does a delamination type of defect. In principle, delamination tendencies can be obviated by providing a parallel wrapped insulator over the liner or reduced by providing an oriented ply which has a greater surface area between adjacent plies.

(U) In the full scale tests, CGW graphite, carbon and graphite phenolic, and Thompsine Tape were utilized as chamber liner materials. All materials performed well for the shorter pulse durations (up to 100 seconds). However, for the longer pulse durations, in excess of 100 seconds, only the CGW graphite exhibited superior resistance to the environment. However, the CGW graphite design was more complex than that employed in the subscale designs to minimize cracking tendencies and improve the reliability of the design approach. Even then, one segment of the CGW graphite cracked but did not cause any performance difficulty.

(U) The Thompsine Tape and carbon and graphite cloth phenolic chamber liners demonstrated thermal shock resistance as expected, and did not spall or chunk during full scale testing. The need for integrating the inner erosion resistant liner and outer more insulative liner by mechanical locking or materials integration for light weight designs was demonstrated by separation at all charred interfaces between graphite or carbon phenolic liners and the silica phenolic insulation. The Thompsine Tape chamber liner demonstrated that complete interface integrity is maintained when the erosion resistant and insulation materials combined during the actual construction of the tape.

(U) Mechanical reliability of the nozzle throat is critical to engine performance, as exemplified by the mechanical failure of the hot-bonded Grafoil nozzle throat insert during subscale testing. Failure occurred by extensive delamination in the

"c" direction in the material. The resulting laminates were forced towards the aft end of the motor by the chamber pressure, causing loss of throat contour.

(U) From a design objectivity standpoint, simple ramp retention of the throat insert is most economical and the easiest provision for the scale-up. To accomplish this, however, tensile and shear strength between plies or laminations must be adequate to prevent failures as noted above. With the exception of the hot-bonded Grafoil, the possible the PTB material, no inadequate strengths for insert materials were noted. Conceivably, orientation of the Grafoil plies in a manner akin to that employed for the Pyroid (PG) throat insert (conical orientation) would have reduced the delamination tendency. Likewise, although no problem occurred with the Carb-I-Tex 700 material, a greater degree of confidence might be exhibited by conical orientation.

(U) The arc-cast hypereutectic hafnium carbide nozzle throat insert tested in a subscale design demonstrated excellent thermal shock resistance even though the insert contained casting defects. The large graphite flakes within the eutectic mixture of carbide plus carbon appears to be the major factor for promoting thermal shock resistance. Potential for scale-up from a mechanical reliability standpoint appears good, but there are, at the present time, limitations on available equipment for arc-casting this material.

(U) Fractures developed in the tantalum carbide prestressed subscale throat insert which did not lead to failure of the insert, but indicated that some uncertainties remain in the design of a prestressed insert. Scale-up of this type of design appears to be expensive because of the precise design requirements, but there are no apparent technical limitations in fabricating larger components.

(U) Thermal shock was not a problem with the subscale thoriated tungsten on any of the three pulses. While fabrication scale-up can be readily accomplished, the erosion was significant and doubt remains as to the true scalability aspects of thermal shock relations. Recrystallization was noted which ordinarily promotes thermal shock tendencies, especially in large sizes where OD to ID ratios are small in order to save weight.

(U) The performance of the Thompsine Tape throat insert was comparable to that of the ablative concepts of similar materials, and therefore is not recommended as throat material for this environment. However, the advantages of Thompsine Tape as an engineering material in ablative designs were demonstrated. It was shown that Thompsine Tape can be fabricated in thickness and at diameters not possible with conventional bias tape construction and that complete dissimilar material interface integrity can be maintained in the charred condition.

(U) During the tests of the Thompsine Tape throat insert, a severe local loss of material occurred. Following the tests, the thrust chamber was sectioned axially into several segments revealing localized large cavernous areas beneath the surface which were not evident from the surface. These cavernous areas resulted from the severe attack of the quartz substructure by the fluorine containing exhaust gases which had apparently penetrated through a delamination. Although this problem occurred only during the test of the Thompsine Tape thrust chamber, it is a potential area of concern in any design employing siliceous materials and thus, very careful attention must be given to insure exclusion of fluorinated propellant specie from these subsurface areas.

(U) Of the other throat insert materials, PG, CGW, and Carb-I-Tex 700, thermal shock was not expected to be a problem and this was verified during the tests. Both the PG, and Carb-I-Tex 700 materials were tested in subscale and full size configurations. Although thermal shock was not a problem with the PG insert, a significant number of cracks occured in the full scale throat structure during fabrication. As a result some break-up and loss of material occured during the test of this insert, although the throat geometry was retained as the PG exhibited the lowest overall erosion. However, the loss of the PG material during the test lowers the confidence of this design approach. It is felt that the integrity of the pyrolytic graphite structure can be improved by modifying the fabrication procedure while maintaining the basic design concept.

2. EROSION RESISTANCE

(U) Erosion rates for the inserts can be calculated from measured diameter changes and the length of firing time. However, rate of erosion of a particular material is a function of engine pressure, efficiency (C*), wall temperature, firing pulse duration, and gas composition as well as other possible factors. For this series of thrust chamber tests, chamber pressures, wall temperatures, and efficiency varied; thus the measured erosion rates were not directly comparable between the nozzle throat materials. Where possible, calculations were made to compare the performance of the nozzle throat materials on an equal basis. On the corrected basis, as a material class, carbides were best, the graphites and pyrolyzed graphite composites a close second, tungsten -2% thoria a distant third, and ablative material worst.

(U) Thermodynamic equalibrium studies yeilding a theoretical rating of refractory materials exposed to HF, the major constituent of the propellant gases, indicate graphite has superior resistance to erosion than either tantalum carbide below wall temperatures of 5840°F or tungsten below wall temperatures of 6320°F (see figure 119). Tantalum carbide is close to tungsten in this theoretical rating, with the maximum difference occuring at 6000°F. Calculated wall temperatures for the throat insert ranged from 4000 to above 6000°F with tantalum carbide and tungsten -2% thoria being equal at a wall temperature of 4700°F during subscale firing.

(U) Subscale thrust chamber test results show tantalum carbide and hypereutectic hafnium carbide to be the most erosion resistant materials. However, laboratory tests where materials were exposed to a hydrogen-fluorine flame found both graphite and tungsten to have less percentage weight loss than the above carbides. Reactivity tests indicated a graphitic material, Carb-I-Tex 700, was best. Tungsten developed less erosion in the reactivity tests than either of the carbides, but grade CGW graphite developed extensive erosion during this laboratory test.

(U) There are several possible reasons for the better performance of the carbides. The N_2H_4 blend fuel contains some water, and the water content produces oxidizing specie of gas in the propellant constituents. Reactivity tests have found carbides to be relatively erosion resistant in oxidizing gases, when compared to graphite. Moreover, tungsten also has less oxidation resistance than carbides, and therefore would be expected to develop more erosion. However, the weight of oxidizing specie in the propellant constituents has been calculated to be relatively low, thus casting doubt on this explanation.

(U) A second possibility is the presence of unreacted fluorine in the gas stream affecting the relative rates of erosion of the nozzle materials. Fluorine rich flames are known to greatly increase the reaction rates and material loss (2); however which

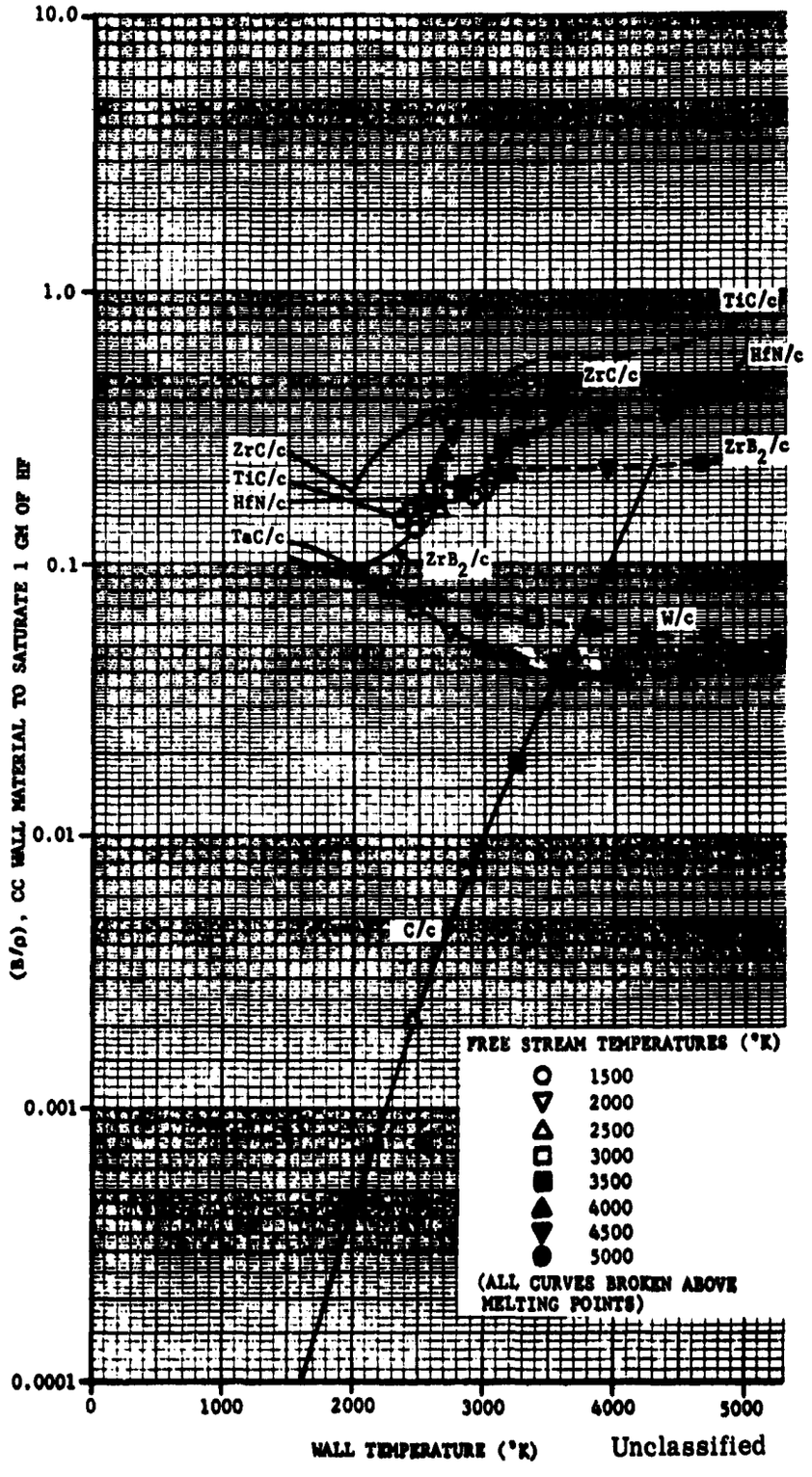

FIGURE 119 (U) Theoretical Rating of Refractory Materials Exposed to HF at 1000 psia (2)

materials would be affected most is not know, although tungsten would, of course, be suspected.

(U) Of the graphite materials evaluated in the subscale test program, pyrolytic graphite performed best. Due to the high axial thermal expansion in the "c" direction and the ply orientation used, the effective throat diameter grew smaller for part of the firing test. However, the erosion measured after firing indicated an erosion rate somewhat greater than tantalum carbide and nearly equivalent to hypereutectic hafnium carbide (considering engine efficiency during firing, etc.) Erosion rate of CGW graphite was higher, as would be anticipated because of the lower density of the monolithic graphite (1.80 gms/cc) compared to the pyrolytic graphite (2.18 gms/cc). Performance of the Carb-I-Tex 700 material should be nearly equivalent to the CGW graphite because of similarities in density and basic chemical structure. However, performance of the Carb-I-Tex 700 was much better and may be due, in part, to the existance of slight volumes of uncharred resin, increased shearing resistance due to the oriented plies, and lower chemical diffusion rates through the structure.

(U) Pyrolytic graphite also performed best in the full scale evaluation program by exhibiting low erosion for a long duration pulse. Carb-I-Tex 700 demonstrated excellent erosion resistance for pulse durations of 100 seconds or less, however significant erosion was experienced during a pulse of greater duration. Although the difference in materials densities would account for some of the difference in erosion, the greatest affect was probably the difference in the throat surface temperature. The pyrolytic graphite was utilized in a unique heat sink design. The planes of high thermal conductivity were oriented such that heat was rapidly conducted away from the throat surface which reduced the rate of temperature increase at throat surface. As a result, the throat surface temperature and thus the reactivity potential of the graphite material with the combustion specie was lower.

(U) An attempt was made to correlate erosion as a function of temperature and pressure by reducing the subscale and full scale test data to a comparable form. To do this, the erosion rate was assumed diffusion rate controlled and was correlated as suggested in references (3), (4), and (5) by assuming an equation of the form

$$\frac{dr}{dt} = K_o P_c^{n} e^{-k_1/T_w}$$

where $\frac{dr}{dt}$ = Erosion rate in in/sec.

P_c = Chamber pressure in psia

K_o = Function of effective collision frequency

k_1 = Function of activation energy

n = Order of reaction (assumed equal to $\frac{1}{2}$)

T_w = Wall surface temperature in °R

(U) The variations in throat diameter, chamber pressure, and throat surface temperature for selected test runs from subscale and full scale tests are given in Figures 64, 65, 66, 67, and 92 through 94. Throat materials included in these data are tantalum carbide, hypereutectic hafnium carbide, PTB, and CGW graphite from the subscale data and Carb-I-Tex 700, pyrolytic graphite, and Thompsine Tape from the full scale data.

(U) This erosion rate of the selected materials corrected for chamber pressure is plotted versus the inverse of the wall surface temperature in Figure 120. A semi-logrithmic scale was used for the figure since, if the erosion rate varied as suggested by the theoretical model, the erosion data for each material would yield a straight line plot. Data for the first 20 seconds of the selected test runs were not used since they were distorted by rocket motor start up transients (see dip in P_c in Figure 92 for example). This limitation, unfortunately, eliminated some low temperature data.

(U) With reference to Figure 120, characteristic trends of the various materials are observed and these trends agree in general with that predicted by the theory. The subscale test data is within the inverse temperature band from 0.2 to 0.3 (wall temperatures were lower than those realized from full scale testing due to lower combustion performance of the test injector). The CGW graphite and the PTB prepyrolyzed composite essentially show the same erosion rate at corresponding temperatures. The activation energy appears similar for both CGW and PTB as can be assessed by the similarity in slope of these two curves. Both the TaC and HfC + C have better erosion resistance than either the CGW or PTB.

(U) The full scale test data is for greater material wall temperatures. The data indicate the PG has a greater erosion resistance than the Carb-I-Tex 700. This is as expected since PG has a higher density than Carb-I-Tex 700 (approximately 2.15 gm/cc as compared to approximately 1.45 gm/cc respectively). The reason for the good erosion resistance for the Thompsine Tape is not clear except that the mass transfer due to ablation would be expected to reduce surface reaction. The fact that the general slopes of the subscale and full scale test data are so different suggests the influence of throat size and test conditions are significant. Also, the effect of chamber pressure may be greater than suggested by the diffusion rate control model.

(U) The large affect that wall temperature has on the surface erosion can be observed by comparing the relative erosion rates of Figure 120 with the full scale throat surface temperatures at various elasped firing times (see Figures 92, 93, and 94). The heat sink affect of the PG throat design, which in part accounted for its excellent performance, significantly reduced the throat surface temperature rise as compared to that of the Carb-I-Tex 700 and the Thompsine Tape. For instance, for a throat surface temperature of approximately 5700°F (0.16 on the inverse temperature plot of Figure 120), the elapsed firing time is 90 and 140 seconds for the Carb-I-Tex 700 and PG respectively. The Thompsine Tape surface temperature is predicted to exceed 6000°F within the first 5 seconds.

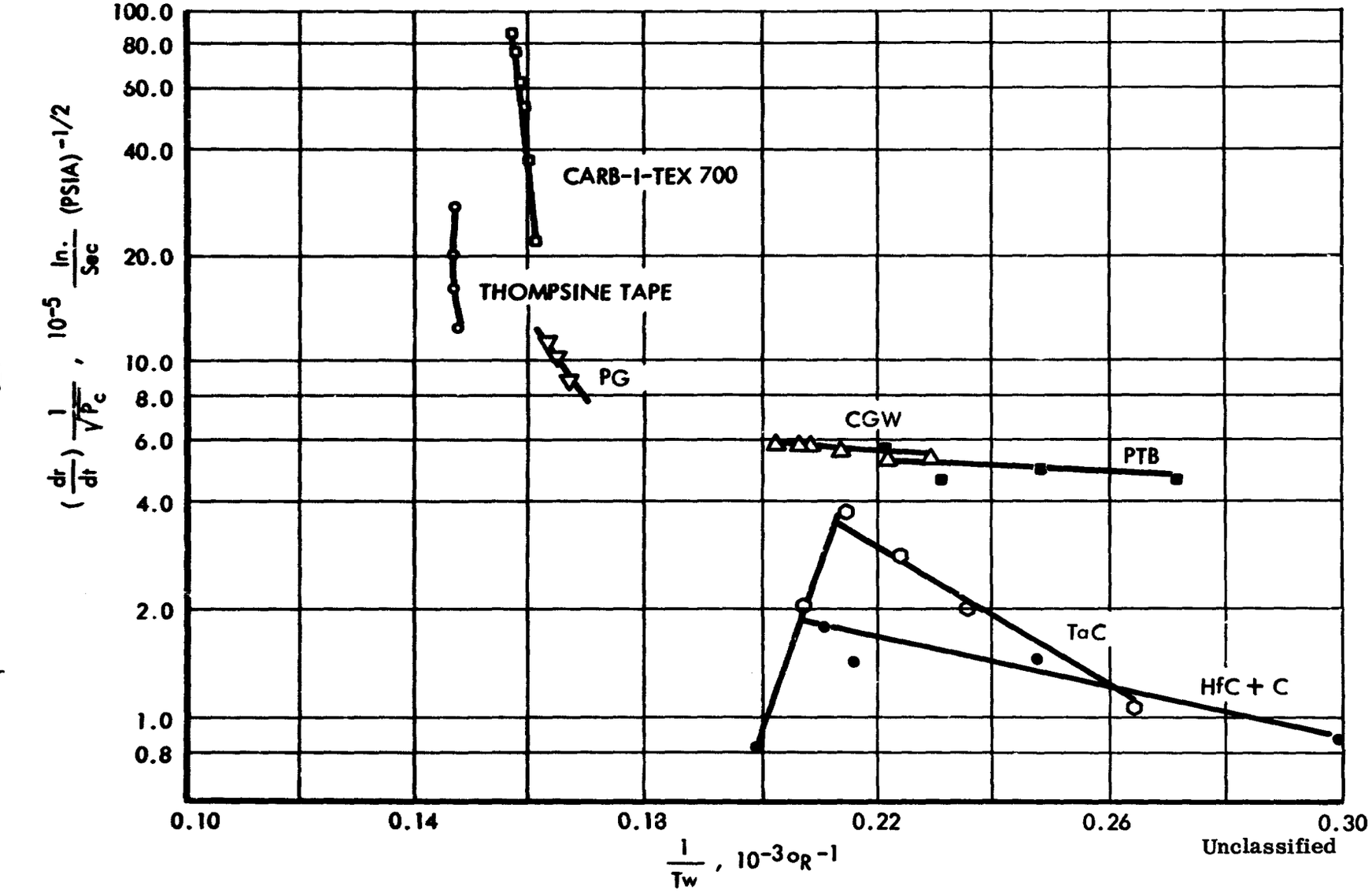

FIGURE 120 (U) CORRELATED EROSION DATA

SECTION VIII

CONCLUSIONS AND RECOMMENDATIONS

(U) The conclusions and recommendations of the technical effort are presented in this section. In review, as presented in Section III, the technical plan presented a systematic approach to accomplish certain specific objectives. Basically, these objectives are the development of candidate materials and design concepts leading toward improved performance capabilities, the definition of operational limitations, the evaluation of thrust chambers and design concepts in liquid fluorine/hydrazine blend propellant exhaust environment, and the analytical correlation of material performance and predicted behavior with test data. As a result of this effort, recommendations for future effort are presented.

1. CONCLUSIONS

(U) The technical effort was pursued in the following areas--literature survey, laboratory materials investigation, and design concept evaluation through subscale and full scale testing. As a result of the effort, the following conclusions are reached:

A. Information obtained through the literature search indicates fairly conclusively that the materials which will have the best performance, i.e., lowest reactivity with the high temperature combustion products of fluorine propellants, are essentially carbon base materials--carbides, graphites, and pyrolyzed (graphite) composites. There is some indication that certain carbides -- specifically TaC--may have superior resistance to HF reaction at very high temperature (above 5840°F wall temperatures). Refractory metals do not appear to be promising for this environment.

B. Laboratory reactivity test data supports the results of the literature survey with one exception. In both static and dynamic tests, the graphite materials ranked highest. The fine grained graphite structures reflected lower reactivity than did the courser grained, high density graphites. The carbides were lower on the scale; however, specimen temperatures were lower than 5800°F in each case. Tungsten performed well in reactivity tests despite literature data to the contrary, but subsequent firing tests did substantiate marginal performance.

C. Test evaluation of both subscale and full size design concepts indicate that satisfactory levels of performance can be achieved by self-resistant materials, without resort to cooling, for the imposed test conditions, i.e., 100-200 psia chamber pressure for pulse lengths up to approximately 200 seconds. While gross survivability can be achieved for more severe conditions, projections of material performance for high pressure environments indicate erosion rates will be excessive for all but relatively short pulses for these materials in an uncooled state.

D. In ranking of the various throat materials used, judgment must be made for difference in C*, pulse duration and chamber pressure occurring during test, and size. On a comparative basis, the following estimated ranking of throat insert materials subjected to the LF_2/N_2H_4 blend propellant system for this program is presented in descending order from best to worst:

Pyroid (PG)

Carb-I-Tex 700

TaC

HfC + C

CGW

Tungsten

PTB

Grafoil

This ranking was established as a result of subscale testing and subsequently confirmed for Pyroid and Carb-I-Tex 700 through full scale testing. In presenting this ranking, it must be recognized that performance differences for the best materials were small making the total effect on material usability subject to other design factors and fabrication capability as well. Thompsine Tape, as has been previously stated, is not recommended for use as a throat material since ablative materials do not appear to have application except for very short pulses (approximately 20 seconds maximum) and in therefore not included on the list.

E. The hypereutectic carbide structure demonstrated insensivity to thermal shock in a nozzle firing. Hypereutectic hafnium carbide demonstrated good erosion characteristics; however, it appears to erode at a greater rate than tantalum carbide. Current fabrication limitations prevent scale-up potential for hypereutectic materials except for future requirements. This type of structure appears attractive for potential lightweight applications.

F. The prestressed design concept shows promise toward utilization of highly thermal shock sensitive material such as the pure carbides (stockiometric mixtures). However, it is very sensitive to the design and therefore requires very accurate design information relating to the material behavior properties such as thermal expansion, strength characteristics, etc. Scale-up potential for this concept also appears limited. This design approach is also quite complex.

G. Carb-I-Tex 700 demonstrated structural reliability and freedom from thermal shock under single or multi-pulse conditions. Although erosion appeared somewhat greater than for pyrolytic graphite for the long duration pulses (in excess of 100 seconds), the inherent durability and simplicity of design requirements make this material attractive. For multi-element construction, scale-up can easily be accomplished yielding a lightweight design.

H. High density, monolithic graphite (CGW) performed adequately and again offered simplicity in design utilization. In view of other industry tests, however, some question occurs as to the ability of monolithic graphite to withstand repeated thermal cycling without cracking. Also application in scaled-up designs increases overall design complexity.

I. In the Pyroid (PG) design, advantage was taken of anisotropic properties of pyrolytic graphite to minimize the surface temperature of the throat insert. By making the planes conical, as opposed to the conventional washer configuration, heat was channeled forward into the cooler forward region and the support graphite heat sink, and axial expansions were minimized. This design concept, though more complex, provided excellent results in both sustained pulses and cyclic applications.

J. Hot-bonded Grafoil appears attractive based on erosion in limited testing. However, due to its low strength characteristics and test performance, it is evident that a complex design is required to provide adequate axial support. In this configuration, it may approach a conventional washer stack which will then compromise its uniqueness from a fabrication flexibility standpoint.

K. The advantages of Thompsine Tape as an engineering material for application in lightweight structures were demonstrated. It was shown that Thompsine Tape can be fabricated in thickness and at diameters not possible with conventional bias tape construction and that complete dissimilar interface integrity can be maintained in the charred conditon.

2. RECOMMENDATIONS

(U) Recommendations for future effort to extend the current state-of-the-art are presented:

A. Pyrolytic graphite and Carb-I-Tex 700 have demonstrated satisfactory performance in rocket motor operating environment created by LF_2/N_2H_4 blend propellant combusted at a chamber pressure of 100 to 200 psia. Additional data is required about the performance of these materials in more severe operating environments (higher chamber pressures) and in other fluorinated propellant systems. Flightweight designs should also be investigated.

B. Although an ablative Thompsine Tape structure is not a recommended candidate throat material in a high pressure fluorine environment, a pyrolysed Thompsine Tape structure would offer improved performance. It has been demonstrated by both TRW and others that pyrolysed materials offer greatly improved dimensional stability. Essentially, these materials consist of normal ablative materials that are post-cured, reimpregnated, carbonized, and in some cases graphitized. These latter steps create a fibrous composite enjoying a stable carbon-to-carbon bonding. The same approach can be utilized to creat a pyrolyzed Thompsine Tape structure. TRW has been employing in-house money to demonstrate feasibility. This type of structure would offer the dual advantages of a pyrolysed chamber and throat liner with an integral insulating support structure.

C. Tantalum or hafnium carbide materials are recommended because they are potentially good candidates for high temperature service; however, their susceptibility to thermal shock failure must be improved. At present, only the arc-cast hypereutectic carbide structure has been demonstrated. Other more scalable forms, such as hot pressed or composite reinforced, have not been sufficiently verified to warrant use at this

time. Preliminary experiements at TRW have shown that improvements in thermal shock resistance may be accomplished by compositing the carbides with reinforcement fibers such as graphite.

REFERENCES

(1) "Thermal Properties of Ablative Chars" Contract AF-33(615)-3809, The Boeing Company, Aerospace Group Second Quarterly Progress Report, September 15, 1966.

(2) *D. L. Peters, "Chemical Corrosion of Rocket Liner Materials and Propellant Performance Studies," Final Technical Report, Volume One of Two, Contract No. W-61-0905-c, Task E, (Dec. 15, 1963).

(3) P. A. McCuen, et al, "A Study of Solid-Propellant Rocket Motor Exposed Materials Behavior," Final Technical Report No. AFRPL-TR-65-33, Vidya Corporation, Palo Alto, California, February 26, 1965.

(4) S. M. Scala, "The Ablation of Graphite in Dissociated Air, Part I: Theory" General Electric Report No. R62SD72, September, 1962.

(5) L. Stag, "Materials for Re-Entry Heat Protection of Satellites," ARS Journal, September, 1960.

---

*Indicates technical information has been extracted from this report.

APPENDIX

MATERIAL AND PROCESS, RESEARCH AND DEVELOPMENT REPORT

TABLE OF CONTENTS

LIST OF FIGURES

LIST OF TABLES

SECTION I

INTRODUCTION

(U) This report is a Materials and Process, Research and Development Report. This report describes the details of the literature survey, laboratory investigation, and the application of a unique ablative composite material called Thompsine Tape.[1] This work was conducted in conjunction with a program to investigate and evaluate materials and design concepts for nonregenerative thrust chambers with improved capabilities for use with liquid fluorine oxidizer and hydrazine blend propellant systems for the Air Force Rocket Propulsion Laboratory, Edwards, California.

[1]TRW has applied for a patent on this material.

SECTION II

PERFORMANCE HISTORY SURVEY

(U) A comprehensive review of materials was made early in the program relative to the combination of high combustion gas temperature and chemical reactivity potential which exists in a liquid fluorine/hydrazine blend propellant system. The following is a summarization of information obtained from various reports of work performed with materials exposed to the influence of high temperature, reactive rocket engine gases containing fluorine. The information was selected to closely apply to the conditions which will exist with hardware produced in support of this contract. Also included is applicable information obtained through contacts with material producers.

(U) The information is presented under general material classification headings -- such as carbides, graphites, etc., and appropriate references are included. In all, a total of approximately 90 reports and articles were reviewed in search for applicable data. Many of these were not pertinent, and only those considered applicable are included in the list of references.

1. CARBIDES

(U) Thermodynamic studies(1)[1] yielding equilibria data on corrosion of refractory rocket nozzle materials by hot combustion gases containing fluorine compounds indicate differences in the resistance of various carbides. Such calculations show, for example, that TaC offers significantly greater resistance to corrosion in HF, a major constituent of the propellant species under consideration, than do the carbides TiC and ZrC. In fact these data predict that, although carbon or graphite have superior resistance to HF attack below 6740°F flame temperature (5840°F hot wall temperature), TaC is superior at high temperatures.

(U) The corrosion of carbides in an HF environment is theorized to result in the formation of metal fluorides, i.e.: ZrF_4, SiF_4, TiF_4, which evolve as gases. This mechanism of corrosion has been supported by laboratory tests conducted by Ebner(2) and Blaes, et al(3). In the former, various refractory materials, including SiC, were exposed to both the well-mixed stoichiometric portion and the unmixed fluorine-rich portion of a hydrogen-fluorine diffusion flame. Samples of the reaction gases from each of the tests were collected for subsequent analyses. In the case of the SiC specimen, the principal reactions were:

$$SiC(s) + 4\,HF \xrightarrow{1455°C} SiF_4\uparrow + C(s) + 2H_2\uparrow \qquad (1)$$

$$C(s) + 4\,F \longrightarrow CF_4\uparrow \qquad (2)$$

(U) After the primary fluorination by HF (equation (1)), carbon remained on the SiC sample surface and was identified by a chemical spot check. This carbon was further fluorinated by the dissociated fluorine in the flame (equation (2)). It was indicated that carbon fluorination was the rate-limiting step and thus inhibited the primary reaction (equation (1)) and rate at which the sample ablated.

---

[1] Numbers in parentheses pertain to References.

(U) In the latter reference (3), phenolic plastics reinforced with ZrO_2 fiber were pyrolyzed in argon, argon/CO_2, and argon/CO_2/HF to evaluate reactions which must be considered during pyrolysis in combustion product environment. It was found that the ZrO_2 reacted with the carbonaceous char to form ZrC and that the ZrC subsequently reacted with HF to form gaseous zirconium fluoride (ZrF_4). Proof of these reactions was provided by actual analyses. X-ray examination of material pyrolyzed in argon only revealed the presence of large quantities of zirconium carbide and smaller amounts of cubic zirconium dioxide. However, when the ploymer was pyrolyzed in the presence of HF, little to no zirconium was found in the charred material.

(U) Unfortunately, very little information exists on the performance of rocket nozzle throat inserts of the more refractory carbides in fluorine-containing propellant combustion gases. This is undoubtedly because of the extreme thermal shock sensitivity of the stoichiometric carbides, and the fact that only recently have such materials as the hypereutectic carbides, and the graded or layered carbides, been available as design approaches for utilizing carbide materials with improved thermal shock resistance. A compilation (4) prepared by Thiokol Chemical Corporation lists data on a large number (409 total) of nozzle firing tests conducted during the past six years involving various refractory throat materials and propellants, both solid and liquid (primarily solid). Unfortunately none of the very few propellant types containing fluorine involved carbide throat inserts.

(U) Wolfson and Thielbahr (5) reported the results of various nozzle materials tested with solid fluorocarbon propellants at the U. S. Naval Ordnance Test Station (NOTS), China Lake, California. Four experimental carbide-coated throat inserts prepared by Carborundum (by hot pressing techniques) were tested for 31 to 35 seconds with a 6600°F flame temperature solid fluorocarbon propellant with zirconium additive, at an average chamber pressure of 425 psia. The coatings consisted of carbides of tantalum, columbium, hafnium and zirconium, each backed-up with a compacted substrate of 30 v/o columbium carbide and 70 v/o graphite. It was noted that when localized coating failures occurred in throat areas extensive erosion developed in the back-up material. The sections of coating that did remain retained their original thicknesses, demonstrating erosion resistance even in the throat. It was indicated that pyrolytic graphite had the best overall performance in the fluorinated propellant environment (also tested in this series). However, the PG took advantage of its high heat sink capability for short firing durations, and did not suffer any local spalling losses due to thermal stresses (as in the case of the layered carbide). It is significant to note that when the carbide layer remained intact practically no erosion occurred -- indicating an erosion resistant capability toward high-temperature, solid metallized fluorocarbon propellant.

(U) Information obtained from Wolfson (6) and Foster (7) covering hypereutectic hafnium carbide inserts produced by Battelle and test fired at China Lake, California (NOTS) indicate significant performance characteristics in these carbide materials. The inserts, with less than ½inch diameter throats, were tested in 6200°F flame temperature solid fluorocarbon propellants with chamber pressures of approximately 3000 psia and final average pressures of around 1400 psia. The results indicated that there was some cracking, but no complete fractures leading to loss of material. The graphite was preferentially attacked by the combustion gases (metallographic examination) and some surface melting had occurred at the hot I.D. wall.

(U) A limiting factor hindering the use of carbides for nozzle throat inserts has been the extreme thermal shock sensitivity of these materials. Approaches for improved thermal shock resistance have been developed. One involves the utilization of "grading" or "layering," whereby an essentially stoichimetric carbide layer is formed for the exposed inside (I.D.) surface and is backed-up by successive layers of carbide-graphite mixtures with increased graphite content toward the O.D. surface. This approach has been found to produce a more thermal shock resistant outer surface by reducing tensile stresses developed during the early stages of firing. An outer layer containing at least 70 v/o graphite has been found adequate for preventing thermal shock cracking. Carborundum Company (8) has produced a large number of such throat inserts involving carbides of TaC, HfC, CbC, TiC, and ZrC with various combinations of graphite-carbide mixtures as the substrate. These shapes are produced by hot pressing techniques. Tests at TRW (9) on graded carbides have shown promising thermal shock resistant properties. Firing test data on the graded or layered carbides has been conflicting, however, with some firing data indicating good thermal shock resistance and other data indicating spalling tendencies with the carbide layer. A part of the problem may be in achieving optimum thermal expansion matches between the various carbide-graphite mixtures.

(U) The second very promising approach for promoting thermal shock resistance in carbides involves increasing the carbon content well beyond the stoichiometric content, in fact beyond the eutectic of carbide and graphite, to form what are termed "hypereutectic carbides." These materials are produced by arc casting and develop large graphite platelets within the eutectic mixture of carbide and graphite. The graphite flake appears to be a major factor for promoting thermal shock resistance, but the mechanism is not yet understood. As an approach for producing a hypereutectic carbide in large shapes (because of limited arc melting capacity), hot pressing techniques have been applied (3). Three sources of carbon were used for mixing with TaC, i.e.: lamp black, graphite flake, and crushed and screened ATJ molded stock. Only the material produced with the flake graphite exhibited resistance to thermal shock; all of the other materials were cracked upon thermal exposure.

(U) Kendall (10) reports excellent thermal shock resistance for the arc-cast hypereutectic carbides evaluated at Aerospace Corporation by plasma arc tests. The hypereutectic carbides survived, without cracking, a heat flux of 3000 $BTU/ft^2/$ sec which produced specimen temperatures above 3000°C at one atmosphere pressure and sonic velocities. Tests at a pressure of 50 atmospheres were conducted on hypereutectic HfC and the material survived these conditions without cracking or surface recession.

(U) Studies have also been conducted at Aerospace Corporation (10) to determine variations in carbon (graphite) content which will still provide thermal shock resistance. For the HfC-C system, carbon contents slightly below the eutectic (hyproeutectic) will still provide thermal shock resistance.

(U) Because of the higher eutectic melting temperature for the TaC-C system -- 6700°F (as opposed to 5600°F for HfC-C) -- this material should be optimum for the extremely high temperatures encountered with fluorine propellant systems. However, Foster (7) at Battelle reports difficulty in producing hypereutectic TaC. The problem is related to the higher vapor pressure for

carbon at the TaC-C eutectic melting temperature (approximately 5 atmospheres, as opposed to 1 atmosphere at the HfC-C eutectic melting temperature). This promotes carbon "boil" and loss in the system. A potential solution involves pressurized arc melting facilities which are currently being constructed.

(U) Another possibility for producing hypereutectic TaC involves the co-pyrolysis of hydrocarbon gas with a metallic halide with flow rates adjusted to co-deposit any composition desired. The reactions are accomplished at a relatively low temperature (approximately 2000°F). Materials producers--such as Raytheon, Cadillac Gage Company (11) and others -- have successfully produced carbide-graphite alloys, as well as straight monocarbides. Such materials have been produced as free-standing shapes, plate, or as coatings on graphite substrates. The anisotropic property characteristics of restrained shapes produced by pyrolytic deposition of materials impose severe restrictions upon the thicknesses that can successfully be developed without delamination or cracking in cylindrically-shaped sections (t/r ratio approximately 0.05). Consequently, where heavy nozzle insert sections are required for erosion resistance, generally it is necessary to employ special design approaches utilizing material produced in plate form -- such as the "washer" type nozzle throat insert construction.

(U) The Raytheon Company has produced quantities of graphite-hafnium alloys containing 20 w/o Hf in the form of plate 2" X 6" X $\frac{1}{4}$" thick. This is very graphite-rich, well above the usual hypereutectic compositions employed for the arc-cast material (approximately 13-14 w/o C, 87-86 w/o Hf). Other compositions of higher metal content can be produced (18).

(U) Pyrolytic deposition of refractory carbide-graphite alloys is attractive because of the flexibility in controlling compositions. As indicated, hypereutectic compositions of very high carbon content -- not easily obtained by other processes -- can be provided by pyrolysis. Also, this process may provide favorable characteristics related to microstructure or purity which would advance performance. Pyrolytically deposited material can also be processed into powder form for subsequent hot pressing, or hot-isostatic compaction.

(U) To permit the use of near-stoichiometric carbides as free-standing nozzle throat inserts, TRW has developed pre-stressing techniques to overcome the thermal shock problem. This was recently successfully demonstrated with a hot pressed TaC throat insert developed and tested in a NASA sponsored program (20).

(U) The principle of the concept involves encompassing the throat insert with a close-fitting (or in certain cases, pre-shrunk) back-up support made from a refractory metal, which in turn is supported by the nozzle shell. The material comprising this close fitting back-up support is selected so as to always expand at a rate slower than the carbide throat insert during the transient heat-up period. Since brittle materials failing in thermal shock characteristically initiate tensile failures on the O.D., inclusion of this tight fitting support superimposes a compressive stress on the O.D., tending to reduce or eliminate the tensile stress. The elastic modulus and allowable stress at temperature for the selected pre-stressing ring must be known for designing to prevent yielding of the ring prior to reaching a quasi-ductile state on the O.D. of the carbide insert. The desing calculations, though complex, have been proven to yield satisfactory results.

2. GRAPHITES

(U) On a thermodynamic basis (1) graphite appears to be the most corrosion resistant material in the presence of hydrogen fluoride (the major constituent of the combustion gases of the propellant system under consideration) for flame temperatures up to 6740°F (5840°F wall temperature). This prediction has been supported by a substantial number of rocket nozzle test firings involving fluorine propellants. Graphite, particularly edge oriented pyrolytic graphite, has shown relatively low erosion rates with these propellant types. In the PG firings, advantage was taken of the optimum orientation for high heat transfer rates and heat sink capability, yielding extremely low erosion rates for short duration exposures. Uncooled nozzle firing test data (12) on edge oriented PG (PG washers with graphite sleeve heat sink) have shown average throat erosion rates of 0.15 mil/sec with LH_2 + LF_2 at 7000°F flame temperature, 300 psia chamber pressure, 0.75 inch throat diameter, and 150 seconds total firing time.

(U) In small nozzle tests conducted at NOTS, China Lake, California (5) which involved metallized solid fluorocarbon propellants, the conventional monolithic graphites (AHDG, ATJ, CVD, H-205-85, H-207, H-243, and RBD) exhibited high erosion rates -- 1.55 to 1.9 mils/second. Pyrolytic graphite (edge oriented for heat sink capability), however, showed excellent performance as contrasted with other nozzle insert materials. For example, in firing tests involving various propellant mixtures and chamber pressures, the throat radius regression rate per unit pressure for pyrolytic graphite was 3.7 X 10-4 mil/psi-sec; whereas, for copper infiltrated tungsten and JTA graphite composite, this rate was 4.4 X 10-3 mil/psi-sec -- an order of magnitude greater. Additional information obtained from these firing tests involving solid fluorocarbon propellants indicated that: (a) throat erosion was directly related to pressure; (b) chemical corrosion of graphite was accelerated at material temperatures above 5000°F (a major reason for superior performance of "heat-sink oriented" PG over conventional graphite); (c) chemical corrosion is a major removal mechanism for refractory insert material with solid fluorocarbon propellants; (d) infiltrated tungsten and pyrolytic graphite were two of the best insert materials tested with the solid fluorocarbon propellants, although tungsten was preferred for the more highly oxidizing atmospheres, and pyrolytic graphite in the fluorinated ones; and (e) upstream ablative shielding can afford protection to throat inserts during firing and reduce nozzle throat erosion.

(U) Tests by Ebner (2) in a hydrogen-fluorine diffusion flame indicated superior performance with graphite. The materials tested -- graphite, silicon carbide, zircon, alumina, zirconia, and magnesia were decreasingly resistant to the test flame in the order indicated. The rate of ablation was about three times more rapid and the average surface temperatures 130° to 745°C higher where the flame was fluorine-rich. The principal ablation reactions for graphite were described as follows:

$$\gamma C(\text{graphite,s}) + \eta F \rightarrow (CF)_\eta \uparrow, \quad (s) < 450°C \qquad (1)$$

$$4\,(CF)_\gamma \ (s) \rightarrow \gamma CF_4 \uparrow + .3\,\gamma C, (s) = 450°C \text{ (est.)} \qquad (2)$$

$$C\ (\text{graphite,s}) + 4F \rightarrow CF_4 \uparrow, (s) > 450°C \qquad (3)$$

Test movies of graphite in the flame showed that initially a gray-white substance was formed on the surface accompanied by abundant spark formation. As the surface was heated above approximately 450°F, the white material decomposed and the sparking stopped. The white material is reported to be the (CF) compound, and the sparking due to carbon formation. The (CF) compound decomposes into CF_4 and C (equation 2)), and above 450°C CF_4 is formed from graphite and fluorine (equation (3)). It was reported (2) that the dissociation of HF and the volatilization of carbon both influence the reaction of HF with carbon as a function of temperature. Farlow and Joyce (13) observed a negligible reaction between HF and the carbon below 2200°C in an electric arc, when HF was not dissociated and the vapor pressure of carbon was negligible. When HF was substantially dissociated and carbon vapor pressure low, principally CF_4 was formed. When HF was dissociated and carbon vapor pressure high, as developed in an arc reactor, a variety of hydrocarbons and fluorocarbons was formed, of which C_2H_2, $C_2H_4F_2$, CHF_3, C_2F_4, and CF_4 are typical (13).

(U) In tests with small rocket motors (14) using F_2/H_2 as the propellants, both polycrystalline and pyrolytic graphite employed as combustion chamber liners (2" I.D. X 8" long) were reported to show no erosion or dimensional change. The test firings were for 30 seconds at a nominal flame temperature of 6960°F and 256 psia chamber pressure. In the instance of the polycrystalline graphite liner (Speer Carbon Company, Grade 3474D), localized burning in a scalloped pattern was visible adjacent to the injector. This burning, or "streaking", was attributed to local impingement of unreacted fluorine -- which is markedly more reactive with graphite than HF. The PG liner showed some slight cracking on the surface, as well as exfoliation or delamination. The latter condition is a characteristic problem with PG and requires special design considerations to eliminate or minimize its effects.

(U) Considerable work has been done with alloying pyrolytic graphite for improved strength properties and oxidation resistance. Oxidation tests of straight PG, ZrC-PG and HfC-PG in which air heated by an arc plasma was passed through an 0.25-inch orifice and impinged on small (1 X 1 inch) samples of the pyrolytic materials indicate increased resistance to oxidation with the alloyed PG at temperatures below the melting point of the protective oxides which are formed (15). In these tests, straight PG indicated erosion rates of 3 mils/second at 4400°F, and 5 mils/second at 5400°F. An alloy of about 20 w/o Zr in PG showed a lower erosion rate of 0.6 mil/sec at 4400°F. At 5060°F, however, slightly above the melting point of ZrO_2, (4868°F), the erosion rate increased to 5 mils/second (about the same as for the straight PG). A sample of HfC-PG containing 78.6% PG alloy tested at 5270°F (slightly above the melting point of HfO_2) had an extremely high erosion rate of 13 mils/second, which was worse than straight PG at that temperature. Additional tests on a PG alloy containing 75% Hf be weight resulted in only 0.6 mil/sec erosion rate at 4930°F and 5240°F. It was postulated that the melting temperature of HfO_2 (5252°F) was not exceeded in the latter test.

(U) Evaluation of the results of flexure strength tests conducted (15) on ZrC-PG alloys showed that a significant strengthening resulted from the addition of the carbide to the structure. Room temperature flexure strengths measured in the "a" direction exhibited increases from about 20,000 psi to an average of 95,000 psi (range 75,000 to 115,000) for a 20% by weight zirconium alloy of ZrC-PG. The alloy approaches the ductility of pyrolytic graphite which is much less brittle than a pure ZrC. Although no data were obtained on the

on the strengthening effect of hafnium, it is believed that a similar behavior would result. The increased room temperature strengths of the carbide-graphite alloys over that of straight PG also persist at elevated temperatures.

(U) Other elements, such as tungsten and boron have been alloyed with pyrolytic graphite. However, neither element appears to improve oxidation resistance. Boron does not seem to add to the strength or oxidation resistance, and there is some evidence that delaminations occur more readily in the boron alloy (16).

(U) Alloys of ZrC and HfC in pyrolytic graphite are considered (16) to be promising new pyrolytic materials for use in highly oxidizing gases. By contrast, practically no effort has been put into producing pyrolytic alloys of TaC and PG. This is presumably because most of the interest has been centered around the more oxidizing propellant systems, such as N_2O_4 oxidizer with 50% N_2H_4-50%UDMH fuel, and the tantalum oxide Ta_2O_5 (M.P.; 4868°F) or HfO_2 (M.P.; 5252°F). However, in a fluroine containing propellant system where HF was the major constituent of the rocket engine combustion gases, a TaC-PG alloy could offer advantages because of the resistance of TaC to HF attack (1) and the high melting point of the TaC-C eutectic (17).

(U) Contact with producers of pyrolytic materials -- such as Cadillac Gage (11) and Raytheon (18) -- has revealed that pyrolytic alloys of tantalum with graphite could be produced to any compsoition desired. No special problems are envisioned which would make this more difficult to produce than the other graphite mixtures involving carbides such as TiC, ZrC, or HfC. However, all sources indicated that development involving at least 4 or 5 months of effort would be required to establish the necessary parameters for controlling the process.

3. OXIDES

(U) The high flame temperatures of fluorine containing propellants limit the range of suitable oxides on the basis of maximum temperature capability. Thoria has the highest melting point of any oxide -- 5970°F (19) -- and on the basis of temperature capability may be satisfactory for the wall temperatures encountered with short duration firings. Other high melting point oxides are MgO, HfO_2, and ZrO_2. All have melting points slightly above 5000°F, and, as such, must be considered marginal in temperature capability. Of the available oxides, thoria and zirconia have received the greatest amount of effort in attempting to develop thermal shock resistant, reinforced or refractory laminate throat insert structures.

(U) Experimental data by Ebner (2) show that refractory oxides are attacked in both stoichiometric and fluorine rich hydrogen -- fluorine flames. In these tests, ZrO_2 suffered an order of magnitude greater penetration in the stoichiometric hydrogen -- fluorine flame than did graphite, but the difference in penetration was reduced to about 2-fold when the flame was fluorine rich.

(U) Ebner's (2) data indicate some differences in the resistance of various oxides to fluorine environments. $ZrSiO_4$ (Zircon), Al_2O_3 ZrO_2 and MgO were decreasingly resistant to the test flame (stiochiometric HF) in the order listed. No data were found in the literature for either ThO_2 or HfO_2.

(U) Based on either the maximum useful temperature or chemical reactivity with fluorine compounds there appears to be no advantage for at least some of the oxides over either graphite or carbides. However, where oxidizing species such as H_2O, O_2, or CO_2 are present in significant quantities in the rocket engine combustion gases, oxides have the best capabilities for resisting attack.

(U) Progress is being made in developing thoria and zirconia oxide composites for thermal shock resistant throat inserts. (20) Early zirconia composites reinforced with tungsten-rhenium wires showed good thermal shock resistance but had a tendency to form cracks during fabrication. Efforts are now being made to reduce the cracking tendency during fabrication, while still retaining thermal shock resistance. Thoria composite specimens reinforced with tungsten-rhenium have also been fabricated but the samples exhibited a large amount of cracking and porosity, and spalled extensively during machining. Recent efforts (21) utilizing hot pressing techniques appear much more promising.

(U) Fabrication of the refractory laminate throat insert design does not require development of the fabrication techniques for the oxides. Present technology is capable of producing discs of oxides (thoria or zirconia) as required by the laminated ("stacked washer") design (22).

4. PYROLYZED AND ABLATIVE COMPOSITES

(U) Little information is available in the industry on the performance of ablative materials in the corrosive environment of the fluorine/hydrazine propellant exhaust. Work done at Philco (3) indicates the unsuitability of zirconium oxide reinforced phenolic composites in the fluorine environment. The mechanism of failure observed during tests was consistent with predicted thermodynamic considerations in which the ZrO_2 reacted with the char to form ZrC, and the ZrC then reacted with the HF present to form gaseous zirconium fluorides. One of the important conclusions drawn was ". . .possible reactions of the reinforcement with the char must be considered to be as important as, and prior to, reactions of the reinforcement with the combustion species".

(U) A paper by Kaufman, Armour, and Green (14) based on work done for the Missile Propulsion Division, Bureau of Naval Weapons, Contract No. w 60-0363-d discussed the testing of a nylon reinforced phenolic and a silica reinforced phenolic as cylindrical chamber liners. These liners were tested in a rocket motor using an F_2/H_2 weight mixture of 8.1:1 and a chamber pressure of 256 psia, corresponding to a nominal flame temperature of 6500°F.

(U)In the case of the silica reinforced phenolic, an absence of liquid (silica) run-off was attributed to the silica melting within the substrate and vaporizing as it approached the surface. However, another explanation -- as suggested from work by Ebner (2) -- is that the SiO_2 reacted with HF to form gaseous SiF_4 which evolved from the surface; e.g.:

$$SiO_2\ (s) + 4HF \longrightarrow SiF_4 \uparrow + 2\ H_2O \uparrow$$

The measured char layer thickness averaged between 0.15 and 0.16 inches in the downstream half of the chamber. The char was reported to be strong and dense with some silica fibers reinforcing the section next to the virgin material. The results obtained with the nylon-phenolic liner were qualitatively similar,

but showed a higher mass loss rate and a weaker and less dense char layer. In the experiments described, the chars formed by reinforced plastic thrust chamber liners were strong enough to resist the small fluid shearing stresses present in the low velocity region and showed no surface regression. However, it is unlikely that such char layers would be stable enough to withstand the high shearing stresses present in a nozzle throat section, at least in motors operating at conventionally high pressures.

(U) In another study (Contract Number AF 04(611)9366) of ablative chamber liners for use in a fluorine environment, Aerojet General Corporation used a carbon-phenolic composite. Preliminary information indicates that spalling was experienced during firing and that this phenomenon was also observed in a later firing with a chamber of the same material, but which had no holes drilled into the surface to permit gas release.

(U) A more recent approach in this series has been to completely pyrolyze the carbon-phenolic composite under laboratory conditions and then back-fill with an epoxy-novalac resin. Implications are that this approached yielded very favorable results during firing.

(C) A series of interesting experiments were performed by D.W. Gibson and D.W. Smith (23). The abstract reads as follows:

> "Various silica, carbon and graphite fabrics, and phenolic laminates were exposed to hydrogen fluoride environments at high temperatures in order to determine the effects upon the stability and properties of these materials. These materials were evaluated at temperatures of 2000°, 3500°, and 5000°F for relatively long periods of time. The results of these experiments demonstrate the stability of both graphite and carbon materials, and the instability of high silica materials to these extreme thermal and corrosive conditions. Recent thrust chamber firings, along with theoretical thermochemical considerations, have confirmed these results."

(C) In addition to their own work, the authors reported the results of two firings at Rocketdyne Research Laboratory, Santa Susanna, California. The first firing was conducted with a duplex chamber using both silica-phenolic and modified silica-phenolic. The throat was constructed of graphite cloth phenolic. The following firing conditions were used:

Weight ratio F_2/H_2	12:1
Corresponding Flame Temp.	6710°F
Chamber Pressure	79 psia (constant)
Number of Firings	3
Average Time of Each Firing	39 seconds
Total Firing Time	116 seconds

The silica materials were considerably affected, expecially the modified silica. However, with reference to the throat, it was noted that, "there was no increase in throat diameter or evidence of erosion in this section after firing."

(C) The second firing was conducted with hydrazine with the following conditions:

Weight Ratio F_2/N_2H_4	2:1
Corresponding Flame Temp.	7180°F
Chamber Pressure	150 psia
Total Firing Time	Approximately 35 seconds

The comment was: "Again, there was no erosion or increase of the diameter of the graphite-phenolic throat."

(C) In their own experiments the authors subjected swatches of graphite cloth, carbon cloth, silica cloth, slabs of phenolic resin (Monsanto Chemical Co. SC-1008), and laminates constructed of these materials to a high temperature HF environment. All of the laminates were carbonized under laboratory conditions at 1500°F prior to initiation of the tests. Exposures were made up to 43 minutes with a flow of 18 CHF of anhydrous HF at temperatures of 2000°F, 3500°F, and 5000°F.

(C) The resin slabs lost 53% weight in the HF exposure. It was noted that: "Rapid heat treatment to these temperatures in the absence of HF gives the same percent weight loss." These percentage losses are consistent with TRW pyrolysis experiments, and indicate that HF does not significantly react with the phenolic resin. With respect to the performance of the other materials, the concluding section stated: "Based upon both theoretical and experimental evaluation, graphite fabric was shown to be the most stable material for use in rocket engines utilizing fluorine-base fuels in the absence of oxygen."

(U) These favorable comments on the performance of graphite materials are not surprizing in the light of previous TRW work, and the data given above in the section on graphites. Other corroborating statements on the performance of pyrolyzed composites were made by representatives of both Basic Carbon Corporation (24) and Union Carbide Corporation (25).

(U) A chamber of PT grade pyrolyzed material was reported fired for 80 seconds in a fluorine environment-- and was to be fired again, without alteration, after an examination of the chamber.

(U) Basic Carbon Corporation personnel indicated that a carbonized composite designated Carb-I-Tex 100 had been successfully used in three separate liquid nozzle firings at 150 psig for 180 seconds with the following propellant combinations: fluorine/hydrazine, fluorine/hydrogen, and 60% fluorine-40% oxygen/hydrazine. Of course, the firing with oxygen in theoxidizer produced higher erosion rates, but performance was described as quite good in all cases.

5. REFRACTORY METALS

(U) From the standpoint of thermal shock resistance and fabricability, the refractory metals are very acceptable rocket nozzle materials. However, the high flame temperatures encountered with fluorine base propellants require nozzle throat insert material of extremely high temperature capability. Unalloyed tungsten and thoriated tungsten alloys have sufficient temperature

capabilities to be considered for throat inserts, at least for shorter duration nozzle firings. Longer duration firing with the high temperature fluorine propellants utilizing an uncooled tungsten insert could cause insert wall temperatures to approach or exceed the melting point of tungsten (6170°F). Other refractory metals or alloys, with melting temperatures lower than that of tungsten could not be considered.

(U) Theoretical equilibrium studies (1) of the reaction between tungsten and hydrogen fluoride indicate that tungsten is more susceptible than carbon to HF attack at all material wall temperatures below the melting point of tungsten. At approximately 6300°F, the equilibrium potentials of tungsten and carbon are equal (1). Literature sources (26,27) indicate that metals combine with free fluorine, even at relatively low temperatures and fluroeine pressure. No data were uncovered regarding the reactivity of free fluorine with tungsten. However, it is expected that the fluorination product, tungsten hexafluoride would be formed. This material volatilizes at room temperature (19.5°C) (28), and thus a tungsten insert could be corrosively attacked and material removed by free fluorine in the exhaust gases.

(U) Firing data on porous tungsten infiltrated with 25 volume percent copper, utilizing high temperature fluorocarbon propellants, indicated the major insert material removal mechanism was chemical corrosion (5). Erosion of the infiltrated tungsten was similar to results for JTA graphite-composite material.

(U) Tungsten does not appear to possess any advantage over high density graphite for use with fluorine-containing propellants being considered. Wolfson, et al, (5) have classified infiltrated tungsten and pyrolytic graphite as leading condidate materials for fluorine-containing propellants, with tungsten preferred for oxidizing environments and pyrolytic graphite for fluorinated ones. The propellant exhaust gas composition involved in the present program has only a very minor amount of oxidizing gas specie, but considerably greater content of fluorinating gas specie. It, therefore, appears that carbonaceous materials have greater potential for the proposed propellant systems.

6. CONCLUSIONS

(U) The survey implies several conclusions as follows:

A. Analysis of the information obtained through the literature search and contacts with material producers indicates fairly conclusively that the materials which will have the best performance (i.e.: lowest reactivity with the high temperature combustion products of fluorine propellants) are the essentially carbon base materials -- i.e.: the graphites, carbides, and pyrolyzed composites. This is true when the contents of the combustion gases are low in oxidizing species.

B. There is some theoretical information, and some meager test data which indicate that certain carbides -- specifically TaC -- may have superior resistance to HF reaction at very high temperatures, above 3500°K (5840°F) wall temperature.

C. The oxides do not appear promising because of reaction with HF to form either gaseous or liquid metal fluorides. However, where no

specific information exists in the literature, certain selected oxides should be evaluated in high temperature reactivity tests with HF to verify performance capabilities.

D. The refractory metals do not appear to offer any advantage over graphites in an environment dominated by fluorine reactions. However, where oxidizing species exist, or predominate, tungsten (as do the oxides) shows an improved performance capability. Since tungsten is a prime material candidate for many rocket nozzle applications, this material should be evaluated by laboratory tests for comparison with other candidate materials.

SECTION III

MATERIALS INVESTIGATION

(U) A laboratory materials screening program was designed to evaluate candidate materials with reference to their ability to resist attack by environments of hydrogen fluoride, the predominant specie in the combustion gases of the propellants under consideration. Two separate studies were conducted to determine the relative reactivity of various materials under consideration.

(U) A series of laboratory bench torch tests involving hydrogen-fluoride mixtures were performed on materials of interest for the prestressed design nozzle. This design concept required critical components of materials other than that of a throat insert (such as a prestressing ring) which might be subjected to exhaust gases. Such materials would be required to provide adequate resistance to the less severe environments upstream or downstream from the throat plane in order to assure satisfactory performance for the prestressed design.

(U) A more extensive laboratory materials screening program was also conducted to evaluate candidate throat and chamber liner materials with reference to their ability to resist attack by hydrogen fluoride environments.

1. HYDROGEN FLUORIDE TORCH TESTS

(U) An existing in-house propellant exhaust environment test setup was utilized. The apparatus was designed to permit evaluation of the resistance of materials to exhause species of hydrogen-fluorine propellant combinations. Test on the refractory materials were conducted as follows.

(U) Test samples were situated in a copper chamber on a peg and holder plate so that each sample tested was positioned at the same distance from the tip of the torch. All samples were 0.5 inches in diameter by 0.5 inches long with a mounting hole at one end, 0.25 inches in diameter by 0.25 inches deep. After the chamber was purged with argon, the samples were subject to a ten second H_2 - F_2 flame exposure having a 1.0 volume ratio. This ratio yields an adiabatic flame temperature of 4984°K (8512°F) which is very near the theoretical peak adiabatic temperature for the H_2 - F_2 system. The total flow rate was 8000 ml per minute. After firing, the chamber was purged again with argon to cool the sample without exposing it to the oxidizing atmosphere. Since some of the samples tested have poor thermal shock resistance, all samples were given an initial thermal "soak" for five seconds to heat them slowly. An 0.2 mixture ratio (F_2 - H_2) was used to reduce the severity of the "soak" flame (T_F - 2724°K; 4444°F). Post metallorgraphic analysis of the samples indicated that some cracking did occur. The data in Table I gives the sample weight before test, weight loss, per cent weight loss and volume loss. Volume loss was obtained using published densities rather than actuals. Thus, a more meaningful interpretation of the results is obtained from percent weight loss, since all samples were very close to the same size. The materials are listed in order of decreasing resistance to the environment. The test data substantiate the findings of the literature and demonstrate the superior behavior of graphite materials.

(U) The lower loss rate of ATJ graphite, as opposed to that of the higher density CFZ, could possibly be attributed to its finer grain structure. ATJ graphite is produced from fine graphite particles of 0.006" maximum size;

Table I (U) Propellant Exhaust Environment Test

Material	Density* gm/cm^3	Weight Before gm	Weight Loss gm	% Weight Loss	Volume Loss cm^3
ATJ	1.80	2.6461	nil	0	0
CFZ	1.90	2.9180	0.004	0.01	0.0021
PG	2.2	3.3650	0.019	0.56	0.0086
W	19.3	25.9003	0.190	0.73	0.0098
TaC	14.37	21.2939	0.160	0.75	0.0111
TZM	10.15	12.9617	0.114	0.88	0.0112
Z_rC	6.78	9.9777	0.111	1.11	0.0163
Ta (carborized)	16.6	23.6965	0.277	1.20	0.0166
HfC C (arc cast)	10.0	21.5643	0.307	1.42	0.0307
Ta - 10W (carborized)	16.8	22.2652	0.552	2.48	0.0328
FS 85	10.8	14.4328	0.372	2.58	0.0344
Ta	16.6	22.0227	0.742	3.37	0.0446
Ta - 10 W	16.8	23.3236	0.798	3.40	0.0475

Unclassified

* Densities are published values.

whereas, the CFZ is produced from much coarser materials (0.030" maximum size). The finer materials reduce permeability and, thus, tend to confine reaction to the surface.

(U) PG, because of its dense, impermeable structure, should exhibit for the graphite materials the highest resistance to reaction by the corrosive gasses. However, because of its highly anisotropic nature it can -- with orientation so as to present an insulative face to the reacting flame front -- result in much higher surface temperatures and, consequently, higher reaction rates.

2. LABORATORY MATERIALS SCREENING PROGRAM

(U) This program plan initially involved exposing selected graphites, oxides, carbides and tungsten to a stagnant hydrogen fluoride atmosphere at sub-ambient pressures and temperatures to 4500°F. The most satisfactory materials were then subjected to a second generation test which involved a dynamic hydrogen fluoride atmosphere and a mixture of oxygen and HF to simulate the actual propellant exhaust specie. From these tests, the relative reactivity of the candidate materials were defined as a function of temperature. The optimum materials were then selected for the actual firing evaluations.

a. Materials

(U) A summary of test materials is presented in Table II. Two grades of dense graphite - CGW and pyrolytic - were evaluated along with wrought tungsten. Both hafnium carbide and tantalum carbide produced by hot pressing techniques were included in the program. Although these materials as homogeneous structures are thermal shock sensitive and, therefore, not applicable for nozzle inserts, they can be used as composites with graphite to produce a usable component. The zirconium oxide was evaluated as a plasma spray coating on a tungsten substrate. Two Carb-I-Tex materials were evaluated. The 100 designation indicates a carbon cloth reinforcement with binder pyrolyzed to carbon. The 700 designation represents an all-graphite system -- graphite cloth reinforcement with binder and impregnants pyrolyzed to graphite. The PTB material is produced from graphite cloth and binder, macerated, molded, and pyrolyzed to graphite. Subsequent reimpregnation with resin produces a final product with ablative characteristics. The carbon cloth phenolic was included as representative ablative material applicable for thrust chambers. All the materials were either received or machined to $\frac{1}{4}$" diameter by 2" long test specimens.

b. Experimental Procedure

(U) The reactivity tests involved resistance heating of $\frac{1}{4}$" diameter by 2" long specimen in the presence of a hydrogen fluoride environment and measuring the change in specimen dimensions after a specific exposure time. The apparatus for conducting the tests is shown in Figures 1 and 2, while a schematic illustration of the heating chamber is shown in Figure 3. During later tests, shorter evacuation times were obtained by eliminating the scrubber from the test set-up and simply using a liquid nitrogen cooled chamber to trap the hydrogen fluoride vapor.

Table II (U) Materials for Evaluation in Fluorine Environments

Material	Type	Form	Vendor
Graphite	CGW	Blocks	Union Carbide
Graphite	Pyrolytic	$\frac{1}{4}$" dia. x 2" rods	Super Temp
Tungsten	Unalloyed	$\frac{1}{4}$" dia. x 2" rods	General Electric
Carbide	TaC (Hot pressed)	3/4" dia. x 2" rods	Carborundum
Carbide	HfC (Hot pressed)	3/4" dia. x 2" rods	Carborundum
Oxide	ZrO_2	0.010 plasma coating on $\frac{1}{4}$" dia. x 2" W rods	TRW
Pyrolyzed Plastic	Carb-I-Tex 700	$\frac{1}{4}$ dia. x 2" rods	Carborundum (Graphite Specialties)
Pyrolyzed Plastic	Carb-I-Tex 100	$\frac{1}{4}$" dia. 2 rods	Carborundum (Graphite Specialties)
Pyrolyzed Plastic	Union Carbide PTB (PT-0145)	$\frac{1}{4}$" dia. x 2" rods	Union Carbide
Carbon Cloth Phenolic	MX-4926	Blocks	TRW

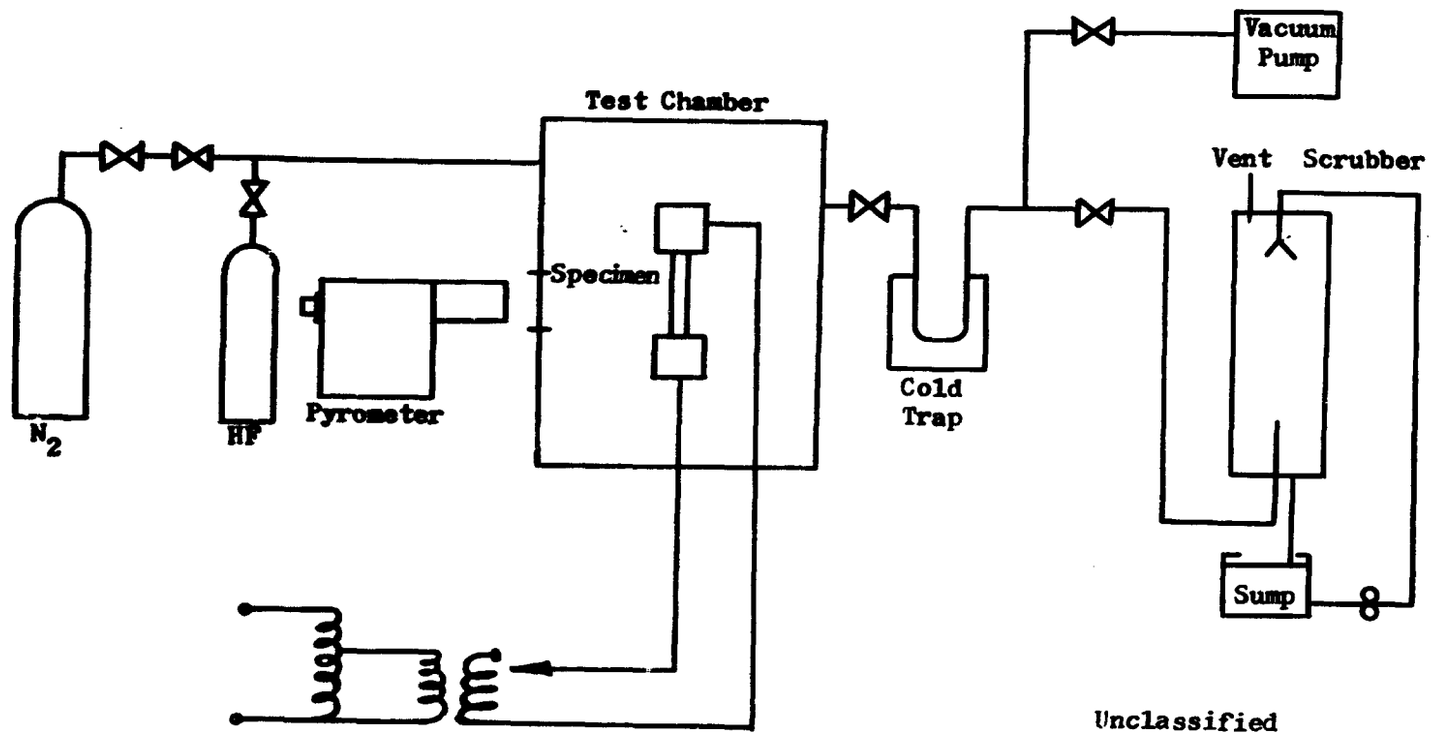

FIGURE 1 (U) Schematic of Reactivity Test Apparatus

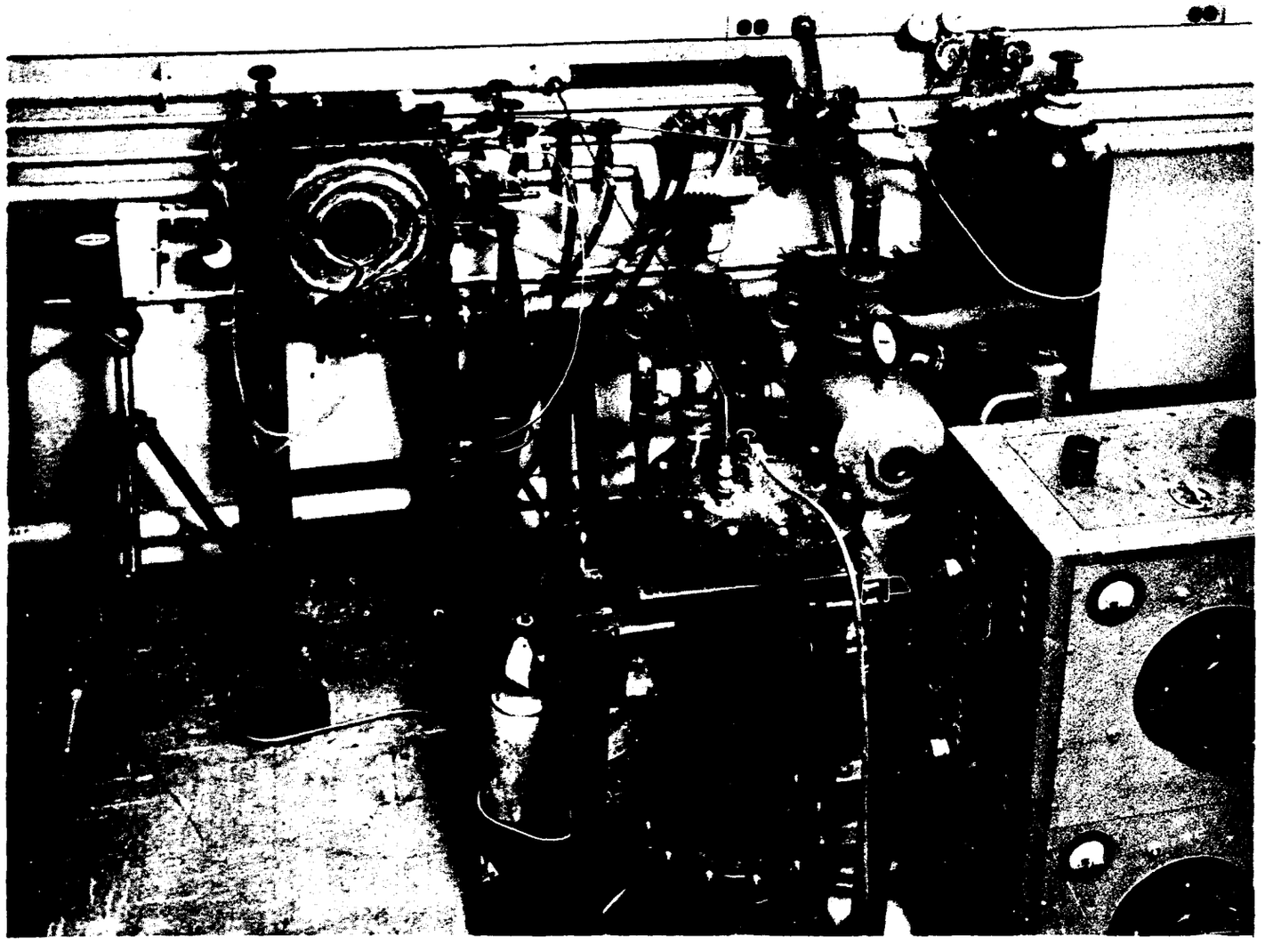

Unclassified

Figure 2 (U) Reactivity Test Apparatus

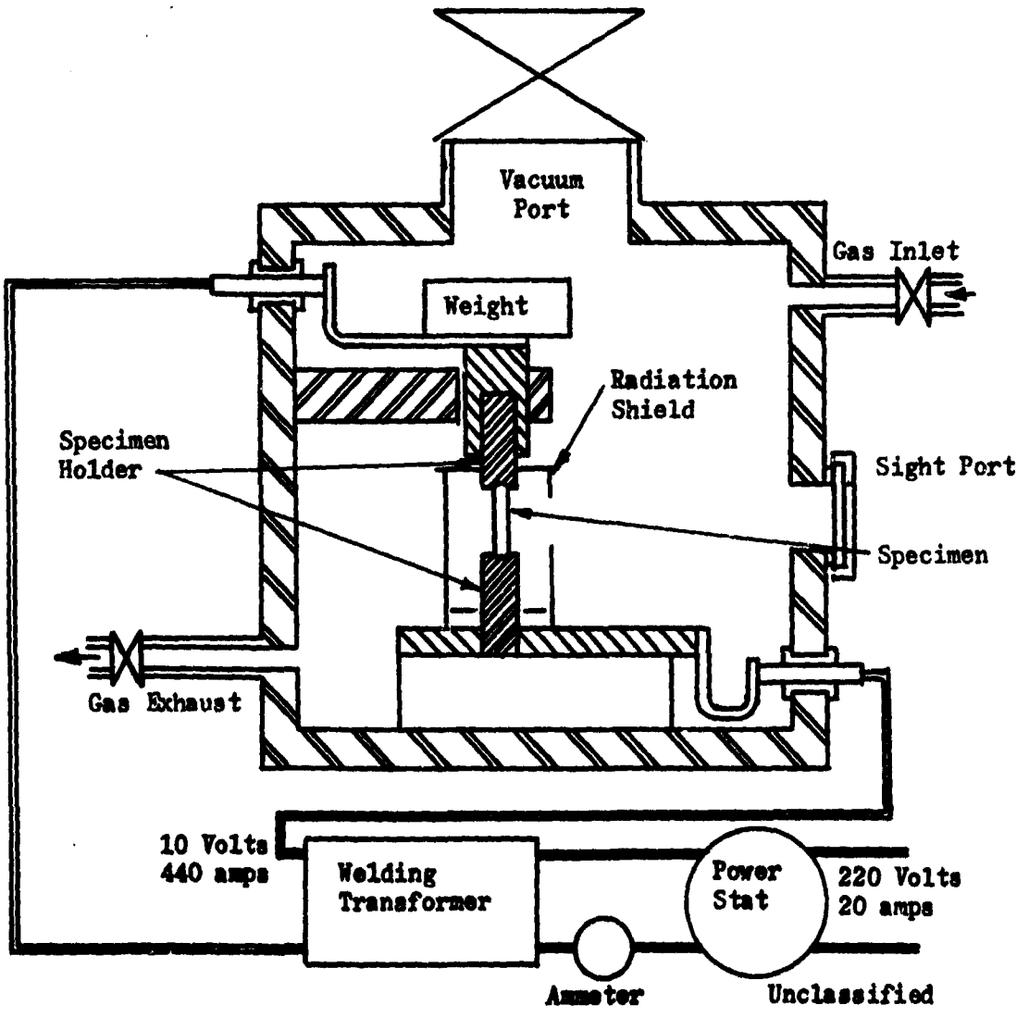

FIGURE 3 (U) Schematic Diagram of Furnace for Compatability Studies

(U) The test procedure involved mounting the specimen in a vertical position in the chamber which was then sealed. The chamber was evacuated to the limit of the mechanical pump (about 0.05 Torr) for at least one hour to assure the complete removal of water vapor absorbed by the internal insulating materials and system surfaces. The specimen was heated to the desired test temperature, the vacuum pump was valved-off, and the test started by admitting HF to the chamber at a rate which brought the chamber pressure to 10 psia in approximately one minute. The total test time was measured as the period from the admission of the HF to the termination of the heating current. After the test, the chamber was evacuated by pumping the fluoride gas through the cold trap. The temperature was measured prior to each test with a two color pyrometer focused on the specimen. During the test, some clouding of the chamber window occurred and constant temperature was maintained by keeping the power input to the specimens constant. The degree of reactivity was determined by measuring the diameter change of the specimen with pin-tip micrometers. Selected specimens were also sectioned for structural examination.

c. Results and Discussion

(U) Data were obtained for tungsten, tantalum carbide, hafnium carbide, graphite grade CGW, pyrolytic graphite, pyrolyzed plastics Carb-I-Tex 700, Carb-I-Tex 100, zirconium oxide, and phenolic reinforced with carbon cloth. Attempts to test type PTB graphite were unsuccessful. The filler resin boiled out during initial heating in vacuum and the resulting structure failed mechanically under loads imposed by the fixture.

(U) A summary of the test results is presented in Table III and Figure 4. In all the tests, the specimens were heated to approximately the maximum temperature obrainable in the test apparatus, depending upon the electrical resistance characteristics of the individual materials.

(U) The results indicate that the pyrolyzed material reinforced with graphite cloth (Carb-I-Tex 700) had the greatest resistance to the hydrogen fluoride environment. Exposure to HF at 4200°F for 3 minutes produced a dimensional change less than 0.001" in the direction normal to the plies. After exposure, the specimen was slightly darker in color and the plies stood out slightly in relief indicating that they had greater resistance to attach than the matrix.

(U) The Carb-I-Tex 100 material showed the greatest degree of dimensional loss, despite the fact that a reaction temperature of only 3400°F was evaluated. Considerable binder was evolved during heat-up and thedimensional change took place predominantly in the direction normal to the plies.

(U) Tungsten exhibited moderately good resistance to hydrogen fluoride attack up to 4500°F. Exposure to HF resulted in the etched-type surface, which indicates preferential grain boundary attack.

(U) The pyrolytic graphite was slightly more resistant than CGW, but not as good as Carb-I-Tex 700. Although the tests were conducted with "c" direction normal to the specimen rod axis, no variation in reactivity as a function of orientation was apparent. The CGW graphite test exhibited a slightly "sooty" surface.

Table III (U) Summary of Reactivity Test Results with HF

Material	Test Temperature, °F	Test time, Min.	Dia. Change 10^{-3} inches
Carb-I-Tex 700	4240	3	0
Carb-I-Tex 700	4200	3	0
W	4000	3	-2.1
W	4520	3	-2.2
W	4420	3	-2.3
W	4520	3	-2.5
PG	4000	3	-2.8
W	4500	6	-3.2
TaC	4480	3	-4.2
ZrO_2	4500	3	-5.0
CGW	4200	3	-5.5
HfC	4500	3	-5.5
Carb-I-Tex 100	3400	3	-6.0*
Carbon Cloth Phenolic	4000	3	-1.8 to 5.0

*Loss occurred only in one direction, normal to the plies, producing an elliptical cross-section.

Unclassified

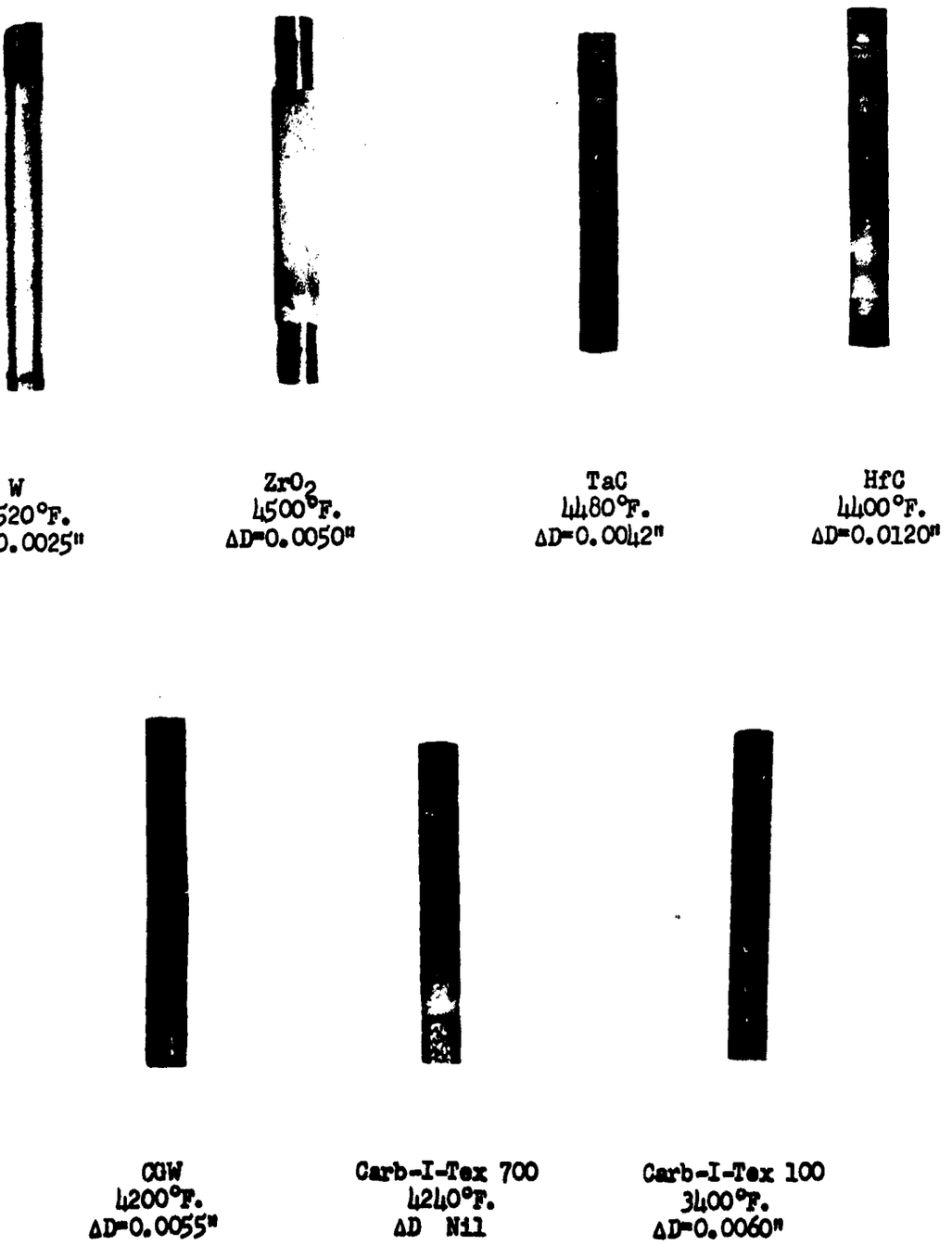

Unclassified

Figure 4 (U) Reactivity Tests in Hydrogen Fluoride Environment

(U) Tantalum carbide offered better resistance to HF attack than hafnium carbide, in agreement with thermodynamic predictions. Zirconium oxide showed resistance to HF attack which was comparable to the hafnium carbide.

(U) The carbon cloth phenolic exhibited a strongly anisotropic expansion on heating and exposure to HF. The plies increased in their plane and stood out in relief. Visible warping of the specimen was also observed.

(U) Since actual service conditions involve dynamic environments and a propellant with a slight quantity of oxygen in addition to hydrogen fluoride, the question arises as to whether these variables will significantly alter the ratings obtained in the screening tests. To answer these questions, additional evaluations were made on tungsten and CGW graphite. The first series of tests involved introducing the HF as a stream impinging directly on the specimen. The test results shown in Table IV indicate that this test modification produced no significant difference in the reactivity characteristics of either the tungsten or the graphite material.

(U) Using a spacing of 5/8" between the hydrogen fluoride jet and the specimen, the tungsten exhibited a loss in diameter of 2.5×10^{-3} inches after a three minute exposure, which is comparable to that observed under steady-state conditions. When the spacing between the nozzle and the specimen was reduced to 3/16", a 4×10^{-3} inch localized pit was developed at 4500°F in the specimen, along with a general loss in diameter of approximately 2×10^{-3} inches. The CGW tested at 4000°F with a 3/16" spacing between the jet and specimen sustained a maximum dimensional loss of 2×10^{-3} inches.

(U) A second series of tests involved introducing 0.1% volume of air into the reaction chamber along with the HF gas. As illustrated in Table IV, this quantity of oxygen, which was chosen to simulate the relative percentage in the exhaust specie involved in the current firing program, did not produce results different from those obtained in the 100% HF environment. It should be emphasized, however, that higher quantities of oxygen can produce severely degrading results. During a test with HF on tungsten, a slight leak developed in the chamber. The appearance of the specimen after three minutes is shown in Figure 5. The reactivity for this material in the HF -- air mixture was significantly greater than that produced by either air or HF alone. The results indicate that propellants which contain fluorine and a greater quantity of oxygen than currently being used can produce severely reactive conditions.

d. Conclusions

(U) The results of the reactivity tests indicate that the graphite base Carb-I-Tex 700 material exhibited the greatest resistance to attack by HF at temperatures up to 4200°F. Wrought tungsten also showed moderately good resistance to attack at temperatures as high as 4500°F. Additions of 0.1% air and theuse of an impinging gas stream did not significantly alter the results obtained with the static HF environment.

3. MECHANICAL PROPERTY EVALUATION

(U) In addition to the reactivity testing to screen various candidate materials, mechanical property tests were conducted on hot-bonded graphite.

Table IV (U) Dynamic and Oxygen Addition Test Results

Material	Test Temperature (°F)	Test Time (min.)	Test Condition	Change In Diameter (10^{-3} in.)
Tungsten	4500	3	Jet impingement 5/8" nozzle - specimen spacing	2.5
Tungsten	4500	3	Jet impingement 3/16" nozzle - specimen spacing	2.0 4.0
CGW Graphite	4000	3	Jet impingement 3/16" nozzle - specimen spacing	2.0
Tungsten	4500	3	HF + 0.1 v/o air	2.5
CGW Graphite	4000	3	HF + 0.1 v/o air	0.7

Unclassified

Unclassified

Figure 5 (U) Tungsten Specimen after Exposure in HF Plus Air Mixture

This is a relatively new graphite material development incorporating layers of pyrolytic graphite foil bonded together into billet form by hot pressing. The resultant material has anisotropic properties similar to pyrolytic graphite. Reactivity tests were not conducted on this material since it is an alternate form of deposited pyrolytic graphite and, therefore, would be expected to exhibit reactivity characteristics similar to those of the pyrolytic graphite material which was tested for reactivity (see the previous section).

(U) Tensile and flexure strengths determined for the hot-bonded graphite are tabulated in Table V. Tensile strength along the "a-b" planes was considerably greater than the tensile strength across the "a-b" planes ("c" direction). However, the actual tensile strength along the "a-b" planes could not be measured because the specimens failed in the grips during test and thus the ultimate load carrying ability was not recorded. Failure in the grips occurred by shear across the "c" direction where the radius from the specimen shoulder goes into the gage length (refer to Figure 6b, Series A). With the loss of the shoulders on the specimen, there was an insufficient area to grip. Tensile strength in the "a-b" plane are the maximum values recorded, but are below the ultimate capability of the material. Strength of the hot-bonded graphite in the "c" direction was low, approximately one-fourth of the strength value reported for pyrolytic graphite tested in the "c" direction.

(U) Flexure strength of the hot-bonded graphite averaged 3,800 psi in Series A tests, 6,600 psi in Series B tests and 361 psi in Series C tests. The low value recorded in Series c flexure tests resulted from applying the principle stress in the "c" direction. This is a low strength direction (across the "a-b" planes) as shown in the tensile test results. Flexure strengths of the Series A tests were 10 times greater than Series C tests, while the Series B tests had flexure strengths nearly 20 times that of the Series C tests because the principle stresses during testing occurred along the higher strength "a-b" planes. Modulus of elasticity was significantly higher for the Series B tests than for either the Series A or Series C tests.

Table V (U) Hot Bonded Grafoil Tensile and Flexure Data

Tensile Data

0.020 in/min Cross-Head Speed

Specimen No.	Orientation	Maximum Load	Maximum Stress
A-1	Figure 6a,	180*	1,800 psi
A-2	Series A	167*	1,700 psi
A-3		232*	2,300 psi
C-1	Figure 6a,	14.6	145 psi
C-2	Series B	8.0	79 psi
C-3		16.0	159 psi

Flexure Data

0.080 in/min Cross-Head Speed

Specimen No.	Orientation	Maximum Load	Maximum Stress Psi	Modulus of Elasticity -psi x 10^6
A-1	Figure 6b,	17.5	4,500	1.27
A-2	Series A	17.1	4,200	1.10
A-3		10.7	2,700	1.24
B-1	Figure 6b,	20.7	6,[illegible]00	2.67
B-2	Series B	22.0	6,600	2.67
B-3		21.2	6,400	2.81
C-1	Figure 6b,	1.3	331	1.00 (est.)
C-2	Series C	1.5	387	1.00
C-3		1.4	367	1.01

Unclassified

* Specimen broke in grip area by shear through the "C" direction (along the "a-b" planes).

a. Tensile Test Specimens

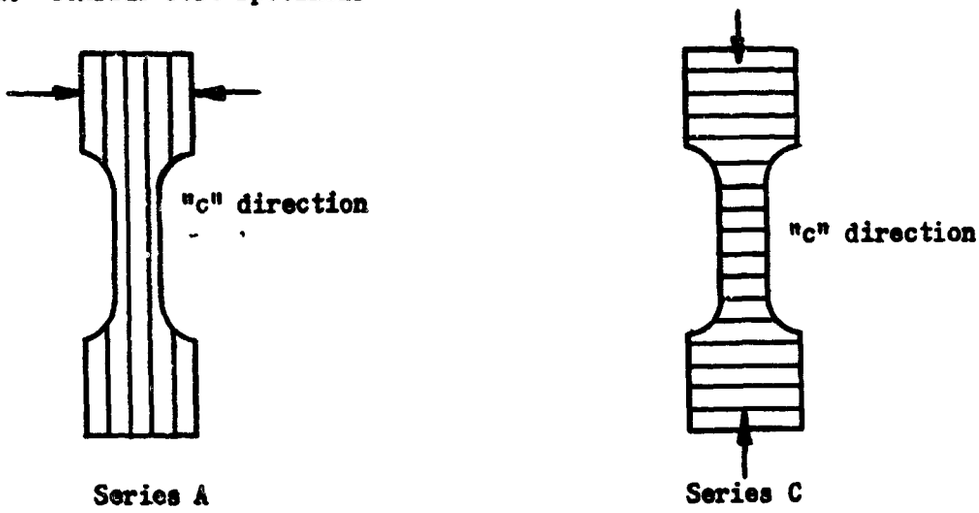

b. Flexure Specimens

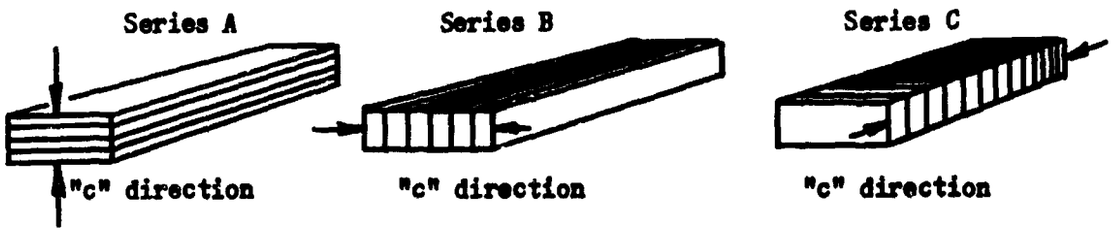

Unclassified

FIGURE 6 (U) Grain Orientation of Hot-Bonded Grafoil Test Specimens

SECTION IV

APPLICATION OF THOMPSINE TAPE

(U) Thompsine tape is a unique configuration of ablative composite reinforcing fibers developed as a means of solving several problems existant in rocket nozzle and reentry vehicle hardware. The material was developed by TRW and up to the current program had been demonstrated on a laboratory basis to be a feasible approach. Limited ablation and erosion data were available from plasma jet evaluations which indicated that the material concept could be competitive with conventional reinforcement forms relative to ablative performance and at the same time provide substantial fabricability and component reliability. The Thompsine tape concept was introduced into the non-regenerative thrust chamber program as a means of solving some of the material integrity problems with restart operation and to demonstrate the capabilities of this material form. It was the objective of the unit S/N 3 demonstration to produce sufficient tape to fabricate one full scale motor assembly, to demonstrate the fabricability characteristics of the material, and investigate the ablative performance without further development of the material.

1. DISCUSSIONS

(U) Thompsine tape is a composite fabric of monolithic design, consisting of currently available high temperature reinforcing yarns. The unique feature of this tape construction is the sinusoidal placement of the longitudinal reinforcing fibers as depicted in Figure 7. For clarity, the schematic view shows one layer, whereas the actual tape ply consists of three layers. Each of these three layers has a similar geometric configuration, with a phase lag of 120° relative to the other two. As indicated in the schematic view, the construction consists of three distinctly different fibers. The main fiber, of course, is the primary reinforcing fibers. The wale fiber (longitudinal linear fiber) provides the restraint or control of the sinusoidal placement of the reinforcing fibers. The "tie" fibers simply tie the ablative yarns into position onto the wale fiber. In Thompsine Tape produced to date, an elastomeric fiber has been utilized as the wale fiber to provide an extensibility feature to the tape, yielding greater tape wrapping diametral ratio capability than that obtainable with the use of standard or preconditioned bias tape slit from standard textile weaves. It will be noted that ablative fibers do not follow an over and under pattern which is typical of standard weaves, but lie in one plane. In the transverse direction of the tape, bands of different fiber material are arranged so that the tape width provides, after wrapping on a mandrel, an integrally-bonded, multi-layered cross-section through the thickness of a nozzle wall. Such a graded or layered composite tape construction is possible with the Thompsine weave since no transverse fibers exist as found in conventionally woven tapes. A picture of a short length of resin impregnated Thompsire tape of graphite and quartz yarns is illustrated in Figure 8.

(U) The unique geometric configuration of the Thompsine concept offers the designer great versatility in tailoring a tape to a specific application where reinforcing fibers of the appropriate composition are placed in strategic location and at the proper orientation to achieve a desired performance.

(U) Such versatility is illustrated by the following possibilities:

A. Simultaneous wrapping of two or more dissimilar materials while maintaining a stratified but monolithic section.

B. Design for any desired diametral ratio wrap.

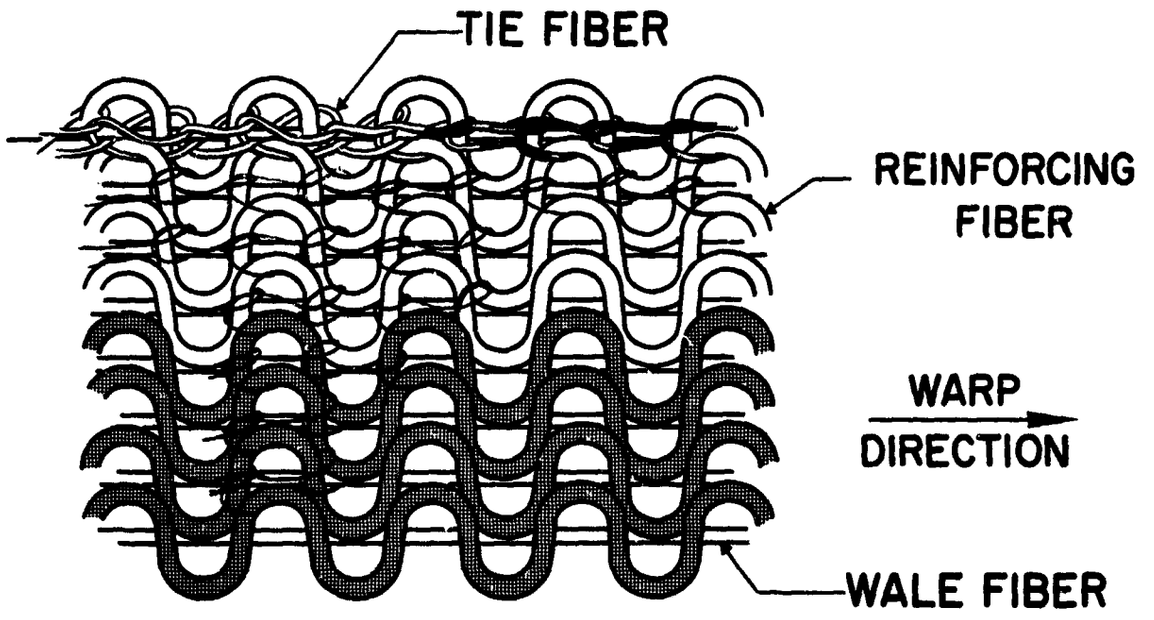

Unclassified FIGURE 7 (U) Schematic of Thompsine Tape construction (one layer)

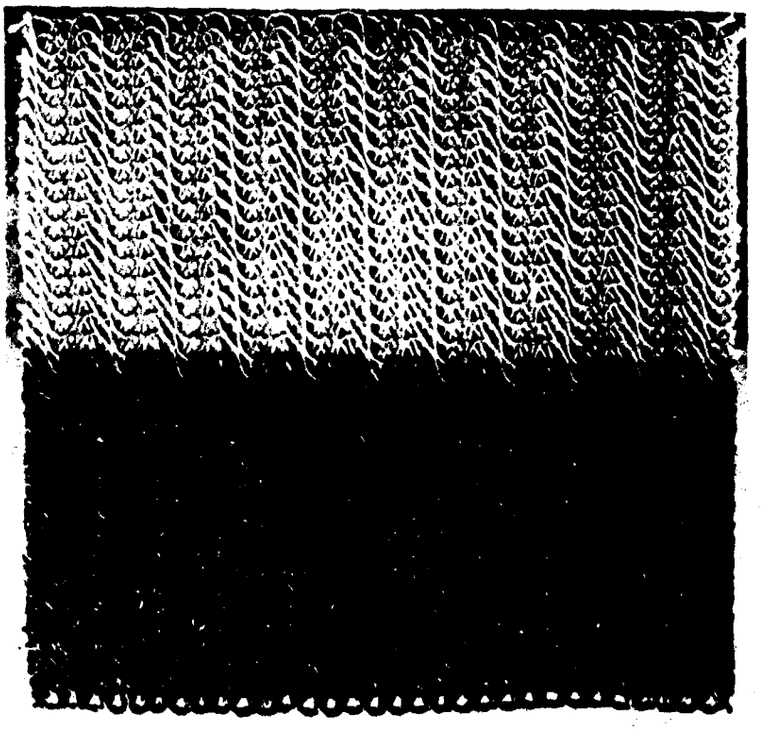

FIGURE 8 (U) Sample of Impregnated composite tape.

C. Transversely varying tape thickness for wrapping at continuously varying orientations.

D. Varying amplitudes and/or frequencies of the sine wave configuration of the reinforcing yarns to provide desired end-grain effects.

E. Interspersing dissimilar fibers in a programmed pattern to achieve a graded cross-section effect.

(U) One of the desirable features of the sinusoidal placement of reinforcing fibers is the end-grain effect obtained when tape wrapping at an orientation. In this situation, all fibers will be placed in a position essentially perpendicular or end-grain to the thermally exposed surface. Each elemental fiber at the exposed surface will be firmly embedded in virgin substrate. The sine pattern can be altered by changing the amplitude and/or frequency to obtain a specific design configuration desired.

(U) For the purpose of this program it was established that for the unit S/N 3 non-regenerative thrust chamber, a specific approach would be taken. First of all, the program was not to be a materials development or improvement program but Thompsine tape, as it was known at that time, was to be used in the design. The material variables that were to be considered were limited to the selection of reinforcement and the width of each side of the tape which would be determined by preliminary heat transfer analysis and predicted erosion profiles. The fibers selected for incorporation into the tape consisted of quartz and graphite yarn. Graphite was selected over carbon as a result of a previous compatibility evaluation on the program which indicated a greater degree of chemical resistance of a graphite structure compared to carbonaceous materials to HF.

(U) Although very limited experience had been gained in impregnation of Thompsine Tape prior to this program, it was determined that the best methods available would be used without an extensive developmental effort. A commercial impregnating source was selected and arrangement for coating the tape with a conventional phenolic resins system was arranged. It was also established that no attempts to use particulate fillers would be made on the program.

(U) Because of lack of experience in producing Thompsine Tape in quantity, a trial run on a preliminary quantity of material was to be produced and impregnated prior to the commitment of the material for hardware fabrication. This trial lot of 15 pounds of material was to be a forerunner which could preclude serious difficulties in the actual fabrication and loss of both schedule time and materials.

2. RESULTS

(U) After considerable thought and consultations with Air Force representatives, a design was finalized for the incorporation of Thompsine Tape into the full scale motor designated unit S/N 3. It was deemed expedient not to use Thompsine Tape throughout the full length of the chamber and exit assembly but also to provide an opportunity to compare the performance of Thompsine Tape with conventional ablative composites in the same motor. The resulting design, therefore, utilized a tape wrapped graphite phenolic composite liner in the forward portions of the thrust chamber approximately 5 inches in axial length. Thompsine tape was used from that point aft through the remainder of the barrel portion of the chamber progressing through the throat approach and throat area. Conventional carbon cloth phenolic was

used in the exit portion of the motor to the expansion area ratio designated by the basic motor design. The entire assembly was overwrapped with 181 E-glass phenolic to provide additional insulation and to build up the varying diameter to provide a cylindrical external surface. Precise details of motor design are included in Section VI of the final report.

(U) One of the many significant aspects of the design, however, was the selection of tape width involved for the Thompsine material. Several factors were involved with the first being the wall thickness necessary of each material to provide the required erosion resistant inner liner and insulative outer liner. Another aspect was the selection of tape width based upon the predicted "neck down" resulting from tape wrapping of the material in a conical development configuration. Because of the variation in erosion and heat transfer at the various stations, it would be desirable to use a separate tape width for each station. However, because of the limited quantity of material to be procured, it was deemed advisable from a logistics standpoint to select a single tape width which would represent a tape width trade-off between all areas considered. The final tape design was a $3\text{-}\frac{1}{4}$ inches overall width with a 2-1/16 inches of graphite fibers. A specification was then generated defining all parameters of the tape construction, the yarns to be used and the other projections necessary for producing acceptable quality material. The target specification requirements are listed in tabular form in Table VI.

a. Trial Run Material

(U) Several samples consisting of a few feet of tape were produced by the weaving vendor to establish the loom parameters necessary to produce the desired construction. One of the approaches considered and attempted was to provide a non-extensible thread along one side of the tape (graphite side) which would assist in eliminating premature stretch-out of the tape during impregnation and during tape wrapping. Preliminary history had indicated that such stretch-out can occur causing change of tape width as well as ultimate extensibility. This concept was discontinued after the trail lot, however, due to added cost and lack of complete effectiveness. When the desired configuration was achieved or adequately approached, approval was granted the weaver to proceed and a quantity of 6.8 pounds was produced. The lot was sampled and evaluated for conformance to the specification requirements. The results of this evaluation are also shown on Table VI. It will be noted that compliance to the target specification was generally good with the exception of the amplitude and period, (which were lower than specified but felt adequate), and the extensibility. Laboratory evaluation indicated, however, that no difficulty would be experienced in achieving the desired diametral wrap ratio required by motor design. Also, the organic fiber content was higher than desired although it was found necessary to use this much tie and wale material to maintain tape integrity. The material was then impregnated by the impregnating source using EC-201 phenolic resin from Evercoat Chemicals. This resin was selected on the basis of its performance in ablative applications and ease of handling.

(U) It was recognized that the graphite and quartz portions of the tape would absorb resin at different levels necessitating the coating of each side of the tape independently. Several approaches were considered, the one settled on being the use of a "W" configuration dip tank in which the tape was draped over the center peak of the "W" such that the interface between the graphite and silica coincided with the peak. Phenolic resin solutions of different concentrations and specific gravities were used in each side of the shaped chamber as required to

Table VI (U) Thompsine Tape Construction

Trial Lot of Tape

Materials	Target Specification	Measured Values
Quartz Yarn	J.P.Stevens Style 300 4/4	JPS Style 300 2/10
Graphite Yarn	Union Carbide WYB 85 1/2	UCC WYB 125 1/5
Tie Fiber	Polypropylene 30 Denier Monofilament	Same
Wale Fiber	460 Denier Lycra P.P. served	Same
Selvage Fiber	Glass yarn	Deleted
Construction		
Amplitude, inches	0.375 ± 0.050	0.250
Period, inches	0.375 ± 0.050	0.250
Yarns/in. tape width	12 minimum	12
Width Total, inches	3-1/4 ± 1/8	3-1/4
Graphite, inches	2-1/16 ± 1/16	2-1/16
Quartz, inches	1-3/16 ± 1/16	1-3/16
Layers	3	3
Phase lag between layer	120°	120°
Elongation at 15#/in load	150% minimum	118%
Neckdown at 15#/in load	No requirement	52%

Organic Content

		Quartz	Graphite
Polypropylene		4.04%	4.88%
Lycra		1.31	2.05
Total	3% maximum	5.35	6.93
Volatile Loss/at Temp. (1 hr.)		0.24%/950°	1.64%/850°
Yield Pounds	15	6.8 received	

Unclassified

achieve the desired resin pickup on the graphite and quartz web. Though not an automated arrangement it was adequate for the limited quantity of material to be coated. Following impregnation the tape was passed through a horizontal "B" staging tower supported by a skrim carrier. A specification had been prepared which designated the resin content desired and the "B" staging conditions thought desirable for tape wrapping. The material was received and evaluated for conformance to the specification. The specification limits of acceptability and the results achieved are presented in Table VII. The yield from the 6.8 pounds of tape after using several short lengths for trial runs through the treater, was 7.2 pounds of prepregged tape. This was felt adequate for preliminary evaluation.

(U) It became apparent immediately, both from the laboratory tests and from the tape wrapping trials, that the tape exhibited very little tacking qualities necessary for successful tape wrapping and debulking operations. Good extensibility was achieved and it was found that the neck-down when tape wrapping on a 3 inch diameter cylindrical mandrel at 75° orientation (simulating the unit S/N 3 throat) a 10-12% neck-down was obtained. These values are much lower than that obtainable with conventional bias slit broadgoods materials. For instance, on the 3 inch mandrel, the maximum bias tape width that could be wrapped would be 1.75 inches and a 34% neck-down would be experienced. On the 4 inch diameter, 75° configuration, the maximum tape width which could be wrapped with bias material would be 0.875 inches. The fabricability, from a tape wrapping configuration standpoint, was thus established for Thompsine Tape.

(U) Because of the low tacking characteristics of the prepreg tape, it was not possible to wrap a preformed billet. In an attempt to improve the tape characteristics a quantity of 1.8 pound was returned to the impregnator for reimpregnation in hopes that some tack could be developed in the tape. Upon return of the material some improvement of the wrapping properties was noted although still insufficient to be considered good tape wrapping grade material. From the laboratory test and from the tape wrapping trials, it was possible to make the necessary decisions on the design and procurement of the tape required for the fabrication of unit S/N 3.

(U) Flat laminates were prepared to establish preliminary composite properties. Table VIII presents property data obtained including interply tensile strength interlaminar shear strength and specific gravity.

b. Fabrication of Unit S/N 3

(U) On the basis of the trial runs, the tape was redesigned to be ¼inch narrower than previously considered to achieve the desired wall thickness. A quantity of 28 pounds of tape was then produced and evaluated for conformance. The new specification allowables and the results of this evaluation are presented in Table IX.

(U) The material was impregnated using the same procedure as on the trial run with the exception that special care was given to reduce the amount of staging, thereby developing more tack. The material was received and evaluated, the results of which are presented in Table X. It was noted that the material was very pliable and was, in fact, extremely sticky.

(U) The sequence of fabrication operations used in manufacturing unit S/N 3 is given in abbreviated detail but sufficient to demonstrate the general approach taken.

Table VII (U) Thompsine Tape Prepreg Properties

Trial Lot of Material

	Specification Target		TRW Test Results		Vendor Test Results		Vendor Results On Recoated Material	
	Quartz	Graphite	Quartz	Graphite	Quartz	Graphite	Quartz	Graphite
Resin Solids %(1)	28.1 ± 2.0	36.0 ± 2.0	26.43	39.26	27.11	40.95	32.8	41.7
Volatile Content %(2)	3.5 ± 1.0	3.5 ± 1.0	2.70	3.22	3.14	4.22	6.5	8.75
Flow, Dry Laminate %(3)	5.5 ± 1.5	5.5 ± 1.5	6.37	1.87	4.21	2.16	21.4	22.5
IRPI (4)	0.95 ± .05	0.95 ± .05			1.66	1.64		
Yield, pounds			7.2					

(1) Determine by DMS Extraction

(2) Air circulating oven 325°F, 20 minutes

(3) 200 psi, value is resin expulsion only exclusive of volatile loss

(4) Infrared polymerization index, zero base line

Table VIII (U) Thompsine Tape Composite Properties

Trial Lot of Tape

Values obtained from molded flat laminates, 310°F, 1000 psi

Interply Tensile Strength (1)	
Quartz Thompsine Composite	1290 psi(2)
Graphite Thompsine Composite	565 psi
Silica phenolic (MX-2600)	695 psi
Graphite phenolic (FM-5014)	1080 psi
Interlaminar Sheat Strength(3)	
Quartz Thomspine Composite	2550
Graphite Thompsine Compoiste	1300
Specific Gravity	
Quartz Thompsine	1.80
Graphite Thompsine	1.27

(1) TRW Test using 1" diameter specimen from ½" laminate

(2) Average of three values

(3) TRW Double Shear specimen 1/2 x 7/16 x 1/2

Table IX (U) Thompsine Tape Construction, Unit S/N 3

Materials	Specification	Test Results
Quartz Yarn	J.P. Stevens Style 300 3/10	Same
Graphite Yarn	Union Carbide WYB 125 1/5	Same
Tie Fiber	Polypropylene 30 Denier Monofilament	Same
Wale Fiber	460 Denier Lycra P.P. served	Same
Construction		
Amplitude	0.250 ± .050	0.240
Period	0.250 ± .050	0.240
Yarns/in tape width	10	10
Width Total	3 ± 1/8	3.0
Graphite	1 13/16 ± 1/16	1 13/16
Quartz	1 3/16 ± 1/16	1 3/16
Layers	3	3
Phase lag between layers	120°	120°
Elogation	150% minimum	85%
Weight, lbs/linear yd.	No requirement	0.103
Yield, lbs.		28

Unclassified

Table X (U) Thompsine Tape Prepreg Properties, Unit S/N 3

	Specification		Vendor Test Results	
	Quartz	Graphite	Quartz	Graphite
Resin Solids, %	28.0 ± 2.0	36.0 ± 2.0	33.8	46.1
Volatile Content, %	3.5 ± 1.0	3.5 ± 1.0	10.3	12.8
Flow, Dry laminate, %	5.5 ± 1.5	5.5 ± 1.5	26.4	30.7
IRPI	0.95 ± 0.05	0.95 ± 0.05	1.41	1.38

Unclassified

A. Tape wrap graphite phenolic on 30° starting ring in the area adjacent to the injector.

B. Overwrap parallel to center line carbon phenolic and then silica phenolic

C. Hydroclave cure.

D. Machine O.D. and 45° starting angle at aft end of wrap.

E. Tape wrap Thompsine Tape at 45°for a length of approximately 3 inches.

F. Machine 75° angle.

G. Tape wrap Thompsine Tape at 75° throat approach and throat sections.

H. Hydroclave cure.

I. Machine O.D. contour and 40° starting ramp.

J. Tape wrap carbon phenolic exit cone section at 40°.

K. Machine carbon preform.

L. Overwrap entire assembly with glass phenolic.

M. Hydroclave cure.

N. Machine inside motor chamber contour and cylindrical O.D.

O. Assemble into steel shell.

(U) The graphite phenolic 30° wrap and subsequent overwrap and cure processing without event. It became immediately apparent when wrapping the Thompsine Tape that the material was excessively tacky and difficulty was experienced in processing the material through the tensioning and guide rolls of the Edwards Wrapmaster. It was also found that the resulting preform was extremely soft and the degree of densification achieved was low. Because of these factors difficulty was experienced in maintaining a tape alignment and hence, the positive positioning of the interface between the graphite and quartz.

(U) A double set of quartz heaters was mounted on the Edwards Wrapmaster in order to effect additional staging, and tape wrapping of the aft end of the chamber proceeded. Although staging was not fully adequate, sufficient tack was developed to wrap the 45° oriented portion.

(U) The 75° interface was machined and attempts were made to wrap the 75° oriented wrap. The immediate problem encountered was the inward flow of 45° oriented Thompsine quartz at the interface. This was caused by the sliding of the quartz down the 45° incline (see sketch in Figure 9). This can be explained by the fact that sufficient tension had been developed in the outer elastomeric layers during the 45° wrap to cause an appreciable radial force. Since the graphite yardage of several plies had been removed in the machining of the 75° interface, the quartz portions remaining had no support other than tack to retain the wrapped positions. With the application of even a minimal amount of heat to activate the 75° wrap, the

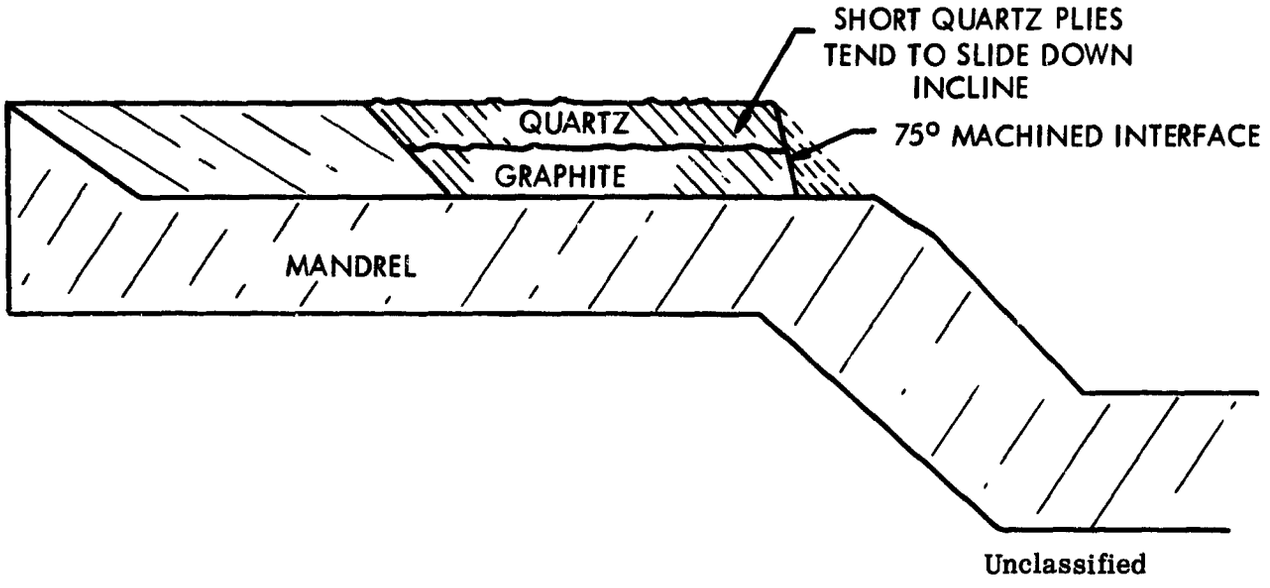

Figure 9 (U) Schematic of Wrap Following 75° Interface Machining

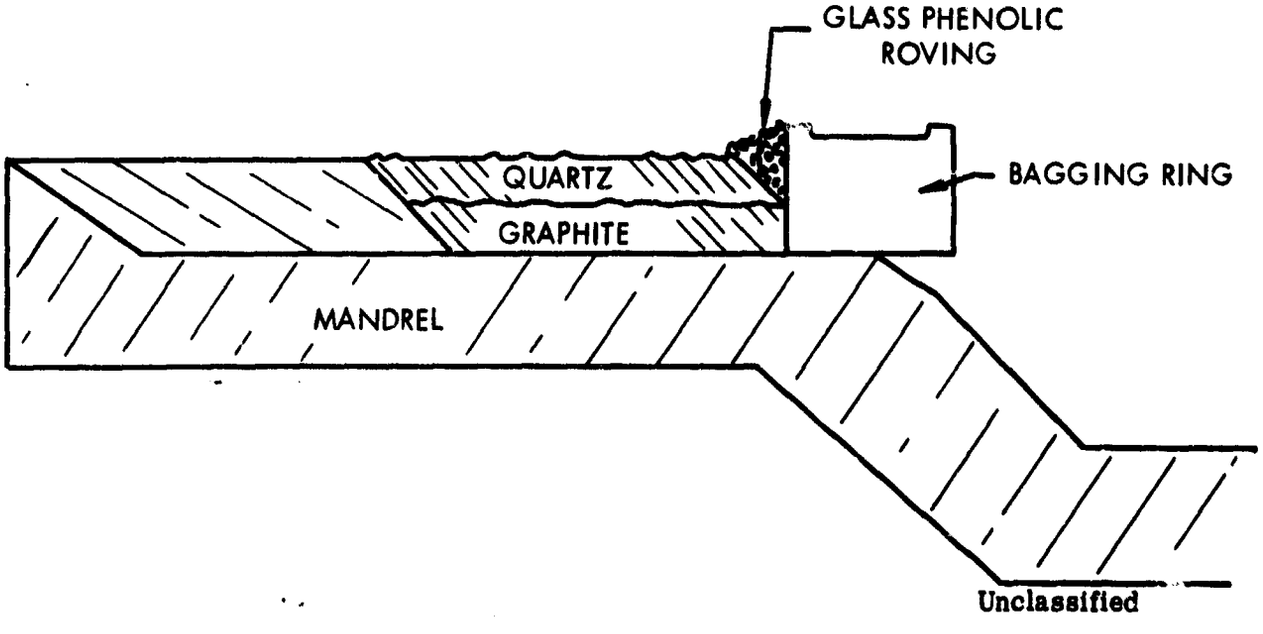

FIGURE 10 (U) Schematic of 75° Interface Repair Procedure

tack was reduced sufficiently to be overcome by the radial force. With the removal of these unsupported quartz plies, the flat starting face for the 75° wrap was destroyed. In order to restore the required starting face, phenolic impregnated glass roving was filament wound over the quartz in this region. Axial restraint in the aft direction was provided by temporarily mounting one of the bagging end rings so that it would butt against the wrapped part (see Sketch in Figure 10). A sufficiently thick section was filament wound to assure an adequate starting face. The bagging ring was then removed and a 75° starting face machined.

(U) Since it was evident that the Thompsine raw material was in need of additional staging, a temporary staging sequence was set up for the next wrap. This consisted of five separate infrared heat sources mounted in series. The tape was positioned in a manner which allowed maximum heat input to the quartz portion in order to advance its resin to a greater degree, thereby imparting better tape wrapping qualities. After being subjected to these heat sources, the tape was passed over the specially fabricated pressure roll and onto the mandrel. Both the pressure roll and the wrapped mass were cooled with liquid CO_2 during wrapping. During the wrap, extreme difficulty was experienced in wrapping the throat approach area. This was caused by inadequate tack coupled with the continual tendency for the outer quartz fibers to slide down the ply causing a puckering of the ply. After several adjustments of heat and coolant inputs, the entire 75° oriented portion was successfully tape wrapped. Diametral ratio attained in the throat area was 2.3 to 1.

(U) While tape wrapping was in progress, several tests were made on the raw material to determine an adequate cure cycle. These tests resulted in the inclusion of a 3 hour staging period in the cycle, to be accomplished at 195°F and atmospheric pressure.

(U) The part was bagged, subjected to the above staging cycle, and then hydroclave cured at 1000 psi. While unbagging, it was noted that, in spite of the staging cycle, excessive flow had occurred. This indicates that a longer stage is desired when handling material in this condition. It was also found that much of the fiber orientation had been lost and that several "puckers" existed.

(U) After cure, the outside diameter of the Thompsine wrap was machined for the overwrap, and an end ring cut for testing purposes. Test results were as follows:

Test	Method	Quartz	Graphite
Specific Gravity	TAP-DAP-101	1.70	1.26
Resin Solids Content	TAP-DAP-103	28.0	----
Residual Volatile Content	TAP-DAP-122	3.0	3.0

Specific gravities attained are somewhat lower than those normally expected with the same basic reinforcing materials. This fact can be understood by examining the structure of Thompsine, which consists of a quantity of organic fibers having a specific gravity in the neighborhood of 1.0. Flat laminate tests have indicated that ultimate specific gravities to be expected with this particular style of Thompsine are 1.80 and 1.27 for the quartz and graphite respectively.

(U) Measurements of the Thompsine wrap taken before and after cure indicate that approximately 80% debulk was achieved during wrap.

(U) The final tape wrapping activities then took place without incident, consisting of the 40° oriented Fiberite MX 4926 exit cone, and the parallel to centerline Fiberite MX 4600 overwrap. The part was bagged and hydroclave cured.

(U) During the machining of the 40° starting ramp for the carbon cloth exit cone portion an end ring was removed from the molding and examined microscopically. A photograph of a cross section of this end ring is shown slightly magnified (5X) in Figure 11 illustrating the graphite and quartz portions of the composite and the ragged mechanical interlock obtained between them. An indication is also apparent in the photo of the loss of fiber orientation. Photographs taken at higher magnification are presented in Figures 12, 13, and 14. Figure 12 is particularly interesting since it shows the distribution of organic elastomeric fibers which are considerably larger in diameter than the graphite fiber. What is not apparent in the photograph but can be seen through the microscope is the loss of fibrous indentification of the organic tie fiber and the fiber used to serve the elastomer wale fiber as a means of controlling extensibility. These fibers were apparently melted in the hydroclave curing operating and appear as islands or pools of organic matter around the elastomeric fibers. This, however, is of little significance since at this point there is no longer need for retention of tape integrity by the tie fiber. The chemical nature of the tie fiber is such as to provide additional ablative cooling to the composite and thus acts as a contributor to the overall performance of the composite.

(U) In Figure 13 the wale fiber is shown in considerable enlargement in the graphite composite while in Figure 14 some degree of porosity is seen in the quartz material indicating poor wetting of the fibers by the resin.

3. SUMMARY AND CONCLUSIONS:

(U) From the experience gained in the processing of the material and the fabrication operations it may be concluded that the desirable forming characteristics of Thompsine Tape have been demonstrated. The wrap at the throat, representing the most severe forming problem, gave a diametral wrap ratio (OD/ID) of 2.3. This is far in excess of the 1.4 achievable with normal bias tape of 1.9 with special handling and tooling techniques.

(U) The wrapping demonstrated the need for additional effort in control of the impregnation process and the "B" staging of the tape to achieve the necessary handling and tacking characteristics. It is apparent that steps must be taken to stage each side of the tape separately since the two fibers, graphite and quartz do not accept and advance the resin equally. The temporary infrared tower set up with the wrapping operation demonstrated that individual staging is feasible.

(U) It was also learned that tape design can and should be revised to reduce the amount and the stretch of the elastomeric fiber. Not only would an improved ablative performance be anticipated but the difficulty with the tape sliding down the wrapping interface could thus be eliminated.

(U) The results of the firing of this motor are presented elsewhere in this report and need not be discussed in this section. It is sufficient to say that the results indicate that the integrity of the Thompsine Tape, both from the standpoint of delamination resistance and, to even a greater extent, the integrity of the interface between dissimilar materials (graphite and quartz) were maintained in and after motor firing. It is felt that the capability of the Thompsine Tape concept has been demonstrated and, although not optimized, is sufficient to warrant

Unclassified FIGURE 11 (U) Cross-section of Thompsine Tape Specimen

FIGURE 12 (U) Cross-section of Thompsine Tape Graphite Specimen, 50X

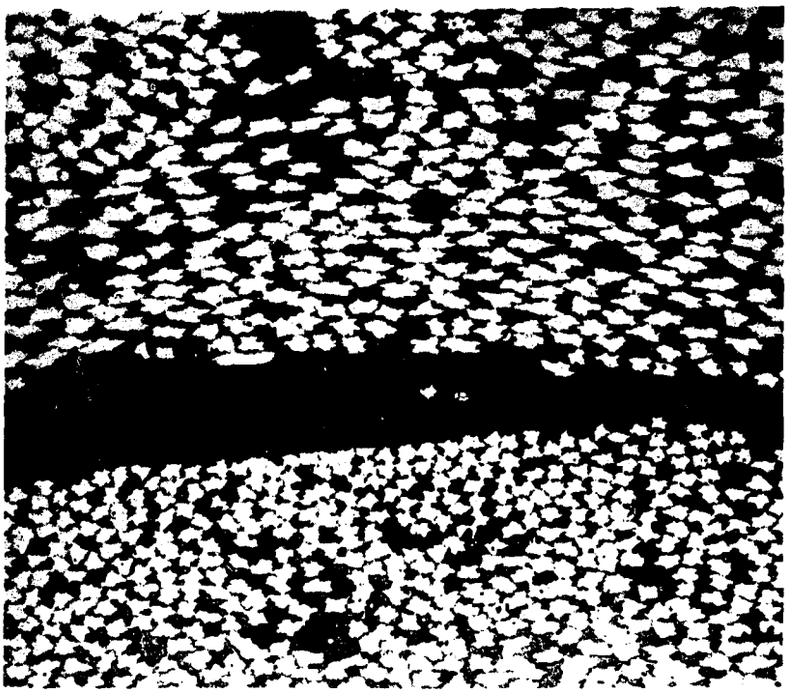

FIGURE 13 (U) Cross-section of Thompsine Tape Graphite Specimen, 250X
Unclassified

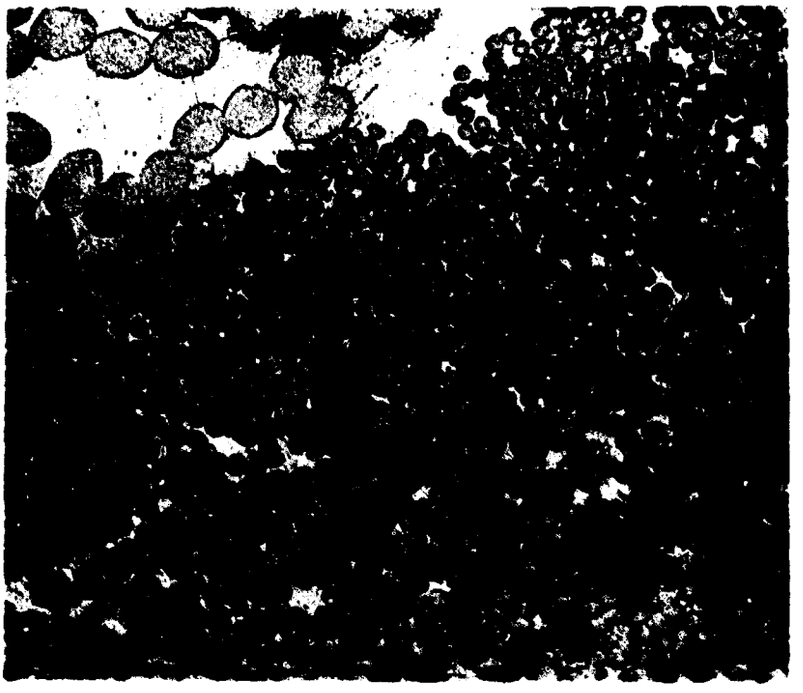

FIGURE 14 (U) Cross-section of Thompsine Tape Quartz Specimen, 250X
Unclassified

further consideration.

(U) It may be concluded that:

A. Thompsine Tape can be produced to specification with a good degree of predicatability as to the configuration.

B. Although reasonable success was achieved in the impregnation, it is apparent that work is necessary in the control of the resin pickup on each side of the tape and the control of the advancement of resin to provide the necessary tape wrapping qualities. It may be necessary to construct a specially designed staging tower to advance to each side of the tape individually and independently.

C. The high degree of tape wrapping ability of Thompsine Tape was demonstrated in achieving high fiber orinetation angles on very small diameters. The material is capable of fabrication in designs far beyond that of conventional bias tape construction.

D. The erosion characteristics of Thompsine Tape were found to be equivalent to conventional ablative materials and the superior integrity obtained by the dissimilar materials was fully demonstrated.

(U) It is felt that considerable technology has been gained about the design and fabrication of Thompsine Tape which will be of value on this and subsequent programs.

REFERENCES

(1)* D. L. Peters, "Chemical Corrosion of Rocket Liner Materials and Propellant Performance Studies", Final Technical Report, Volume One of Two, Contract No W-61-0905-c, Task E, (Dec. 15, 1963).

(2) M. Ebner, "Stability of Refractories in Hydrogen-Fluorine Flames", Sixty-Second Annual Meeting, The American Ceramic Society, Philadelphia, Pa., April 27, 1960 (Refractories Division, No. 28-R-60).

(3) H. B. Blaes, et al, "Application of Materials to Advanced Rocket Nozzle and Hot Gas Control Systems", Third Quarterly Progress Report, Contract AF 33(657)-11217 (April 15, 1964).

(4) S. P. Gualillo, "Phase Report on the Evaluation of Nozzle Materials", Contract DA-01-021-ORD-11919, Modification 33 April 7, 1965.

(5) Milton R. Wolfson and William H. Thiebahr, "Nozzle Material Testing with Solid Fluorocarbon Propellants", 1965 Western Metal Congress (February 22-26, 1965).

(6) Milton R. Wolfson (NOTS-China Lake, Cal.) -- Private Communication (July 8, 1965).

(7) Ellis Foster (Battelle) -- Private Communication (July 15, 1965).

(8) B. R. Miccioli (Carborundum) -- Private Communications (Various, November 1964 to present).

(9) "Improved Throat Inserts for Ablative Thrust Chambers", Second Interim Progress Report ER 6130-Q2 (TRW), Contract No. 3-6280, Control No. CRSD-2093 (Nov.-Dec. 1964).

(10) E. G. Kendall (Aerospace Corp.) -- Private Communication (July 8, 1965).

(11) P. F. Woerner and R. G. Teeg (Cadillac Gage) -- Private Communications (July 8 and July 19, 1965).

(12) High Temperature Materials Co. data sheet titled "Pyrolytic Materials Exhibit High Performance in Uncooled Rocket Nozzles" (October 1, 1962).

(13) M. W. Farlow and R. M. Joyce, Jr., "Aliphatic Fluorine Compounds", U.S. Pat. 2,709,183, May 24, 1955.

(14) Warren F. Kaufman, et. al, "Thermal Protection of Fluorine-Hydrogen Thrust Chambers by Carbonaceous Materials", ARS Journal, pp 1600 through 1602 (October 1962).

---

*Indicates technical information has been extracted from this report.

(15) J. S. Campbell and C. D. Coulbert, "Refractory Thrust Chambers for Spacecraft Engines", Final Report, Contract NAS 7-262, Project 342 (March 22, 1965).

(16) J. S. Campbell, et al, "Pyrolytic Refractory Thrust Chamber Development", Final Report, Contract NAS 7-54, Amendment 1, Project 264 (August 15, 1963).

(17) Ellis Foster (Battelle) -- Private Communication (December 9, 1964).

(18) James Pappis (Raytheon) -- Private Communication (July 23, 1965).

(19) "Refractory Ceramics of Interest in Aerospace Structural Applications - A Materials Selection Handbook" - ASD-TIR-63-4102 (October 1963).

(20) "Improved Throat Inserts for Ablative Thrust Chambers", ER 6130-9 (TRW), Contract No. 3-6280 (August 1965).

(21) "Improved Throat Inserts for Ablative Thrust Chambers", Fourth Quarterly Progress Report, ER 6130-Q4 (TRW), Contract No. 3-6280 (July 1965).

(22) Vendor contract, Zirconium Corporation of America, Solon, Ohio, (June 1, 1965).

(23)* D. W. Gibson and D. W. Smith, "Properties of Silica, Carbon and Graphite Fabric Materials Before and After Exposure to High Temperature Hydrogen Fluoride Environments", pp 359-369, Bulletin of the 6th Liquid Propulsion Symposium, 23-25 September 1964, (Classified, CONFIDENTIAL).

(24) G. Hanna and W. Carlson (Basic Carbon Corp.) -- Private Communication (June 14, 1965).

(25) P. A. Liptrot and H. N. Townsend (Carbon Products Division of Union Carbide Corporation) -- Private Communication (July 29, 1965).

(26) J. L. Margrove and A. K. Kuriakose "Kinetics of the Reactions of Elemental Fluorine with Zirconium Carbide and Zirconium Diboride at High Temperatures", The Journal of Physical Chemistry, Vol. 68, No. 2 (February 1964).

(27) J. J. Hardwood "The Metal Molybdenum" pp 366, ASM, 1956.

(28) "Handbook of Chemistry and Physics", Chemical Rubber Publishing Company, 41st Edition (1959-1960).

Confidential
Security Classification

DOCUMENT CONTROL DATA - R&D

(Security classification of title, body of abstract and indexing annotation must be entered when the overall report is classified)

ORIGINATING ACTIVITY (Corporate author) TRW Inc. 23555 Euclid Avenue, Cleveland, Ohio 44117	2a. REPORT SECURITY CLASSIFICATION Confidential 2b GROUP 4

3 REPORT TITLE

Thrust Chamber Materials and Design Concepts Evaluation (U)

4 DESCRIPTIVE NOTES (Type of report and inclusive dates)

Final Report, June 1965 through May 1967

5 AUTHOR(S) (Last name, first name, initial)

Parks Jr., Edgar G; Poulos, E. N.; Smith, K. J.; Crump, D. N.; Pearson, J. B.

6 REPORT DATE	7a. TOTAL NO. OF PAGES	7b. NO. OF REFS
October, 1967	253	33

8a. CONTRACT OR GRANT NO.	9a. ORIGINATOR'S REPORT NUMBER(S)
AF04 (611) - 10807 b. PROJECT NO. 3058 c. Program Structure No. 7506 d	ER 6383 - 19 9b. OTHER REPORT NO(S) (Any other numbers that may be assigned this report) AFRPL - TR - 67 - 175

10 AVAILABILITY/LIMITATION NOTICES

" In addition to security requirements which must be met, this document is subject to special export controls and each transmittal to foreign governments or foreign nationals may be made only with prior approval of AFRPL (RPPR/STINFO), Edwards, California 93523."

11 SUPPLEMENTARY NOTES	12. SPONSORING MILITARY ACTIVITY
	AFRPL, Edwards, California

13 ABSTRACT

(U) A program was conducted to investigate and evaluate new and unique designs of non-regenerative combustion chambers and nozzles using new materials or new techniques for applying the best materials. The technical effort on this program was divided into two phases. This is the final report on the program.

(U) The technical activity was pursued in three areas--literature survey, laboratory materials investigation, and design concept evaluation in rocket motor tests. The limitation that such parameters as chamber pressure, chemical reaction, firing duration, multiple starts, thermal shock, and structural requirements impose are evaluated in several design concepts. Scaling relations, effect of flow parameter changes on design requirements, and relative ratings on ease of fabrication and reliability of advanced thrust chamber design concepts are evaluated.

(U) Analysis of information obtained through literature search, contact with material suppliers, and laboratory testing indicates that materials which will have the best performance, i.e. lowest reactivity with high temperature fluorniated propellant combuation products, are essentially carbon base materials--graphites, carbides, pyrolyzed composites. Rocket motor tests were conducted using LF_2/ hydrazine blend propellant composition which is equivalent to a theoretical combustion temperature of over 7000°F to evaluate candidate materials and to demonstrate design concepts and scaling relations.

DD FORM 1 JAN 64 1473

Confidential
Security Classification

Confidential

KEY WORDS	LINK A		LINK B		LINK C	
	ROLE	WT	ROLE	WT	ROLE	WT
Non-Regenerative Thrust Chambers						
Materials Evaluation in LF_2/N_2H_4 Blend Propellant System						
Thrust Chamber Design Concept						

INSTRUCTIONS

1. **ORIGINATING ACTIVITY**: Enter the name and address of the contractor, subcontractor, grantee, Department of Defense activity or other organization *(corporate author)* issuing the report.

2a. **REPORT SECURITY CLASSIFICATION**: Enter the overall security classification of the report. Indicate whether "Restricted Data" is included. Marking is to be in accordance with appropriate security regulations.

2b. **GROUP**: Automatic downgrading is specified in DoD Directive 5200.10 and Armed Forces Industrial Manual. Enter the group number. Also, when applicable, show that optional markings have been used for Group 3 and Group 4 as authorized.

3. **REPORT TITLE**: Enter the complete report title in all capital letters. Titles in all cases should be unclassified. If a meaningful title cannot be selected without classification, show title classification in all capitals in parenthesis immediately following the title.

4. **DESCRIPTIVE NOTES**: If appropriate, enter the type of report, e.g., interim, progress, summary, annual, or final. Give the inclusive dates when a specific reporting period is covered.

5. **AUTHOR(S)**: Enter the name(s) of author(s) as shown on or in the report. Enter last name, first name, middle initial. If military, show rank and branch of service. The name of the principal author is an absolute minimum requirement.

6. **REPORT DATE**: Enter the date of the report as day, month, year, or month, year. If more than one date appears on the report, use date of publication.

7a. **TOTAL NUMBER OF PAGES**: The total page count should follow normal pagination procedures, i.e., enter the number of pages containing information.

7b. **NUMBER OF REFERENCES**: Enter the total number of references cited in the report.

8a. **CONTRACT OR GRANT NUMBER**: If appropriate, enter the applicable number of the contract or grant under which the report was written.

8b, 8c, & 8d. **PROJECT NUMBER**: Enter the appropriate military department identification, such as project number, subproject number, system numbers, task number, etc.

9a. **ORIGINATOR'S REPORT NUMBER(S)**: Enter the official report number by which the document will be identified and controlled by the originating activity. This number must be unique to this report.

9b. **OTHER REPORT NUMBER(S)**: If the report has been assigned any other report numbers *(either by the originator or by the sponsor)*, also enter this number(s).

10. **AVAILABILITY/LIMITATION NOTICES**: Enter any limitations on further dissemination of the report, other than those imposed by security classification, using standard statements such as:

(1) "Qualified requesters may obtain copies of this report from DDC."

(2) "Foreign announcement and dissemination of this report by DDC is not authorized."

(3) "U. S. Government agencies may obtain copies of this report directly from DDC. Other qualified DDC users shall request through _____."

(4) "U. S. military agencies may obtain copies of this report directly from DDC. Other qualified users shall request through _____."

(5) "All distribution of this report is controlled. Qualified DDC users shall request through _____."

If the report has been furnished to the Office of Technical Services, Department of Commerce, for sale to the public, indicate this fact and enter the price, if known.

11. **SUPPLEMENTARY NOTES**: Use for additional explanatory notes.

12. **SPONSORING MILITARY ACTIVITY**: Enter the name of the departmental project office or laboratory sponsoring *(paying for)* the research and development. Include address.

13. **ABSTRACT**: Enter an abstract giving a brief and factual summary of the document indicative of the report, even though it may also appear elsewhere in the body of the technical report. If additional space is required, a continuation sheet shall be attached.

It is highly desirable that the abstract of classified reports be unclassified. Each paragraph of the abstract shall end with an indication of the military security classification of the information in the paragraph, represented as *(TS), (S), (C), or (U)*.

There is no limitation on the length of the abstract. However, the suggested length is from 150 to 225 words.

14. **KEY WORDS**: Key words are technically meaningful terms or short phrases that characterize a report and may be used as index entries for cataloging the report. Key words must be selected so that no security classification is required. Identifiers, such as equipment model designation, trade name, military project code name, geographic location, may be used as key words but will be followed by an indication of technical context. The assignment of links, rules, and weights is optional.

DD 1473 Abstract Continued:

Eight 100 pound and three 3750 pound thrust chambers were tested at chamber pressures of 150 and 200 psia. Material and design concepts included prestressed tantalum carbide, arc cast hypereutectic hafnium carbide, pyrolyzed composites of Carb-I-Tex 7000 and PTB, heat sink design of pyrolytic graphite, tungsten, high-density graphite, hot-bonded Grafoil, and Thompsine Tape.

(U) The experimental findings were supplemented with technical and analytical support in an effort to establish the limitations that the propellant environment imposes on the selected materials and design concepts. The erosion or chemical reaction of liner materials appear to be diffusion controlled in most instances and a method for prediction of erosion based upon surface temperature and chamber pressure is reported. Conclusions and recommendations for further work are offered.